Department of MEDICINE, HEMATOLOGY
CENTRO DE INVESTIGACIÓN DEL CÁNCER-IBMCC
(USAL-CSIC)

VNiVERSiDAD D SALAMANCA

CAMPUS OF INTERNATIONAL EXCELLENCE

Doctoral Dissertation

Molecular Characterization of B-Acute Lymphoblastic Leukemia (B-ALL):

Genomic and functional analysis of Acute Lymphoblastic Leukemia and an *in vitro* model of targeted genetic modification

Promotor:
Prof. Dr. Jesús María Hernández Rivas

Supervisor:
Dra. M del Rocío Benito Sánchez
Dra. Teresa Gonzáles Martínez

Adrián Montaño Brioso

November 2020

This doctoral thesis corresponds to a compendium of publications, consisting of the following articles:

Paper I: Adrián Montaño, Jesús Hernández-Sánchez, Maribel Forero-Castro, María Matorra-Miguel, Eva Lumbreras, Cristina Miguel, Sandra Santos, Valentina Ramírez, Jose Luís Fuster, Natalia de Las Heras, Alfonso García-de Coca, Magdalena Sierra, Julio Dávila, Ignacio de la Fuente, Carmen Olivier, Juan Olazabal, Joaquín Martínez, Nerea Vega-González, Teresa González, Jesús María Hernández-Rivas, Rocío Benito. *Comprehensive custom NGS panel validation for the improvement of the stratification of B-Acute Lymphoblastic Leukemia patients*. J. Pers. Med. 2020, 10, 0137; doi:10.3390/jpm10030137.

Paper II: Maribel Forero-Castro*, Adrián Montaño*, Cristina Robledo, Alfonso García de Coca, José Luis Fuster, Natalia de las Heras, José Antonio Queizán, María Hernández-Sánchez, Luis A. Corchete-Sánchez, Marta Martín, Jordi Ribera-Salas, Josep-María Ribera, Rocío Benito, Jesús M. Hernández-Rivas. *Integrated genomic analysis of chromosomal alterations and mutations in B-cell acute lymphoblastic leukemia reveals distinct genetic profiles at relapse*. Diagnostics 2020, 10(7), 455. doi:10.3390/diagnostics10070455. **These authors contributed equally to this work.*

Paper III: Adrián Montaño, Jose Luis Ordoñez, Verónica Alonso-Pérez, Jesús Hernández-Sánchez, Sandra Santos, Teresa González, Rocío Benito, Ignacio García-Tuñón, Jesús María Hernández-Rivas. *ETV6/RUNX1 Fusion Gene Abrogation Decreases the Oncogenicity of Tumour Cells in a Preclinical Model of Acute Lymphoblastic Leukaemia*. Cells 2020, 9(1), 215. doi: 10.3390/cells9010215.

In addition, two review articles were published, showed in the Annexes:

Paper IV: Adrián Montaño, Maribel Forero-Castro, Darnel Marchena-Mendoza, Jesús María Hernández-Rivas, Ignacio García-Tuñón, Rocío Benito. *New Challenges in Targeting Signaling Pathways in Acute Lymphoblastic Leukemia by NGS Approaches: An Update*. Cancers (Basel). 2018 Apr 7,10(4). pii: E110. doi: 10.3390/cancers10040110.

Paper V: Adrián Montaño, Maribel Forero-Castro, Jesús María Hernández-Rivas, Ignacio García-Tuñón I, Rocío Benito. *Targeted genome editing in acute lymphoblastic leukemia. A review*. BMC Biotechnology. 2018, 18: 45. doi: 10.1186/s12896-018-0455-9.

D. **Jesús María Hernández Rivas**, Doctor en Medicina, Catedrático del Departamento de Medicina de la Universidad de Salamanca, Médico Adjunto del Servicio de Hematología del Hospital Clínico Universitario de Salamanca e Investigador del Centro de Investigación del Cáncer de Salamanca,

D.a **María del Rocío Benito Sánchez**, Doctora en Ciencias Biológicas e Investigadora del Centro de Investigación del Cáncer de Salamanca,

D.a **Teresa González Martínez**, Doctora en Ciencias Biológicas e Investigadora del Centro de Investigación del Cáncer de Salamanca,

CERTIFICAN:

Que D. Adrián Montaño Brioso, graduado en Biotecnología por la Universidad de Cádiz, ha realizado bajo nuestra dirección el trabajo de Tesis Doctoral titulado "Molecular Characterization of B-Acute lymphoblastic leukemia (B-ALL): Genomic and functional analysis of Acute Lymphoblastic Leukemia and an *in vitro* model of targeted genetic modification", y que éste reúne, a nuestro juicio, las condiciones de originalidad y calidad científica requeridas para su presentación y defensa ante el tribunal correspondiente para optar al grado de Doctor, con mención "Doctor Europeus", por la Universidad de Salamanca.

La tesis doctoral ha sido escrita en inglés y, de acuerdo con la normativa de la Universidad de Salamanca para la obtención del título de Doctor, el doctorando presenta un resumen significativo en castellano de esta. Además, será presentada por compendio de artículos.

Y para que así conste a los efectos oportunos, firmamos el presente certificado en Salamanca, a 20 de octubre de 2020.

Fdo: HERNANDEZ RIVAS JESUS MARIA - 06541691P
Firmado digitalmente por HERNANDEZ RIVAS JESUS MARIA - 06541691P
Fecha: 2020.10.20 19:35:07 +02'00'

BENITO SANCHEZ MARIA DEL ROCIO - 07875452E
Firmado digitalmente por BENITO SANCHEZ MARIA DEL ROCIO - 07875452E
Nombre de reconocimiento (DN): c=ES, serialNumber=IDCES-07875452E, givenName=MARIA DEL ROCIO, sn=BENITO SANCHEZ, cn=BENITO SANCHEZ MARIA DEL ROCIO - 07875452E
Fecha: 2020.10.20 19:13:16 +02'00'

Prof. Dr. Jesús M. Hernández Rivas

Dra. M. del Rocío Benito Sánchez

Dra. Teresa González Martínez

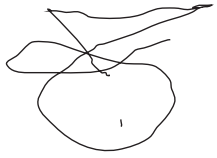

This Thesis was performed being Adrián Montaño Brioso fully supported by a predoctoral grant of the "Junta Provincial de la Asociación Española Contra el Cáncer de Salamanca (AECC-JP Salamanca)".

Acknowledgments:

- Asociación Española Contra el Cáncer -Junta Provincial de Salamanca (AECC-JP Salamanca).
- Consejería de Educación, Junta de Castilla y León, Fondos FEDER (SA085U16, SA271P18).
- Regional Council of Castilla y León SACYL, (GRS 2062/A/19, GRS 1847/A/18).
- Fundación Castellano Leonesa de Hematología y Hemoterapia (FUCALHH 2017).
- Proyectos de investigación en Biomedicina, gestión sanitaria y atención sociosanitaria del IBSAL (IBY17/00006)
- Centro de Investigación Biomédica en Red de Cáncer (CIBERONC CB16/12/00233).
- SYNtherapy. Synthetic Lethality for Personalized Therapy-based Stratification In Acute Leukemia (ERAPERMED2018-275)

***A mi sobrina Gabriela**,*

para que te sirva de inspiración.

Con esfuerzo podrás conseguir todo lo que te propongas.

Agradecimientos

Ahora, que veo como todo va acabando, soy más consciente de todo lo que ha significado para mis estos años en Salamanca y tengo la sensación de que me voy siendo alguien distinto a aquel gaditano bailarín al que casi ni entendían al hablar. De esta ciudad eterna me llevo mucho más que una tesis doctoral bajo el brazo, me llevo algo que es incluso más importante y que difícilmente consiga plasmar en el papel. No obstante, lo intentaré, porque son muchas las personas las que se cruzaron conmigo en el camino y que de una manera u otra han marcado esta etapa de mi vida.

En primer lugar, y sin duda alguna, me gustaría agradecer a mi director, el profesor Jesús María Hernández Rivas, por tu generosidad al abrirme las puertas del laboratorio y por darme a conocer de tu mano el apasionante mundo de la hematología. Por tus sabios consejos y tus enseñanzas que me ayudaron a crecer profesionalmente.

A mis codirectoras, Rocío y Teresa. Rocío, gracias por tu bendita paciencia, por tu esfuerzo y tus ánimos. Siempre con buenas palabras para todos y al pie del cañón ante cualquier adversidad. No he conocido a persona más noble y buena que tú. Teresa, gracias porque has sido un gran apoyo para mi y siempre has sabido darme buenos consejos. Al final va a resultar que Galicia y Cádiz no estaban tan lejos… Gracias de corazón a las dos por todo.

A la junta provincial de la Asociación Española Contra el Cáncer de Salamanca (AECC). Los ángeles que velan por todos esos enfermos que más que nunca necesitan del apoyo de los demás. Gracias infinitas por vuestra labor y en especial por confiar en mi y hacer posible la realización de este proyecto.

Gracias a los miembros del tribunal, así como a los expertos extranjeros que se comprometieron con la revisión de esta tesis. Gracias también a todos los clínicos que colaboraron en este proyecto mediante la cesión de muestras y datos clínicos. Y sin duda, gracias a todos los pacientes y familiares por vuestra colaboración, requisito indispensable para la investigación.

Al Servicio de Hematología del Hospital Universitario de Salamanca, con la Dra. María Consuelo del Cañizo y más tarde el Dr. Marcos González a la cabeza, y con ello a todos los profesionales que forman parte de esta familia. Echaré mucho de menos las cenas de navidad en las que de año en año conseguíamos reunirnos todos para acabar bailando la conga de la mano de la DJ Manoli.

Al centro de investigación del cáncer y con ello a todo el personal de los distintos servicios, administración, conserjería, mantenimiento, almacén y cocina. Gracias a todos por vuestro buen hacer y vuestra simpatía. Y por supuesto, gracias especialmente al laboratorio 12, cuánto orgullo he sentido siempre al decir que formaba parte de este equipo. Gracias a todos y cada uno de vosotros.

A Maribel, mi predecesora de la LAL, que aún en la distancia siempre la he sentido cerca. Gracias por tu apoyo y cercanía. Echaré de menos nuestro "LAL Team" y hasta tus interminables audios por

whatsapp que necesitaba ir anotando para no olvidarme de lo primero que me habías contado. Gracias también por aceptar ser parte del tribunal, demostrándome tu apoyo hasta el último momento.

A mis queridas Sara e Irene, mil gracias por ser mis manos en muchas ocasiones y por vuestro cariño. De tu mano, Irene, comencé mi aventura en el mundo de la secuenciación y te puedo asegurar que no hay mejor profesora que tú. Gracias a las dos por estar siempre dispuestas a ayudar con una sonrisa de por medio. Me llevo un bonito recuerdo de aquellos ensayos de la coreografía que preparamos, y por supuesto, de la cara de ilusión y sorpresa de Sara cuando la música sonó y corriendo fui a la mesa de los novios para invitarla a ver lo que con tanto cariño habíamos preparado.

A Eva, gracias por tu inmenso cariño. Nunca me hubiera imaginado que la más gruñona de todas iba a ser también la que más amor me iba a dar. Gracias por esos ratitos y esas charlas a última hora de la tarde antes de irme a casa, que me hacían sonreír incluso en los peores días. Espero que nadie me quite el puesto y seguir siendo siempre tu "rubio gaditano favorito".

A mis chicas, Sofía, Valentina, Claudia, Elena y María M. Gracias por vuestro cariño y amistad. Con vosotras aprendí que como mejor se ahogan las penas es con unas buenas risas de por medio. Sofía, el caprichoso destino nos quiso volver a unir, y ¿quién sabe?, quizás vuelva a hacerlo de nuevo. Valentina, contigo vuelve el frente colombiano y lo hace pisando fuerte. Gracias por tu comprensión y por tus halagadoras palabras que me dieron fuerza en esta última etapa. Claudia, no hay mejor compañera de laboratorio y de fiesta que tú. Gracias por tu confianza. Elena, la princesita de la menos 3 que ha conseguido hacerse hueco un este apretado corazón. Gracias por tu apoyo y por nuestras charlas conciliadoras cargadas de humor y una buena dosis de ironía. María M, contigo aprendí mucho más de lo que te enseñé. Gracias por tu esfuerzo y por hacerme sentir acompañado.

A mi Ana, que si no le dedicaba un párrafo para ella sola no sé de lo que hubiera sido capaz. Gracias por tanto, tu incansable insistencia y tozudez al final han hecho mella en mi. Entraste en el grupo de forma tímida y coqueta para acabar arrasando con todo el que pasaba por tu lado, ¡hasta en mi casa te metiste! Pero he de decir que lo has conseguido, voy a echarte mucho de menos. Gracias por tu amistad, por tu cariño e incluso por tus consejos, aunque a veces fueran un tanto desalentadores. Contigo me llevo a una gran amiga a la que incluso le podría preparar un sándwich a altas horas de la madrugada.

A Marta y Miguel, porque con vosotros empecé este camino. Muchas gracias por vuestra ayuda y por los buenos ratos que pasamos en los congresos. Me siento muy orgulloso de haber sido vuestro compañero.

A las veteranas Anita, María A, María H y Mónica. Gracias por guiarnos y aconsejarnos en todo momento. Gracias, Anita, por tu generosidad, por estar siempre dispuesta a ayudar y por los buenos ratitos que me hiciste pasar cuando nos contabas tus anécdotas y batallitas. A María A, gracias especialmente por los ánimos y por ayudarme tanto en esta última etapa de la tesis, no lo pudiste hacer

con más mimo y cariño. Es curioso que tuvieras que irte a Berlín para que pudiera conocerte más de cerca. María H, muchas gracias también por tu ayuda, por ser mi guía durante el primer año, por tu paciencia y tu esfuerzo. Espero que no me guardes rencor por haberme pasado al equipo de la LAL y si algún día necesitas algo, recuerda que solo tienes que decir "Ok google, llamar a Adrián" y ahí estaré. Mónica, una pena haber coincidido tan poco tiempo contigo, pero gracias por tus consejos y por supuesto por darme a conocer tan bien la que fue tu ciudad por unos años, New York.

A los veteranos, Nacho y Jose Luis. Nacho, tú me ha enseñado lo que es la ciencia, pero la ciencia verdad, a la que no le gustan los guantes, pero ojo, tampoco las contaminaciones de plásmidos. La ciencia que rompe con las reglas y la que se discute con café y cigarrillo en mano. Eres muy grande y ojalá hubiera más científicos como tú. Jose Luís, mil gracias por tu bondad y por tu entera disposición. Contigo hacer ciencia da gusto, siempre muy correcto pero bromista a la vez. De hecho, sigue siendo difícil adivinar cuando estás de broma y cuando no.

A las chicas del IDI, que bien parece el título de una serie de Netflix. ¡Qué habría hecho sin vosotras! Sandra y Cris, sois un cañón de alegría que arrasa con todo aquel que esté a vuestro lado, seguid siempre contagiando vuestras risas y vuestra espontaneidad. Muchas gracias por vuestro esfuerzo y por hacerme todo mucho más fácil. Inma, el mejor fichaje de la temporada, contigo la LAL se queda en buenas manos. Gracias por tu apoyo y comprensión. A los chicos bioinformáticos, Alex, Javier, Jony, Fernando y a la última incorporación estadística, Ángela, gracias por hacernos las cosas más fáciles, porque sois un pilar fundamental de este grupo.

A los que ya se fueron del labo, a Vero, Kamila, Jesús y Cristina. Cuanto te he echado de menos "tata", como me gusta llamarte. Gracias por escucharme, entenderme y aconsejarme. Contigo me llevo a una gran persona con un corazón de los que no caben en el pecho y con una alegría que logra contagiar a los demás. Gracias, Kamila, por tu paz y tu cariño, la biblioteca no volvió a ser la misma desde que te fuiste. Jesús, gracias por tu apoyo y tus buenas ideas que han sido fundamentales para poder realizar esta tesis. Cristina, gracias también por tu apoyo y por ser un referente durante el primer año.

A mis compañeros del grupo de mieloma. Si hay que estar apretaditos en el laboratorio, qué mejor que con vosotros. Muchas gracias a todos por estar siempre dispuestos a ayudar y por hacernos sentir tan cómodos. Por las comidas de navidad y los congresos compartidos. En especial a Dalia, gracias por tu dulzura y tu cariño. Qué cierto es que son los pequeños detalles los que marcan la diferencia. Gracias también por acompañarme y apoyarme en esta última etapa de la tesis.

Ai miei colleghi italiani durante il mio soggiorno, che, sebbene breve a causa di questa pandemia, è stato anche molto intenso. Grazie per il vostro aiuto e per avermi fatto sentire a casa, per il caffè dopo pranzo, le risate e i dolci momenti accompagnati da un delizioso "bacio perugina".

A los amigos que la ciencia me regaló. A mis compañeros de carrera, especialmente a Alberto, Merchi, Alba, Sonia, Belén y Ángela, gracias por esos reencuentros en los que el pueblo vuelve a despertar una noche más y todo es como antes. A Jose Luis, mi "Wey". Gracias por tu amistad sincera y por sentirte siempre cerca.

Gracias a todas las amistadas que forjé en esta maravillosa ciudad. Carlos, Javi, Amador, Dani, Carlitos y todos los que el mundo del baile me brindó. Gracias por todos los momentos que me habéis regalado, por vuestro amor y vuestra generosidad.

Salamanca, que tendrás que todo el que te pisa se enamora. Gracias por haberme cruzado a todas esas personas en el camino y por hacerme sentir en familia estando a la vez tan lejos de la mía. Salamanca, como dice la canción, eres esas noches de invierno de quiero un abrazo, en las que las calles te arropan y el frío empieza a hacerse querer. Eres esos cambios de aire en cada estación, bailando a destiempo y sin explicación. Eres el primer lunes de abril bajo el puente y el bebernos el mundo de este a oeste, encontrar el amor en cada rincón, como la rana que no tiene miedo al chapuzón, por si le falla el nenúfar o el corazón. Prométeme que al volver todo estará tal y como lo dejé. No puede ser simple casualidad haber dado con algo tan especial (David Rees).

Y como no, gracias al mejor regalo que Salamanca me dio. Mi fiel compañero, Alejandro. Gracias por tu inmenso amor, por cuidarme, mimarme y alegrarme los días. Gracias por estar siempre ahí y ayudarme a levantarme cada vez que caía. Gracias también a tu familia por hacerme sentir uno más, especialmente a la yeya Paqui, en la que encontré a la abuela que tanto necesitaba.

A mis amigos del alma, los de siempre. Gracias por seguir regalándome tanto incluso en la distancia, y es que con nosotros está demostrado que no hay kilómetros que consiga separarnos. Gracias por ayudarme a recargar las pilas y darme fuerzas cada vez que bajaba a casa. Porque siempre nos quede ese atardecer del último día del año con la arena de la playa entre nuestros pies y una copita de manzanilla para brindar.

Por último, dar gracias a lo más importante de mi vida, mi familia. Gracias, mamá, papá y hermana, por vuestro incansable apoyo y hacerme sentir tan orgulloso. Gracias, Juan, por cuidar de mi madre cuando no he podido estar y por el inmenso cariño que siempre nos has mostrado. A mi Gabi, porque a pesar de que no has crecido a mi lado, siempre he sentido como se te iluminaban los ojos cada vez que llegaban "los titis". A mis abuelos, tíos y primos. Especialmente a ellas, que se fueron durante esta etapa sin poderles dar mi último adiós. Gracias, tata Loli, gracias, abuela Mercedes, porque vuestro orgullo me hizo sentir el hombre más especial del mundo.

"La amistad duplica las alegrías y divide las angustias por la mitad"

Francis Bacon

"We ourselves feel that what we are doing is just a drop in the ocean.

But the ocean would be less because of that missing drop"

Mother Teresa

TABLE OF CONTENTS

LIST OF ABBREVIATIONS

ALL	Acute lymphoblastic leukemia
AYA	Adolescent and young adults
Allo-HSCT	Allogeneic hematopoietic stem cell transplantation
aCGH	Array-based comparative genomic hybridization
B-ALL	B-cell Acute Lymphoblastic Leukemia
BTG1	B-cell translocation gene 1
CAR-T cells	Chimeric antigen receptor-modified T cells
CNV	Copy number variation
Ara-C	Cytosine arabinoside
DSB	Double-stranded breaks
EBF1	Early B-cell factor 1
EGIL	European Group for the immunological classification of leukemias
FAB	French-American-British
HR	Homologous recombination
WBC	Initial white blood cell
iAMP21	Intrachromosomal amplification of chromosome 21
6-MP	Mercaptopurines
MTX	Methotrexate
MRD	Minimal residual disease
MFC	Multichannel flow cytometry
MLPA	Multiplex Ligation-dependent Probe Amplification
NGS	Next-generation sequencing
NHEJ	Non-homologous end-joining
OS	Overall survival
PAR1	Pseudoautosomal region 1
RFS	Relapse-free survival
RNA-seq	RNA sequencing
CRISPR	Short palindromic repeats interspersed with regular intervals
aSNP	Single nucleotide polymorphism arrays
PETHEMA	Spanish program in Hematology Treatment
SEHOP	Spanish Society of Pediatric Hematology and Oncology

T-ALL	T-Acute Lymphoblastic Leukemia
TALEN	Transcription activator-like effector nuclease
TKI	Tyrosine kinase inhibitor
WES	Whole exome sequencing
WGS	Whole genome sequencing
WHO	World Health Organization
ZNF	Zinc-finger nuclease

LIST OF TABLES AND FIGURES

Introduction

Chapter I

Chapter II

Chapter III

INTRODUCTION

"The starting point of all achievement is desire"

Napoleon Hill

1. ACUTE LYMPHOBLASTIC LEUKEMIA (ALL)

1.1 Epidemiology, etiology and pathogenesis

Acute lymphoblastic leukemia (ALL) is a hematological neoplasm that originates in the lymphoid stem cell and can affect both the B and T lineages, being B-cell Acute Lymphoblastic Leukemia (B-ALL) much more frequent, encompassing up to 80% of patients [1].

In Europe, the incidence was estimated at 1.28 per 100000 people annually, comprising almost 12% of all incident leukemia cases worldwide, and being the most common cancer of childhood: almost 80% of acute leukemias in children and 20% of adult acute leukemias [2,3]. Around 60% of acute lymphoblastic leukemia patients are diagnosed before the age of 20 years, with the maximum peak of incidence being observed between 1-4 years. In adults, a second gradual increase of cases is observed from the age of 45 onwards [4].

B-ALL originates in a series of alterations that cause the blockage of differentiation, leading to incorrect maturation and uncontrolled proliferation of lymphoid precursors which replace the normal hematopoietic cells of the marrow. The disease mainly affects the bone marrow, and can invade the blood and extramedullary sites, such as lymph nodes, spleen and central nervous system [5,6].

The etiology of B-ALL is unknown. However, inherited genetic susceptibility and environmental risk factors such as exposure to pesticides, paints, or even maternal habits during pregnancy have been deemed to be possibly responsible for the development of the disease [6–9]. In most patients a primary event has been identified that could be the trigger for the leukemic process. This event is defined by a series of recurrent alterations characteristic of these patients, mainly translocations and aneuploidies, and in most cases, they have been shown to be present from the uterus [10,11]. It has been demonstrated that some of these alterations, such as *KMT2A* (*MLL*) rearrangements, are sufficient by themselves to initiate the development of leukemia [12]. However, sometimes these aberrations are not enough for the clinical development of leukemia, so the appearance of second events are required [13,14]. Therefore, these external factors, together with inherited genetic susceptibility, could lead to the development of the "first hit" during the early stages of gestation. The same factors could trigger, during the first months of life, the leukemia transformation through the achievement of second alterations [15]. These second hits often affect key pathways in the development of the disease such as lymphoid development, cell cycle regulation or transcription regulation [16,17].

The development of T-Acute Lymphoblastic Leukemia (T-ALL) is also based on a multi-step process, in which an accumulation of genetic aberrations takes place, corrupting tumor suppressor genes and developmental pathways implicated in cell growth control, proliferation, differentiation and survival [18]. It is worth noting the presence of mutations in the NOTCH pathway such as *NOTCH1* and *FBXW7* genes, which are largely related to the development of the disease [19,20].

Once leukemia has developed, there is controversy about whether these secondary alterations or primary events are responsible for the evolution of the disease, and therefore of the leukemic phenotype. This is, for example, the case of t(12;21), the most frequent translocation in pediatric B-ALL children, and which causes the genetic fusion between *ETV6* and *RUNX1* genes. This fusion gene is known to be a primary event in leukemogenesis and has been reported to appear from the uterus, but additional postnatal genetic events are required for the development of clinically overt leukemia [21]. Some of these events are also present at the time of relapse, suggesting that they may be driving the evolution of the disease [22–25]. However, other studies suggest that the fusion gene not only drives the leukemic transformation, but also the maintenance and propagation of leukemia cells [26]. For these reasons, the true role of the *ETV6/RUNX1* fusion gene in the pathogenesis of ALL as well as its involvement in the evolution of the disease needs to be further explored.

1.2 Diagnosis and classification systems

The clinical diagnosis of acute lymphoblastic leukemia is based on morphological, immunophenotypic and cytogenetic criteria, integrating a series of conventional techniques assessed in the guidelines of the world health organization (WHO) 2016 classification [27].

Firstly, a morphological evaluation by cell microscopy is performed in order to identify lymphoblasts and to determine the level of infiltration in bone marrow and peripheral blood. By definition, the bone marrow must have at least 20% lymphoblasts, presenting these a very variable morphology [28]. While B-ALL usually has a high degree of infiltration, T-ALL usually has an associated lymphomatous mass in the mediastinum or other sites [29].

On the other hand, immunophenotyping using multiparameter flow cytometry (MFC) has become the gold standard in the diagnosis and subclassification of ALL, allowing the evaluation of B and T lineages and the presence of aneuploidies. MFC also provides critical clues for detecting and monitoring minimal residual disease (MRD) [30,31]. The European group for the immunological classification of leukemias (EGIL) proposed in 1995 a classification system exclusively based on the expression of immunological markers and classified B-ALL into four groups, based on the expression of CD19, CD79a (mb-1) and CD22 markers: B-I (pro-B) ALL; B-II (common) ALL; B-III (pre-B) ALL and B-IV (mature-B) ALL. In the same way, but this time based on the expression of CD3, CD7, CD2,

CD5, CD8 and CD1a markers, T-ALL was also classified into four groups: T-1 (pro-T) ALL; T-II (pre-T) ALL; T-III (cortical T) ALL and T-IV (mature T) ALL [32,33]. This system allows the classification of B-ALL patients but is not useful for prognosis stratification. Due to the lack of standardization between the different centers, the "AIEOP-BFM group" developed the first consensus guideline for flow cytometric immunophenotyping of pediatric ALL. This guideline seeks to ensure the reproducibility of diagnostic tests, including instructions for sample processing, staining, acquisition and analysis and was updated in 2016 [34].

Genetic analysis using conventional cytogenetic techniques such as karyotype and FISH is also mandatory in the clinical management of ALL, allowing to stratify patients according to the WHO classification [27].

The system of classification of ALL patients has changed in recent decades, as the landscape of techniques available in the clinical routine has evolved. The first classification was carried out by the French-American-British (FAB) group in 1976, dividing ALL into three subtypes (L1, L2 and L3). This classification was based on morphological and cytochemical criteria, taking into account cell size, cytoplasm, nucleolus, vacuolation and basophilia [35]. In 1997, the WHO attempted to establish another system based on cell morphology and cytogenetic profiles, which was finally published a few years later [36]. This system is still in use today, although it has undergone several modifications. In 2008 the first review was carried out, which included, in addition to morphology and cytogenetics, the use of flow cytometry. The incorporation of cytogenetic studies into the diagnostic workup have made it possible to refine the stratification of patients, especially in the B-ALL group, in which a series of cytogenetic alterations, mainly translocations, were identified. Following guidelines of the WHO 2016 classification, B-ALL belongs to the 'B-lymphoblastic leukemia/lymphoma' category and is classified into two main groups: B-ALL patients with recurrent genetic alterations and undefined patients. Then, the group with recurrent abnormalities were subclassified into: hyperdiploidy (>50 and <60 chromosomes), hypodiploidy (<45 chromosomes), t(12;21)(p13;q22) *TEL/AML1* (*ETV6/RUNX1*), t(v;11q23) *KMT2A* (*MLL*) rearranged, t(1;19)(q23;p13) *E2A/PBX1* (*TCF3/PBX1*), t(9;22)(q34;q11.2) *BCR/ABL1* and t(5;14)(q31;q32) *IL3/IGH.* The 2016 revision also included two new provisional entities: patients with intrachromosomal amplification of chromosome 21 (iAMP21), defined by the presence of multiple copies of the *RUNX1* gene (≥5 signals per cell by FISH), and those with translocations involving tyrosine kinases or cytokine receptors (*BCR/ABL1*-like or Ph-like ALL) as described by both the Dutch Childhood Oncology Group and the St. Jude Children's Research Hospital [37–39]. This last subgroup is characterized by an expression profile very similar to that of Philadelphia positive patients but lacking the fusion gene. In T-ALL a new provisional entity "Early T-cell precursor lymphoblastic leukemia" was also included (Table 1) [27].

Table 1. WHO classification of acute lymphoblastic leukemia (2016). Table adapted from Arber DA. Blood 2016.

B-cell lymphoblastic leukemia/lymphoma, not otherwise specified
B-cell lymphoblastic leukemia/lymphoma, with recurrent genetic abnormalities
B-cell lymphoblastic leukemia/lymphoma with hypodiploidy[1]
B-cell lymphoblastic leukemia/lymphoma with hyperdiploidy
B-cell lymphoblastic leukemia/lymphoma with t(9;22)(q34;q11.2)[*BCR/ABL1*]
B-cell lymphoblastic leukemia/lymphoma with t(v;11q23)[*MLL* rearranged]
B-cell lymphoblastic leukemia/lymphoma with t(12;21)(p13;q22)[*ETV6/RUNX1*]
B-cell lymphoblastic leukemia/lymphoma with t(1;19)(q23;p13.3)[*TCF3/PBX1*]
B-cell lymphoblastic leukemia/lymphoma with t(5;14)(q31;q32)[*IL3/IGH*]
B-cell lymphoblastic leukemia/lymphoma with intrachromosomal amplification of chromosome 21 (iAMP21)
B-cell lymphoblastic leukemia/lymphoma with translocations involving tyrosine kinases or cytokine receptors ('*BCR/ABL1*–like ALL')
T-cell lymphoblastic leukemia/lymphomas
Early T-cell precursor lymphoblastic leukemia

[1] Hypodiploidy was refined as low hypodiploidy (<44 chromosomes) and hypodiploidy with *TP53* mutations

1.3 Prognostic markers

Prognostic markers are relevant in the management of diseases since they help us to predict the evolution of patients and therefore, to define therapeutic options. Age is one of the most relevant clinical parameters in the risk stratification of ALL patients. Nevertheless, the genetic markers at the time of diagnosis as well as the achievement of a negative MRD after treatment are also considered (together with the age) the most important prognostic factors in ALL [6].

Historically, age allows us to establish two large prognostic groups, children (<18 years) and adults, characterized by marked differences in survival rates. While children have achieved survival rates above 90%, adults have not exceeded 40% [40]. Increasing age is thus related to a worse prognosis. Several studies have also proposed to subdivide these groups into different age groups, although no consensus has been reached. As an example, the National Cancer Institutes defined a new subgroup compounded of adolescent and young adults (AYA) (15–39 years), which have been shown to have an intermediate prognosis with survival rates of about 60-70% [41,42].

Other factors, such as white blood cell (WBC) count at diagnosis also helps us to define the risk, being high WBC (WBC ≥30x10^9/L for B-ALL and WBC ≥100x10^9/L for T-ALL) associated with high

risk patients, and the presence of central nervous system involvement has been associated with patients at high risk of relapse (3-5% of patients at diagnosis versus 30-40% at relapse) [43–47].

In last decades, the detection of MRD has also become very important, increasingly used in clinical practice as an independent prognostic marker for the duration of complete remission [48,49]. Persistence of MRD has been associated with reduced relapse-free survival (RFS) and reduced overall survival (OS) [50].

Although clinical factors play an important role in guiding therapy, genetic changes have a significant role in risk determination. In fact, each of the cytogenetic alterations established by the WHO classification demonstrated to have prognostic value. Whereas, the presence of hyperdiploidy or *ETV6/RUNX1* fusion gene are associated with a good prognosis and low risk, the presence of hypodiploidy, *BCR/ABL1* fusion gene, *MLL* rearrangements, iAMP21 or the *BCR/ABL1*-like subgroup are associated with an adverse prognosis and high risk [51–57]. Nevertheless, the development of new therapies has had a great impact on risk stratification. In particular, the survival of patients carrying the Philadelphia chromosome (*BCR/ABL1*) has improved dramatically in recent decades with the incorporation of tyrosine kinase inhibitors (TKIs) to treatment. Thus, the Philadelphia positive subgroup, historically considered to have a poor prognosis, is now considered to have a better prognosis [58]. On the other hand, patients carrying t(1;19) (*TCF3/PBX1*) and t(5;14) (*IL3/IGH*) are considered as intermediate risk group, and those patients who do not present any of the recurrent genetic alterations would therefore be considered to be of uncertain risk [59,60]. This last subgroup of patients is also known as "B-Others" [61].

In the case of T-ALL, no cytogenetic subgroups with prognostic value have been described. However, recurrent alterations that could have some impact on the clinical course of these patients have been detected [62,63]. In approximately 50% of T-ALL patients, chromosomal translocations affecting some transcription factor genes are detected: *TAL1*, *TAL2*, *LYL1*, *OLIG2*, *LMO1*, *LMO2*, *TLX1* (*HOX11*), *TLX3* (*HOX11L2*), *NKX2-1*, *NKX2-2*, *NKX2-5*, *HOXA*, *MYC*, *MYB* and *TAN1*. The particularity of these rearrangements is that the translocated transcription factor gene is placed under the control of strong T-cell specific enhancers (T-cell receptor α, β, and δ) resulting in its aberrant expression [64].

Sometimes several prognostic factors can be correlated with each other, such as age and recurrent genetic alterations. In particular, the large differences observed in survival rates between children and adults are partly attributed to the distribution of different genetic subtypes among age groups. While genetic subtypes associated with low risk such as hyperdiploidy or *ETV6/RUNX1* fusion gene are common in children, alterations associated with high risk, such as *BCR/ABL1* fusion,

are more common in adults [65]. The following figure shows the distribution of the different genetic subgroups among age groups (Figure 1).

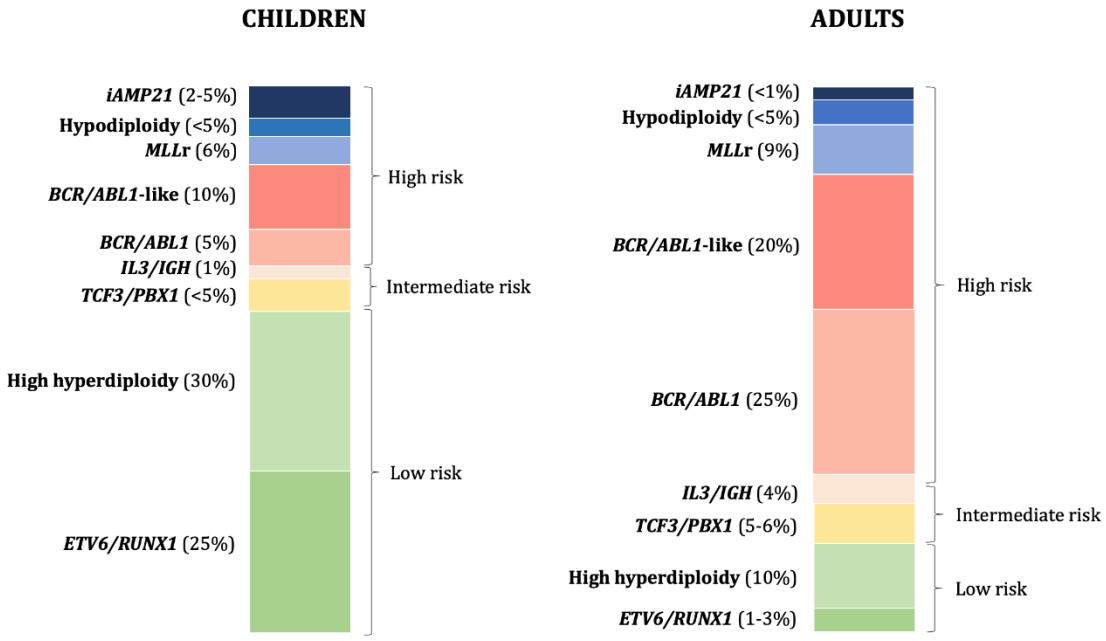

Figure 1. Frequency of primary chromosomal abnormalities in children and adults with B-ALL.

The determination of the different clinical and biological factors at diagnosis is thus essential in patients risk stratification, which has a direct impact on therapy decision-making.

1.4 Treatment

Current protocols for the treatment of ALL are based on the determination of the most appropriate therapeutic option according to the risk group to which the patient belongs. These protocols also differentiate between children and adults. In Spain the pediatric protocol is defined by the Spanish Society of Pediatric Hematology and Oncology (SEHOP), while the adult protocol is established by the Spanish program in Hematology Treatment (PETHEMA). In these protocols, genetics plays a key role in therapy decision-making. In the latest version of the PETHEMA protocol for adults with Philadelphia chromosome-negative, factors such as positive MRD (≥0.01%) and the presence of unfavorable genetics are key in the treatment algorithm decision. Hypodiploidy (<40 chromosomes), *MLL* rearrangements, deletions/mutations of *TP53* in homozygosity, concomitant deletions of *IKZF1* and *CDKN2A/B* in B-ALL, and non-mutated *NOTCH1/FBXW7* or mutated *RAS/PTEN* in T-ALL are considered to be unfavorable genetic markers in this protocol.

Current treatment regimens significantly improve the survival of ALL patients, being these changes especially evident in children with a modest effect in adults. It is therefore not surprising

that current adult protocols seek inspiration from pediatric treatments [66]. These protocols follow mainly two strategies, chemotherapy and allogeneic hematopoietic stem cell transplantation (allo-HSCT).

The chemotherapeutic regimen is divided into three phases. The first one is the induction of remission which aims to achieve complete remission by restoring normal hematopoiesis. During this phase the combination of glucocorticoids, vincristine, L-asparaginase and anthracyclines is generally used. Later, an intensification or consolidation phase (six months to a year), in which the use of glucocorticoids, vincristine, high doses of methotrexate (MTX), cytarabine (cytosine arabinoside, ara-C) and asparaginase are included. Finally, the maintenance phase, which is mainly based on the combination of drugs used during the previous phases administered for 2-3 years, and also incorporates the use of mercaptopurines (6-MP) (Figure 2). Most of these drugs are based on the induction of apoptosis by the arrest of the cell cycle, the inhibition of DNA synthesis or expression of oncogenes.

On the other hand, allo-HSCT has proven to be a very effective treatment to prevent relapses. However, allo-HSCT is a complex therapeutic procedure involving many issues which may potentially influence the results, so its use is reserved for patients with persistent positive MRD or very high-risk groups [67].

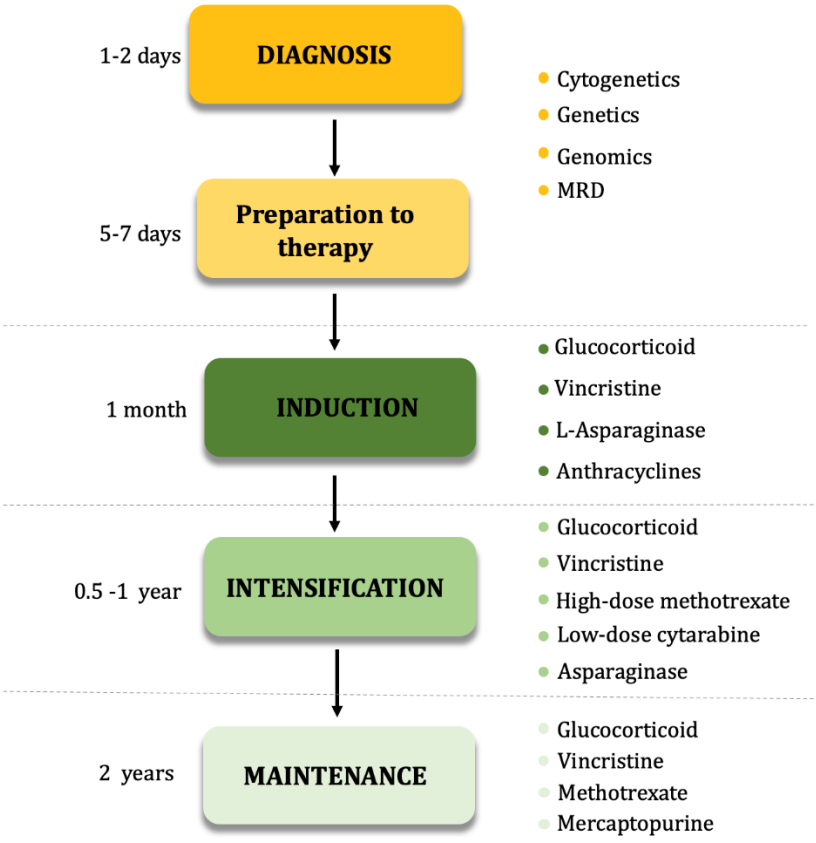

Figure 2. General scheme for the treatment of ALL patients.

One of the main problems with chemotherapy is the side effects. In fact, a high incidence of ALL patients with side effects that may even be permanent sequelae has been demonstrated [68,69]. The most common side effects include hypersensitivity reactions, neuro, cardio and hepatotoxicity, digestive tract and kidney toxicity, as well as myelosuppression and osteonecrosis [70]. Proper stratification of patients can help to decrease overall toxicity, while individual toxicity is often caused by genetic variants in genes responsible for drug metabolism and could be prevented by specific genetic testing.

Advances in new techniques such as next-generation sequencing (NGS) have allowed the detection of multiple mutations and polymorphisms, that are present at the time of diagnosis or that even appear during therapy, which have been strongly associated with treatment resistance and relapse [71,72]. Table 2 shows some of the most important polymorphisms associated with the metabolism of several drugs used in the treatment of ALL, such as those found in metabolizing enzymes (*GSTM1* or *TPMT*) and transporters (*ABCC4*) [73]. Of note, three SNPs have been described in *TPMT* gene, which codes for the enzyme that metabolizes 6-MP, associated with a loss of its catalytic activity [74].

Table 2. Polymorphisms associated with response to drugs. The following table shows some of the main genes in which polymorphisms associated with the response of the following drugs have been identified.

Drug	Genes	Reference
Glucocorticoids	*SMARCB1, ABCB1*	[73,75]
L-asparaginase	*GRIA1, NFATC2, NFATC2, FCHSD1, GALNT10, C5orf3, SLC36A3*	[73,76–78]
Methotrexate	*MTHFR, PDE4B, SLCO1B1, ARID5B, ABCC2, ABCC4, ABCB1*	[70,73,79–84]
Mercaptopurine	*IMPDH1, XDH, ABCC4, SLC28A3, FAM8A6P, HIVEP2, NME1, PAG1, KCNMA1, FRMD4B, CDH12, GNG2, SLC24A3, NUDT15, TPMT, APEX1, ITPA*	[85–93]
Vincristine	*CYP3A4, CYP3A5 and MDR1*	[94]
Cytarabine	*PTPRS, GIT1, C3orf6, SLC25A37, P2RX1, CCDC24*	[95]
Anthracyclines	*CYP1B1*	[96]

The identification of new molecular alterations affecting critical oncogenic pathways in the evolution of ALL has also allowed the emerging development of new drugs, which are combined with "classical" drugs with the aim to improve patient response rates. These novel drugs include kinase inhibitors (*ABL1* kinase inhibitors, aurora kinase inhibitors, janus kinase inhibitors and TKIs), other molecular or signaling inhibitors (proteasome, mammalian target of rapamycin-mTOR, Farnesyltransferase, γ-Secreatase, angiogenesis, apoptosis inducers and chemokine receptor-CXCR4 antagonists), and epigenetic therapy (DNA methyltransferase, histone methyltransferase and histone deacetylase inhibitors) [97,98,107,99–106]. As an example, the incorporation of TKIs during the induction phase in the treatment of the Philadelphia positive subgroup has dramatically improved the outcome of these patients, who previously had a very poor prognosis [58]. The use of TKIs has evolved in recent years, from those considered first-generation such as imatinib, through second-generation such as dasatinib or nilotinib, to the third generation with ponatinib [108–111]. The outcome of patients has gradually improved with the use of the different TKIs, reaching higher event-free and overall survival rates [112].

On the other hand, immunotherapy and cellular therapy have had a great development in the last years. In fact, a large number of clinical trials have been conducted and many are still ongoing. In B-ALL, antibodies against CD19 (blinatumomab), CD20 (rituximab and ofatumumab) and CD22 (epratuzumab, inotuzumab or moxetumomab) have been developed. In addition, the use of chimeric antigen receptor-modified T cells (CAR-T cells) directed against CD19 and CD22 for B-ALL, and against CD38 for T-ALL has shown promising results, having revolutionized the treatment of ALL in both children and adults (Figure 3) [6]. CAR-T cells are genetically engineered T cells that express the antigen-binding domain and produce the activation and proliferation of cytotoxic T cells by binding to T cells [6,113].

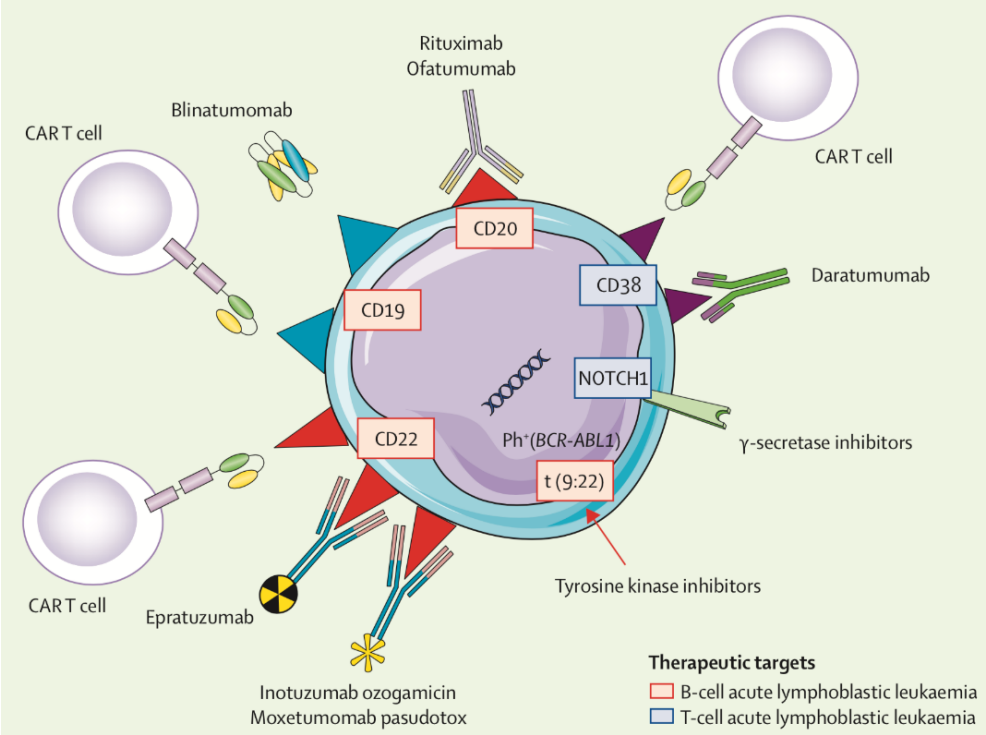

Figure 3. New-targeted therapy for acute lymphoblastic leukemia [6]. The following figure shows different immunotherapies designed against specific markers for the treatment of ALL.

1.5 Relapse and clonal heterogeneity in ALL

Survival rates have increased in recent decades, largely due to current treatment regimens; however, 15-20% of children and 40-50% of adults still relapses [114–117]. Furthermore, the prognosis after relapse is usually very poor, mainly because patients often have a greater resistance to chemotherapy compared to the time of diagnosis [118–120]. This therapeutic resistance is induced by the persistence of a series of genetic alterations as a result of the clonal selection carried out during treatment [121]. The interaction with the microenvironment could play a role to protect leukemia cells from being eliminated by the immune system response and chemotherapeutic agents, and facilitates the development of treatment resistance [122]. Relapse is also present in patients who are considered to have a good prognosis, as carriers of t(12;21), in which a high incidence of late relapses has been observed [123]. Therefore, relapse along with toxicity, is one of the main problems in the clinical management of ALL patients.

The development of high-performance technologies has made it possible to identify a large number of frequent alterations in patients who relapse, including variations in the number of copies (CNVs), mutations and changes in the expression profile. These alterations could underlie the biological processes responsible for drug resistance and the ultimate leukemia relapse. An example of this is the loss of *IKZF1*, which is already considered a strong predictor of relapse, as well as

mutations in *TP53* gene. Both events have been frequently detected in relapsed B-ALL patients and therefore have been associated with a higher relapse rate [39,124–127]. Furthermore, many of these identified alterations have been shown to affect the signaling pathway of drugs, driving resistance and ultimately ALL relapse. An example of this is the somatic deletion and consequently decreased expression of the *MSH6* gene, which has been associated with thiopurine resistance, as well as the suppression of the *BTG1* and *NR3C1* genes, associated with glucocorticoid resistance [128].

However, the clonal basis of the relapse is very heterogeneous and not yet completely clear. Approximately 94% of relapses have their origin in persistent leukemic clones that were already present at the time of diagnosis [129]. This explains why common alterations have been found between the relapse clone and the major leukemic clone at diagnosis. In addition, novel alterations may appear in the relapse clone, suggesting that they come from a minor subclone already present at diagnosis and that undergo clonal evolution, or that they are newly acquired during the clinical course of the disease. On the other hand, only 6% of the clones at relapse have been observed to be genetically distinct from those at diagnosis, representing the development of a second "de novo" leukemia instead of being a real relapse (Figure 4) [24,130,131].

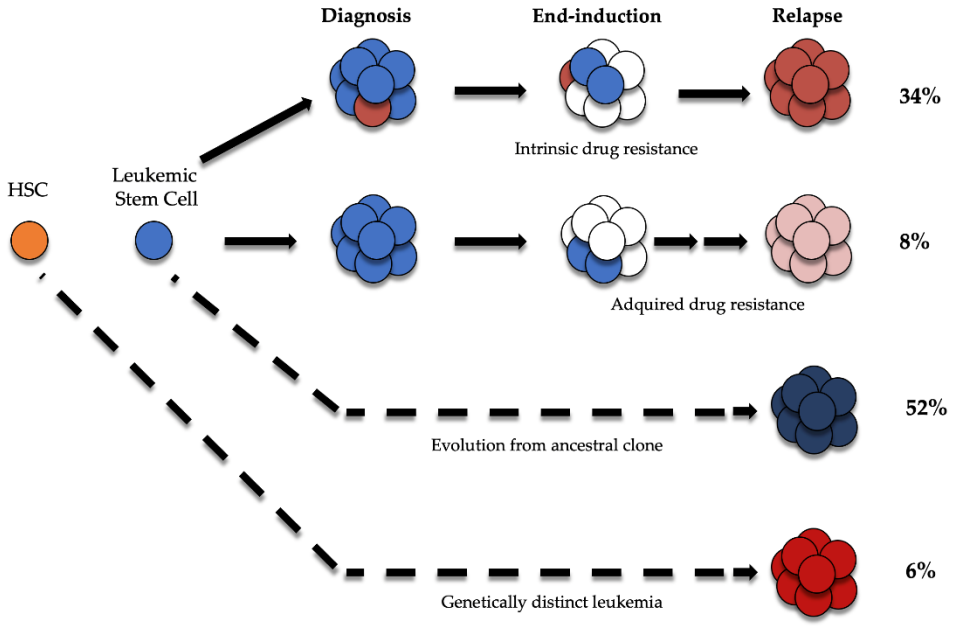

Figure 4. Clonal evolution of relapsed leukemia. 94% of relapsed clones exhibit a clear relationship to the clone seen at diagnosis. Intrinsically drug resistant clones can exist at low levels at diagnosis and survive treatment while other times, the drug resistance may be acquired. The majority of cases reveal a relapsed clone that has directly evolved from the leukemic stem cell. Rarely, the clone seen at relapse is genetically distinct from that at diagnosis and represents a new leukemia. Adapted from Pierro et al. [129].

In summary, relapse of ALL is a complex process and, although many efforts have been made to characterize the genomic landscape of relapses, much remains to be discovered and learned. The integrated use of genetic platforms, as well as the development of functional studies, will be essential for the identification of potential targets or biomarkers of resistance and relapse.

2. GENETICS OF ACUTE LYMPHOBLASTIC LEUKEMIA

The "gold standards" for determining genetic analysis in the clinical practice are still the conventional cytogenetic techniques that include karyotype and FISH for numerical/structural changes. Furthermore, other techniques are also routinely implemented in the clinic such as: I) arrays technologies; II) Multiplex Ligation-dependent Probe Amplification (MLPA) assay, both to assess smaller CNVs and large losses/gains; III) qPCR for transcript and MRD determination; as well as IV) Sanger sequencing for the evaluation of specific genetic variants.

The development of array-based comparative genomic hybridization (aCGH) allowed to analyze the presence of CNVs that were not usually detected by conventional techniques, increasing notably the detection resolution [132]. Arrays technology is based on the competitive co-hybridization between the differentially labeled test (e.g., tumor) and the diploid control DNA in an array platform, which allows the detection of imbalances caused by a higher or lower proportion of DNA in the tumor sample compared to the reference [133]. The incorporation of Single nucleotide polymorphism arrays (SNPa) also allowed the detection of loss of heterozygosity or copy neutral uniparental disomy, which are often involved in the development of cancers [134].

On the other hand, MLPA has also been used in research studies to identify clinically relevant CNVs profiles. This technique is based on a multiplexed PCR using up to 40 probes, each directed at a specific region, to evaluate the relative number of copies of each DNA sequence [135]. Although some studies have shown a high level of concordance between CNVs detection by aSNPs and MLPA, the latter is limited to the number of genes interrogated [136].

Taken together, the application of arrays and MLPA to the study of B-ALL allowed the identification of numerous alterations affecting genes involved in normal B cell development and they have positioned themselves as powerful tools that help during the diagnostic process of patients [137,138]. However, one of the limitations of the use of these tools is that it is necessary to integrate all these methodologies together to obtain a complete molecular analysis of ALL patients, which is actually tedious and time-consuming [139–141]. In addition, these techniques have great limitations themselves, regarding they show some difficulties in detecting some specific alterations. For

example, karyotype analysis has shown to have a wide margin of error due to, in many cases, the lack of metaphases to analyze [142]. The use of high-throughput techniques such as NGS, however, have proven to be a valuable tool with which identify the genomic alterations for the purposes of diagnosis, risk determination and treatment selection in B-ALL, even increasing the detection sensitivity. The following table shows a summary of the main techniques available for the detection of the main genetic alterations and polymorphisms associated with B-ALL patients (Table 3).

Table 3. Available techniques for the detection of the main genetic alterations and polymorphisms associated with B-ALL patients.

Tech.	Type					Limitations
	Rearr.	CNVs	Aneuploidies	Targeted mutation	SNPs	
Karyotype	X		X			High error rate due to lack of metaphases and problems in hypodiploid detection.
FISH	X	X				Only balance rearrangements and cannot detect small rearrangements (e.g., deletions <100 kb or duplications >500 kb). Limited number of targets.
aCGH	X	X	X			Only unbalanced translocations. Cannot detect copy neutral loss of heterozygosity. Low throughput.
aSNP	X	X		X	X	Cannot detect small rearrangements (e.g., deletions or duplications <100 kb). Low throughput.
MLPA		X		X	X	Limited number of targets and throughput. Only INDELs. Cannot detect copy neutral loss of heterozygosity.
qPCR	X	X				Limited number of targets. Test optimization and efficiency is a concern.
Sanger				X	X	Small DNA fragments (300-1000 bp). Limited number of targets and throughput.
NGS	X	X	X	X	X	Sophisticated bioinformatics systems, fast data processing and large data storage capabilities

Technique (Tech). Rearrangements (Rearr.)

2.1 High throughput sequencing in the study of B-ALL

The automated Sanger method has been the most used sequencing method for more than two decades since it was first commercialized in 1986. However, in the last few years, due to the higher levels of coverage provided by NGS techniques, new mutations in genes involved in hematological malignancies, specifically in B-ALL have been identified. The most widely used is Illumina's

technology, which is based on a technique known as "bridge amplification", in which a solid support containing small sequences of oligonucleotides is used. These sequences are homologous to those of the adapters that are attached to the ends of the DNA to be sequenced. Once the DNA is attached to the solid carrier, the adapters also serve as substrates for the amplification synthesis reaction to take place repeatedly (Figure 5).

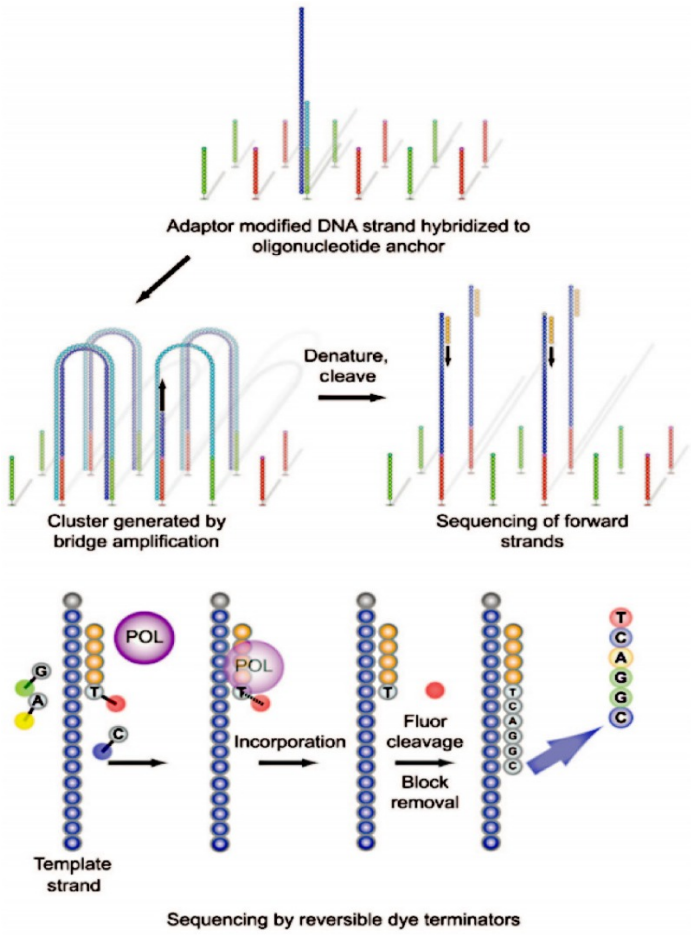

Figure 5. Illumina sequencing by synthesis. Adapter-modified, single-stranded DNA is added to the flow cell and immobilized by hybridization. Bridge amplification generates clonally amplified clusters. Clusters are denatured and cleaved; sequencing is initiated with addition of primer, polymerase (POL) and 4 reversible dye terminators. Post incorporation fluorescence is recorded. The fluor and block are removed before the next synthesis cycle [143].

The application of NSG to the study of B-ALL allowing the identification of a large number of mutations in genes involved in the pathogenesis of the disease. This technology allows the performance of whole genome sequencing (WGS); whole exome sequencing (WES), used for point mutation investigation and target gene sequencing, for the study of specific regions [144].

NGS can follow several enrichment methods, the most commonly used being amplicon-based target enrichment and capture-based target enrichment. The first uses specific probes for

enrichment, while the second requires a PCR reaction. In this thesis, the amplicon-based deep sequencing workflow was followed using Illumina and/or Roche/454 FLX platform (Results: Chapter I & II). Roche platform is based on "pyrosequencing" in which the incorporation of nucleotides complementary to the template strand triggers an enzymatic cascade, which in turn produces a chemiluminescent signal [145]. The second type of NGS strategy involves capture hybridization-based sequencing and was applied in the last part of this thesis (Results: Chapter I). Targeted capture sequencing is less error-prone and a more homogeneous coverage is obtained [146].

The application of targeted panels has managed to identify particularly relevant genes associated with poor prognosis such as mutations in *TP53* and *JAK2* [126]. Many of these studies focus on the study of samples from children and adults separately. While mutations in genes of the RAS pathway, such as *KRAS*, *NRAS* and *FLT3*, have been frequently reported in children, mutations in the *FAT1*, *SF1*, *CRLF2*, *TET2* and *PTPN11* genes are more frequent in adults [147].

Targeted NGS panels are starting to be used in the clinical practice in the study of diseases such as immune deficiencies and several forms of inherited cancer and are being implemented over the others mainly due to costs reduction and simplicity of analysis [148–152]. Several panels have been developed and used for the study of cancer such us the Oncomine™ Childhood Cancer Research Assay from Ion Torrent. However, these panels are very general and do not include alterations specific to B-ALL. In addition, targeted panels designed for the study of ALL generally require the use of RNA, which is much less stable than DNA and therefore much more laborious for its use in the clinical practice.

The use of WES and WGS in B-ALL patients, has allowed, on the other hand, the study of a greater number of genes and with it the most complete study of the different biological pathways. WES studies, on the one hand, showed how the PI3K-RAS pathway was altered in up to 47% of B-ALL patients. In children, it was shown that the most common alterations affect B-cell development (49.4%), TFs (45.8%), tumor suppressor genes (32.7%), cytoplasmic transport (27.3%), and RAS signaling (26.7%). According to other studies, mutations in *NRAS*, *KRAS*, *FLT3*, *PAX5* and *CREBBP* were the most frequent in these patients. Furthermore, these mutations are clustered into eleven pathways (Ras, JAK/STAT, epigenetics, matrix, cytoplasmic transport, receptor, B-cell development, tumour suppressor, channel and others) [153]. The application of WES in diagnostic samples and relapse also reported that mutations in *CREBBP* with mutations in *KRAS*, suggesting that both could be leading cells to relapse [154].

The integration of WGS also allowed defining alterations in the RTK-RAS pathway and histone modifiers in high-hyperdiploid patients [155]. In patients with *MLL* rearrangements, the presence of mutations in the PI3K-RAS pathway was also identified, as well as epigenetic mutations. The use of

WES and WGS also allowed the identification of two subtypes of hypodiploid patients. The near haploid cases (24-31 chromosomes) had alterations directed to the tyrosine kinase receptor, RAS signaling and *IKZF3*, while the low hypodiploid ALL (32-39 chromosomes) had alterations in *TP53*, *IKZF2* and *RB1* [156].

RNA sequencing (RNA-seq) has also become an almost essential tool at the molecular biology laboratory level, especially for the analysis of differential gene expression. This methodology shares the same rationale as DNA sequencing, except that the enrichment takes place at the mRNA level and the synthesis of the cDNA needs to be carried out [157]. Thanks to lower costs, RNA-seq is now the method of choice for expression studies, thus prevailing over conventional microarray methods. Using RNA-seq it is possible to directly determine gene identity and exon-content/usage, which is crucial for the identification of new transcripts and analysis of unknown genes [158]. The application of RNA-seq is of special interest in the study of B-ALL due to the recurrence of gene rearrangements in these patients [159]. The increased sensitivity of NGS in comparison to other sequencing techniques has also allowed the detection of undetected alterations such as *MLL*r partner genes [160].

The integration of transcriptomic analysis into the study of the B-ALL has allowed the identification of new entities through the detection of new fusion genes and gene expression signatures. The best example of this is the Ph-like subgroup, which is now considered as a new provisional entity by the most recent WHO classification [27]. One of the main limitations of RNA-seq is the complexity of the analysis, since it is necessary to process a very large data set that cannot be interpreted without an extensive analysis [161].

NGS studies have thus been more focused on the development of new exploratory studies and were therefore more focused on the area of research. Nevertheless, the use of NGS in the clinical practice is becoming increasingly widespread thanks to the development of new methodologies that have made it possible to substantially reduce costs and turnaround time, as well as to simplify the analysis of results. In fact, the incorporation of NGS into the clinic has already proven to be a powerful tool for the study of hematological malignancies, including B-ALL. In particular, NGS has been proposed for the detection of MRD due to the increased sensitivity compared to conventionally employed techniques [162,163]. The use of NGS has been shown to achieve a sensitivity of 10^{-4}, similar to that achieved by the use of flow cytometry, the gold standard so far along with quantitative PCR for the detection of MRD [163,164]. Furthermore, the NGS has already been tested for the genetic characterization of patients. Specifically, the St. Jude Children's Research Hospital group integrated the use of RNA-seq into clinical practice along with the routine techniques used in diagnosis. They

demonstrated that it was a very valuable tool with which to identify therapeutic targets for precision personalized medicine, especially in the high-risk patient group [165].

2.2 Genetic events associated with B-ALL patients

The integration of results of several techniques, i.e. gene expression profiling, aSNP analysis, and currently NGS, have permitted a better definition of the molecular landscape of ALL and the identification of a constellation of novel mutations. These mutations affect key pathways in the development of ALL such as lymphoid cell differentiation and development (e.g., *PAX5*, *IKZF1*, *EBF1*), *JAK/STAT* signaling (e.g., *JAK1*, *JAK2*, *IL7R*, *CRLF2*), *RAS* signaling (e.g., *NRAS*, *KRAS*, *PTPN11*, *FLT3*, *NF1*), cell cycle regulation and tumor suppression (e.g., *TP53*, *RB1*, *CDKN2A/B*), Wnt/β-catenin signaling (e.g., *Wnt*, *FAT1*), *NOTCH* signaling pathway (e.g., *NOTCH1*, *NOTCH2*, *NOTCH3*, *FBXW7*, *HES1*, *JAG1*, *JAG2*), chromatin structure modifiers and epigenetic regulators (e.g., *PHF6*, *EZH2*, *DNMT3A*), and non-canonical pathways or other/unknown genes (e.g., *CREBBP*, *NT5C2*, *TBL1XR1*) [16,17]. Figure 6 shows the pathways as well as the significantly mutated genes in ALL patients. A revision is included in Supplementary Appendix (Annex IV) which lists the main altered pathways in ALL identified by NGS [166].

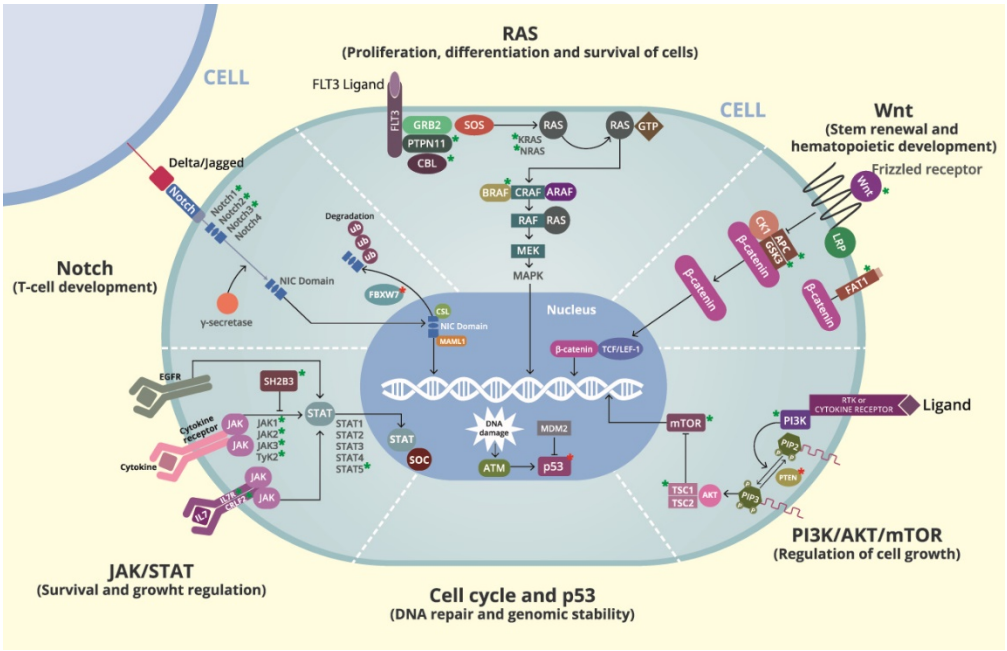

Figure 6. Cellular pathways affected by genes significantly mutated in ALL. Asterisks show the genes that are mutated in each cellular program and the biological effect of these mutations on the pathway (Green: activation mutation; Red: inactivating mutation).

These alterations help to identify new therapeutic targets and establish new prognostic markers, which is especially interesting for patients without defined genetic alterations. However,

recurrent alterations have also been detected in different already established genetic subtypes, which could be considered as risk factors in the future, helping to refine the stratification of these patients. For example, recurrent mutations in *IKZF3* and *FLT3* genes were identified in patients with near-haploidy and *TP53* mutations in those with low hypodiploidy [167]. Mutations in the *RAS* pathway were frequently detected in patients with high hyperdiploidy [155]. Mutations in the *RAS* pathway accompanied by mutations in the *PI3K* pathway were also frequently observed in patients with *MLL* rearrangement [168]. In patients with *TCF3/HLF* fusion gene, frequent loss of *PAX5*, *VPREB1* and mutations in the non-translocated *TCF3* allele were observed [169]. Furthermore, B-other patients showed a large number of mutations and CNVs [170].

In addition to somatic mutations, recurrent CNVs involved in pathways associated with B- ALL pathogenesis have been reported among different genetic subgroups through the development of genome-wide analysis. These include the genes involved in B-cell development (e.g. *IKZF1*, *EBF1*, *PAX5*, *ETV6*), cell cycle and proliferation (e.g. *CDKN2A*, *CDKN2B*, *RB1*, *BTG1*), and cytokine receptors (e.g. *CRLF2*) [137,171].

The loss of *IKZF1* has been established as a powerful and independent marker of poor prognosis in B-ALL [39,172]. This can be a full or a partial loss, but the most commonly observed types are the loss of exons 4 to 7 (Δ4-7), exons 2 to 7 (Δ2-7) and 4 to 8 (Δ4-8) [173]. *IKZF1* deletions have been observed in approximately 15% of children and 40% of adult patients with B-ALL [174–176]. This higher proportion seen in adults is due to the fact that this alteration occurs very frequently in Philadelphia positive (~ 80%) and Ph-like patients (~ 70%), both enriched in the adult population [39,177,178]. The presence of *IKZF1* deletion has also been associated with a poor response to treatment in high-risk patients, especially, with an increased resistance to glucocorticoids [57,179,180]. *IKZF1* deletions have also been associated with a worse response to treatment in Ph-negative patients [181,182]. The loss of *IKZF1* has also been strongly associated with the loss of other genes such as *PAX5*, *EBF1* and *BTG1*, as well as the presence of *CRLF2* rearrangements. This suggests a cooperative effect of these lesions on leukemogenesis [173].

Recurrent loss of Early B-cell factor 1 (*EBF1*) and *PAX5*, both essential factors for proper lymphoid development, has been reported. The loss of *EBF1* is very rare, although it usually appears in a higher percentage in patients with relapse (~25%), which justifies its strong association with a lower RFS [183,184]. *PAX5*, instead, is altered in approximately 30% of B-ALL patients, either through deletions, rearrangements or specific mutations. Loss of *PAX5* has not been associated with poor prognosis, but rather with improved sensitivity to glucocorticoids [185].

Another recurrent CNV is the loss of the *ETV6* gene, especially enriched in the subgroup of *ETV6/RUNX1* positive patients (~70%). The loss of this gene has not been associated with a particular prognosis [185].

CDKN2A and *CDKN2B* are two tumor suppressor genes and their loss has shown to be an important prognostic marker [186]. Both are found consecutively on the short arm of chromosome 9, a region that is recurrently lost in B-ALL patients. Therefore, the loss of one usually leads to the loss of the other. The same occurs with *PAX5*, also in the 9p arm, which explains the high co-occurrence between the loss of these three genes [187].

RB1 gene is a cell cycle regulator, the loss of which has been reported in ~7% of patients. The loss of this gene seems to be associated with a worse response to treatment, although its true prognostic value is not entirely clear. The loss of *RB1* in almost half of the cases is associated with the loss of the q-arm of chromosome 13 [185,187].

The B-cell translocation gene 1 (*BTG1*) has a role in several crucial cellular processes, such as proliferation and apoptosis. Its loss has been associated with a deficient response to glucocorticoids [188]. *BTG1* loss has been observed in about 8% of B-ALL patients, although with a much higher incidence in patients with Down syndrome [189].

Overexpression of the *CRFL2* gene has also been reported on a recurring basis, mainly due to the presence of some point mutations or its rearrangement with *P2RY8* or *IGH@* gene. Specifically, gene fusion between *CRLF2/P2RY8* is caused by the loss of a region known as pseudoautosomal region 1 (PAR1). This region includes the genes located between *CRLF2* and *P2RY8*, so, when it is lost, *CRLF2* is placed under the control of the *P2RY8* promoter which activates it constitutively [190]. *CRFL2* overexpression has also been associated with an unfavorable prognosis, although this is probably due to the high frequency of these alterations detected in the poor prognostic group, Ph-like patients [170,177].

Taken altogether, the detection of these alterations generates great interest in the management of B-ALL patients, but especially in the Ph-like positive subgroup. The diagnosis of these patients is often determined by the gene expression profile, although it is still a challenge due to the lack of a recurrent genetic alteration that allows their unequivocal identification. However, a genetic signature specific to these patients has been established, characterized by *CRFL2* rearrangements, alterations in the *JAK/STAT* pathway (including mutations and rearrangements), ABL-class fusions, *RAS/MAPK* pathway alteration, as well as the recurrent loss of *IKZF1*, *PAX5*, *EBF1* and *BTG1* genes [137,191–193]. Therefore, the detection of these recurrent alterations could help in the identification of this subgroup of patients.

The integration of transcriptomic analyses also allowed the identification of new additional minority subgroups (<10% of ALL patients) such as those with *DUX4, ZNF384* and *NUMT1* rearrangements or the *ETV6/RUNX1*-like subgroup [174,194–200]. Interestingly, the St. Jude Children's Research group identified two new subgroups of B-ALL through the expression profile, one of them being characterized by alterations in *PAX5* (rearrangements, amplifications or intragenic mutations) and the other one by the p.Pro80Arg (P80R) point mutation in *PAX5* [201].

On the other hand, with the development of pharmacogenetics and pharmacogenomics, associations between different genetic alterations and response to treatment have been established [191,192]. In fact, numerous polymorphisms and mutations have been associated with the response to drugs, both being related to susceptibility and resistance, especially in those genes that mediate drug transport and metabolism. In addition to the examples mentioned above, it is worth noting the *ABL1* mutations, which have been shown to generate resistance to TKI, or the activating mutations of the *NT5C2* gene, which are associated with a high risk of relapse by decreasing the effectiveness of mercaptopurines. Particularly, this gene encodes an enzyme that makes the drug inactive [202,203]. In most cases, no response to treatments results in the ultimate relapse of the disease. In this way, a greater approach to personalized medicine has been achieved, which main aim is to select and, therefore, offer the best therapeutic option based on the genetic profile of patients.

Many of the alterations identified by the application of the NGS studies in ALL have also been established as promising therapeutic targets. For example, alterations in the RAS/MAPK pathway, which has been associated with resistance to chemotherapy and poor outcome, could be considered a therapeutic target, as many compounds have been developed and used to inhibit molecules downstream this pathway (MEK inhibitors) [204]. Drugs such as trametinib, selumetinib, and cobimetinib have already been designed for this purpose, although none of them have yet been tested for ALL patients [205]. Drugs targeting the JAK/STAT pathway, such as ruxolitinib, are already being tested on ALL patients harboring alterations in this pathway [206]. Specifically, the COG AALL1521 phase 2 trial is currently investigating the safety and efficacy of the combination of ruxolitinib with post-induction chemotherapy in children, adolescents and young adults with high-risk ALL (NCT02723994). In addition, possible tailored treatment strategies for patients with *CRLF2* rearrangement have been identified such as USP9X inhibitors, the histone deacetylase inhibitor "givinostat", anti-TSLPR/CRLF2 antibodies and cell immunotherapy with TSLPR-directed CAR T-cells [207–209]. Conversely, *IKZF1* gene alterations, which are mainly associated with high-risk patients, have not yet been proved to be a potential therapeutic target. However, preclinical studies have demonstrated the efficacy of retinoic acid and FAK inhibitors in ALL models with *IKZF1* deletion [210,211].

Therefore, B-ALL is a very heterogeneous disease at the biological level with a large number of recurrent genetic alterations that can help in the risk stratification and clinical management of patients. The following table shows an overview of the main genetic alterations identified in B-ALL patients, including genomic rearrangements, CNVs, aneuploidies and alterations in potentially targetable genes and cellular pathways, as well as their association with the different biological groups established by the WHO classification and their associated prognostic value (Table 4).

Table 4. Main genetic alterations associated to B-ALL patients. In the first column the type of alteration, followed by the genetic alteration, the genetic subtype of the WHO with which it is associated, the prognosis with which it has been related and finally the references.

Type	Alteration	WHO 2016	Prognosis	Reference
Rearrangements	*ETV6/RUNX1*	*ETV6/RUNX1*	Favorable	[52]
	BCR/ABL1	Philadelphia	Poor (improved with tyrosine kinase inhibitors)	[54]
	MLLr	*MLLr*	Very poor	[55]
	TCF3/PBX1	*TCF3/PBX1*	Intermediate	[59]
	CRFL2r	Ph-like	Poor	[212]
	ABL-class tyrosine kinase genes			
	JAK2			
	EPOR			
	TCF3/HLF	B-Other	Poor	[213]
	DUX4		Favorable	[184]
	MEF2D		Poor	[214]
	ZNF384		Intermediate	[215]
	NUMT1		Favorable	[216]
	PAX5		Intermediate to poor	[201]
CNVs	*IKZF1*	Ph, Ph-like and B-Others	Poor	[39,178,217]
	CDKN2A/B	Ph-like	Poor	[186,212]
	PAX5	Ph-like, Ph and *TCF3/PBX1*	Uncertain	[137,218]
	BTG1	-	Poor	[188]
	ETV6	*ETV6/RUNX1*	Unclear	[185]
	EBF1	Ph	Poor	[184]

	VPREB1	*ETV6-RUNX1*, Ph and Ph-like	Poor	[219]
	RB1	iAMP21	Unclear	[185,220]
	ERG	B-Other	Favorable	[184]
	SH2B3	iAMP21	Undefined	[220]
	iAMP21	iAMP21	Poor	[221]
Aneuploid	High hyperdiploid	Hyperdiploid	Favorable	[51]
	High hypodiploid	Hypodiploid	Poor	[53,222]
	Low hypodiploid			
	Near-haploid			
Targeted mutation targets for targeting therapy	*PAX5* P80R	B-Other	Unclear	[201]
	TP53	Hypodiploid	Poor	[126,156,167]
	JAK/STAT	Ph-like	-	[223]
	PI3K/AKT/mTOR	Hypodiploid, Ph-like	-	[156,223]
	ABL	Ph, Ph-like	Poor (treatment resistance)	[223,224]
	FLT3	*MLL*r, hyperdiploid	-	[225,226]
	RAS	Hypodiploid, Ph-like	-	[156]

Nevertheless, more studies are required to establish the true prognostic value of many of these alterations.

3. FUNCTIONAL STUDIES

With the development of NGS techniques, a big need arose to interpret at functional level, by using both *in vitro* and *in vivo* models, the large number of new alterations identified. These models may allow us to elucidate the mechanisms of action of the different alterations, to establish which pathways could be affected and, therefore, to identify novel targets and design new drugs. In addition, functional studies allow us to evaluate the effect of new or already established drugs in the presence or absence of these alterations.

3.1 Genome editing systems in the study of B-ALL

Genetic editing systems are mainly based on the generation of DNA double-stranded breaks (DSB) through directed nucleases that stimulate the activation of DNA's intrinsic repair mechanisms.

The repair mechanisms, which include homologous recombination (HR) and non-homologous end-joining (NHEJ), induced alterations at the breaking point [227]. These alterations can be directed if HR is stimulated by the use of a donor template, or the breakage can be corrected by NHEJ, which is prone to errors, generating deletions and/or insertions that change the reading frame and that, in most cases, a knock-out is generated [228,229].

Genetic editing systems have evolved over the years. Zinc-finger nucleases (ZNFs) and transcription activator-like effector nucleases (TALENs) were the first systems to appear, although they were quickly replaced by another faster, simpler and cheaper system called "short palindromic repeats interspersed with regular intervals" or commonly known as CRISPR system (Figure 7) [230]. This system is based on the use of nucleases, being Cas9 the most commonly used nuclease, which is guided by a 20-nucleotide single-stranded RNA molecule to produce the desired targeted cut on the DNA [231].

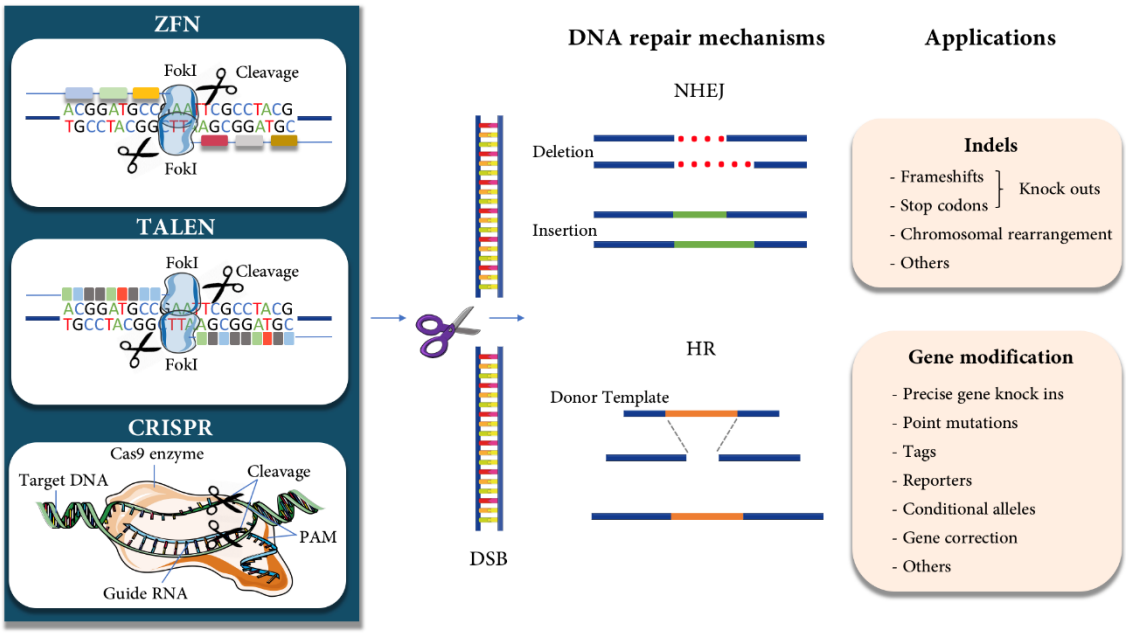

Figure 7. The nuclease genome editing technologies. The three most commonly used types of nucleases include programmable nucleases like Zinc Finger Nucleases (ZFNs), transcription activator-like effector nucleases (TALENs) and CRISPR systems (Clustered Regularly Interspaced Short Palindromic Repeats). These nucleases were able to induce double-strand breaks (DSBs) in the target followed by the activation of DNA repair mechanisms. On induction of double-stranded breaks or nicks at targeted regions, repairing is done by either Non-homologous end joining (NHEJ) or Homologous recombination (HR) pathway. NHEJ is an error prone repair mechanism where joining of broken ends takes place, which generally results in heterogeneous indels (insertions and deletions) whereas HR is a precise repair method in which homologous donor template DNA is being used in repair DNA damage target site. HR is the ideal strategy for generating knock in models [232].

CRISPR/Cas9 systems have been used in the study of several hematological malignancies, including ALL. Most of these studies were focused on the generation of knock-out models in order to elucidate the functional effect of transcription factors (e.g. *IZKF1*, *PAX5*); fusion genes (e.g. *MLL/AF4*, *ETV6/RUNX1*) or possible therapeutic targets among others. Interestingly, the use of genome editing

systems in the study of B-ALL has made it possible to clarify the role of these alterations, not only in the evolution of the disease, but also in its development. For example, the British's group conducted a study in which they produced an ETV6/RUNX1 Knock-in model, demonstrating that the expression of this fusion gene resulted in the induction of a partial block of the maturation of B lymphocytes. During the maturation block, the second events necessary for the development of leukemia occur [233]. On the other hand, these CRISPR/Cas9 systems // genome editing systems also play a key role in the process of developing new therapies, especially during the generation of CAR-T cells-based immunotherapy. This was demonstrated by the study carried out by Michel Sadelain's group, in which they used the CRISPR/Cas9 system to improve the therapeutic potential of these CAR-T cells [234]. A more extensive review of the main genetic editing studies carried out in ALL is included in the Supplementary Appendix (Annex V) at the end of this thesis [232]

HYPOTHESIS

B-Acute lymphoblastic leukemia patients are characterized by a great biological heterogeneity that has a big impact on the clinical course of the disease. The presence of a series of recurrent alterations is the basis of the current classification systems, which have also become powerful prognostic markers. In this way, we can predict the clinical outcome of patients based on the genetic alterations they present. Therefore, it is important to correctly and quickly detect these alterations in the diagnostic process of these patients. A non-correct stratification could lead to an inappropriate treatment selection, wrong dosage and, consequently, problems of refractoriness as well as treatment toxicity.

The recent development of omic techniques, such as next generation sequencing and arrays, have allowed the study of a large number of genetic alterations with great sensitivity and precision. Their application in the study of B-ALL has thus made it possible to identify a series of new recurrent alterations that are often also correlated with clinical outcomes such as reduced survival, increased relapse rates or treatment toxicities. These alterations include a wide spectrum of genetic events such as mutations, CNVs and translocations. Most of these alterations are not yet taken into account in the clinical practice. However, these biomarkers could be established as new prognostic markers in the near future. Thus, the integrative study of the wide spectrum of genetic alterations present in B-ALL could help to establish novel and better prognostic markers to be applied in the clinical practice for the risk stratification of patients and to identify predictive and prognostic markers of the response to treatment. Consequently, we could achieve a reduction in relapse rates, one of the main problems in the clinical management of ALL patients.

The integration of NGS in the clinical practice could make it possible to detect, in one single assay, the main B-ALL risk-associated alterations, thus becoming a powerful tool for the diagnosis of these patients. Therefore, the design of a comprehensive targeted gene-panel that simultaneously may detect the main alterations present in B-ALL, in addition to the cooperating abnormalities that have some impact on patients clinical course, could be of great interest and very useful to improve ALL risk stratification, classification and in therapy decision making.

The relapse of ALL is characterized by a great clonal heterogeneity, composed by a wide number of alterations that could be driving the relapse process. The integrated use of different genomic techniques can be useful to assess the genetic landscape of relapsed patients and thus determine factors that could predict the risk of relapse.

Functional studies, by using *in vitro* and *in vitro* models, are also of crucial importance in determining the possible biological effect (mechanisms of action) of either the presence or absence of the different genetic alterations, as well as to assess them as potential therapeutic targets by drug testing analyses. The t(12;21), the most frequent translocation in pediatric B-ALL. The role of the

fusion gene in the development of leukemia has been well established, determining that it is not capable of initiating the disease by itself. In this sense, the role of *ETV6/RUNX1* is controversial. While some studies suggested that the fusion gene acts exclusively in the early stages of the disease, others claim that he also plays a key role in maintaining the leukemia. Thus, an *ETV6/RUNX1* knock-out model could help demonstrate that the fusion protein is key to maintain the oncogenic potential of tumor cells, making it a possible therapeutic target that potentially could reduce the relapse rate in these patients.

In summary, I guess the combination of the new omic technologies and CRISPR will help us to elucidate the genetic abnormalities in B-ALL at both diagnosis and progression. Moreover, the use of CRISPR will provide new insights in the knowledge of the molecular mechanisms of the translocations involved in B-ALL as well as will open new avenues in the disease management.

AIMS

Specific aims:

I. To design and validate of a comprehensive custom NGS panel for the detection of the main B-ALL risk associated genetic alterations at diagnosis.

II. To elucidate the genetic profile driving the relapse of B-ALL patients through the integrative study of mutations and CNVs by NGS, MLPA and aCGH.

III. To evaluate the role of *ETV6/RUNX1* fusion gene in the maintenance of the leukemic phenotype by generation of an *in vitro* and xenograft models.

RESULTS

This section includes the experimental work performed on this thesis, including Material and Methods, Results and Discussion. This section has been divided into three chapters:

Chapter I: Adrián Montaño, Jesús Hernández-Sánchez, Maribel Forero-Castro, María Matorra-Miguel, Eva Lumbreras, Cristina Miguel, Sandra Santos, Valentina Ramírez, Jose Luís Fuster, Natalia de Las Heras, Alfonso García-de Coca, Magdalena Sierra, Julio Dávila, Ignacio de la Fuente, Carmen Olivier, Juan Olazabal, Joaquín Martínez, Nerea Vega-González, Teresa González, Jesús María Hernández-Rivas, Rocío Benito. *Comprehensive custom NGS panel validation for the improvement of the stratification of B-Acute Lymphoblastic Leukemia patients.* J. Pers. Med. 2020, 10, 0137; doi:10.3390/jpm10030137.

Chapter II: Maribel Forero-Castro*, Adrián Montaño*, Cristina Robledo, Alfonso García de Coca, José Luis Fuster, Natalia de las Heras, José Antonio Queizán, María Hernández-Sánchez, Luis A. Corchete-Sánchez, Marta Martín, Jordi Ribera-Salas, Josep-María Ribera, Rocío Benito, Jesús M. Hernández-Rivas. *Integrated genomic analysis of chromosomal alterations and mutations in B-cell acute lymphoblastic leukemia reveals distinct genetic profiles at relapse*. Diagnostics 2020, 10(7), 455. doi:10.3390/diagnostics10070455. **These authors contributed equally to this work.*

Chapter III: Adrián Montaño, Jose Luis Ordoñez, Verónica Alonso-Pérez, Jesús Hernández-Sánchez, Sandra Santos, Teresa González, Rocío Benito, Ignacio García-Tuñón, Jesús María Hernández-Rivas. *ETV6/RUNX1 Fusion Gene Abrogation Decreases the Oncogenicity of Tumour Cells in a Preclinical Model of Acute Lymphoblastic Leukaemia*. Cells 2020, 9(1), 215. doi: 10.3390/cells9010215

Chapter I. Comprehensive custom NGS panel validation for the improvement of the stratification of B-Acute Lymphoblastic Leukemia patients.

Adrián Montaño[1], Jesús Hernández-Sánchez[1], Maribel Forero[2], María Matorra-Miguel[1], Eva Lumbreras[1], Cristina Miguel[1], Sandra Santos[1], Valentina Ramírez-Maldonado[1], Jose Luís Fuster[3], Natalia de Las Heras[4], Alfonso García-de Coca[5], Magdalena Sierra[6], Julio Dávila[7], Ignacio de la Fuente[8], Carmen Olivier[9], Juan Olazabal[10], Joaquín Martínez[11], Nerea Vega-García[12], Teresa González[7], Jesús María Hernández-Rivas*[1,7] Rocío Benito[1].
**Correspondence.*

[1]IBSAL, IBMCC, Universidad de Salamanca, CSIC, Centro de Investigación del Cáncer (CIC), Salamanca, España. [2]Colegio de ciencias biológicas (GICBUPTC grupo de investigación), Universidad pedagógica y tecnológica de Colombia (UPTC), Colombia. [3]Departamento de pediatría oncohematológica- Hospital Universitario Virgen de la Arrixaca, Murcia, España. [4]Departamento de Hematología - Hospital Virgen Blanca, León, España. [5]Departamento de Hematología - Hospital Clínico de Valladolid, Valladolid, España. [6]Complejo Sanitario de Zamora, Zamora, España. [7]Departamento de Hematología - Hospital Universitario de Salamanca, Salamanca, España. [8]Departamento de Hematología - Hospital Rio Hortega, Valladolid, España. [9]Servicio de Hematología y Hemoterapia - Complejo Sanitario de Segovia, Segovia, España. [10]Departamento de Hematología - Hospital Universitario de Burgos, Burgos, España. [11]Departamento de Hematología - Hospital Universitario 12 de Octubre, Madrid, España. [12]Laboratorio de Hematología, Instituto de Investigación, Hospital Sant Joan de Déu, Barcelona, España.

J. Pers. Med. 2020, 10, 0137; doi:10.3390/jpm10030137.

Journal of *Personalized Medicine*

MDPI

Article

Comprehensive Custom NGS Panel Validation for the Improvement of the Stratification of B-Acute Lymphoblastic Leukemia Patients

Adrián Montaño [1], Jesús Hernández-Sánchez [1], Maribel Forero-Castro [2], María Matorra-Miguel [1], Eva Lumbreras [1], Cristina Miguel [1], Sandra Santos [1], Valentina Ramírez-Maldonado [1], José Luís Fuster [3], Natalia de Las Heras [4], Alfonso García-de Coca [5], Magdalena Sierra [6], Julio Dávila [7], Ignacio de la Fuente [8], Carmen Olivier [9], Juan Olazabal [10], Joaquín Martínez [11], Nerea Vega-García [12], Teresa González [7], Jesús María Hernández-Rivas [1,7,*] and Rocío Benito [1,*]

1 IBSAL, IBMCC, Universidad de Salamanca, CSIC, Centro de Investigación del Cáncer (CIC), 37007 Salamanca, Spain; adrianmo18@gmail.com (A.M.); jesus807@gmail.com (J.H.-S.); mariammzamora@gmail.com (M.M.-M.); a21093@usal.es (E.L.); cristinamiguelgarcia@gmail.com (C.M.); sandruskism90@gmail.com (S.S.); vramirem@gmail.com (V.R.-M.)
2 Escuela de Ciencias Biológicas (Grupo de investigación GICBUPTC), Universidad Pedagógica y Tecnológica de Colombia, Tunja 150003, Colombia; maribel.forero@uptc.edu.co
3 Sección de Oncohematología Pediátrica, Hospital Clínico Universitario Virgen de la Arrixaca, Instituto Murciano de Investigación Biosanitaria (IMIB), 30120 Murcia, Spain; josel.fuster@carm.es
4 Departamento de Hematología—Hospital Virgen Blanca, 24008 León, Spain; nherasr@saludcastillayleon.es
5 Departamento de Hematología—Hospital Clínico de Valladolid, 47003 Valladolid, Spain; agarciaco@saludcastillayleon.es
6 Complejo Sanitario de Zamora, 49022 Zamora, Spain; msierrap@saludcastillayleon.es
7 Departamento de Hematología—Hospital Universitario de Salamanca, 37007 Salamanca, Spain; juldaval@hotmail.com (J.D.); teresa.gonzalez.mart@gmail.com (T.G.)
8 Departamento de Hematología—Hospital Rio Hortega, 47012 Valladolid, Spain; ifuentegr@saludcastillayleon.es
9 Servicio de Hematología y Hemoterapia—Complejo Sanitario de Segovia, 40002 Segovia, Spain; colivierco@gmail.com
10 Departamento de Hematología—Hospital Universitario de Burgos, 09006 Burgos, Spain; jolazabal@saludcastillayleon.es
11 Departamento de Hematología—Hospital Universitario 12 de Octubre, 28041 Madrid, Spain; jmarti01@med.ucm.es
12 Laboratorio de Hematología, Instituto de Investigación, Hospital Sant Joan de Déu, 08950 Barcelona, Spain; nvega@fsjd.org
* Correspondence: jmhr@usal.es (J.M.H.-R.); beniroc@usal.es (R.B.)

Received: 18 August 2020; Accepted: 19 September 2020; Published: 21 September 2020

Abstract: Background: B-acute lymphoblastic leukemia (B-ALL) is a hematological neoplasm of the stem lymphoid cell of the B lineage, characterized by the presence of genetic alterations closely related to the course of the disease. The number of alterations identified in these patients grows as studies of the disease progress, but in clinical practice, the conventional techniques frequently used are only capable of detecting the most common alterations. However, techniques, such as next-generation sequencing (NGS), are being implemented to detect a wide spectrum of new alterations that also include point mutations. Methods: In this study, we designed and validated a comprehensive custom NGS panel to detect the main genetic alterations present in the disease in a single step. For this purpose, 75 B-ALL diagnosis samples from patients previously characterized by standard-of-care diagnostic techniques were sequenced. Results: The use of the custom NGS panel allowed the correct detection of the main genetic alterations present in B-ALL patients, including the presence of an aneuploid clone in 14 of the samples and some of the recurrent fusion genes in 35 of the

samples. The panel was also able to successfully detect a number of secondary alterations, such as single nucleotide variants (SNVs) and copy number variations (CNVs) in 66 and 46 of the samples analyzed, respectively, allowing for further refinement of the stratification of patients. The custom NGS panel could also detect alterations with a high level of sensitivity and reproducibility when the findings obtained by NGS were compared with those obtained from other conventional techniques. Conclusions: The use of this custom NGS panel allows us to quickly and efficiently detect the main genetic alterations present in B-ALL patients in a single assay (SNVs and insertions/deletions (INDELs), recurrent fusion genes, CNVs, aneuploidies, and single nucleotide polymorphisms (SNPs) associated with pharmacogenetics). The application of this panel would thus allow us to speed up and simplify the molecular diagnosis of patients, helping patient stratification and management.

Keywords: acute lymphoblastic leukemia; NGS; genetic alterations; diagnosis

1. Introduction

B-acute lymphoblastic leukemia (B-ALL) is a malignancy of hematopoietic stem cells, which originates in the B-line lymphoid and is characterized by the presence of a series of genetic alterations, mainly translocations, which determine the course of the disease. Each alteration is associated with a low, intermediate, or high risk. The current WHO classification system is based on the presence or absence of these genetic alterations, which allows stratification of approximately 80% of children and 75% of adults with B-ALL [1,2]. However, there is still a high percentage of patients, commonly referred to as "B-other" cases, who do not have any of the recurrent genetic alterations and, therefore, cannot be stratified according to risk. There is also great clinical heterogeneity within each of the different prognostic subgroups [3,4].

In the last decade, technical advances in microarray and sequence analysis have allowed the development of multiple comprehensive exploratory studies, through which a number of candidate prognostic markers for ALL risk stratification have been identified and published. These alterations range from point mutations; changes in copy number, which affects key genes in B-ALL development, such as *IKZF1*, *PAX5*, *CDKN2A*, *ETV6*, *BTG1*, and *RB1*; new rearrangements, such as those affecting the *CRLF2* gene [2,5–8]. Some of them have already been considered as biological markers of poor prognosis, especially the loss of *IKZF1* [9]. In addition, a number of polymorphisms and mutations directly associated with the response to treatments have been identified [10–13]. Most of them are not yet considered in clinical practice, nor are they even routinely identified at diagnosis, although in the future, they are likely to contribute to the risk stratification of patients and be taken into account in therapeutic decisions [2,8,11].

Diagnostic techniques, such as karyotyping and fluorescence in situ hybridization (FISH), remain the gold standard in clinical practice in the diagnosis of B-ALL patients [14,15]. In addition, other conventional techniques, such as SNPs arrays and multiplex ligation-dependent probe amplification (MLPA), are often used to identify smaller CNVs and larger losses/gains [16]. However, these techniques are not always sufficient to identify the broad spectrum of new alterations detected in the disease and also have significant limitations in terms of detection sensitivity [9,17,18].

The development of mass sequencing techniques in recent years has allowed their implementation in the study of hematological malignancies, such as B-ALL. Consequently, they have become a promising tool for the clinical management of the disease. These techniques include the study of DNA, RNA, and miRNA and can involve a variety of strategies, including whole-genome sequencing (WGS), whole-exome sequencing (WES), and targeted panels. However, WGS and WES, which currently allow the detection of the largest number of alterations, remain expensive, slow, and labor-intensive in the clinical laboratory [19,20]. For this reason, in recent years, targeted panels have taken priority over

WGS and WES [21,22]. This study, therefore, proposed the use of specific panels as the best option for clinical practice, through which detection sensitivity can be improved and data analysis simplified.

In this study, we proposed the use of a specific DNA-based panel to help overcome the limitations of the techniques conventionally used in clinical practice during the process of patient diagnosis. The incorporation of selective sequencing approaches in clinical practice could allow the single-step detection of the main genetic alterations present in B-ALL with greater sensitivity, in a fast, simple, and economic way. In addition, the applicability of this could be guaranteed since it is designed for use in bench-top sequencers. These alterations include: (a) aneuploidies, high hyperdiploid (>51 chromosomes), low hypodiploid (31-39 chromosomes), and near-haploid (24–30 chromosomes); (b) recurrent fusion genes (*ETV6/RUNX*1, *BCR/ABL1* and *MLL*r); (c) intrachromosomal amplification of chromosome 21 (iAMP21) and *CRLF2* rearrangements; (d) CNVs, in particular, alterations in *IKZF1*, *PAX5*, *CDKN2A*, *ETV6*, *BTG1*, and *RB1* genes; (e) candidate actionable genes, which can only be detected by NGS; (f) polymorphisms or germinal mutations associated with treatment response.

In this work, we designed a customized DNA-based NGS panel, whose validation by standard diagnostic tests is expected to allow us to use a unique methodology to detect the main genetic alterations present in B-ALL and to achieve a better stratification of patients according to risk. The study included 75 samples that had previously been characterized by conventional techniques. The use of the custom NGS panel would allow the correct stratification, as well as a refined prognosis of patients by a genuinely comprehensive assessment of the molecular spectrum of alterations (CNVs, nucleotide mutations, SNPs associated with pharmacogenetic and fusion genes), as well as cooperating genetic aberrations (e.g., *IKZF1, CDKN2A*, *PAX5*, *BTG1*, and *CRLF2* rearrangements).

2. Materials and Methods

2.1. Selection of Patients and Samples

Seventy-five B-ALL patients at diagnosis referred from 22 Spanish centers to the Hematology Service at the University Hospital, Salamanca, were analyzed in this study. The diagnosis of B-ALL patients was based on the morphological, immunophenotypic, and genetic characteristics of leukemic blast cells, as described above [23]. Standard-of-care diagnostics also include genetic characterization by conventional cytogenetic analysis, karyotype, and FISH.

The samples were also studied using other methodologies to validate them: 62 of the samples were sequenced using other sequencing methodologies; 44 were sequenced by 454 Junior sequencing (Roche, Basel, Switzerland); one was sequenced by an amplicon-based NGS panel (Illumina, San Diego, CA, USA); 17 samples were sequenced using both methodologies. The characteristics of these panels are detailed below in the section on validation assays.

Sixty-two of the 75 samples were also studied by MLPA (for *IKZF1*, *CDKN2A/B*, *PAX5*, *EBF1*, *ETV6*, *BTG1*, and *RB1* genes, as well as genes from the X/Y PAR1 region) and microarray-based comparative genomic hybridization (aCGH) [24]. The loss of *IKZF1* in these patients was also verified by PCR.

The cohort of patients included: 10 *BCRL/ABL1*-positive patients; 10 *ETV6/RUNX1*-positive patients; 10 patients with a high hyperdiploid clone (>51 chromosomes); 10 patients with *MLL*r; 3 patients with a low hypodiploidy clone (<40 chromosomes); 3 patients with iAMP21, and 29 without recurrent disorders or B-other patients (two of whom had the *CRLF2* rearrangement). The characteristics of the patients are shown in Tables S1 and S2.

ALL cell lines were also used for technical validation. The REH cell line was obtained from Deutsche Sammlung von Mikroorganismen und Zellkulturen (DMSZ) German collection (ACC 22). It was established from the peripheral blood of a patient with ALL, who carried t (12;21) and del (12), producing respective *ETV6/RUNX1* fusion and deletion of *ETV6*. This cell line has a series of mutations described in previous studies, which are collated online at https://cansarblack.icr.ac.uk/cell-line/REH/mutations. In addition, different clones generated in the laboratory from the REH line by single-cell sorting were

used, in which the expression of the fusion protein *ETV6/RUNX1* was truncated using the clustered regularly interspaced short palindromic repeats-cas9 (CRISPR/Cas9) system [25].

The study was approved by the local ethical committee, the Comité Ético de Investigación Clínica del Área de Salud de Salamanca, at the University Hospital, Salamanca (ethical approval code: PI 2019 03 230). Written informed consent was obtained from each patient or legal guardian before patients entered the study.

2.2. DNA Extraction

Genomic DNA was extracted from frozen bone marrow or fixed peripheral blood cell samples with a QIAmp DNA mini kit (Qiagen, Valencia, CA, USA), following the manufacturer's recommendations. DNA quantity was assessed by Qubit 4.0 using a double-strand kit (high/broad sensitivity) (Invitrogen Life Technologies, Carlsbad, CA, USA).

2.3. Next-Generation Sequencing

2.3.1. Custom NGS Panel Design

A custom NGS panel was made using SureDesign Studio (Agilent Technologies, Santa Clara, CA, USA) with 57,680 probes targeting 1522 regions, including specific exons for 150 genes associated with B-ALL; 165 SNPs associated with the pharmacogenetics of ALL treatment, breakpoint sequence of *ETV6/RUNX1, BCR/ABL1*, *MLL*r, *CRLF2*r, including *CRLF2/P2YR8* and *IGH/CRLF2* fusion gene; specific regions for CNV detection in *IKZF1*, *CDKN2A*, *PAX5*, *BTG1*, *RB1,* and *ETV6;* probes randomly distributed between chromosomes 4, 8, 10, and 21 for hyperdiploidy detection, and chromosomes 7 and 17 for hypodiploidy detection. The final design covered ~500 kb (Tables S3–S7).

2.3.2. Library Construction and Illumina Sequencing

Genomic DNA from each sample was fragmented and used to prepare the NGS libraries for the Illumina platform using a hybridized capture-based target-enrichment approach (SureSelect) developed by Agilent Technologies. Regions of interest were enriched for each library using the SureSelectQXT Target Enrichment Kit following the manufacturer's instructions (Agilent). Enriched DNA was precipitated with streptavidin-coated beads and washed, eluted, and amplified with index tags to identify each sample and pooled for sequencing. After quality control was measured by the 4200 TapeStation (Agilent) and quantified using Qubit® 4.0 Fluorometer, the libraries were sequenced on an Illumina NextSeq or MiSeq platform (Illumina Inc., San Diego, CA, USA). Paired-end sequencing (151-bp reads) was run. At the end of the process, this platform collects all the information in demultiplexed and paired FASTQ files for subsequent bioinformatic analysis.

2.3.3. Sequence Data Processing: Mutational Analysis

Raw data quality control was performed with FastQc (v0.11.8) and Picard tools (v2.2.4) to collect sequencing metrics. Clonal reads were removed, and low-quality sequence tails were trimmed, with a threshold Phred quality score of ten. The trimmed sequence reads were aligned to the reference genome (hg38/GRCh38) and to mark PCR duplicates, BWA v0.7.12, and GATK v3.5.

A minimum quality score of Q30 was required to ensure high-quality sequencing results. Variant calling and annotation were performed using an in-house pipeline based on the VarScan v2.3.9, SAMTools v1.3.1., and ANNOVAR bioinformatic tools. The dbSNP, COSMIC, ClinVar, 1000 Genomes Browser, and exome aggregation consortium (ExAC) databases and in silico predictors of functional effects, such as mutationAssessor, sorting intolerant from tolerant (SIFT), and polymorphism phenotyping v2 (PolyPhen-2), were used for annotation. General information about variants was obtained using the Varsome web tool (https://varsome.com) [26]. To consider SNPs, variants with a minor allele frequency (MAF) of <0.01 were selected. In addition, variants with a variant allele frequency (VAF) of 40–60% or >90% were reviewed, prioritizing variants described by in silico predictors of

functional effects and ClinVar as deleterious, damaging, pathogenic, or likely pathogenic. Aligned reads were manually reviewed with the integrative genomics viewer (IGV) to confirm and interpret variant calls, fusion genes, and microdeletions and reduce the risk of false positives. Any mutation in driver genes previously described in seminal papers was considered in the analysis.

2.3.4. Sequence Data Processing: Copy Number Variation Analysis

Data were processed using a previously described in-house pipeline [27]. First, a reference was generated with control samples (unaltered karyotype). To that end, the mean coverage depth of each individual target of a sample was first normalized for the total amount of the DNA template loaded onto sequencing flow cells based on the total reads of that sample. The mean coverage of each individual target from the reference samples obtained in this was used as the reference for a specific region. To detect CNVs, the normalized coverage of each target of a test sample was compared with the mean coverage of the same region in the reference file generated, as described above. Whole-genome profiles of $\log_2$ ratios of mean coverage of individual targets of a region normalized to that of the reference were plotted against the target. The x-axis shows the targets in the panel plotted by relative genome order. The y-axis corresponds to the $\log_2$ ratio of mean coverage of testing to that of the reference. CNVs were called using fixed thresholds, representing the minimum $\log_2$ ratio for gains (0.40) and the maximum $\log_2$ ratio for losses (−0.55). An atypical $\log_2$-normalized coverage ratio <0.5 suggests a heterozygous deletion.

2.3.5. Sequence Data Processing: Fusion gene and IKZF1 microdeletion Analysis

Manta software (Illumina) was used to detect medium and large structural variants (>50 bp), including *IKZF1* deletions and translocations [28].

2.4. Analytical Validation: Sensitivity, Specificity, and Reproducibility Analysis

To determine the reproducibility of the custom NGS panel, three additional samples that did not belong to the series of patients described in the previous section were included in duplicate. In addition, two healthy control samples were added to avoid the detection of false positives.

Sensitivity and specificity were determined by comparing the variants reported by the custom NGS panel with those reported by the techniques routinely employed to detect each of the alterations. Mutational information obtained through other sequencing methodologies—454 Junior sequencing (Roche) and a targeted TruSeqCustom amplicon (TSCA) panel for ALL (pre-beta test plan for Illumina)—was used to validate the mutations. MLPA data were used to determine the sensitivity and specificity of the custom NGS panel for detecting CNVs, and karyotyping and FISH were used to validate the aneuploidies and fusion genes, respectively. To determine sensitivity, true positives (TPs) were taken into account, considering these to be the alterations detected by at least two techniques. False negatives (FNs) were considered to be those alterations reported by other techniques but not by NGS (sensitivity = TP/TP + FN). Specificity was calculated, taking into account the true negatives (TNs), considered to be alterations not reported by NGS or other techniques, and false positives (FPs), such as those alterations detected by NGS, which were not reported by any other technique (specificity = TN/TN + FP).

Data from 454 Junior sequencing included the mutational status of *JAK2* (E12-16, NM_004972.3), *TP53* (E4-11 NM_000546.5), *IL7R* (E6 NM_002185.5), *PAX5* (E2-3 NM_016734.3), *CRLF2* (E6, NM_022148.4), and *LEF1* (E2-3, NM_016269.5) genes. These data were previously published by Forero-Castro et al. [29]. ALL targeted TSCA panel included the mutational status of 52 genes (Montaño A. EHA-SWG, 2018) (Table S8).

The PCR amplification-based method (amplicons) was used for the validation tests of the mutations. PCR libraries were prepared using a Nextera XT DNA sample preparation kit (Illumina) and indexed using a Nextera XT index kit (Illumina). The indexed libraries were then purified using Agencourt AMPure XP beads (Beckman Coulter, Brea, CA, USA), quality checked on a Bioanalyzer DNA 1000 chip

(Agilent), and then quantified by fluorometry using a Qubit HS dsDNA assay kit (Invitrogen, Carlsbad, CA, USA). The libraries were then diluted to an equimolar concentration of 4 nM before pooling for sequencing. The pooled library concentration was confirmed for a final time by a fluorometric measurement before denaturing and sequencing. The pooled genomic libraries were then sequenced using the Illumina NextSeq or MiSeq platform (Illumina). Samples were processed using V3 MiSeq sequencing chemistry in a 2 × 151-bp run (8 samples per run).

Sanger sequencing (SS) in an ABI 3130 automated sequencer was used to validate polymorphism and fusion genes through the design of region-specific oligonucleotides. The specific forward and reverse primers were designed using Primer3 (http://bioinfo.ut.ee/primer3/). Genomic DNA was amplified with the Fast Start High Fidelity PCR System (Roche) following the manufacturer's instructions, with some variations in the annealing temperature. DNA sequences were evaluated using Chromas Lite v2.1.1 (Technelysium, South Brisbane, Australia) and DS Gene v1.5 (Accerlys, San Diego, CA, USA) software. Data were analyzed using the annotations of genome version hg38/GRCh38. Table S9 shows the oligonucleotide pairs used for confirmation of fusion genes that were not previously reported by conventional techniques.

MLPA reactions were performed using the SALSA MLPA P335-B1 ALL-IKZF1 probe mix (MRC-Holland, Amsterdam, The Netherlands), according to the manufacturer's instructions. DNA samples from three healthy donors were used as controls. The P335-B1 probe mix contains probes for the genes *IKZF1*, *CDKN2A/B*, *PAX5*, *EBF1*, *ETV6*, *BTG1*, and *RB1* and those from the X/Y PAR1 region. MLPA amplification products were analyzed on an ABI 3130xl Genetic Analyzer (Applied Biosystems, Foster City, CA, USA) with GeneMapper software V.3.7, using the Genescan 500LIZ internal size standard (Applied Biosystems). The copy number at each locus was estimated according to the method of Schwab et al. [30].

aCGH experiments were carried out in an aCGH 12X135K array platform (Roche NimbleGen, Madison, WI, USA). The segmentation analysis was performed using the CGHweb tool 8. The Database of Genomic Variants from Toronto (DGV, http://dgv.tcag.ca/dgv/app/home) was used to exclude DNA variations located in regions with defined CNVs. All copy number changes with more than 50% overlap with respect to those reported in the DGV were excluded. The data discussed in this publication have been deposited in NCBI's Gene Expression Omnibus [24] and are accessible through GEO Series accession number GSE75671 (http://www.ncbi.nlm.nih.gov/geo/query/acc.cgi?token=ufczceaqvvudfup&acc=GSE75671).

3. Results

3.1. NGS Panel Performance

Results obtained from sequencing showed an average of 3.5×10^6 reads/sample. At least 99.4% of the regions of interest were sequenced. The average sequence depths ranged from 800× to 20×. Due to the design, the regions corresponding to mutations had a median frequency of 342 (24.6–767.4) reads. The coverage depth obtained in the regions corresponding to mutation detection allowed the detection of variants in case of up to 5% VAF, thus allowing the presence of subclones to be determined. The regions with low VAF that obtained a depth coverage <250 were confirmed by amplicon-based sequencing. The regions corresponding to the SNPs associated with pharmacogenetics had a median read frequency of 73.7 (0–417.8). The CNVs and fusion gene regions had median read frequencies of 355.1 (81.9–647.1) and 570.2 (408.5–701.2), respectively.

A total of 868 variants (SNV/INDELS) were reported in the cohort of patients. Fourteen and 46 samples showed the presence of aneuploidy and CNVs in some of the genes studied, respectively. Thirty-five patients showed some of the recurrent fusion genes included in the panel design. No SNVs/INDELs were reported in control samples. The controls also showed an unaltered CNV profile. The NGS panel was highly reproducible compared with the duplicate sequenced samples and

the results obtained from sequencing the different types of samples, such as fresh cells, cryopreserved cells, and tumor tissue (Table S10).

Validation assays determined sensitivity and specificity of 96.3% and 90.0% for SNV/INDEL detection compared with other sequencing methodologies; 89.7% and 100% for detecting fusion genes compared with FISH; 93.3% and 100% for aneuploidy detection compared with karyotyping, and 95.5% and 100% for the detection of CNVs compared with MLPA (Table S11).

Most of the alterations (>90%) detected with the custom NGS panel could be validated by other techniques (karyotyping, FISH, MLPA, aCGH, PCR, or other sequencing methodologies) and showed high levels of concordance.

3.2. High Sensitivity and Reproducibility in SNV/INDEL Detection

A total of 86.7% of the analyzed samples (65/75) featured a mutation in at least one of the genes studied, with a mean of 1.8 mutations per patient (range 0–6). One hundred and fifty-three variants were selected after applying the quality filters and removing SNPs and possible sequencing artifacts, of which most were non-synonymous SNVs (83.1%). These variants were detected in 55 of the genes studied. The most frequently altered gene was *NRAS*, which was detected in 30% of patients, followed by *KRAS*, *JAK2*, *PAX5*, and *IKZF1*, which were detected in more than 8% of the cohort (Figure 1). Over 70% of the mutations detected in the *NRAS* and *KRAS* genes were the hotspots located at codons 12 and 13. Furthermore, mutational hotspots R683 and T875 of *JAK2* were the most recurrent mutations observed in this gene (Table S12).

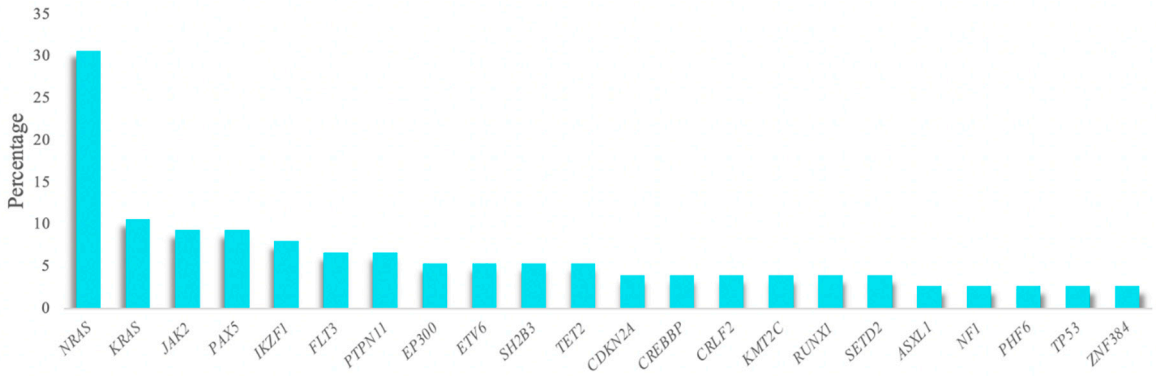

Figure 1. Genes most frequently mutated in the patient series. The histogram shows the genes detected in more than 2% of the patient series.

The mutational status of *JAK2*, *TP53*, *IL7R*, *PAX5*, *CRLF2*, and *LEF1* genes, determined by 454 Junior sequencing in 62 of patients, and the mutational status of 52 genes, determined by an amplicon-based NGS panel (Illumina) in 18 patients, were used for custom NGS panel validation in mutation detection. In this way, the regions common to all panels were analyzed (454 Junior sequencing/amplicon panel vs. custom NGS panel). The analysis revealed 18 samples to have mutations in at least one of these common regions. The mutations reported by the NGS custom panel faithfully reproduced the alterations detected by the other sequencing methodologies, yielding an almost identical VAF in almost all samples (Table 1).

Table 1. Correlation between mutations detected by the custom NGS panel and 454 Junior sequencing. The table lists the patients who presented some mutations in the genes studied by sequencing with 454 Junior. The first column contains the patient identifier (ID) in bold, followed by the gene, altered nucleotide in coding sequence (CDS mutation), an altered amino acid (AA mutation), and variant allele frequency (VAF) detected by 454 Junior sequencing and the custom NGS panel.

ID	Gene	CDS Mutation	AA Mutation	VAF (%)		
				454 Junior (Roche)	TSCA (Ilumina)	Custom NGS Panel
ID5	***RUNX1***	**c.G239A**	p.R80H	-	30.58	40.76
ID43	*TP53*	c.560-1G->A	Splice_Intron 5 SA	41	-	42.27
ID23	*FLT3*	c.G2503T	p.D835Y	-	19.24	12.86
	KRAS	c.G35T	p.G12V	-	19.29	14.68
	JAK3	c.C23T	p.T8M	-	55.23	41.18
ID64	FLT3	c.G580A	p.V194M	-	49.33	43.79
ID73	*CRLF2*	c.695T>G	p.F232C	21.5	-	25.69
	JAK2	c.2049A>T	p.R683S	13.79	-	14.96
ID24	*CRLF2*	c.660G>T	p.E220D	75.73	5.28	5.19
ID25	*PAX5*	c.399T>A	p.S133R	20.4	31.22	23.08
	TP53	c.818G>C	p.R273P	3.5	2.72	0
ID41	*PAX5*	c.215A>G	p.Y72C	54.65	53.98	50.66
	PAX5	c.239C>G	p.P80R	39.62	0	44.13
ID60	*JAK2*	c.2047A>G	p.R683G	11.79	5.51	6.67
	JAK2	c.2624C>A	p.T875N	-	16.68	16.85
ID74	*JAK2*	c.2047A>G	p.R683G	40	-	41.10
ID40	*ETV6*	c.1165_1166del	p.M389fs	-	40.41	35.19
	FLT3	c.T1733C	p.M578T	-	45.13	36.51
ID42	*TP53*	c.G242A	p.R81Q	-	82.16	88.82
	NF1	c.C4537T	p.R1513X	-	82.17	69.35
	CRLF2	c.G394A	p.V132M	-	46.61	46.18

Table 1. *Cont.*

ID	Gene	CDS Mutation	AA Mutation	VAF (%)		
				454 Junior (Roche)	TSCA (Ilumina)	Custom NGS Panel
ID26	*SH2B3*	c.C464T	p.P155L	-	52.52	51.58
ID72	*NRAS*	c.G35A	p.G12D	-	0	3.97
ID71	*PHF6*	c.G55A	p.R129X	-	29.64	18.42
	RUNX1	c.C385T	p.A19T	-	0	46.68
ID34	*PAX5*	c.T800A	p.V267D	-	84	48.12
	KRAS	c.G35T	p.G12V	-	14.4	13.39
ID20	*NRAS*	c.G35A	p.G12D	-	8.48	4.49
ID29	*NRAS*	c.G35A	p.G12D	-	6.41	5.13

In the ID24 sample, the variant p.E220D in the *CRLF2* gene was detected by all sequencing techniques but with discrepancies in the VAF. While similar VAFs (about 5%) were obtained with the custom panel and the amplicon panel, a higher VAF (75%) was observed with 454 Junior sequencing. Similarly, the mutation in *PAX5* (p.V267D) observed in the sample ID34 showed discrepancies in the VAF estimated by the different panels. On the other hand, a mutation in the *TP53* gene detected by the 454 Junior and amplicon panels was not detected by the custom NGS panel in ID25, probably because it was present in such a low percentage of cells (VAF ~3%). By contrast, two other mutations in the ID71 and ID72 samples were only detected by the custom NGS panel (Table 1).

Mutations previously described in the REH cell line were also detected in the genes included in the panel: *TBLX1R1*, *IKZF1*, *NOTCH1*, *IL27*, *TP53*, *GATA3*, and *BCL11B*. These mutations were also maintained in several clones established from the REH cell line. Only two mutations of the parental cell line (REH) were not detected in the analyzed clones because they were established by single-cell sorting and were not present in 100% of the pool of parental cells (VAF ~30%) (Table S13).

SNPs associated with the response to drugs included in the panel were also successfully detected in genes, such as *MTHFR* and *SCOL1B1*, associated with methotrexate (MTX) metabolism, as well as in *NUDT15* and *ITPA*, to which 6-mercaptopurine (6-MP) toxicity levels are related. Table S14 shows the observed frequencies of pharmacogenetic SNPs in the patient cohort.

3.3. Accurate Aneuploidy Detection

To validate high hyperdiploid detection, 10 samples previously characterized by their karyotype and aCGH were included in the study. Five of them were selected because the presence of the high hyperdiploid clone was confirmed by aCGH, but not by karyotype, either because of a lack of mitoses or due to the failure of the malignant clone to grow. These 10 samples also included two samples in which the high hyperdiploid clone was detected in fewer than 20% of the cells per karyotype. Using the custom NGS panel, the high hyperdiploid clone was detected in all 10 samples analyzed, as reported by both the cytogenetic and aCGH approaches. In addition, two more samples with high hyperdiploid clone were identified, stratified within the *BCR/ABL1*-positive subgroup. Thus, the trisomies observed by NGS faithfully reproduced the findings observed by both techniques (Table 2). The NGS panel showed even greater sensitivity in detecting trisomies than aCGH, achieving more gains in all cases analyzed by the two methodologies. For high hyperdiploid detection, probes were distributed between the most frequently gained chromosomes in this subgroup of patients: chromosomes 4, 8, 10, and 21. However, due to the design of the panel, the probes distributed throughout the genome also enabled trisomies in other chromosomes to be detected (Figure 2A). The most frequently gained chromosomes were numbers 6 and 21: their trisomies were observed in 100% of patients, followed by those of chromosomes 10 and X, which were found in 92% of patients (Figure S1).

Table 2. High hyperdiploid cases detected by the custom NGS panel. Twelve cases (listed by ID in bold) with high hyperdiploid clone detected by next-generation sequencing (NGS), with their corresponding karyotype and fluorescent in situ hybridization (FISH), microarray-based comparative genomic hybridization (aCGH), and custom NGS panel results are shown.

ID	Karyotype	aCGH	NGS
ID2	55-60,XY,+Y,+4,+5,+7,+8,t(9;22)(q34;q11),+9,+11,add(12)(p12) [15]	+4, +18, +X	+4, +6, +10, +11, +14, +17, +21, +X
ID10	Karyotype failure	+2, +4, +6, +10, +14, +21	+2, +4, +6, +10, +14, +21, +X
ID31	51-58,XX,+5,+6,+9,+10,+21 [14]/46,XX [6]	ND	+4, +6, +14, +17, +21, +X
ID32	48-52,XX,+2,+6,+8,+10,+12,+21 [12]/46,XX [3]	ND	+4, +6, +8, +9, +10, +17, +21, +X
ID33	51,XX,+21,4mar [4]/46,XX [17]	+10, +18, +21	+5, +6, +9, +10, +17, +21, +X
ID34	50-52,XX,+10,+17,+18,+21,+mar [3]/46,XX [8]	+10, +14, +21	+6, +8, +9, +10, +14, +19, +21, +X
ID35	Karyotype failure	+4, +5, +6, +8, +10, +14, +21, +X	+4, +5, +6, +8, +10, +14, +17, +21, +X
ID36	46,XX [10]	+6, +8, +13, +14, +19, +21	+5, +6, +8, +10, +12, +13, +14, +19, +21
ID37	46,XX [10]	+4, +6, +9, +10, +14, +17, +21	+4, +6, +9, +10, +17, +21, +X
ID38	46,XX [6]/46,XX,add(3)(q)(21) [2]	+10, +14, +17, +21	+4, +6, +9, +10, +17, +21, +X
ID39	46,XY [10]	+14, +17, +18, +21, +22, +X	+4, +6, +9, +10, +14, +17, +21, +22, +X
ID40	60,XY,+X,+4,+5,+6,+8,+10,+10,+16,+17,+18,+21,+22,+mar [14]	ND	+4, +5, +6, +8, +10, +16, +17, +21, +22, +X

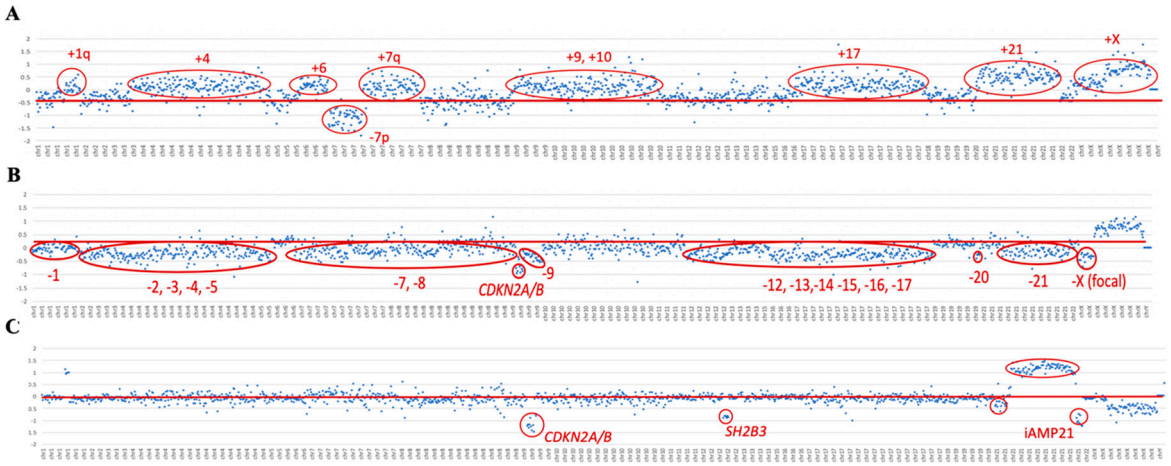

Figure 2. Dot plot of copy number variations (CNVs). This figure shows the dot plots of three samples for the detection of CNVs. The x-axis represents the chromosome regions included in the custom NGS panel, in increasing order from chromosome 1 to X. The y-axis shows the values of the $\log_2$ ratio. The red lines indicate the reference, and in the red circles, there are the chromosomal regions above or below the reference, showing the respective gain or loss of that region. (**A**) Dot plot of the ID37 sample, showing a high hyperdiploid clone with the gain of chromosomes 1q, 4, 6, 7q, 9, 10, 17, 21, and X, in addition to the loss of 7p. (**B**) Dot plot of the ID43 sample, showing a near-haploid clone with the loss of chromosomes 1, 2, 3, 4, 5, 7, 8, 12, 13, 14, 15, 16, 17, 20, and 21. (**C**) Dot plot of the ID44 sample, showing the loss of the *CDKN2A/B* and *SH2B3* genes, and of iAMP21.

The hypodiploid clones were studied with respect to the distribution of probes along chromosomes 7 and 17. Using the panel, the presence of a hypodiploid clone was detected in two of the three cases included in the study, which were confirmed by karyotyping. Within the subgroup of patients with hypodiploidy, a low hypodiploidy clone (31–39 chromosomes) was observed in the ID42 sample by karyotype and custom NGS panel. In the ID43 sample, more missing chromosomes were identified with the custom NGS panel than by the karyotype, it being possible to identify the presence of a near-haplotype clone (e.g., in Figure 2B). On the other hand, the karyotype of the ID41 sample showed the presence of a clone with low hypodiploidy, but this was not evident from the custom NGS panel. Interestingly, aCGH did not show any chromosomal losses in this sample either.

All three patients included in the study with iAMP21 reported by FISH were confirmed by NGS. The dot plot of these samples showed a characteristic profile in chromosome 21. In particular, a gain of the region described as the common region of amplification (CRA) was observed in all cases, in addition to other regions of chromosome 21 with losses (e.g., see Figure 2C).

The panel design also allowed the detection of CNVs in *IKZF1*, *CDKN2A/B*, *PAX5*, *BTG1*, *RB1*, and *ETV6* genes. These results were validated with the data available from MLPA and aCGH. Microdeletions of the *IKZF1* gene were also confirmed by PCR. Twenty-four patients showed *IKZF1*del, which was mainly enriched in the positive Philadelphia subgroup (33.3% of the cases). Eighteen of them were also reported by one of the other conventional techniques—MLPA, PCR, and/or aCGH. In addition, the NGS custom panel was able to detect all cases of *IKZF1* loss, which were discordant between the three techniques, without giving rise to any false-positive results. Four of these cases had a focal loss of the 7p arm that affected the entire *IKZF1* gene. These cases could not be detected by PCR as there was no region to which the designed primers could hybridize. The remaining six cases could not be confirmed because no previous genetic data were available (Figure 3).

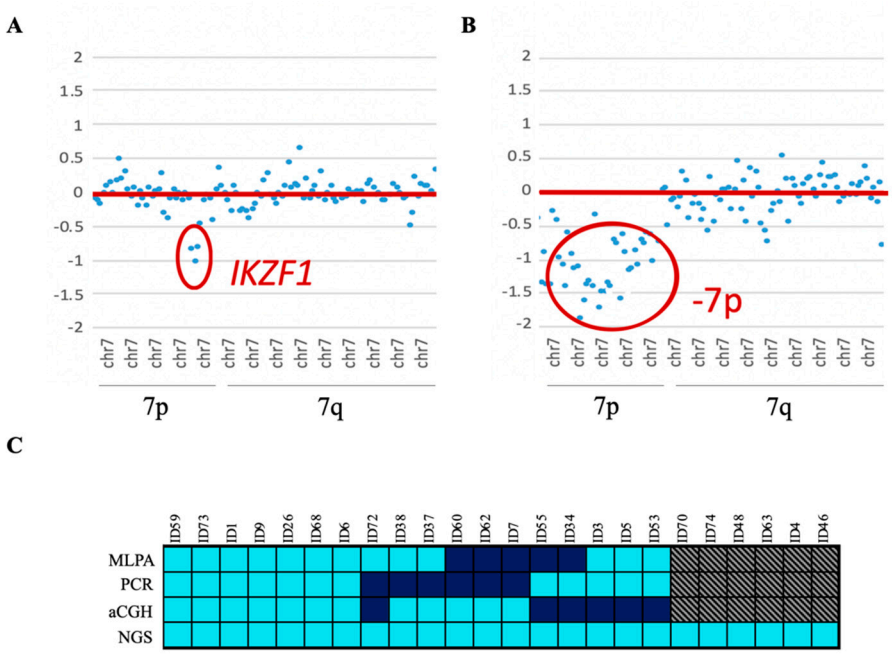

Figure 3. *IKZF1* loss. (**A**) Dot plot of CNV representation, showing *IKZF1* gene loss. (**B**) Dot plot of CNV representation, showing loss of 7p, which includes the *IKZF1* gene. The x-axis represents the chromosome regions included in the custom NGS panel, in increasing order from chromosome 1 to X. The y-axis shows the $\log_2$ ratios. The red lines indicate the reference, and the chromosomal regions above or below the reference are those inside the red circles, indicating the respective gain or loss of that region. (**C**) *IKZF1* loss detected by NGS compared with the results obtained by conventional multiplex ligation-dependent probe amplification (MLPA), PCR, and aCGH techniques. Turquoise, detected; dark blue, not detected; grey, no information available. Each column represents one patient.

One-third of the patients with the *IKZF1* deletion also featured a loss of the *CDKN2A/B* gene. This gene was lost in 20 patients, including all of those identified by the MLPA and/or aCGH (12/12). The loss of the *PAX5* gene was observed in 12 patients and was accompanied in a small majority of cases by the loss of *CDKN2A/B* (7/12), thus giving a detection rate of 92.3% for the cases confirmed by MLPA and/or aCGH. Only one case with *PAX5* loss reported by MLPA was not detected by NGS. This loss was also not reported by aCGH. On the other hand, 83.3% (9/11) of the cases with loss of *ETV6* confirmed by MLPA and/or aCGH were detected by NGS. These two patients had a focal loss of *ETV6* by aCGH, but this loss was also not detected by MLPA. In addition, the loss of *ETV6* was also detected in one patient without previous information. The loss of this gene was mainly detected in the *ETV6/RUNX1*-positive subgroup (7/10). The loss of the *BTG1* gene was detected in nine patients, thereby giving a detection rate of 85.7% of cases (6/7) that were confirmed by MLPA and/or aCGH. The sample in which the loss of *BTG1* by NGS was not detected had a focal loss by aCGH. The loss of *RB1* by NGS was confirmed in 100% of cases observed by MLPA and/or aCGH (2/2), in addition to two other cases with no previous data. Furthermore, the panel design allowed for the detection of CNVs in other genes included in the panel, such as *ERG*, *TP53*, and *VPREB1*, although these were not validated. No false positives were detected.

3.4. Fusion Gene Detection

The use of the custom NGS panel allowed the detection of the *ETV6/RUNX1* and *BCR/ABL1* fusion genes with high sensitivity and specificity. To study the various fusion genes, probes were added throughout the most frequently described regions where the breakpoints occur.

In the case of t(12;21)(p13;q22), probes were added along the intron 5 of *ETV6* (NM_001987.5). The presence of the fusion gene *ETV6/RUNX1* was detected in 11 samples, which represented 90% of

the cases confirmed by FISH (9/10), and two other cases—ID52 and ID61—in which fusion was not reported (Figure 4A). PCR of the detected breakpoint confirmed the presence of the *ETV6/RUNX1* fusion gene in these samples (data not shown). In the sample ID13, in which the *ETV6/RUNX1* fusion gene reported by FISH was not detected, a different translocation was observed between chromosomes 5 and 12, involving the *ETV6* gene (Figure S2). The fusion gene *ETV6/RUNX1* was also analyzed in the REH cell line and the *ETV6/RUNX1* knockout (KO) clones established in previous studies [25]. The *ETV6/RUNX1* fusion gene was detected in 100% of cells from the REH cell line, as expected, and the truncator mutation was also found in 100% of the cells in the KO clones (data not shown).

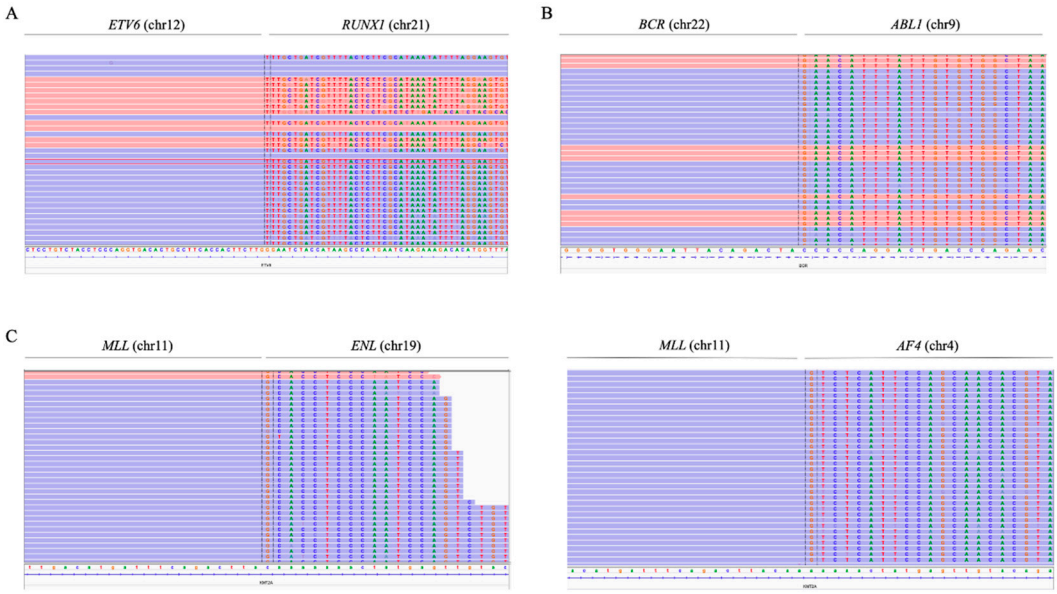

Figure 4. Fusion genes visualized with integrative genomics viewer (IGV). (**A**) *ETV6/RUNX1* fusion gene (sample ID52). In the left region, the reads were aligned with intron 5 of *ETV6*, while in the right, the reads were aligned with intron 3 of *RUNX1*. (**B**) *BCR/ABL1* fusion gene (sample ID63). In the left region, reads were aligned with intron 1 of *BCR*; to the right, reads were aligned with intron 1 of *ABL1*. (**C**) *MLL/ENL* fusion gene (sample ID30) and *MLL/AF4* fusion (sample ID27). In the left region, reads were aligned with intron 10 of *MLL*; to the right, reads were aligned with the intergenic region next to *ENL* and intron 3 of *AF4*, respectively. The position of the breakpoint was determined by MANTA software.

In all ten samples in which the presence of the *BCR/ABL1* fusion gene was reported by cytogenetic techniques, the gene was also detected using the NGS panel. In addition, the fusion gene was detected by cytogenetics in a previously unreported sample (ID63) (Figure 4B). The presence of this fusion gene was confirmed by PCR (data not shown). For its detection, probes were distributed along intron 1 and exons 12-16 of *BCR* (NM_004327.4), which made it possible to distinguish between the two frequent types of rearrangements—the minor p190 (m-BCR) that occurs in *BCR* intron 1 and the major p210 (M-BCR) between *BCR* introns 12-16. The 90% (10/11) of patients showed m-BCR, while the other 10% (1/11) of the samples exhibited M-BCR.

To detect *MLL* rearrangements, probes along exons 9 to 12 of *MLL* (NM_005933.4) were included. Seventy percent of the cases confirmed by karyotype/FISH were also detected by NGS (7/10). The use of the panel also made it possible to determine the partner gene of *MLL* in these cases (Figure 4C). Five patients with *MLL*r detected by the custom NGS panel showed rearrangement with the *AF4* gene (chromosome 4), while in one patient, the rearrangement was observed with the *ENL* gene (chromosome 19) and, in another, with the *EPS15* gene (chromosome 1). By contrast, three cases with an *MLL* rearrangement confirmed by karyotype and/or FISH were not detected by the NGS panel.

To determine the detection sensitivity of the various fusion genes, samples were included in the study in which the fusion gene reported by FISH was found in a low percentage of cells. In this way, using NGS, it was possible to identify the fusion gene *ETV6/RUNX1*, *BCR/ABL1*, and *MLL* rearrangements in samples with percentages less than 12, 26, and 18%, respectively.

Both cases with *CRLF2* rearrangements were successfully detected. In sample ID47, the *CRLF2/IGH* fusion gene was observed as a product of t(14;X) (Figure 5A). Moreover, sample ID48 showed the presence of the *CRLF2/P2YR8* and *CRLF2/IGH* fusion genes. The presence of the *CRLF2/P2YR8* fusion gene was also determined by the detection of the loss of the genes *CSF2RA*, *IL3R*, and *ASMTL* (Figure 5B,C). *CRLF2* rearrangements were observed in four other samples in which the rearrangements were not reported by conventional techniques.

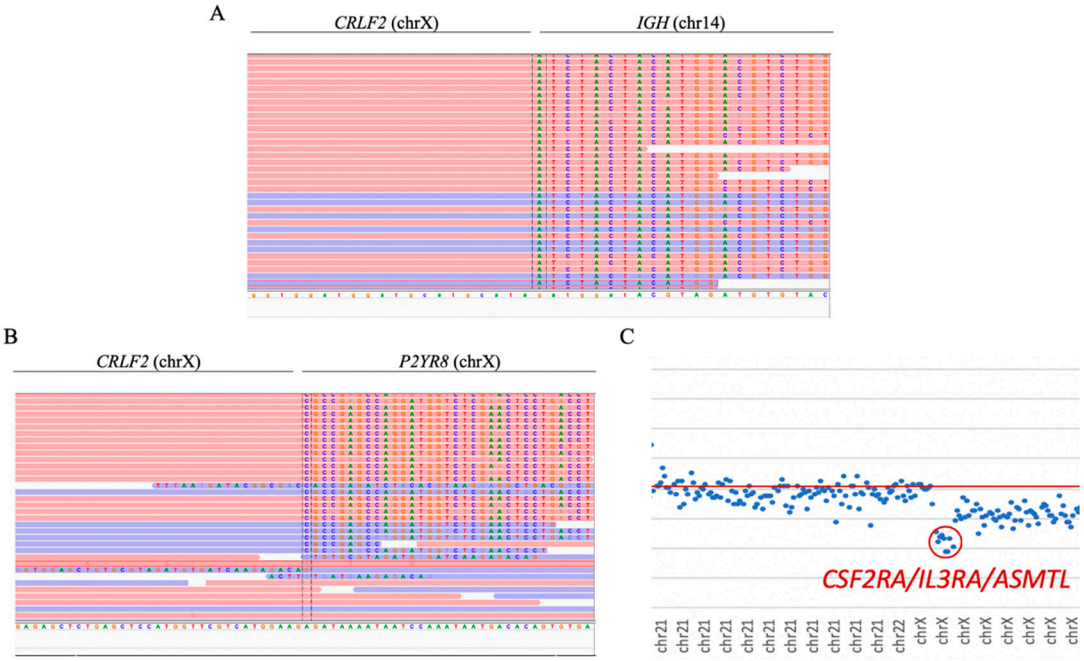

Figure 5. *CRLF2* rearrangement. (**A**) *CRLF2/IGH* fusion gene visualized with IGV software (sample ID47). In the left region, reads were aligned with the intergenic region next to the *CRLF2* gene; to the right, reads were aligned with the 14q32.33 region. (**B**) *CRLF2/P2YR8* fusion gene visualized with IGV (sample ID48). In the left region, reads were aligned with the intergenic region next to the *CRLF2* gene; to the right, reads were aligned with intron 1 of *P2YR8* (NM_178129.5). The position of the breakpoint was determined by MANTA software. (**C**) Dot plot of sample ID70, showing the loss of the genes *CSF2RA*, *IL3R*, and *ASMTL*, resulting in the *CRLF2/P2RY8* fusion gene.

3.5. The Integrative Use of the Custom NGS Panel with Standard-of-Care Diagnostics Allowed the Stratification of More Patients

The integration of the use of the custom panel together with the conventional techniques routinely used in clinical practice was more successful at stratifying patients. In 28% (21/75) of the samples, the karyotype could not be analyzed correctly because there were insufficient metaphases or because the malignant clone did not grow. Some of the recurrent alterations were detected in three of the 29 B-other patients and were re-stratified into their corresponding groups. Of these alterations, 81.3% were detected by both methodologies, while 12% were detected only by the custom NGS panel, and 6.7% only by cytogenetic techniques (Figure 6). In addition, some secondary alterations were identified in 61.3% (46/75) of the samples by the use of the custom NGS panel.

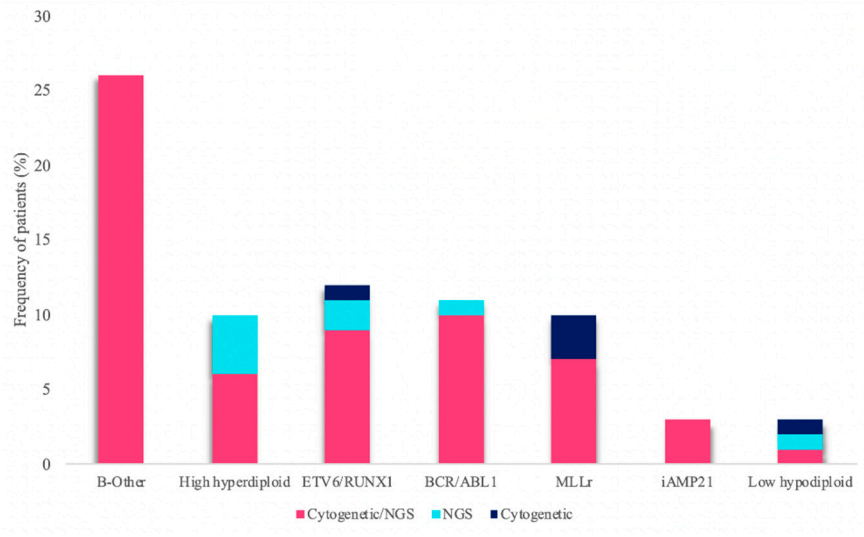

Figure 6. Frequency of genetic subtypes. The bar graph shows the percentage of genetic subtypes identified in the cohort of patients. Bars may be subdivided into three parts: pink, percentage of patients stratified through the combined use of cytogenetic techniques and NGS; turquoise, percentage of patients stratified exclusively by NGS; dark blue, stratified through the use of cytogenetic techniques only.

4. Discussion

We presented the results of a study of the validation of a custom NGS panel designed to improve the stratification of B-ALL patients. Seventy-five samples from B-ALL patients, included in the study at the time of diagnosis, were genetically characterized by conventional techniques. The use of the custom NGS panel was able to detect the main genetic alterations associated with risk in B-ALL patients with high sensitivity and reproducibility, even in some cases that could not be detected by standard-of-care diagnostics. Secondary alterations were also detected by NGS, some of which were associated with prognostic risk, which could help refine the stratification of patients.

The integration of arrays and NGS techniques is currently the only option available for detecting the greatest possible number of alterations [18]. Nonetheless, these techniques are not available in all centers, above all, in less-developed countries, such as those in Latin America, where the survival rate remains very poor, even in children, mainly due to the lack of good clinical diagnosis [31]. In addition, these analyses usually involve the study of the entire genome, which makes it very difficult to interpret the data. Therefore, a tool that allows the detection of a large number of alterations in a single experiment and in a quick and inexpensive way could be very useful in clinical practice to help stratify patients and predict their response to treatments [32–34].

The NGS panel proved to be a robust tool for SNV/INDEL detection. The regions of the panel intended for detecting them had a high read coverage (mean coverage >300 reads), which allowed mutations to be identified in low percentages of cells. SNPs included in the panel design associated with drug responses were also successfully detected. Validation through data obtained by other sequencing techniques and ALL cell lines further demonstrated that the custom NGS panel is capable of detecting genetic variants with high accuracy and reproducibility.

On the other hand, the use of the NGS custom panel was successful at detecting cases with aneuploidies and CNVs. In the case of patients with a high hyperdiploid clone, the panel could detect even those cases that were not reported by karyotyping, and that required the use of aCGH to stratify them correctly. In addition, NGS was more sensitive at detecting trisomies than was aCGH. In the cases with hypodiploidy, the NGS panel also helped refine the stratification, making it possible to detect a case with near-haploid, who was diagnosed as low hypodiploidy by karyotype. These cases sometimes pose a dilemma during the diagnostic process because a near-haploid or low hypodiploid clone can 'double-up' and appear as hyperdiploid/near-triploid when karyotyped [15]. In addition, iAMP21 was

detected in all the cases studied, making it possible to distinguish it from cases with trisomy 21 based on their characteristic profile in the representation of the dot plot of the CNV. In this way, the findings observed by NGS faithfully reproduced what was observed by karyotyping and/or aCGH, but with even greater sensitivity than with the combination of the two. CNVs were also detected in key genes involved in the evolution of B-ALL, effectively reproducing the results observed by MLPA and/or aCGH. NGS also made it possible to detect more genes than those included in the commercial panels of MLPA, thereby avoiding the main limitation of this technique.

Finally, we evaluated the sensitivity and effectiveness of the custom NGS panel in detecting the main fusion genes associated with B-ALL patients: the *ETV6/RUNX1* fusion gene (reported in 25% of children and 1–3% of adults), the *BCR/ABL1* fusion gene (reported in 10% of children and 20% of adults), and *MLL* rearrangements (reported in 6% of children and 9% of adults) [1,2,35]. The NGS panel was able to identify all fusion genes included in the panel. Furthermore, it enabled fusion genes to be detected with high sensitivity, confirming the presence of the various fusion genes in patients with the fusion in a small percentage of cells, detecting even cases that were not reported by conventional techniques. In *MLL*r cases, the NGS panel only detected 70% of the cases confirmed by cytogenetics because only the region where the most frequent *MLL* breakpoints occur was included in the panel design. Twenty percent of *MLLr*-positive patients might present the breakpoint in a different position and, therefore, not be detected by the panel.

The custom NGS panel proved to be a powerful tool for the detection of the main genetic alterations present in B-ALL patients, on which the current classification systems of this disease are based. The use of NGS allowed further refinement of the prognosis of the already established biological groups, especially the high-risk subgroup. In the *BCR/ABL1*-positive cases, we were able to distinguish between the different transcripts because it was possible to identify the *BCR* breakpoint. Although no studies have demonstrated the clinical and prognostic significance of the different *BCR/ABL1* transcripts in B-ALL, it has been demonstrated in CML patients [36]. On the other hand, by using the panel, it was possible to determine the *MLL* partner in rearrangement cases, which is known to have a clinical impact [37,38].

The correct stratification of patients into different risk groups is of vital importance because it has a direct impact on therapeutic decision-making and because poor classification can lead to the choice of inappropriate treatment or dose. The integration of this NGS panel with standard-of-care diagnostics stratified more patients than was possible by using them separately. Therefore, the implementation of this NGS panel in clinical practice could help improve patient stratification, overcoming the limitations of the conventional techniques commonly used in clinical diagnosis. Detection of secondary alterations, such as somatic mutations, SNPs associated with pharmacogenetics, CNVs, and new fusion genes, could also help improve stratification.

The panel design includes the coding regions of up to 150 genes involved in the evolution of B-ALL. Although only *TP53* mutations are currently taken into account in clinical practice, the mutational status of key genes could also be considered in the near future. These genes often affect key pathways in the pathogenesis of the disease, such as the *RAS*, *JAK/STAT*, and *PI3K* pathways, which are known to be promising therapeutic targets [18,39–41]. A total of 164 SNPs associated with pharmacogenetics were also included, which could provide valuable information for clinicians when making therapeutic decisions.

Some CNVs have already been established as new prognostic markers. In particular, the loss of the *IKZF1* gene has been associated with an adverse prognosis and with an even worse prognosis when accompanied by other alterations, such as *CDKN2A/B* deletion, also known as "*IKZF1*^{plus}" [42,43]. The *IKZF1* deletion has also been reported recurrently in Ph-like patients, which is frequently accompanied by the loss of other genes, such as *PAX5* and *BTG1*, as well as somatic mutations, all of which are included in the NGS panel [44]. *CRLF2* rearrangements have frequently been reported in this subgroup of patients, which has also been associated with a worse prognosis [45–47]. The detection of all these alterations could, therefore, be very useful for identifying the genetic signature of Ph-like

patients, for whom there is not yet a well-established or standardized diagnostic method. Although transcriptomic analysis is currently the gold standard for the diagnosis of these patients, it remains a challenge in the clinical routine of many diagnostic centers [48]. Many of these alterations are also possible therapeutic targets, which is of great interest, especially when dealing with patients who have a very poor prognosis.

In conclusion, the design of this custom panel allowed the detection of the main genetic alterations present in B-ALL patients, with which they could be stratified into different risk groups. In addition, a series of secondary alterations of high prognostic value, many of which are also promising therapeutic targets, were identified. The use of this NGS panel could facilitate better patient stratification and the refinement of the established biological groups. Our results demonstrated the advantages of NGS for managing patients, improving detection sensitivity, and solving the problems of conventional techniques (Figure 7). The integration of the NGS panel in clinical practice could complement the standard diagnostic techniques (karyotyping and FISH), while avoiding the use of additional techniques, thereby reducing costs and response time. In addition, the identification of cooperating alterations could be useful in future research that aims to detect new biomarkers and predictors of response to treatment.

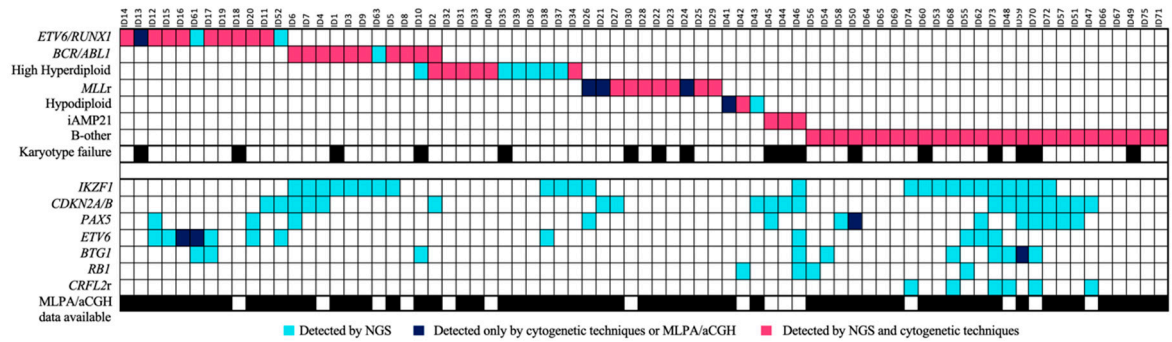

Figure 7. Genetic findings from the combined analysis of the custom NGS panel and standard-of-care diagnostics. The figure summarizes the genetic alterations observed in the series of B-ALL patients, where columns and rows represent patients and genetic alterations, respectively. The upper box shows the alterations that allow patients to be classified by biological risk groups. Turquoise, dark-blue, and pink boxes, respectively, indicate the alterations detected exclusively by the custom NGS panel and cytogenetic techniques and those detected by both. In the lower box, the different secondary alterations detected correspond to the loss of the genes indicated in the different rows and to the rearrangements of the *CRFLF2* gene.

Supplementary Materials: Additional information is available online at http://www.mdpi.com/2075-4426/10/3/0137/s1. Table S1: Genetic characteristics of the patients; Table S2: Clinical and demographic characteristics of the patient cohort; Table S3: List of genes included in the panel design for mutation analysis; Table S4: Chromosomal regions for detecting gene fusions; Table S5: Chromosomes mapped to aneuploidy detection; Table S6: Genes for CNV detection; Table S7: Pharmacogenomic SNPs included; Table S8: Genes included in the targeted TruSeqCustom amplicon (TSCA) panel for ALL (pre-beta test plan for Illumina); Table S9: Oligonucleotide pair for detecting gene fusions; Table S10: List of variants detected in duplicate-sequenced samples; Table S11: Sensitivity and specificity of detection of different types of alterations; Table S12: List of detected mutations; Table S13: Mutations described in REH cell line; Table S14: Frequency of pharmacogenetic SNPs detected in the patient cohort; Figure S1: Frequency of trisomies in high hyperdiploidy cases; Figure S2: t(5;12)(q35;p13) visualized with IGV.

Author Contributions: Conceptualization, A.M., T.G., R.B., and J.M.H.-R.; Methodology, A.M., M.F.-C., M.M.-M., E.L., C.M., S.S., V.R.-M., J.L.F., N.d.l.H., A.G.-d.C., M.S., J.D., I.d.l.F., C.O., J.O., J.M., N.V.-G., and J.M.H.-R.; Software, A.M., J.H.-S., C.M., S.S., and R.B.; Validation, A.M., M.F.-C., T.G., and R.B.; Formal analysis, A.M., J.H.-S., M.F.-C., R.B., and J.M.H.-R.; Investigation, A.M., M.F.-C., R.B., and J.M.H.-R.; Data curation, A.M., J.H.-S., M.F.-C., T.G., R.B., and J.M.H.-R.; Writing—original draft preparation, A.M.; Writing—review and editing, all authors; Visualization, all authors; Supervision, R.B. and J.M.H.-R.; Project administration, R.B. and J.M.H.-R.; Funding acquisition, R.B. and J.M.H.-R. All authors have read and agreed to the published version of the manuscript.

Funding: This work was financially supported in part by a grant from the Consejería de Educación, Junta de Castilla y León, Fondos FEDER (SA085U16, SA271P18), and the Regional Council of Castilla y León SACYL, (GRS 2062/A/19, GRS 1847/A/18), Fundación Castellano Leonesa de Hematología y Hemoterapia (FUCALHH 2017), Proyectos de Investigación en Biomedicina, Gestión Sanitaria y Atención Sociosanitaria del IBSAL (IBY17/00006), Centro de Investigación Biomédica en Red de Cáncer (CIBERONC CB16/12/00233), SYNtherapy. Synthetic Lethality for Personalized Therapy-based Stratification In Acute Leukemia (ERAPERMED2018-275); ISCIII (AC18/00093), co-funded by ERDF/ESF, "Investing in your future" and a grant to AM from the Junta Provincial de Salamanca of the Asociación Española Contra el Cáncer (AECC).

Acknowledgments: The authors would like to thank to Irene Rodríguez, Sara González, Teresa Prieto, María Ángeles Ramos, Filomena Corral, Almudena Martín, Ana Díaz, Ana Simón, María del Pozo, Isabel M Isidro, Vanesa Gutiérrez, Sandra Pujante, and María Angeles Hernández from the Cancer Research Center of Salamanca, Spain, for their technical assistance.

Conflicts of Interest: The authors declare no conflict of interest.

References

1. Moorman, A.V. New and emerging prognostic and predictive genetic biomarkers in B-cell precursor acute lymphoblastic leukemia. *Haematologica* **2016**, *101*, 407–416. [CrossRef] [PubMed]
2. Iacobucci, I.; Mullighan, C.G. Genetic Basis of Acute Lymphoblastic Leukemia. *J. Clin. Oncol.* **2017**, *35*, 975–983. [CrossRef] [PubMed]
3. Pui, C.H.; Chessells, J.M.; Camitta, B.; Baruchel, A.; Biondi, A.; Boyett, J.M.; Carroll, A.; Eden, O.B.; Evans, W.E.; Gadner, H.; et al. Clinical heterogeneity in childhood acute lymphoblastic leukemia with 11q23 rearrangements. *Leukemia* **2003**, *17*, 700–706. [CrossRef] [PubMed]
4. Malard, F.; Mohty, M. Acute lymphoblastic leukaemia. *Lancet* **2020**, *395*, 1146–1162. [CrossRef]
5. Pui, C.H.; Yang, J.J.; Hunger, S.P.; Pieters, R.; Schrappe, M.; Biondi, A.; Vora, A.; Baruchel, A.; Silverman, L.B.; Schmiegelow, K.; et al. Childhood Acute Lymphoblastic Leukemia: Progress Through Collaboration. *J. Clin. Oncol.* **2015**, *33*, 2938–2948. [CrossRef]
6. Stary, J.; Zuna, J.; Zaliova, M. New biological and genetic classification and therapeutically relevant categories in childhood B-cell precursor acute lymphoblastic leukemia. *F1000Research* **2018**, 7. [CrossRef]
7. Vrooman, L.M.; Silverman, L.B. Treatment of Childhood Acute Lymphoblastic Leukemia: Prognostic Factors and Clinical Advances. *Curr. Hematol. Malig. Rep.* **2016**, *11*, 385–394. [CrossRef]
8. Hunger, S.P.; Mullighan, C.G. Redefining ALL classification: Toward detecting high-risk ALL and implementing precision medicine. *Blood* **2015**, *125*, 3977–3987. [CrossRef]
9. Stanulla, M.; Cave, H.; Moorman, A.V. IKZF1 deletions in pediatric acute lymphoblastic leukemia: Still a poor prognostic marker? *Blood* **2020**, *135*, 252–260. [CrossRef]
10. Li, B.; Brady, S.W.; Ma, X.; Shen, S.; Zhang, Y.; Li, Y.; Szlachta, K.; Dong, L.; Liu, Y.; Yang, F.; et al. Therapy-induced mutations drive the genomic landscape of relapsed acute lymphoblastic leukemia. *Blood* **2020**, *135*, 41–55. [CrossRef]
11. Steeghs, E.M.P.; Boer, J.M.; Hoogkamer, A.Q.; Boeree, A.; de Haas, V.; de Groot-Kruseman, H.A.; Horstmann, M.A.; Escherich, G.; Pieters, R.; den Boer, M.L. Copy number alterations in B-cell development genes, drug resistance, and clinical outcome in pediatric B-cell precursor acute lymphoblastic leukemia. *Sci. Rep.* **2019**, *9*, 4634. [CrossRef]
12. Zhang, W.; Kuang, P.; Liu, T. Prognostic significance of CDKN2A/B deletions in acute lymphoblastic leukaemia: A meta-analysis. *Ann. Med.* **2019**, *51*, 28–40. [CrossRef]
13. van Galen, J.C.; Kuiper, R.P.; van Emst, L.; Levers, M.; Tijchon, E.; Scheijen, B.; Waanders, E.; van Reijmersdal, S.V.; Gilissen, C.; van Kessel, A.G.; et al. BTG1 regulates glucocorticoid receptor autoinduction in acute lymphoblastic leukemia. *Blood* **2010**, *115*, 4810–4819. [CrossRef]
14. Harrison, C.J.; Haas, O.; Harbott, J.; Biondi, A.; Stanulla, M.; Trka, J.; Izraeli, S. Biology and Diagnosis Committee of International Berlin-Frankfurt-Munster study, g. Detection of prognostically relevant genetic abnormalities in childhood B-cell precursor acute lymphoblastic leukaemia: Recommendations from the Biology and Diagnosis Committee of the International Berlin-Frankfurt-Munster study group. *Br. J. Haematol.* **2010**, *151*, 132–142. [CrossRef]
15. Rack, K.A.; van den Berg, E.; Haferlach, C.; Beverloo, H.B.; Costa, D.; Espinet, B.; Foot, N.; Jeffries, S.; Martin, K.; O'Connor, S.; et al. European recommendations and quality assurance for cytogenomic analysis of haematological neoplasms. *Leukemia* **2019**, *33*, 1851–1867. [CrossRef]

16. Usvasalo, A.; Elonen, E.; Saarinen-Pihkala, U.M.; Raty, R.; Harila-Saari, A.; Koistinen, P.; Savolainen, E.R.; Knuutila, S.; Hollmen, J. Prognostic classification of patients with acute lymphoblastic leukemia by using gene copy number profiles identified from array-based comparative genomic hybridization data. *Leuk. Res.* **2010**, *34*, 1476–1482. [CrossRef]
17. Mrozek, K. Cytogenetic, molecular genetic, and clinical characteristics of acute myeloid leukemia with a complex karyotype. *Semin. Oncol.* **2008**, *35*, 365–377. [CrossRef]
18. Coccaro, N.; Anelli, L.; Zagaria, A.; Specchia, G.; Albano, F. Next-Generation Sequencing in Acute Lymphoblastic Leukemia. *Int. J. Mol. Sci.* **2019**, *20*. [CrossRef]
19. Rehm, H.L.; Hynes, E.; Funke, B.H. The Changing Landscape of Molecular Diagnostic Testing: Implications for Academic Medical Centers. *J. Pers. Med.* **2016**, *6*. [CrossRef]
20. Rehm, H.L. Evolving health care through personal genomics. *Nat. Rev. Genet.* **2017**, *18*, 259–267. [CrossRef]
21. Miller, E.M.; Patterson, N.E.; Zechmeister, J.M.; Bejerano-Sagie, M.; Delio, M.; Patel, K.; Ravi, N.; Quispe-Tintaya, W.; Maslov, A.; Simmons, N.; et al. Development and validation of a targeted next generation DNA sequencing panel outperforming whole exome sequencing for the identification of clinically relevant genetic variants. *Oncotarget* **2017**, *8*, 102033–102045. [CrossRef]
22. Lionel, A.C.; Costain, G.; Monfared, N.; Walker, S.; Reuter, M.S.; Hosseini, S.M.; Thiruvahindrapuram, B.; Merico, D.; Jobling, R.; Nalpathamkalam, T.; et al. Improved diagnostic yield compared with targeted gene sequencing panels suggests a role for whole-genome sequencing as a first-tier genetic test. *Genet. Med.* **2018**, *20*, 435–443. [CrossRef]
23. Pui, C.H.; Evans, W.E. Acute lymphoblastic leukemia. *New Engl. J. Med.* **1998**, *339*, 605–615. [CrossRef]
24. Forero-Castro, M.; Robledo, C.; Benito, R.; Abaigar, M.; Africa Martin, A.; Arefi, M.; Fuster, J.L.; de Las Heras, N.; Rodriguez, J.N.; Quintero, J.; et al. Genome-Wide DNA Copy Number Analysis of Acute Lymphoblastic Leukemia Identifies New Genetic Markers Associated with Clinical Outcome. *PLoS ONE* **2016**, *11*, e0148972. [CrossRef] [PubMed]
25. Montano, A.; Ordonez, J.L.; Alonso-Perez, V.; Hernandez-Sanchez, J.; Santos, S.; Gonzalez, T.; Benito, R.; Garcia-Tunon, I.; Hernandez-Rivas, J.M. ETV6/RUNX1 Fusion Gene Abrogation Decreases the Oncogenicity of Tumour Cells in a Preclinical Model of Acute Lymphoblastic Leukaemia. *Cells* **2020**, *9*. [CrossRef]
26. Kopanos, C.; Tsiolkas, V.; Kouris, A.; Chapple, C.E.; Albarca Aguilera, M.; Meyer, R.; Massouras, A. VarSome: The human genomic variant search engine. *Bioinformatics* **2019**, *35*, 1978–1980. [CrossRef]
27. Bastida, J.M.; Lozano, M.L.; Benito, R.; Janusz, K.; Palma-Barqueros, V.; Del Rey, M.; Hernandez-Sanchez, J.M.; Riesco, S.; Bermejo, N.; Gonzalez-Garcia, H.; et al. Introducing high-throughput sequencing into mainstream genetic diagnosis practice in inherited platelet disorders. *Haematologica* **2018**, *103*, 148–162. [CrossRef]
28. Chen, X.; Schulz-Trieglaff, O.; Shaw, R.; Barnes, B.; Schlesinger, F.; Kallberg, M.; Cox, A.J.; Kruglyak, S.; Saunders, C.T. Manta: Rapid detection of structural variants and indels for germline and cancer sequencing applications. *Bioinformatics* **2016**, *32*, 1220–1222. [CrossRef]
29. Forero-Castro, M.; Robledo, C.; Benito, R.; Bodega-Mayor, I.; Rapado, I.; Hernandez-Sanchez, M.; Abaigar, M.; Maria Hernandez-Sanchez, J.; Quijada-Alamo, M.; Maria Sanchez-Pina, J.; et al. Mutations in TP53 and JAK2 are independent prognostic biomarkers in B-cell precursor acute lymphoblastic leukaemia. *Br. J. Cancer* **2017**, *117*, 256–265. [CrossRef]
30. Schwab, C.J.; Jones, L.R.; Morrison, H.; Ryan, S.L.; Yigittop, H.; Schouten, J.P.; Harrison, C.J. Evaluation of multiplex ligation-dependent probe amplification as a method for the detection of copy number abnormalities in B-cell precursor acute lymphoblastic leukemia. *Geneschromosomes Cancer* **2010**, *49*, 1104–1113. [CrossRef]
31. Jaime-Pérez, J.C. El problema de la recaída en la leucemia linfoblástica aguda de la infancia. *Rev. De Hematol.* **2017**, *18*, 1–3.
32. Mullighan, C.G. New strategies in acute lymphoblastic leukemia: Translating advances in genomics into clinical practice. *Clin. Cancer Res.* **2011**, *17*, 396–400. [CrossRef]
33. Pui, C.H.; Evans, W.E. Treatment of acute lymphoblastic leukemia. *N. Engl. J. Med.* **2006**, *354*, 166–178. [CrossRef]
34. Inaba, H.; Greaves, M.; Mullighan, C.G. Acute lymphoblastic leukaemia. *Lancet* **2013**, *381*, 1943–1955. [CrossRef]
35. Brown, L.M.; Lonsdale, A.; Zhu, A.; Davidson, N.M.; Schmidt, B.; Hawkins, A.; Wallach, E.; Martin, M.; Mechinaud, F.M.; Khaw, S.L.; et al. The application of RNA sequencing for the diagnosis and genomic classification of pediatric acute lymphoblastic leukemia. *Blood Adv.* **2020**, *4*, 930–942. [CrossRef]

36. Gong, Z.; Medeiros, L.J.; Cortes, J.E.; Zheng, L.; Khoury, J.D.; Wang, W.; Tang, G.; Loghavi, S.; Luthra, R.; Yang, W.; et al. Clinical and prognostic significance of e1a2 BCR-ABL1 transcript subtype in chronic myeloid leukemia. *Blood Cancer J.* **2017**, *7*, e583. [CrossRef]
37. Emerenciano, M.; Meyer, C.; Mansur, M.B.; Marschalek, R.; Pombo-de-Oliveira, M.S.; Brazilian Collaborative Study Group of Infant Acute Leukaemia. The distribution of MLL breakpoints correlates with outcome in infant acute leukaemia. *Br. J. Haematol.* **2013**, *161*, 224–236. [CrossRef]
38. Meyer, C.; Burmeister, T.; Groger, D.; Tsaur, G.; Fechina, L.; Renneville, A.; Sutton, R.; Venn, N.C.; Emerenciano, M.; Pombo-de-Oliveira, M.S.; et al. The MLL recombinome of acute leukemias in 2017. *Leukemia* **2018**, *32*, 273–284. [CrossRef]
39. Paulsson, K.; Lilljebjorn, H.; Biloglav, A.; Olsson, L.; Rissler, M.; Castor, A.; Barbany, G.; Fogelstrand, L.; Nordgren, A.; Sjogren, H.; et al. The genomic landscape of high hyperdiploid childhood acute lymphoblastic leukemia. *Nat. Genet.* **2015**, *47*, 672–676. [CrossRef]
40. Andersson, A.K.; Ma, J.; Wang, J.; Chen, X.; Gedman, A.L.; Dang, J.; Nakitandwe, J.; Holmfeldt, L.; Parker, M.; Easton, J.; et al. The landscape of somatic mutations in infant MLL-rearranged acute lymphoblastic leukemias. *Nat. Genet.* **2015**, *47*, 330–337. [CrossRef]
41. Messina, M.; Chiaretti, S.; Wang, J.; Fedullo, A.L.; Peragine, N.; Gianfelici, V.; Piciocchi, A.; Brugnoletti, F.; Di Giacomo, F.; Pauselli, S.; et al. Prognostic and therapeutic role of targetable lesions in B-lineage acute lymphoblastic leukemia without recurrent fusion genes. *Oncotarget* **2016**, *7*, 13886–13901. [CrossRef]
42. Moorman, A.V.; Enshaei, A.; Schwab, C.; Wade, R.; Chilton, L.; Elliott, A.; Richardson, S.; Hancock, J.; Kinsey, S.E.; Mitchell, C.D.; et al. A novel integrated cytogenetic and genomic classification refines risk stratification in pediatric acute lymphoblastic leukemia. *Blood* **2014**, *124*, 1434–1444. [CrossRef]
43. Stanulla, M.; Dagdan, E.; Zaliova, M.; Moricke, A.; Palmi, C.; Cazzaniga, G.; Eckert, C.; Te Kronnie, G.; Bourquin, J.P.; Bornhauser, B.; et al. IKZF1(plus) Defines a New Minimal Residual Disease-Dependent Very-Poor Prognostic Profile in Pediatric B-Cell Precursor Acute Lymphoblastic Leukemia. *J. Clin. Oncol.* **2018**, *36*, 1240–1249. [CrossRef]
44. Marke, R.; van Leeuwen, F.N.; Scheijen, B. The many faces of IKZF1 in B-cell precursor acute lymphoblastic leukemia. *Haematologica* **2018**, *103*, 565–574. [CrossRef]
45. Harvey, R.C.; Mullighan, C.G.; Chen, I.M.; Wharton, W.; Mikhail, F.M.; Carroll, A.J.; Kang, H.; Liu, W.; Dobbin, K.K.; Smith, M.A.; et al. Rearrangement of CRLF2 is associated with mutation of JAK kinases, alteration of IKZF1, Hispanic/Latino ethnicity, and a poor outcome in pediatric B-progenitor acute lymphoblastic leukemia. *Blood* **2010**, *115*, 5312–5321. [CrossRef]
46. Cario, G.; Zimmermann, M.; Romey, R.; Gesk, S.; Vater, I.; Harbott, J.; Schrauder, A.; Moericke, A.; Izraeli, S.; Akasaka, T.; et al. Presence of the P2RY8-CRLF2 rearrangement is associated with a poor prognosis in non-high-risk precursor B-cell acute lymphoblastic leukemia in children treated according to the ALL-BFM 2000 protocol. *Blood* **2010**, *115*, 5393–5397. [CrossRef]
47. Meyer, L.K.; Delgado-Martin, C.; Maude, S.L.; Shannon, K.M.; Teachey, D.T.; Hermiston, M.L. CRLF2 rearrangement in Ph-like acute lymphoblastic leukemia predicts relative glucocorticoid resistance that is overcome with MEK or Akt inhibition. *PLoS ONE* **2019**, *14*, e0220026. [CrossRef]
48. Chiaretti, S.; Messina, M.; Foa, R. BCR/ABL1-like acute lymphoblastic leukemia: How to diagnose and treat? *Cancer* **2019**, *125*, 194–204. [CrossRef]

Chapter II. Integrated genomic analysis of chromosomal alterations and mutations in B-cell acute lymphoblastic leukemia reveals distinct genetic profiles at relapse

Maribel Forero-Castro[1,†], Adrián Montaño[2,†], Cristina Robledo[2], Alfonso García de Coca[3], José Luis Fuster[4], Natalia de las Heras[5], José Antonio Queizán[6], María Hernández-Sánchez[2], Luis A. Corchete-Sánchez[2,7], Marta Martín-Izquierdo[2], Jordi Ribera[8], José-María Ribera[9], Rocío Benito[2,*,‡] and Jesús M. Hernández-Rivas[2,7,10,*,‡]

*†These authors contributed equally to this work. ‡Sharing senior authorship. *Correspondence.*

[1]Escuela de Ciencias Biológicas, Universidad Pedagógica y Tecnológica de Colombia. Avenida Central del Norte 39-115, Tunja 150003, Boyacá, Colombia. [2]IBSAL, IBMCC, Universidad de Salamanca-CSIC, Cancer Research Center, Campus Miguel de Unamuno, 37007 Salamanca, Spain. [3]Servicio de Hematología, Hospital Clínico de Valladolid, Av. Ramón y Cajal, 3, 47003 Valladolid, Spain. [4]Servicio de Oncohematología Pediátrica, Hospital Universitario Virgen de la Arrixaca, Murcia, Ctra. Madrid-Cartagena, s/n, 30120 Murcia, El Palmar, Spain. [5]Servicio de Hematología, Hospital Virgen Blanca, Altos de Nava s/n, 24071 León, Spain. [6]Servicio de Hematología, Hospital General de Segovia, C/Luis Erik Clavería Neurólogo S/N, 40002 Segovia, Spain. [7]Servicio de Hematología, Hospital Universitario de Salamanca, Paseo de San Vicente, 88-182, 37007 Salamanca, Spain. [8]Acute Lymphoblastic Leukemia Group, Josep Carreras Leukaemia Research Institute, Carretera de Canyet, s/n, Barcelona, 08916 Badalona, Spain. [9]Servicio de Hematología Clínica, Institut Català d'Oncologia, Hospital Germans Trias i Pujol, Josep Carreras Research Institute, Universitat Autònoma de Barcelona, Carretera de Canyet, s/n, Barcelona, 08916 Badalona, Spain. [10]Departamento de Medicina, Universidad de Salamanca, Campus Miguel de Unamuno. C/Alfonso X El Sabio s/n, 37007 Salamanca, Spain.

Diagnostics 2020, 10(7), 455. doi:10.3390/diagnostics10070455

diagnostics

MDPI

Article

Integrated Genomic Analysis of Chromosomal Alterations and Mutations in B-Cell Acute Lymphoblastic Leukemia Reveals Distinct Genetic Profiles at Relapse

Maribel Forero-Castro [1,†], Adrián Montaño [2,†], Cristina Robledo [2], Alfonso García de Coca [3], José Luis Fuster [4], Natalia de las Heras [5], José Antonio Queizán [6], María Hernández-Sánchez [2], Luis A. Corchete-Sánchez [2,7], Marta Martín-Izquierdo [2], Jordi Ribera [8], José-María Ribera [9], Rocío Benito [2,*,‡] and Jesús M. Hernández-Rivas [2,7,10,*,‡]

1 Escuela de Ciencias Biológicas, Universidad Pedagógica y Tecnológica de Colombia. Avenida Central del Norte 39-115, Tunja 150003, Boyacá, Colombia; maribel.forero@uptc.edu.co
2 IBSAL, IBMCC, Universidad de Salamanca-CSIC, Cancer Research Center, Campus Miguel de Unamuno, 37007 Salamanca, Spain; adrianmo18@gmail.com (A.M.); crisrmontero@hotmail.com (C.R.); mahesa2504@hotmail.com (M.H.-S); lacorsan@hotmail.com (L.A.C.-S.); marta.martini@usal.es (M.M.-I.)
3 Servicio de Hematología, Hospital Clínico de Valladolid, Av. Ramón y Cajal, 3, 47003 Valladolid, Spain; agarciaco@saludcastillayleon.es
4 Servicio de Oncohematología Pediátrica, Hospital Universitario Virgen de la Arrixaca, Murcia, Ctra. Madrid-Cartagena, s/n, 30120 Murcia, El Palmar, Spain; josel.fuster@carm.es
5 Servicio de Hematología, Hospital Virgen Blanca, Altos de Nava s/n, 24071 León, Spain; ndelasheras22@hotmail.com
6 Servicio de Hematología, Hospital General de Segovia, C/Luis Erik Clavería Neurólogo S/N, 40002 Segovia, Spain; jqueizan@saludcastillayleon.es
7 Servicio de Hematología, Hospital Universitario de Salamanca, Paseo de San Vicente, 88-182, 37007 Salamanca, Spain
8 Acute Lymphoblastic Leukemia Group, Josep Carreras Leukaemia Research Institute, Carretera de Canyet, s/n, Barcelona, 08916 Badalona, Spain; jribera@carrerasresearch.org
9 Servicio de Hematología Clínica, Institut Català d'Oncologia, Hospital Germans Trias i Pujol, Josep Carreras Research Institute, Universitat Autònoma de Barcelona, Carretera de Canyet, s/n, Barcelona, 08916 Badalona, Spain; jribera@iconcologia.net
10 Departamento de Medicina, Universidad de Salamanca, Campus Miguel de Unamuno. C/Alfonso X El Sabio s/n, 37007 Salamanca, Spain
* Correspondence: beniroc@usal.es (R.B.); jmhr@usal.es (J.M.H.-R.); Tel.: +34-923294812 (R.B.); +34-923291384 (J.M.H.-R.)
† These authors contributed equally to this work.
‡ Sharing senior authorship.

Received: 17 June 2020; Accepted: 2 July 2020; Published: 4 July 2020

Abstract: The clonal basis of relapse in B-cell precursor acute lymphoblastic leukemia (BCP-ALL) is complex and not fully understood. Next-generation sequencing (NGS), array comparative genomic hybridization (aCGH), and multiplex ligation-dependent probe amplification (MLPA) were carried out in matched diagnosis–relapse samples from 13 BCP-ALL patients to identify patterns of genetic evolution that could account for the phenotypic changes associated with disease relapse. The integrative genomic analysis of aCGH, MLPA and NGS revealed that 100% of the BCP-ALL patients showed at least one genetic alteration at diagnosis and relapse. In addition, there was a significant increase in the frequency of chromosomal lesions at the time of relapse ($p = 0.019$). MLPA and aCGH techniques showed that *IKZF1* was the most frequently deleted gene. *TP53* was the most frequently mutated gene at relapse. Two *TP53* mutations were detected only at relapse, whereas the three others showed an increase in their mutational burden at relapse. Clonal evolution patterns

were heterogeneous, involving the acquisition, loss and maintenance of lesions at relapse. Therefore, this study provides additional evidence that BCP-ALL is a genetically dynamic disease with distinct genetic profiles at diagnosis and relapse. Integrative NGS, aCGH and MLPA analysis enables better molecular characterization of the genetic profile in BCP-ALL patients during the evolution from diagnosis to relapse.

Keywords: acute lymphoblastic leukemia (ALL); relapse; next-generation sequencing (NGS); array comparative genomic hybridization (aCGH); multiplex ligation-dependent probe amplification (MLPA); *IKZF1*; *TP53*

1. Introduction

Acute lymphoblastic leukemia (ALL) is a disease with specific genetic alterations associated with drug resistance, treatment failure and disease relapse [1,2]. Despite vast improvements in the treatment of childhood and adult ALL in recent years, the outlook for relapsed leukemia remains poor, highlighting the need for innovative treatment approaches [3]. It is well known that relapsed ALL is a heterogeneous disease and that distinct genetic alterations may be unique to small subgroups of patients [3]. Genomic studies of matched diagnosis–relapse samples from ALL patients have shed light on the clonal evolution that leads to relapse, the pathways associated with chemoresistance, and the potential targets for therapy [4–9]. However, the mechanisms that probably fuel an ALL relapse are not fully understood. A combined analysis of gene mutations and copy number alterations (CNAs) could provide valuable insight into the discovery of the patterns of clonal evolution and the biomarkers that predict a greater likelihood of relapse in ALL [3,10,11]. Here, we have performed an integrated and sequential genomic analysis combining next-generation sequencing (NGS), array comparative genomic hybridization (aCGH), and multiplex ligation-dependent probe amplification (MLPA) to identify the clonal shifts related to ALL progression.

2. Materials and Methods

2.1. Patients

Thirteen paired diagnosis and first relapse samples of B-cell precursor acute lymphoblastic leukemia (BCP-ALL) patients (4 children and 9 adults) were eligible for this study. The patients were treated in accordance with the risk-adapted protocols of PETHEMA (Programa Español de Tratamientos en Hematología) and SEHOP (Sociedad Española de Hematología y Oncología Pediátrica). The diagnosis of ALL was based on morphological, immunophenotypic and genetic features of leukemic blast cells, as described previously [12]. The patients' demographic information, clinical characteristics, risk classification, response to therapy and survival were recorded. The study was approved by the local ethical committee, the Comité Ético de Investigación Clínica, at the Hospital Universitario de Salamanca. Written informed consent was obtained from each patient or their legal guardian before entering the study.

Table 1 shows the characteristics of the patients included in this study. The median age was 31 years (range 4–80 years). The median percentage of blast counts in their bone marrow was 82% (range 45–96%). Fifty-four per cent of the patients had none of the chromosomal abnormalities associated with poor risk (t(9;22), t(v;11q23) or hypodiploidy). Ninety-two per cent of patients died presenting a 5-year overall survival probability of 15% (median: 22 months, 95% CI: 3.2–40.8 (Table 1 and Table S1)).

Table 1. Characteristics of the patients with B-cell precursor acute lymphoblastic leukemia (BCP-ALL) included in the study.

Characteristics	Patients (n = 13)
Age at diagnosis (years), median (range)	31 (4–80)
Male/Female, (%)	3/10 (23.1/76.9)
Bone marrow blast [1], median (range)	82 (45–96)
White blood cell count (×109/L), median (range)	27 (3–168)
Hb count (g/L), median (range)	105 (39–160)
Platelet count (×109/L), median (range)	73 (29–248)
Elevated LDH, (U/L) level, (%)	66.7
Cytogenetics	
Poor risk [2] (%)	46.2
Others (%)	53.8
Risk group [3]	
Low risk (%)	7.7
Intermediate risk (%)	23.1
High risk (%)	69.2
Time to relapse	
Very early relapse [4] (%)	53.8
Early relapse [4] (%)	15.4
Late relapse [4] (%)	30.8
5-year overall survival probability % (median, 95% CI)	15.3 (22, 3.2–40.8)

[1] Estimated by flow cytometry. [2] Includes the unfavorable abnormalities t(9;22), t(v;11q23) and hypodiploidy. [3] Risk group stratification was mainly designated according to the Programa Español de Tratamientos en Hematología (PETHEMA) protocols. [4] Time of relapse criteria: very early, earlier than 18 months after initial diagnosis and less than 6 months after the cessation of frontline treatment; early, more than 18 months after initial diagnosis, but less than 6 months after the cessation of frontline treatment; late, more than 6 months after the cessation of frontline treatment.

2.2. DNA Isolation and Next-Generation Sequencing Assay (NGS)

Genomic DNA was extracted from frozen fixed bone marrow cell samples with a QIAmp DNA Mini Kit (Qiagen, Valencia, CA, USA) following the manufacturer's instructions. The mutational status of the *JAK2* (exons 12 to 16), *PAX5* (exons 2 and 3), *LEF1* (exons 2 and 3), *CRLF2* (exon 6), *IL7R* (exon 5) and *TP53* (exons 4–11) genes was investigated using two preconfigured 96-well primer plates (Roche, Branford, CT, USA) with titanium amplicon chemistry (454 Life Sciences, Branford, CT, USA). The above-mentioned genes were selected due to their well-defined roles as mutational hot spots in BCP-ALL [13–23]. A variant analysis was performed using GS Amplicon Variant Analyzer 2.5.3 (454 Life Sciences, Roche Applied Science) and Sequence Pilot version 3.4.2 (JSI Medical Systems, Kippenheim, Germany) software [24,25]. The variants were filtered to display the sequence variants occurring in more than 2% of bidirectional reads per amplicon in at least one patient [26–28]. All somatic mutations were searched on the online COSMIC database—Catalogue of Somatic Mutations in Cancer (http://cancer.sanger.ac.uk/cancergenome/projects/cosmic) and the IARC *TP53* database—International Agency for Research on Cancer (http://p53.iarc.fr/p53Sequences.aspx) [29]. The sequence variations identified by NGS were independently validated using conventional Sanger sequencing and/or a separate setup of the NGS re-sequencing run.

2.3. Oligonucleotide Array Comparative Genomic Hybridizations (Array-CGH)

All samples were tested on an aCGH 12X135K array platform (Roche NimbleGen, Madison, WI, USA). Raw $\log_2$ ratios were segmented using the copy number R package (version 1.20.0) [30]. We used the GISTIC algorithm—(version 2.0.23) to identify statistically significant minimal common altered regions (MCRs) and the broad CNAs present in the samples [31]. The Database of Genomic Variants from Toronto (DGV, http://dgv.tcag.ca/dgv/app/home) was used to exclude DNA variations located in regions with defined copy number variations. All CNAs with an overlap of more than 50% with respect to those reported in the DGV were excluded.

2.4. Multiplex Ligation-Dependent Probe Amplification (MLPA)

MLPA reactions were performed using the SALSA MLPA P335-B1 ALL-IKZF1 probemix (MRC-Holland, Amsterdam, Netherlands) according to the manufacturer's instructions. DNA samples from three healthy donors were used as controls. The P335-B1 probemix contains probes for the following genes: *IKZF1*, *CDKN2A/B*, *PAX5*, *EBF1*, *ETV6*, *BTG1*, *RB1*, as well as genes from the X/Y PAR1 region (*CRLF2*, *CSF2RA*, *IL3RA* and *P2RY8*). MLPA amplification products were analyzed on an ABI 3130xl Genetic Analyzer (Applied Biosystems/Hitachi) with GeneMapper software V.3.7, using the Genescan 500LIZ internal size standard (Applied Biosystems). The copy number at each locus was estimated according to Schwab et al. [32].

According to the probemix contained in the P335-B1 MLPA kit, an integrative MLPA–aCGH analysis was performed to identify gene deletions in the *IKZF1*, *CDKN2A/B*, *PAX5*, *EBF1*, *ETV6*, *BTG1* and *RB1* genes, as well as genes from the X/Y *PAR1* region (*CRLF2, CSF2RA, IL3RA* and *P2RY8*). The copy number at each locus was estimated according to the method of Schwab et al. [32], whereby values above 1.3, between 1.3 and 0.75, between 0.75 and 0.25, and below 0.25 were considered as gain, normal, hemizygous loss, and homozygous loss, respectively. It was possible to distinguish the gene deletions identified either by MLPA or by aCGH analysis, or by the both methods. The distributions of the probes in each platform are illustrated in Figure S1.

2.5. Statistical Methods

The differences between groups were compared by the chi-square, Fisher's exact, and Mann–Whitney tests, as appropriate. Values of $p < 0.05$ were considered to be statistically significant. Analyses were conducted using IBM SPSS version 21.0 (IBM Corp., Armonk, NY, USA).

The materials, procedures and statistical analyses are described in detail in the Supplementary File 1.

3. Results

3.1. Recurring Genomic Alterations in Matched Diagnosis–Relapse BCP-ALL Samples

The aCGH detected 1451 somatic genetic lesions in 13 paired (diagnosis and relapse) BCP-ALL samples. The number of genetic lesions varied significantly between patients (1–287 lesions; median, 16 per sample). There were no significant differences in the number of CNAs between children and adults ($p = 0.765$), or between patients who had early relapses and those who did not ($p = 0.731$). Figures 1 and 2 and Figure S2 show the main aCGH findings at diagnosis and relapse, with a significant increase in the number of lesions at relapse. There was a median of six alterations per sample at diagnosis and of 47 at relapse ($p = 0.019$).

Figures 1 and 2 and Figure S2 show the patterns and frequencies of DNA copy alterations observed in the 13 paired diagnosis/relapse samples. The most recurrent broad and focal copy number changes observed at diagnosis and/or relapse were: dup(1q) at 23%, dup(X) at 31%, dup(21) at 15%, del(7 or 7p) at 77%, dup(7q) at 31%, del(9p) at 62%, del(12p) at 15%, del(13q) at 23% and del(17p) at 15%. Of these, the deletions located on 7p and 9p were the most frequently focal and broad chromosomal alterations detected at diagnosis and/or relapse (77% and 62%, respectively (Table S1)).

Our integrative MLPA–aCGH analysis showed that the percentages of deleted genes in the following paired diagnosis/relapse BCP-ALL samples were: *IKZF1*, 54% vs. 62%, $p = 0.691$; *CDKN2A/B*, 54% vs. 23%, $p = 0.107$; *PAX5*, 38% vs. 23%, $p = 0.673$; *EBF1*, 23% vs. 15%, $p = 1.000$; *BTG1*, 23% vs. 23%, $p = 1.000$; *ETV6*, 15% vs. 15%, $p = 1.000$; *RB1*, 8% vs. 15%, $p = 1.000$, and *PAR1*, 15% vs. 8%, $p = 1.0$. Thus, no statistically significant differences in the frequency of these gene deletions were found between diagnosis and relapse. Figure 3 compares the main complementary findings at the two points in disease evolution by MLPA and/or aCGH techniques.

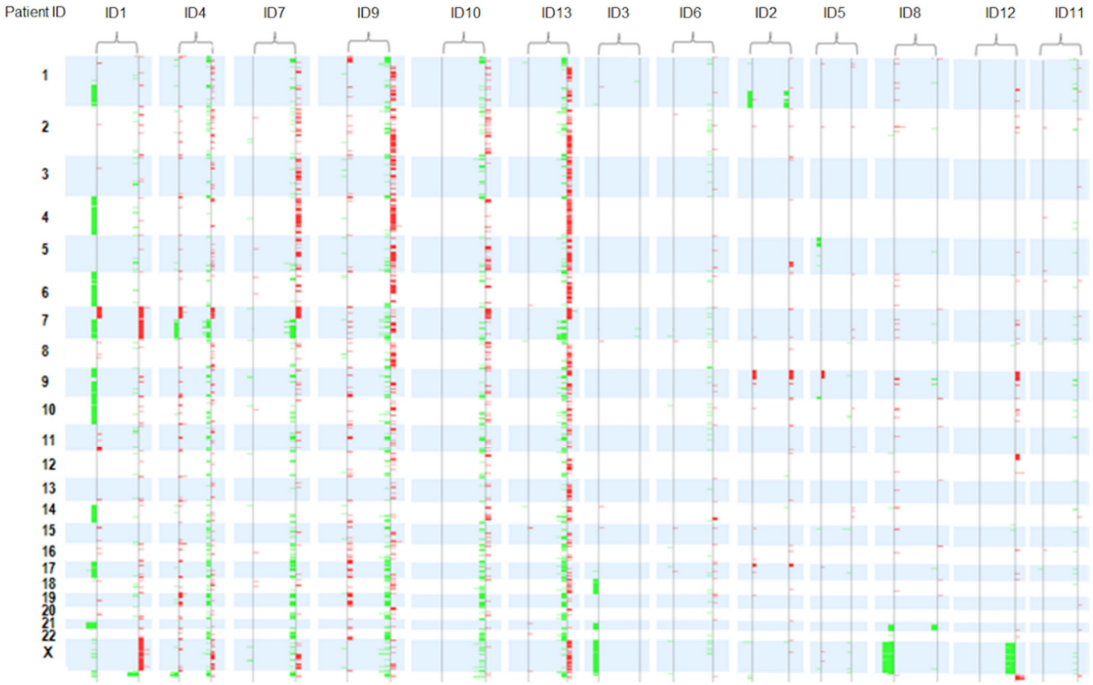

Figure 1. Summary of array comparative genomic hybridization results in 13 paired diagnosis and relapse samples. All patients exhibited heterogeneous changes in the pattern of copy number alterations (CNAs) from diagnosis to relapse. The paired diagnostic/relapse samples were ordered from highest to lowest number of CNAs. Losses: green. Gains: red.

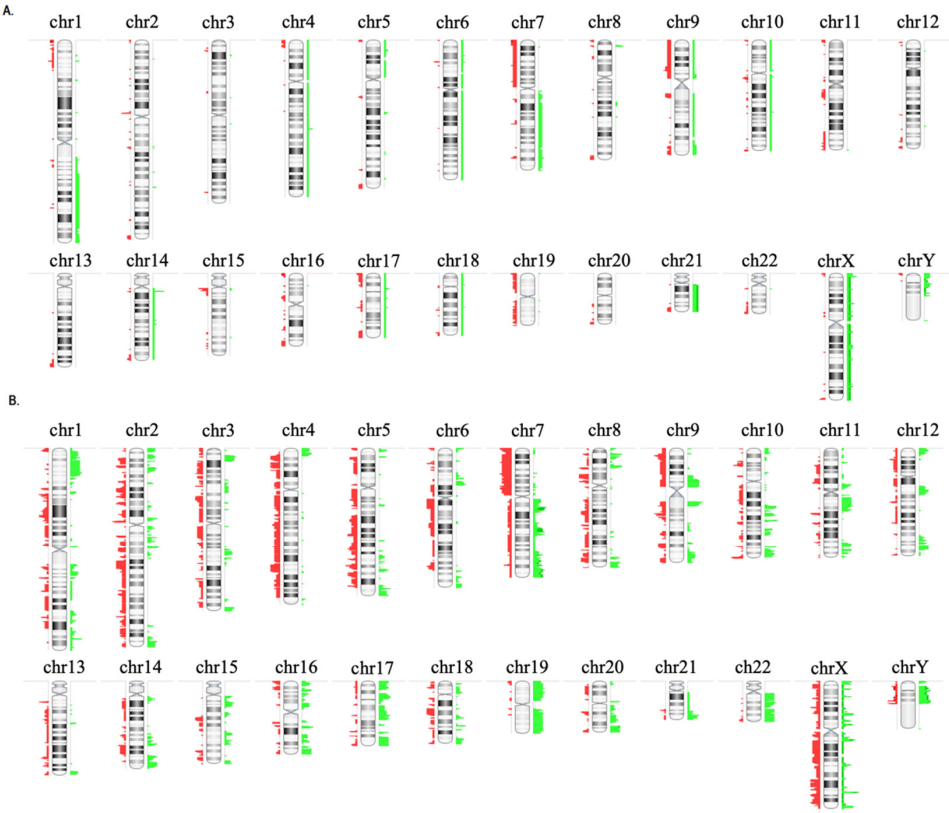

Figure 2. Copy number alterations observed in 13 paired diagnostic/relapse samples. (**A**) CNAs observed in all samples at diagnosis, (**B**) CNAs observed in all samples at relapse. To the right of each chromosome the regions with gains are shown in green and to the left the regions with losses are shown in red.

Patient ID	ID1		ID2		ID3		ID4		ID5		ID6		ID7		ID8		ID9		ID10		ID11		ID12		ID13	
Genes**	D	R	D	R	D	R	D	R	D	R	D	R	D	R	D	R	D	R	D	R	D	R	D	R	D	R
IKZF1	*	+					*	*			*	&		*	*		+	&		+	+		&	*		*
CDKN2A/B			*	*	+				*						*		*		+				*	*		+
PAX5			*	*					*						+		*	&					*	*		
EBF1							+										*	*			*					+
BTG1															*		*	+					*	&		+
ETV6	&																	*					*	*		
RB1															*			+								+
PAR1 region		+					+										+									

Abbreviations: D: diagnosis; R: relapse; *: gene deletions identified by a multiplex ligation-dependent probe amplification (MLPA) and array comparative genomic hybridization (aCGH) analysis; +: gene deletions identified by an aCGH analysis only; &: gene deletions identified by a MLPA analysis only.

Figure 3. Gene deletions identified by an integrative MLPA–aCGH analysis. ** The P335-B1 probemix contains probes for the following genes: *IKZF1* (eight probes at 7p12.2), *CDKN2A/B* (three probes at 9p21.3), *PAX5* (seven probes at 9p13.2), *EBF1* (four probes at 5q33.3), *ETV6* (six probes at 12p13.2), four probes for *BTG1* and the *BTG1* downstream region (at 12q21.33), *RB1* (five probes at 13q14.2), as well as genes from the X/Y *PAR1* region (*CRLF2*, *CSF2RA*, *IL3RA* and *P2RY8* (five probes at Xp22.33)). Additionally, there is one probe at Yp11.31 (*ZFY*) and one at 9p24.1.

A NGS analysis revealed six mutations in 4/13 (31%) patients (three children: ID2, ID3, ID4, and one adult: ID7)) at diagnosis and/or relapse. Notably, three of them (ID2, ID3 and ID4) did not have poor risk cytogenetics at diagnosis. Likewise, it should be mentioned that two of them were treated at diagnosis with high risk protocols (ID2 and ID7), one with an intermediate risk protocol (ID4) and one with a low risk protocol (ID3 (Table S1)). Of these six mutations, a sequence analysis revealed three missense mutations, one splicing site mutation and two deletion-insertions. *TP53* was the most frequently mutated gene (4/13, 31%), whereas *PAX5* was only mutated in one adult patient (ID7 (1/13, 8%)). Interestingly, two *TP53* mutations were only detected at relapse (ID3: c.829_842delins14 and ID7: c.-8_4del12), whereas the remaining were present from diagnosis and maintained at relapse (ID2: 817_821delinsGACCC, ID4: c.832C > T, ID7: c.818G > C (Table 2)).

The complementary integrative genomic analysis using aCGH, MLPA and NGS revealed that 100% of ALL patients showed at least one genetic alteration at diagnosis and relapse (mutation, loss and/or gain, or chromosomal rearrangement identified by Fluorescence in situ hybridization (FISH)). The frontline risk-adapted protocols, outcome, clinical status, karyotype, FISH, NGS, aCGH and MLPA analysis of each patient are shown in Table S1.

3.2. Heterogeneous Patterns of Genetic Evolution in Paired Diagnosis and Relapse Samples

Tables S2–S4 show the regions of statistically significant recurrent amplification and deletion that were retained, lost, or acquired as new lesions at relapse, respectively (*q-value* < 0.05).

The statistically significant peaks retained at relapse included gains on 10q26.13 (*FAM53B)*, 15q11.2 and losses on 1p36.32, 5p15.33, 9p21.3 (*PTPLAD2, MLLT3*), 9p21.2 (*CDKN2A*, *CDKN2B*, *DMRTA1*)

and 10q26.3. The significant peaks lost at relapse included losses on 8q24.3 and 19p13.3 (*TCF3*, *E2A*). Finally, the significant peaks acquired as new lesions at relapse included gains on 1p36, 1q21, 2p13.3 (*DYSF*), 3q21, 4p16, 5q33.1 (*PDGFRB*), 7q36.1 (*EZH*), 10q25.2, (*ADD3*), 14q32.31 (*BCL11B*), and losses on 9q34.2 and 13q34.

Table 2. Description of somatic mutations observed in diagnosis–relapse BCP-ALL patients. All three TP53 mutations retained at relapse increased their mutational burden to relapse (c.818G > C from 3.5% to 26%, c.832C > T from 11% to 21% and 817_821delinsGACCC from 53% to 71%).

Patient ID	Gene	Type of Mutation	Mutation	AA Change	Database	Moment	Mutational Burden
ID2	*TP53-E08*	Indel	c.817_821delinsGACCC	p.R273_V274delinsDP	Undescribed	Diagnosis	53%
						Relapse	71%
ID4	*TP53-E08*	Missense	c.832C > T	p.P278S	COSM10939/*TP53* website http://p53.fr/	Diagnosis	11%
						Relapse	21%
ID7	*PAX5-E03*	Missense	c.399T > A	p.S133R	Undescribed	Diagnosis only	20%
	TP53-E08	Missense	c.818G > C	p.R273P	COSM165077/*TP53* website http://p53.fr	Diagnosis	3.5%
						Relapse	26%
	TP53-E05	Splicing	c.-8_4del12	Splice_Intron 5 SA	*TP53* website http://p53.fr	Relapse only	15%
ID3	*TP53-E05*	Missense	c.829_842delins14	p.C277_D281delinsGPQG	Undescribed	Relapse only	90%

An integrative analysis showed that all patients exhibited heterogeneous changes in the pattern of CNAs from diagnosis to relapse, indicating that the profile of the relapse samples was genomically distinct: 8% of patients acquired only new genetic lesions at relapse, 38% of patients acquired new lesions and lost lesions present at diagnosis, and 54% of the patients simultaneously retained, lost and acquired lesions at relapse (Figures 2–4).

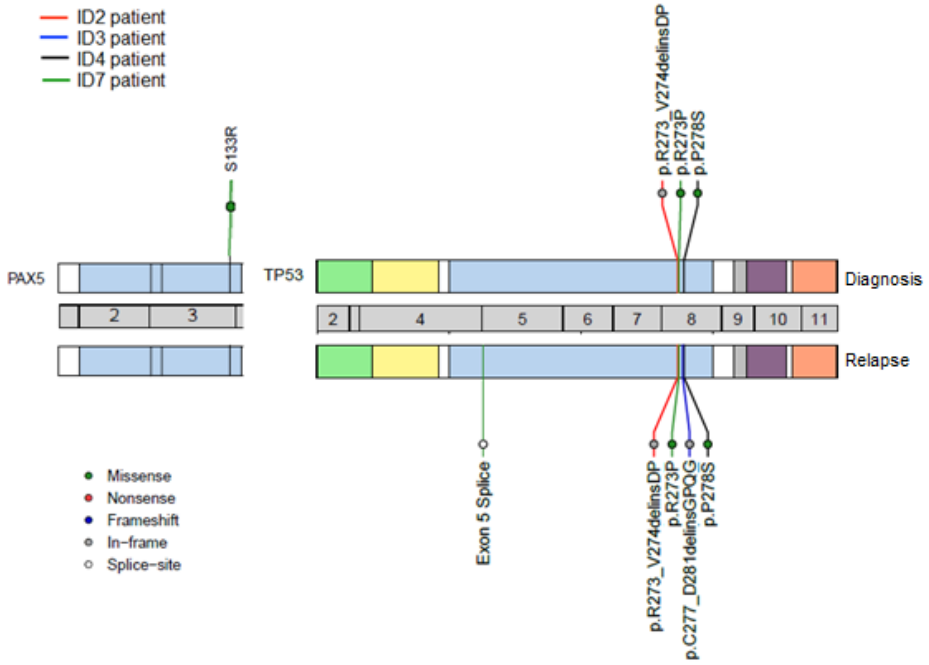

Figure 4. Mutations identified by next-generation sequencing (NGS) showed patterns of genetic evolution in paired diagnostic/relapse samples. Patient ID2 (red line) and Patient ID4 (black line): retained mutations in the *TP53* gene. Patient ID7 (green line): retained one mutation in the *TP53* gene, acquired a new mutation in the *TP53* gene and lost one mutation in the *PAX5* gene at relapse. Patient ID3 (blue line): acquired a new mutation in the *TP53* gene at relapse.

The MLPA–aCGH analysis revealed that most of the patients (5/7, 71%) with deletions of *IKZF1* (7p) at diagnosis retained this genetic alteration at relapse (children: ID1 and ID4, and adults: ID6, ID9 and ID12). By contrast, only three (ID2, ID9, ID12) of seven patients (42.9%) with *CDKN2A/B* and/or *PAX5* deletions (9p) retained these deletions at relapse. It should be noted that the adult patient ID13, who presented an elevated number of CNAs at relapse, acquired new lesions in the chromosomal regions that harbored the *EBF1, CDKN2A/B, IKZF1, BTG1* and *RB1* genes. Finally, the losses on 17p were also identified in two patients (child ID2 and adult ID9) at diagnosis, being retained at relapse in child ID2. An insertion/deletion mutation in *TP53* was also identified in this pediatric patient at diagnosis and relapse (Tables S1 and S2, Figures 1, 3 and 4).

Table 2 details the mutations observed at both times and describes their mutational burden. Interestingly, two *TP53* mutations were acquired at relapse (ID3, ID7), whereas all three *TP53* mutations, which were detected from diagnosis, had an increase in their mutational burden at relapse (ID2, ID4, ID7 (Figure 5)). Thus, in the pediatric patient ID2, an increase in the *TP53* mutant clone burden was observed at relapse (53% to 71%), as well as in the pediatric patient ID4 (11% to 21%) and the adult patient ID7 (3.5% to 26%), respectively.

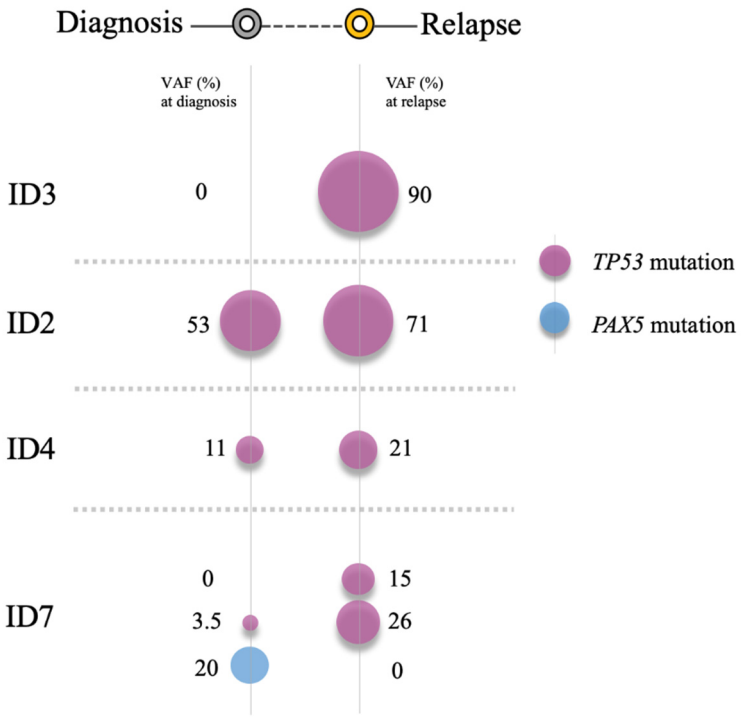

Figure 5. Clonal changes of mutations detected in paired diagnostic/relapse samples. Patient ID2 and Patient ID4 retained TP53 mutations, thereby increasing their mutational burden. Patient ID7 acquired a *TP53* mutation at relapse and maintained another in *TP53* from diagnosis, and showed a loss of *PAX5* mutation at relapse. Patient ID3 had acquired a *TP53* mutation by the time of relapse.

It is worth mentioning that the pediatric patient ID3, who was stratified as at low risk of disease at diagnosis, had acquired a mutation in *TP53* by relapse. Likewise, it should be noted that one adult patient (ID7) showed a co-occurrence of mutations in two different genes, *TP53* and *PAX5*. In the *TP53* gene, the splice mutation (c.-8_4del12) was detected only at relapse (mutational burden: 15%) whereas the missense mutation (c.818G > C) was present at both times (mutational burden: 3.5% vs. 26%). In the *PAX5* gene, only one missense mutation (c.399T > A) was observed at diagnosis (mutational burden: 20%). This patient had also acquired a deletion in the *IKZF1* gene by relapse (Table S1 and Figure 3 and Figure S3). The integrative NGS, aCGH, and MLPA analysis enabled a

better molecular characterization of the genetic profile in ALL patients during the evolution of their disease from diagnosis to relapse.

4. Discussion

The present study, carried out in sequential ALL patients at diagnosis and relapse, showed that all 13 ALL patients exhibited heterogeneous clonal changes in terms of CNAs and mutations between diagnosis and relapse, involving the acquisition, loss and maintenance of lesions at relapse. The shared lesions between the relapse clone and the predominant clone at diagnosis suggest a common pre-leukemic origin [22], while the acquired lesions provide unequivocal evidence of a second clone that was present as a minor population at diagnosis, but acquired different genetic alterations before emerging as the relapse clone [5].

An integrated NGS, aCGH, and MLPA analysis allowed for the identification of alterations on the *IKZF1* (7p) and *TP53* (17p) genes in paired diagnostic and relapse samples; these were more frequent at relapse than at diagnosis. Both genetic events could have strongly influenced disease relapse and the short survival of these patients. In this study, *TP53* is the most frequently mutated gene at relapse (31%). *TP53* abnormalities (deletion and/or mutation) have been associated with a resistance to treatment and worse prognosis in childhood and adult ALL [8,33]. *TP53* gene abnormalities have a key role in ALL relapse, as they independently predict a high risk of treatment failure in ALL patients [8,24,34]. The presence of *TP53* alterations has been associated with a reduced response rate to induction therapy and correlated with a shortened duration of survival, even after successful reinduction therapy [35,36]. Different therapeutic strategies to target mutant p53 have been developed for the high risk *TP53*-mutant ALL, such as the use of the small molecule APR-246 which exhibits antileukemia activity in *TP53*mut BCP-ALL, targeting non-functional mutant p53 and restoring its tumor suppressive function [37].

IKZF1 was the most frequently deleted gene, the incidence of deletions being greater at relapse than at diagnosis. Similarly, as seen in previous studies, the frequency of *IKZF1* deletions was higher in adults than in children [38]. *IKZF1* deletions have been associated with a higher risk of relapse in ALL and have been shown to be a hallmark of *BCR-ABL1*-positive ALL, although they have also been identified in a fraction of *BCR-ABL1*-negative ALL patients [10,38–43], as noted in our study. In recent years, *IKZF1* deletions and *TP53* alterations are being recognized as important markers of poor prognosis in ALL after a first relapse, mainly in children [9,39,44]. Therefore, these alterations could contribute to the re-stratification of risk for ALL patients and to proposing timely therapeutic strategies such as treatment intensification and identifying candidates for transplantation or for inclusion in clinical trials due to their high risk of suffering a second relapse [34,45,46].

In the present study, heterogeneous patterns of genetic evolution in paired diagnostic and relapse samples were observed that are consistent with those reported in previous studies [47]. In particular, two *TP53* mutations were only detected at relapse (patients ID3 and ID7), whereas all three *TP53* mutations increased their mutational burden between diagnosis and relapse (patients ID2, ID4 and ID7). It should be noted that two of the six *TP53* mutations identified had not been reported in the genomic databases.

ALL is clonally heterogeneous and genetic lesions in minor clones may confer resistance to therapy and promote disease relapse (e.g., *TP53*, *IKZF1*, *CREBBP*) [22]. The low proportion of the minor relapse subclone at diagnosis suggests that the leukemia at diagnosis contains genetically diverse subclones. Therapy would aim to select the eventual dominant relapse clone whose alterations confer resistance to treatment [48]. Thus, *TP53* mutations could be considered as driver mutations that probably confer a selective growth advantage on ALL tumor cells at relapse [24]. Preclinical studies and clinical experience have shown that leukemic blasts are more resistant at relapse than at diagnosis. Mechanisms of resistance may include the selection of a pre-existing resistant subclone or the acquisition of additional genomic lesions under the selective pressure of chemotherapy, as observed in our study [4].

5. Conclusions

In summary, the present study provides additional evidence that the clonality of ALL is genetically dynamic from diagnosis to relapse. The integrative NGS, aCGH, and MLPA analysis enabled a better molecular characterization of the genetic profile in ALL patients during the evolution of their disease, showing distinct genetic profiles at diagnosis and relapse. With this study, the utility of simultaneously identifying CNAs and mutations at the time of diagnosis and relapse was evidenced, which is clinically important to predict the evolution of the patients. New genomic strategies to identify various genetic lesions from a single sample and in a single experiment are currently being solved by designing specific panels for each type of hematological disease, which contribute to the improvement of the risk stratification, promoting the use of personalized treatment in ALL.

Supplementary Materials: The following are available online at http://www.mdpi.com/2075-4418/10/7/455/s1. All data analyzed during this study are included in this published article and its Supplementary File 1 which contains: Table S1. Frontline risk-adapted protocols, outcome, clinical status, karyotype, FISH, NGS, aCGH and MLPA analysis in matched diagnosis-relapse BCP-ALL patients; Table S2. Description of somatic mutations observed in diagnosis–relapse BCP-ALL patients; Table S3. Regions of significant recurrent amplification and deletion retained at relapse (*q-value* < 0.05); Table S4. Regions of significant recurrent deletion lost at relapse (*q-value* < 0.05); Table S5. Regions of significant recurrent amplification and deletion acquired at relapse (*q-value* < 0.05); Figure S1. Location of the probes in the X/Y PAR1 region provided in the MLPA probemix and NimbleGen high-density microarray platform; Figure S2. Patterns and frequencies of DNA copy alterations observed in 13 paired diagnostic/relapse samples; Figure S3. Gene deletions identified by integrative MLPA-aCGH analysis and Figure S4. Mutations identified by NGS showed patterns of genetic evolution in paired diagnostic/relapse samples. The datasets generated during the current study are available in the GEO Accession viewer repository (GSE12803), LINK: [https://www.ncbi.nlm.nih.gov/geo/query/acc.cgi?acc=GSE128031].

Author Contributions: Conceptualization, M.F.-C., A.M., R.B., J.M.H.-R., M.H.-S.; Methodology, M.F.-C., A.M., C.R., M.M.-I., A.G.d.C., J.L.F., N.d.l.H., J.A.Q., J.R., J.-M.R., J.M.H.-R.; Software, M.F.-C., R.B. and L.A.C.-S.; Validation, M.F.-C., R.B., L.A.C.-S., C.R. and M.H.-S.; Formal Analysis, M.F.-C., A.M., R.B., J.M.H.-R., M.H.-S. and L.A.C.-S.; Investigation, M.F.-C., A.M., R.B., J.M.H.-R., M.H.-S.; Data Curation, M.F.-C., A.M., R.B., J.M.H.-R., M.H.-S. and L.A.C.-S.; Writing—Original Draft Preparation, M.F.-C. and A.M.; Writing—Review and Editing, All authors; Visualization, All authors; Supervision, R.B. and J.M.H.-R.; Project Administration, R.B. and J.M.H.-R.; Funding Acquisition, M.F.-C., R.B. and J.M.H.-R. All authors have read and agreed to the published version of the manuscript.

Funding: This work was supported in part by a grant from the Consejería de Educación, Junta de Castilla y León, Fondos FEDER (SA085U16, SA271P18), Proyectos de Investigación de la Gerencia Regional de Sanidad, SACYL, (GRS 1847/A/18; GRS 2062/A/19), SYNtherapy. Synthetic Lethality for Personalized Therapy-based Stratification In Acute Leukemia (ERAPERMED2018-275); ISCIII (AC18/00093), co-funded by ERDF/ESF, "Investing in your future", Fundación Castellano Leonesa de Hematología y Hemoterapia (FUCALHH 2017), and Centro de Investigación Biomédica en Red de Cáncer (CIBERONC CB16/12/00233). A grant to AM from the Junta Provincial de Salamanca of the Asociación Española Contra el Cáncer (AECC), a grant to MFC from the Universidad Pedagógica y Tecnológica de Colombia—Vicerrectoría de Investigación y Extensión (Grupo de Investigación en Ciencias Biomédicas UPTC—GICBUPTC, Escuela de Ciencias Biológicas). M. Hernández-Sánchez holds a Sara Borrell post-doctoral contract (CD19/00222) from the Instituto de Salud Carlos III (ISCIII). co-founded by Fondo Social Europeo (FSE) "El Fondo Social Europeo invierte en tu futuro", MM is currently supported by an "Ayuda predoctoral de la Junta de Castilla y León" by the Fondo Social Europeo (JCYL- EDU/556/2019 PhD scholarship) and a grant to JR and JMR from Instituto Carlos III (PI14/01971).

Conflicts of Interest: The authors declare no conflict of interest.

References

1. Roberts, K.G.; Mullighan, C.G. Genomics in acute lymphoblastic leukaemia: Insights and treatment implications. *Nat. Rev. Clin. Oncol.* **2015**, *12*, 344–357. [CrossRef] [PubMed]
2. Malard, F.; Mohty, M. Acute lymphoblastic leukaemia. *Lancet* **2020**, *395*, 1146–1162. [CrossRef]
3. Bhatla, T.; Jones, C.L.; Meyer, J.A.; Vitanza, N.A.; Raetz, E.A.; Carroll, W.L. The biology of relapsed acute lymphoblastic leukemia: Opportunities for therapeutic interventions. *J. Pediatr. Hematol. Oncol.* **2014**, *36*, 413–418. [CrossRef] [PubMed]
4. Bhojwani, D.; Yang, J.J.; Pui, C.H. Biology of childhood acute lymphoblastic leukemia. *Pediatric Clin. N. Am.* **2015**, *62*, 47–60. [CrossRef]

5. Mullighan, C.G.; Phillips, L.A.; Su, X.; Ma, J.; Miller, C.B.; Shurtleff, S.A.; Downing, J.R. Genomic analysis of the clonal origins of relapsed acute lymphoblastic leukemia. *Science* **2008**, *322*, 1377–1380. [CrossRef]
6. Yang, J.J.; Bhojwani, D.; Yang, W.; Cai, X.; Stocco, G.; Crews, K.; Wang, J.; Morrison, D.; Devidas, M.; Hunger, S.P.; et al. Genome-wide copy number profiling reveals molecular evolution from diagnosis to relapse in childhood acute lymphoblastic leukemia. *Blood* **2008**, *112*, 4178–4183. [CrossRef]
7. Mullighan, C.G.; Downing, J.R. Global genomic characterization of acute lymphoblastic leukemia. *Semin. Hematol.* **2009**, *46*, 3–15. [CrossRef]
8. Yu, C.H.; Chang, W.T.; Jou, S.T.; Lin, T.K.; Chang, Y.H.; Lin, C.Y.; Lin, K.H.; Lu, M.Y.; Chen, S.H.; Wu, K.H.; et al. TP53 alterations in relapsed childhood acute lymphoblastic leukemia. *Cancer Sci.* **2020**, *111*, 229–238. [CrossRef]
9. Ishida, H.; Iguchi, A.; Aoe, M.; Takahashi, T.; Tamefusa, K.; Kanamitsu, K.; Fujiwara, K.; Washio, K.; Matsubara, T.; Tsukahara, H.; et al. Panel-based next-generation sequencing identifies prognostic and actionable genes in childhood acute lymphoblastic leukemia and is suitable for clinical sequencing. *Ann. Hematol.* **2019**, *98*, 657–668. [CrossRef]
10. Chen, C.; Heng, E.Y.H.; Lim, A.S.T.; Lau, L.C.; Lim, T.H.; Wong, G.C.; Tien, S.L. Chromosomal microarray analysis is superior in identifying cryptic aberrations in patients with acute lymphoblastic leukemia at diagnosis/relapse as a single assay. *Int. J. Lab. Hematol.* **2019**, *41*, 561–571. [CrossRef]
11. Coccaro, N.; Anelli, L.; Zagaria, A.; Specchia, G.; Albano, F. Next-Generation Sequencing in Acute Lymphoblastic Leukemia. *Int. J. Mol. Sci.* **2019**, *20*, 2929. [CrossRef] [PubMed]
12. Pui, C.H.; Evans, W.E. Acute lymphoblastic leukemia. *N. Engl. J. Med.* **1998**, *339*, 605–615. [CrossRef] [PubMed]
13. Harrison, C.J. Key pathways as therapeutic targets. *Blood* **2011**, *118*, 2935–2936. [CrossRef] [PubMed]
14. Chiaretti, S.; Zini, G.; Bassan, R. Diagnosis and subclassification of acute lymphoblastic leukemia. *Mediterr. J. Hematol. Infect. Dis.* **2014**, *6*, e2014073. [CrossRef]
15. Chiaretti, S.; Gianfelici, V.; Ceglie, G.; Foa, R. Genomic characterization of acute leukemias. *Med. Princ. Pract. Int. J. Kuwait Univ. Health Sci. Cent.* **2014**, *23*, 487–506. [CrossRef]
16. Gowda, C.; Dovat, S. Genetic targets in pediatric acute lymphoblastic leukemia. *Adv. Exp. Med. Biol.* **2013**, *779*, 327–340. [CrossRef]
17. Iacobucci, I.; Papayannidis, C.; Lonetti, A.; Ferrari, A.; Baccarani, M.; Martinelli, G. Cytogenetic and molecular predictors of outcome in acute lymphocytic leukemia: Recent developments. *Curr. Hematol. Malig. Rep.* **2012**, *7*, 133–143. [CrossRef]
18. Loh, M.L.; Mullighan, C.G. Advances in the genetics of high-risk childhood B-progenitor acute lymphoblastic leukemia and juvenile myelomonocytic leukemia: Implications for therapy. *Clin. Cancer Res.* **2012**, *18*, 2754–2767. [CrossRef]
19. Mullighan, C.G. Genomic profiling of B-progenitor acute lymphoblastic leukemia. *Best Pract. Res. Clin. Haematol.* **2011**, *24*, 489–503. [CrossRef]
20. Roberts, K.G.; Mullighan, C.G. How new advances in genetic analysis are influencing the understanding and treatment of childhood acute leukemia. *Curr. Opin. Pediatr.* **2011**, *23*, 34–40. [CrossRef]
21. Woo, J.S.; Alberti, M.O.; Tirado, C.A. Childhood B-acute lymphoblastic leukemia: A genetic update. *Exp. Hematol. Oncol.* **2014**, *3*, 16. [CrossRef] [PubMed]
22. Inaba, H.; Greaves, M.; Mullighan, C.G. Acute lymphoblastic leukaemia. *Lancet* **2013**, *381*, 1943–1955. [CrossRef]
23. Pui, C.H.; Carroll, W.L.; Meshinchi, S.; Arceci, R.J. Biology, risk stratification, and therapy of pediatric acute leukemias: An update. *J. Clin. Oncol.* **2011**, *29*, 551–565. [CrossRef]
24. Forero-Castro, M.; Robledo, C.; Benito, R.; Bodega-Mayor, I.; Rapado, I.; Hernandez-Sanchez, M.; Abaigar, M.; Maria Hernandez-Sanchez, J.; Quijada-Alamo, M.; Maria Sanchez-Pina, J.; et al. Mutations in TP53 and JAK2 are independent prognostic biomarkers in B-cell precursor acute lymphoblastic leukaemia. *Br. J. Cancer* **2017**, *117*, 256–265. [CrossRef] [PubMed]
25. Hernandez, J.A.; Hernandez-Sanchez, M.; Rodriguez-Vicente, A.E.; Grossmann, V.; Collado, R.; Heras, C.; Puiggros, A.; Martin, A.A.; Puig, N.; Benito, R.; et al. A Low Frequency of Losses in 11q Chromosome Is Associated with Better Outcome and Lower Rate of Genomic Mutations in Patients with Chronic Lymphocytic Leukemia. *PLoS ONE* **2015**, *10*, e0143073. [CrossRef] [PubMed]

26. Weissmann, S.; Roller, A.; Jeromin, S.; Hernandez, M.; Abaigar, M.; Hernandez-Rivas, J.M.; Grossmann, V.; Haferlach, C.; Kern, W.; Haferlach, T.; et al. Prognostic impact and landscape of NOTCH1 mutations in chronic lymphocytic leukemia (CLL): A study on 852 patients. *Leukemia* **2013**, *27*, 2393–2396. [CrossRef]
27. Kohlmann, A.; Klein, H.U.; Weissmann, S.; Bresolin, S.; Chaplin, T.; Cuppens, H.; Haschke-Becher, E.; Garicochea, B.; Grossmann, V.; Hanczaruk, B.; et al. The Interlaboratory RObustness of Next-generation sequencing (IRON) study: A deep sequencing investigation of TET2, CBL and KRAS mutations by an international consortium involving 10 laboratories. *Leukemia* **2011**, *25*, 1840–1848. [CrossRef]
28. Grossmann, V.; Roller, A.; Klein, H.U.; Weissmann, S.; Kern, W.; Haferlach, C.; Dugas, M.; Haferlach, T.; Schnittger, S.; Kohlmann, A. Robustness of amplicon deep sequencing underlines its utility in clinical applications. *J. Mol. Diagn. JMD* **2013**, *15*, 473–484. [CrossRef]
29. Leroy, B.; Anderson, M.; Soussi, T. TP53 mutations in human cancer: Database reassessment and prospects for the next decade. *Hum. Mutat.* **2014**, *35*, 672–688. [CrossRef]
30. Nilsen, G.; Liestol, K.; Van Loo, P.; Moen Vollan, H.K.; Eide, M.B.; Rueda, O.M.; Chin, S.F.; Russell, R.; Baumbusch, L.O.; Caldas, C.; et al. Copynumber: Efficient algorithms for single- and multi-track copy number segmentation. *BMC Genom.* **2012**, *13*, 591. [CrossRef]
31. Beroukhim, R.; Getz, G.; Nghiemphu, L.; Barretina, J.; Hsueh, T.; Linhart, D.; Vivanco, I.; Lee, J.C.; Huang, J.H.; Alexander, S.; et al. Assessing the significance of chromosomal aberrations in cancer: Methodology and application to glioma. *Proc. Natl. Acad. Sci. USA* **2007**, *104*, 20007–20012. [CrossRef] [PubMed]
32. Schwab, C.J.; Jones, L.R.; Morrison, H.; Ryan, S.L.; Yigittop, H.; Schouten, J.P.; Harrison, C.J. Evaluation of multiplex ligation-dependent probe amplification as a method for the detection of copy number abnormalities in B-cell precursor acute lymphoblastic leukemia. *Genes Chromosom. Cancer* **2010**, *49*, 1104–1113. [CrossRef] [PubMed]
33. Chiaretti, S.; Brugnoletti, F.; Tavolaro, S.; Bonina, S.; Paoloni, F.; Marinelli, M.; Patten, N.; Bonifacio, M.; Kropp, M.G.; Sica, S.; et al. TP53 mutations are frequent in adult acute lymphoblastic leukemia cases negative for recurrent fusion genes and correlate with poor response to induction therapy. *Haematologica* **2013**, *98*, e59–e61. [CrossRef]
34. Hof, J.; Krentz, S.; van Schewick, C.; Korner, G.; Shalapour, S.; Rhein, P.; Karawajew, L.; Ludwig, W.D.; Seeger, K.; Henze, G.; et al. Mutations and deletions of the TP53 gene predict nonresponse to treatment and poor outcome in first relapse of childhood acute lymphoblastic leukemia. *J. Clin. Oncol.* **2011**, *29*, 3185–3193. [CrossRef] [PubMed]
35. Diccianni, M.B.; Yu, J.; Hsiao, M.; Mukherjee, S.; Shao, L.E.; Yu, A.L. Clinical significance of p53 mutations in relapsed T-cell acute lymphoblastic leukemia. *Blood* **1994**, *84*, 3105–3112. [CrossRef] [PubMed]
36. Li, B.; Brady, S.W.; Ma, X.; Shen, S.; Zhang, Y.; Li, Y.; Szlachta, K.; Dong, L.; Liu, Y.; Yang, F.; et al. Therapy-induced mutations drive the genomic landscape of relapsed acute lymphoblastic leukemia. *Blood* **2020**, *135*, 41–55. [CrossRef]
37. Demir, S.; Boldrin, E.; Sun, Q.; Hampp, S.; Tausch, E.; Eckert, C.; Ebinger, M.; Handgretinger, R.; Kronnie, G.T.; Wiesmuller, L.; et al. Therapeutic targeting of mutant p53 in pediatric acute lymphoblastic leukemia. *Haematologica* **2020**, *105*, 170–181. [CrossRef]
38. Forero-Castro, M.; Robledo, C.; Benito, R.; Abaigar, M.; Africa Martin, A.; Arefi, M.; Fuster, J.L.; de Las Heras, N.; Rodriguez, J.N.; Quintero, J.; et al. Genome-Wide DNA Copy Number Analysis of Acute Lymphoblastic Leukemia Identifies New Genetic Markers Associated with Clinical Outcome. *PLoS ONE* **2016**, *11*, e0148972. [CrossRef]
39. Mullighan, C.G.; Su, X.; Zhang, J.; Radtke, I.; Phillips, L.A.; Miller, C.B.; Ma, J.; Liu, W.; Cheng, C.; Schulman, B.A.; et al. Deletion of IKZF1 and prognosis in acute lymphoblastic leukemia. *N. Engl. J. Med.* **2009**, *360*, 470–480. [CrossRef]
40. Mullighan, C.G.; Miller, C.B.; Radtke, I.; Phillips, L.A.; Dalton, J.; Ma, J.; White, D.; Hughes, T.P.; Le Beau, M.M.; Pui, C.H.; et al. BCR-ABL1 lymphoblastic leukaemia is characterized by the deletion of Ikaros. *Nature* **2008**, *453*, 110–114. [CrossRef]
41. Caye, A.; Beldjord, K.; Mass-Malo, K.; Drunat, S.; Soulier, J.; Gandemer, V.; Baruchel, A.; Bertrand, Y.; Cave, H.; Clappier, E. Breakpoint-specific multiplex polymerase chain reaction allows the detection of IKZF1 intragenic deletions and minimal residual disease monitoring in B-cell precursor acute lymphoblastic leukemia. *Haematologica* **2013**, *98*, 597–601. [CrossRef] [PubMed]

42. Stanulla, M.; Cave, H.; Moorman, A.V. IKZF1 deletions in pediatric acute lymphoblastic leukemia: Still a poor prognostic marker? *Blood* **2020**, *135*, 252–260. [CrossRef] [PubMed]
43. Vairy, S.; Tran, T.H. IKZF1 alterations in acute lymphoblastic leukemia: The good, the bad and the ugly. *Blood Rev.* **2020**, 100677. [CrossRef] [PubMed]
44. Dorge, P.; Meissner, B.; Zimmermann, M.; Moricke, A.; Schrauder, A.; Bouquin, J.P.; Schewe, D.; Harbott, J.; Teigler-Schlegel, A.; Ratei, R.; et al. IKZF1 deletion is an independent predictor of outcome in pediatric acute lymphoblastic leukemia treated according to the ALL-BFM 2000 protocol. *Haematologica* **2013**, *98*, 428–432. [CrossRef] [PubMed]
45. Burki, T.K. Intensified treatment for IKZF1-deleted childhood leukaemia. *Lancet Oncol.* **2018**, *19*, e441. [CrossRef]
46. Yeoh, A.E.J.; Lu, Y.; Chin, W.H.N.; Chiew, E.K.H.; Lim, E.H.; Li, Z.; Kham, S.K.Y.; Chan, Y.H.; Abdullah, W.A.; Lin, H.P.; et al. Intensifying Treatment of Childhood B-Lymphoblastic Leukemia with IKZF1 Deletion Reduces Relapse and Improves Overall Survival: Results of Malaysia-Singapore ALL 2010 Study. *J. Clin. Oncol.* **2018**, *36*, 2726–2735. [CrossRef]
47. Ribera, J.; Zamora, L.; Morgades, M.; Mallo, M.; Solanes, N.; Batlle, M.; Vives, S.; Granada, I.; Junca, J.; Malinverni, R.; et al. Copy number profiling of adult relapsed B-cell precursor acute lymphoblastic leukemia reveals potential leukemia progression mechanisms. *Genes Chromosom. Cancer* **2017**, *56*, 810–820. [CrossRef]
48. Jan, M.; Majeti, R. Clonal evolution of acute leukemia genomes. *Oncogene* **2013**, *32*, 135–140. [CrossRef]

Chapter III. *ETV6/RUNX1* Fusion Gene Abrogation Decreases the Oncogenicity of Tumour Cells in a Preclinical Model of Acute Lymphoblastic Leukaemia.

Adrián Montaño[1], Jose Luis Ordoñez[2], Verónica Alonso-Pérez[2], Jesús Hernández-Sánchez[1], Sandra Santos[1], Teresa González[3], Rocío Benito[1], Ignacio García-Tuñón[*2] and Jesús María Hernández-Rivas[1,2,3,4*]
**Correspondence.*

[1]IBSAL, IBMCC, Universidad de Salamanca-CSIC, Cancer Research Center; Salamanca; Spain. [2]Unidad de Diagnóstico Molecular y Celular del Cáncer, Centro de Investigación del Cáncer-IBMCC (USAL-CSIC), Salamanca, Spain. [3]Dept of Hematology, Hospital Universitario de Salamanca; Salamanca; Spain. [4]Dept of Medicine, Universidad de Salamanca, Spain.

Cells 2020, 9(1), 215. doi: 10.3390/cells9010215

cells

MDPI

Article

ETV6/RUNX1 Fusion Gene Abrogation Decreases the Oncogenicity of Tumour Cells in a Preclinical Model of Acute Lymphoblastic Leukaemia

Adrián Montaño [1], Jose Luis Ordoñez [1,2], Verónica Alonso-Pérez [1], Jesús Hernández-Sánchez [1], Sandra Santos [1], Teresa González [1,3], Rocío Benito [1], Ignacio García-Tuñón [1,*,†] and Jesús María Hernández-Rivas [1,3,4,*,†]

1 IBSAL, IBMCC, Cancer Research Center, Universidad de Salamanca-CSIC, 37007 Salamanca, Spain; adrianmo18@gmail.com (A.M.); jlog@usal.es (J.L.O.); alonsoperezveronica@gmail.com (V.A.-P.); jesus807@gmail.com (J.H.-S.); sandruskism90@gmail.com (S.S.); teresa.gonzalez@mundo-r.com (T.G.); beniroc@usal.es (R.B.)
2 Department of Biochemistry and Molecular Biology, University of Salamanca, Campus Unamuno s/n, 37007 Salamanca, Spain
3 Department of Hematology, Hospital Universitario de Salamanca, 37007 Salamanca, Spain
4 Department of Medicine, Universidad de Salamanca and CIBERONC, 37007 Salamanca, Spain
* Correspondence: ignacio.tunon@uah.es (I.G.-T.); jmhr@usal.es (J.M.H.-R.); Tel.: +34-923291384 (J.M.H.-R.); Fax: +34-923294624 (J.M.H.-R.)
† These authors share senior authorship.

Received: 7 December 2019; Accepted: 13 January 2020; Published: 15 January 2020

Abstract: Background: The t(12;21)(p13;q22), which fuses *ETV6* and *RUNX1* genes, is the most common genetic abnormality in children with B-cell precursor acute lymphoblastic leukaemia. The implication of the fusion protein in leukemogenesis seems to be clear. However, its role in the maintenance of the disease continues to be controversial. Methods: Generation of an in vitro *ETV6/RUNX1* knock out model using the CRISPR/Cas9 gene editing system. Functional characterization by RNA sequencing, proliferation assays, apoptosis and pharmacologic studies, and generation of edited-cell xenograft model. Results: The expression of *ETV6/RUNX1* fusion gene was completely eliminated, thus generating a powerful model on which to study the role of the fusion gene in leukemic cells. The loss of fusion gene expression led to the deregulation of biological processes affecting survival such as apoptosis resistance and cell proliferation capacity. Tumour cells showed higher levels of apoptosis, lower proliferation rate and a greater sensitivity to PI3K inhibitors in vitro along as a decrease in tumour growth in xenografts models after *ETV6/RUNX1* fusion gene abrogation. Conclusions: ETV6/RUNX1 fusion protein seems to play an important role in the maintenance of the leukemic phenotype and could thus become a potential therapeutic target.

Keywords: acute lymphoblastic leukaemia; ETV6/RUNX1; CRISPR/Cas9; genome edition

1. Background

The gene fusion between the transcription factors *ETV6* (*TEL*) and *RUNX1* (*AML1*), generated by t(12;21)(p13;q22), is the most frequent chromosomal translocation in children with acute lymphoblastic leukaemia (ALL). This translocation fuses the 5′ non-DNA binding region of the ETS family transcription factor *ETV6* to almost the entire *RUNX1* locus [1,2]. Patients carrying this translocation are associated with a good prognosis and excellent molecular response to treatment. However up to 20% of cases relapse [3–7]. Furthermore, the response to treatment of some relapse cases is associated with resistance

to treatments such as glucocorticoids (GCs) [8], and these patients must be treated with stem cell transplantation [9].

ETV6/RUNX1 (E/R) protein is known to play a role in the development of B-ALL, but by itself it is not capable of initiating the disease. Postnatal genetic events are required for the development of clinically overt leukaemia. These second events are usually mutations or deletions, such as the loss of wild type (WT) allele of *ETV6* [10]. Recent studies suggest that E/R is responsible for the initiation of leukaemia and is also essential for disease progression and maintenance, through deregulation of different molecular pathways that contribute to leukemogenesis. E/R regulates phosphoinositide 3-kinase (PI3K)/Akt/mammalian target of rapamycin (mTOR) (PI3K/Akt/mTOR) pathway, which promotes proliferation, cell adhesion and DNA damage response; *STAT3* pathway involved in self-renewal and cell survival and *MDM2*/*TP53* whose deregulation induces the inhibition of apoptosis and consequently cell survival [11].

However, the functional studies carried out by the silencing of *E/R* fusion gene expression, mediated by siRNA and shRNA, reveal that there is still controversy about the role of the oncoprotein in the maintenance of the leukemic phenotype. Thus E/R silencing by siRNA neither induced cell cycle arrest/apoptosis nor attenuated clonogenic potential of cells. Therefore, the E/R fusion protein may be dispensable for the survival of definitive leukemic cells [12]. By contrast, other studies showed that E/R expression was critical for the survival and propagation of the respective leukaemia cells in vitro and in vivo [13,14]. These results arise some doubts about the implications of the fusion protein in tumour cells.

The implementation of new genetic editing strategies has allowed the development of functional studies by generation of gene and gene fusion Knock-out (KO) models, both in vitro and in vivo [15]. In this study, we completely abrogated the expression of E/R fusion protein in REH ALL cell line using the CRISPR/Cas9 editing system and we observed the deregulation of different biological processes such as apoptosis resistance and cell proliferation. Consequently, leukaemia cells showed greater sensitivity to death and less proliferative advantage after gene fusion abrogation. E/R KO cells also showed an increased sensitivity to PI3K inhibitors and a decrease of the oncogenicity in vivo. In summary, we provide evidence that fusion protein has a key role in the maintenance of the leukemic phenotype.

2. Material and Methods

2.1. Cell Lines and Culture Conditions

REH, obtained from Deutsche Sammlung von Mikroorganismen und Zellkulturen (DMSZ) German collection (ACC 22), is a cell line established from the peripheral blood of a patient with ALL who carried t (12,21) and del(12) producing respective *E/R* fusion and deletion of residual *ETV6*. REH was maintained in RPMI 1640 (Life Technologies, Carlsbad, CA, USA) supplemented with 15% foetal bovine serum (FBS) and 1% of Penicillin/Streptomycin (P/S) (Life Technologies). Stromal HS-5 cell line was obtained from American Type Culture Collection (ATCC) collection (CRL-11882) and maintained in DMEM (Life Technologies, Carlsbad, CA, USA) supplemented with 10% FBS and 1% of P/S. Both cells lines were maintained at 37 °C with 5% CO_2.

2.2. Sgrnas Design and Cloning

Based on the methodology of CRISPR/Cas9, two single guides RNAs (sgRNAs) (G1 and G2) were designed with the Broad Institute CRISPR designs software (http://www.broadinstitute.org). One of them directed towards the end of exon 5 of *ETV6* and other directed towards the beginning of intron 5–6, both before the fusion point, with the intention of producing indels or deletions that modify the open reading frame of the oncogene, and, therefore, the gene expression. These sgRNAs were cloned into a vector containing the Cas9 nuclease coding sequence and GFP, pSpCas9(BB)-2A-GFP (PX458) (Addgene plasmid #48138) (Ran 2013) as described previously [15] (Table S1). Then, they were electroporated into the REH cells.

2.3. Sgrna Transfections

REH ALL cells (4×10^6 cells) were electroporated with 4 µg of both plasmid constructs (Garcia tunon 2017) (PX458 G1 and PX458 G2) using the Amaxa electroporation system (Amaxa Biosystem, Gaithersburg, MD, USA) according to supplier's protocol.

2.4. Flow Cytometry Analysis and Cell Sorting

Seventy-two hours after sgRNAs transfection, GFP-positive cells were selected by fluorescence-activated cell sorting (FACS) using FACS Aria (BD Biosciences, San Jose, CA, USA). Single-cells were seeded in 96-well plate by FACS, establishing the different KO and control clones.

2.5. Sequencing of sgrNA Targets Sites

Genomic DNA was extracted using the QIAamp DNA Micro Kit (Qiagen, Hilden, Germany) following the manufacturer's protocol. To amplify the region of *E/R* fusion, PCR was performed using the following primers: forward 5′-ACCCTCTGATCCTGAACCCC–3′ and reverse 5′-GGATTTAGCCTCATCCAAGCAG–3′. PCR products were purified using a High Pure PCR Product Purification Kit (Roche, Basilea, Switzerland) and were sequenced by the Sanger method using each forward and reverse PCR primers (Table S2).

The editing efficiency of the sgRNAs and the potential induced mutations were assessed using Tracking of Indels by Decomposition (TIDE) software (https://tide-calculator.nki.nl; Netherlands Cancer Institute), which only required two Sanger sequencing runs from wild-type cells and mutated cells.

2.6. Off-Target Sequence Analysis

The top four predicted off-target sites obtained from "Breaking Cas" website (http://bioinfogp.cnb.csic.es/tools/breakingcas/) were analysed by PCR in the different clones (Table S2) before to functional and xenograft experiments.

2.7. RT-qPCR

Total RNA extraction was performed with the RNeasy Kit (Qiagen) as suggested by the manufacturer. Real-time reverse transcriptase–polymerase chain reactions (RT-qPCRs) were performed as described [16]. The primers for *E/R* (sense, 5-CTCTGTCTCCCCGCCTGAA-3 antisense, 5-CGGCTCGTGCTGGCAT-3), were designed. These oligonucleotides were designed outside the editing region (exon 5 of *ETV6* and exon 4 of *RUNX1*) and with a distance between them in mRNA of 143 base pairs (bps) (Figure S2). RT-qPCR data shown include at least 3 independent experiments with 3 replicates per experiment.

2.8. Transcriptome Sequencing

RNA-seq was performed by using TruSeq Stranded mRNA (Illumina). In all samples, RNA was analysed following manufacturer's recommendations for the protocol "TruSeq Stranded mRNA Reference Guide-Illumina". Libraries were sequenced in the NextSeq550 platform (Illumina) according to manufacturer's description with a read length of 2×75 nucleotides.

Briefly, bcl files were demultiplexing on BaseSpace (Illumina Cloud based resource) to generate fastq files. Raw data quality control was performed with fastQc (v0.11.8), globin contamination was assessed with HTSeq Count, FastQ screen evaluated ribosomal RNA contamination and other external possible resources of contamination (*Mus musculus*, *Drosophila melanogaster*, *Caenorhabditis elegans* and *mycoplasma*). STAR (v020201) was used for the alignment (hg19 reference genome) and Feature Counts (v1.4.6, University of Melbourne, Parkville, Australia) to generate the read count matrix. Finally, DESeq2 was used for differentially gene expression analysis. DESeq2 model internally corrects for library size therefore normalizes the values and enables paired comparisons. Heatmap was performed in R.

Go enrichment analysis (http://geneontology.org) to evaluate whether a set of genes was significantly enriched between the different comparisons was used. The most significant biological mechanisms, pathways and functional categories in the data sets of genes selected by statistical analysis were identified through PANTHER Overrepresentation Test. REVIGO was used to cluster biological processes (http://revigo.irb.hr) [17].

The data discussed in this publication have been deposited in NCBI's Gene Expression Omnibus (Hernandez-Rivas JM et al., 2019) and are accessible through GEO Series accession number GSE140980 (https://www.ncbi.nlm.nih.gov/geo/query/acc.cgi?acc=GSE140980).

2.9. Western Blotting

Protein expression was assessed by SDS-PAGE and western blotting (WB). The antibodies were obtained from Cell Signalling Technology (Danvers, MA, USA) including a human anti-Bcl-2 antibody (1:1000; 2872) for Bcl-2, a human anti-Bcl-xL antibody (1:1000; 2762) for Bcl-xL, a human anti-phospho Akt antibody (1:1000; 4060) for p-Akt (Ser473) and a human anti-phospho mTOR antibody (1:1000;2971) for p-mTOR (Ser2448). Anti-rabbit IgG horseradish peroxidase-conjugated (1:5000, 7074) was used as a secondary antibody. Antibodies were detected using ECL^{TM} WB Detection Reagents (RPN2209, GE Healthcare, Chicago, IL, USA). ImageJ software was used for densitometric analysis [18,19].

2.10. Cell Viability, Cell Cycle Analysis and Proliferation Assays

Cell viability was measured by flow cytometry based on non-vital dye propidium iodide (PI) labelling. Briefly, 5×10^5 cells were collected and washed twice in PBS and labelled with PI, allowing the discrimination of living-intact cells (PI-negative) and apoptotic cells (PI-positive). In parallel, cell distribution in the cell cycle phase was also analysed by measuring DNA content (PI labelling after cell permeabilization). These experiments were carried out after 24, 48 and 72 culture hours.

For proliferation measuring, MTT assays and labelling of cells with CellTrace Carboxyfluorescein Succinimidyl Ester (CFSE) Cell Proliferation Kit (Thermo Fisher, Madison, WI, USA) were used. In MTT assays, cells were plated on 96-well plates, cell density varied according to the days of the experiment, in a range between 3×10^4 and 5×10^3 cells (24–240 h). MTT solution (3-(4,5-cimethylthiazol-2-yl)-2,5-diphenyl tetrazolium bromide) was added at concentration of 0.5 µg/µL (Merck, Darmstadt, Germany). After incubation for 3–4 h at 37 °C, cells were lysed with the solubilization solution (10% SDS in 0.01M HCl) and absorbance was measured in a plate reader at 570 nm. For labelling of cells, 3×10^5 cells were stained with CellTrace-CFSE following the manufacturer's instructions and plated on 6-well plates. After 48 h, CFSE expression was measured by flow cytometry.

2.11. B-ALL-Stromal Cell Co-Culture

HS-5 human mesenchymal stromal cells (MSCs) were plated at a density of 1×10^5 cells per coverslip in 6-well plates. After 24 h, control cells and E/R KO clones were stained with Celltrace-CFSE and 3×10^5 cells placed on top of the stromal cell monolayer. Cells were co-cultured during 48h in RPMI 1640 supplemented with 15% FBS and 1% of P/S at 37 °C with 5% CO_2.

2.12. Drugs and Treatments

The followings drugs were used: Vincristine and Copanlisib (BAY 80–6946) were obtained from Selleckchem (Houston, TX, USA) and Prednisolone (P6004) obtained from Merck. All drugs were prepared at the appropriate stocking concentrations in DMSO (Merck) and stored at −20 °C until use.

2.13. Mouse Xenograft Tumourigenesis

Sixteen four to five-week-old female NOD/SCID/IL2 receptor gamma chain null (NSG) mice (Charles River, Barcelona, Spain) were used. 5×10^6 tumour cells from REH or control clone were subcutaneously injected into the left flank and tumour cells from KO clones (KO1, KO2 and KO3) were

injected in the right flank as described previously [15]. Groups were established as follows: REH vs. KO2 in group 1, REH vs. KO3 in group 2, control clone vs. KO1 in group 3 and control clone vs. KO2 in group 4 (4 mice per group). The study received prior approval from the Bioethics Committee of our institution and followed the Spanish and European Union guidelines for animal experimentation (RD 53/2013 and 2010/63/UE).

Tumour diameters were measured every 2–3 days with a calliper. Tumour volume was calculated as described elsewhere by the formula a2bπ/6 (a and b being, respectively, the smallest and the biggest diameters). Mice were sacrificed by anaesthesia overdose when tumour volume reached 2 cm^3 or 48–62 days after cell injection, upon which the tumours were collected and weighted.

2.14. Histopathology and Immunohistochemistry

Excised tumours were sampled just after sacrifice and representative areas were (a) formalin-fixed (24 h) (Merck Millipore, Burlington, MA, USA) and paraffin-embedded and (b) snap-frozen in OCT and stored at 80 °C as previously described [20]. Tissue sections 2 μM thick were stained with hematoxilin & eosin (H&E) and prepared for immunohistochemistry (IHC). IHC was performed as previously described [20] using the anti-Ki67primary antibody (Merck Millipore). The number of mitotic figures were counted in 6 high-power field.

2.15. Statistical Analysis

Statistical analysis was performed using GraphPad Prism 6 Software (San Diego, CA, USA). Differences in relative expression of E/R and cell viability after treatments were tested by Tukey's multiple comparisons test. Differences in protein expression, proliferation and apoptosis levels were tested by unpaired *t*-test. Differences in tumour masses over time were tested by non-parametric Mann Whitney U test followed by Tukey's multiple comparisons test and parametric Student's t test. Statistical significance at values of $p \leq 0.05$ (*), $p \leq 0.005$ (**) and $p \leq 0.001$ (***) was noted.

3. Results

3.1. CRISPR/Cas9 Edited Lymphoid Cell Line Showed a Loss of E/R Functionality

The fusion gene product between *ETV6* and *RUNX1* genes is generated by the union of *ETV6* intron 5 and *RUNX1* intron 1–2. *E/R* sequence was edited by CRISPR/Cas9 and evaluated by Sanger sequencing in REH cells (Figure S1). The edition efficiency evaluated through TIDE was 76.5% with sgRNA G1 and 86.2% with sgRNA G2. The most frequent generated mutations were insertions up to 4 bps.

Single-edited cells were seeded into a 96 well plate to obtain clones with a single edition that predicted a KO sequence for the oncogene. Only 48 single cell clones proliferated in culture. These clones were screened by sanger sequencing and the results revealed that more than 50% of clones (25/48) presented an edited *E/R* sequence. Among them, three single-edited cell clones "KO1, KO2 and KO3 clones" with a predicted *E/R* KO sequence were selected for the study. These clones had different editions in their sequences. KO1 clone carried an insertion of two cytosines at the end of *ETV6* exon 5, near the Protospacer Adjacent Motif (PAM) sequence of the sgRNA G2, thus a frameshift mutation that generated a stop codon before finishing the exon. On the other hand, KO2 and KO3 had an insertion of 5 and 3 nucleotides respectively near the PAM sequence within exon 5, followed by a deletion of 100 bps approximately between both sgRNAs. These alterations modified the open reading frame, generating the stop codon in the next exon. In addition, the loss of the splicing region prevented the correct processing of the protein. Additionally, two single-edited cell clones with WT *E/R* sequence were used as control clones "Control 1 and Control 2" (Figure S2).

In order to check the functionality of the *E/R* alleles carrying these clones, the expression of the fusion transcript E/R was quantified by RT-qPCR. Quantification revealed a total loss of E/R mRNA expression in KO2 and KO3 clones as compared to control clones ($p < 0.001$) and a leaky expression in KO1 clone ($p < 0.001$) (Figure 1). The loss of E/R expression was also observed by total RNA-seq in E/R KO clones.

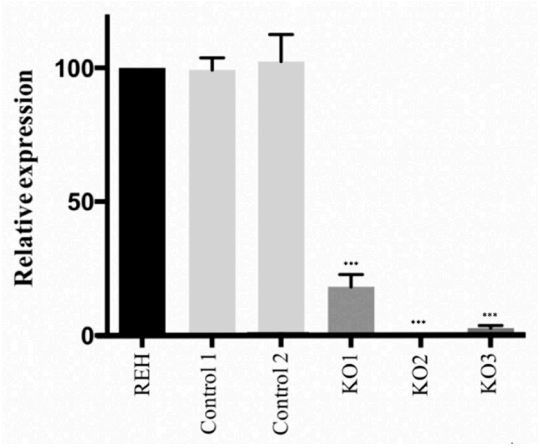

Figure 1. E/R expression levels by Reverse Transcription–quantitative real-time Polymerase Chain Reaction (RT-qPCR). Control clones showed an expression of E/R similar to it was observed in the parental REH cells. In E/R KO clones, whose sequence was edited by the CRISPR/Cas9 system, KO2 and KO3 showed a total loss of E/R expression and KO1 showed a leaky expression. All the experiments were carried out by triplicate, the means with the standard deviations for each clone were represented. *** $p \leq 0.001$ (unpaired *t*-test).

The four most likely off-target sequences from both guides were analysed by Sanger sequencing into the different clones. Results of Sanger sequencing revealed the lack of editing in those regions, confirming the absence of CRISPR/Cas9 off-targets (data not shown).

3.2. Transcriptomic Analysis of E/R KO Lymphoid Cell Line Generated by CRISPR/Cas9 Showed a Distinct Expression Signature and a Deregulation of Its Downstream Signalling Genes

The gene expression profile of E/R KO clones versus REH cells and controls clones, analysed by total RNA-sequencing, showed a total of 342 genes differentially expressed ($q < 0.05$), 182 upregulated and 160 downregulated (Table S3). The heatmap of the top50 of the most deregulated genes according to fold change (FC) values showed a distinct expression signature of E/R KO clones as compared with REH cells and control clones (Figure 2).

In order to elucidate the effect of *E/R* fusion gene abrogation on a functional level, the significantly deregulated genes were grouped into biological processes according to their function by enrichment analysis (Table S4 and Figure S3A). These biological processes were classified into 11 cluster representative: Germinal centre formation, regulation of response to external stimulus, positive regulation of multicellular organism process, negative regulation of apoptotic/necroptotic process, regulation of GTPase activity, I-kappaB kinase/NF-kappaB signalling, cellular calcium ion homeostasis, regulation of protein localization, regulation of cell adhesion, cytoskeleton organization and actin filament-based process (Figure S3B).

Some of these biological processes include genes whose deregulation has been described in ALL patients [21–26]. Among them we observed a downregulation of *CXCR7*, *LCK*, *PTPRG*, *VPS34*, *PTPRK*, *ARHGEF12*, *RGM* and *HAP1* genes and an upregulation of *RXRA*, *CXXC5*, *ARX*, *SORBS2*, *RGS16*, *TLR7*, *mir-146* and *TP63* genes. It is worth mentioning that *RGS16* and *PTPRK* genes are involved in PI3K/Akt/mTOR pathway, and *mir-146* and *TP63* are involved in the regulation of apoptosis. Both biological processes were proposed as key factors in maintenance of the oncogenicity of E/R-positive cells.

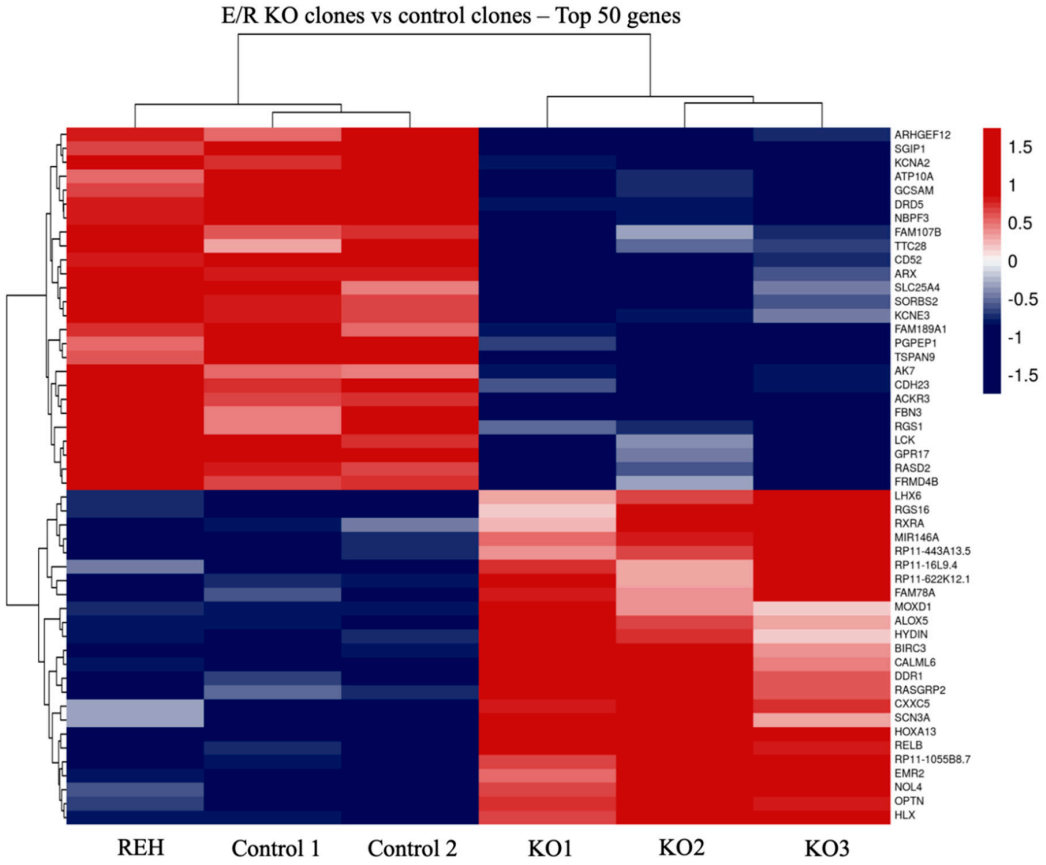

Figure 2. Transcriptomic analysis of E/R KO clones. Heat map of TOP50 differentially expressed genes in E/R Knock-out (KO) clones as compared with REH cells and control clones. Each row represents one differentially expressed gene; each column represents one clone. The dendrogram on the top reveals the sample clustering; the dendrogram on the left reveals the gene clustering.

3.3. E/R Abrogation Reduces Proliferative Capacity and Resistance to Apoptosis In vitro

To elucidate the biological effects of abrogation of E/R expression in the KO clones, functional studies were performed. MTT proliferation studies were performed at 24 h intervals up to 240 h. The results showed no proliferation differences between KO clones and REH cells or control clones (Figure S4). We simultaneously analysed the cell cycle distribution of the different cells by permeabilization followed by PI staining. No differences were observed between the different clones (Figure 3A). Moreover, no significant differences were observed through the expression of CFSE by flow cytometry (Figure 3B). By contrast, E/R KO clones showed a significantly lower proliferation rate than control clones when they were co-cultured with MSCs (HS-5) ($p < 0.05$) (Figure 3C).

Deregulation of genes such as *miR-146a* or *TP63* observed by expression analysis suggested the alteration of cellular processes such as the regulation of apoptosis. Levels of anti-apoptotic factor such as *Bcl-2* or *Bcl-xL* gene have shown to play a key role in the survival of E/R-positive cells, protecting from programmed death [27,28]. To check these findings, Bcl-2 and Bcl-xL expression levels were measured through WB. Suppression of the fusion protein produced a decrease of 60% and 47% in the expression of Bcl-2 and Bcl-xL proteins respectively ($p = 0.003$; $p = 0.043$), thus reducing the resistance to apoptosis provided by the antiapoptotic factors of this family (Figure 4). In agreement with this observation, we detected an increase in the late apoptotic levels assessed by propidium iodide staining in E/R KO clones as compared with control clones (8.99 ± 2.08 vs. 2.135 ± 0.065) ($p < 0.05$) (Figure 3D). Treatment with Vincristine (1 μM) induced a greater late apoptotic rate in E/R KO clones as compared with control clones (75.8 ± 9.59 vs. 32.7 ± 2.1) ($p < 0.05$) (Figure 3E).

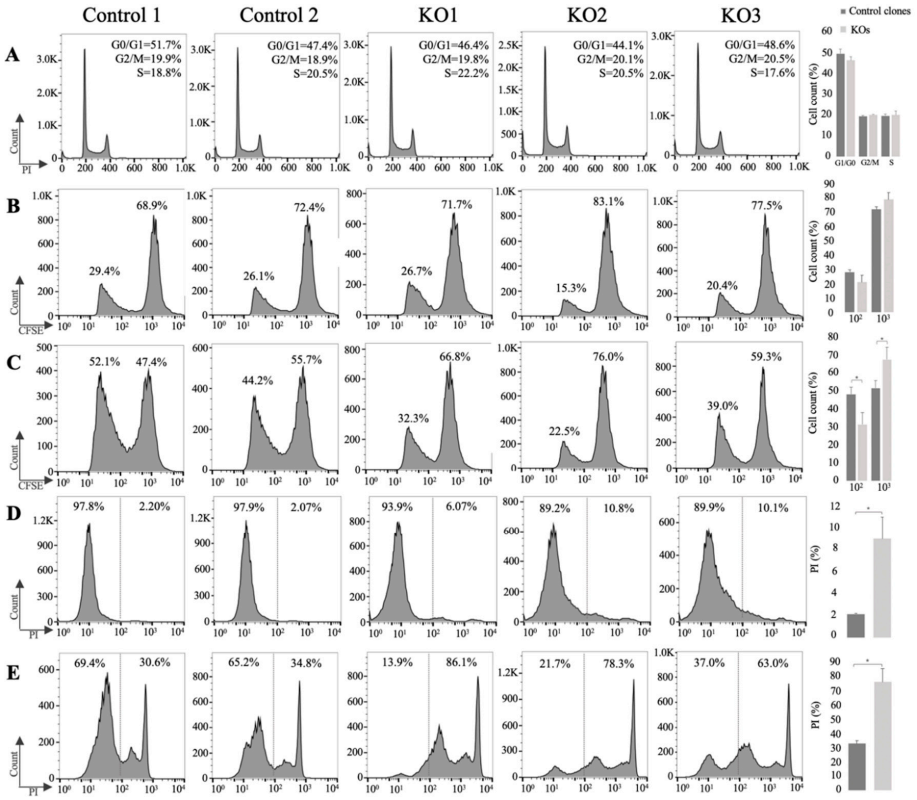

Figure 3. In vitro functional studies after E/R abrogation. (**A**) Cell cycle distribution of control clones and E/R KO cells at 48 h. (**B**) Carboxyfluorescein Succinimidyl Ester (CFSE) quantification by flow cytometry after 48 in culture. The peak on the right (10^3) represents the percentage of cells that have not divided and the left peak (10^2) represents the percentage of cells that have divided and therefore diluted their CFSE expression. (**C**) CFSE expression by flow cytometry of cells co-cultured with Mesenchymal Stromal Cells (MSC) cell line HS-5 at 48 h. (**D**) Apoptosis level quantification by Propidium Iodide (PI) expression. The figure shows the percentage of PI negative cells (left) and PI positive cells (right) at 48 h. (**E**) Apoptosis level quantification by PI expression after treatment with Vincristine (1 μM) at 48 h. On the right is represented the mean distribution of control clones (dark grey) and E/R KO clones (grey) of different experiments. All the experiments were carried out by triplicate. * $p \leq 0.05$ (unpaired *t*-test).

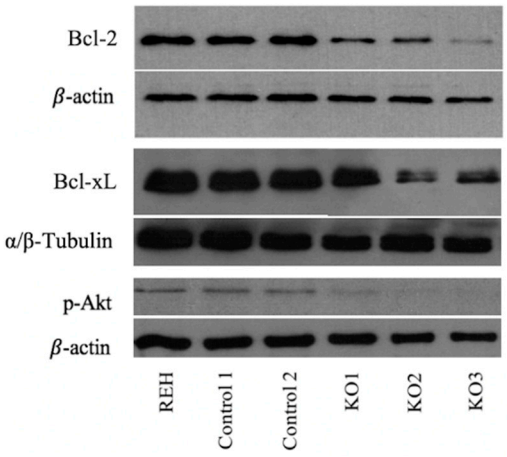

Figure 4. Western blot analysis of E/R targets expression. Lower phospho-Akt (60 kDa), BCL-XL (30 kDa) and BCL-2 (28 kDa) expression levels were observed in all E/R KO clones compared with parental cell line (REH) and control clones. This experiment had three replicates.

3.4. Abrogation of ETV6/RUNX1 Expression Enhances Sensitivity to the PI3K Inhibitor Copanlisib

Deregulation of *RGS16* or *PTPRK* genes also suggested the alteration of the PI3K/Akt/mTOR pathway. Several studies have already suggested that E/R may be key in the maintenance of the leukemic phenotype through the activation of different pathways, including the PI3K/Akt/mTOR pathway, resulting in proliferation and cell survival of leukemic cells. Akt phosphorylation levels measured through WB showed a reduction of 90% in Akt activity in the KO clones relative to REH cells and control clones ($p = 0.003$), suggesting the decrease in PI3K/Akt/mTOR activity as a result of the elimination of the expression of E/R (Figure 4).

A large proportion of relapsing E/R-positive patients become resistant to GCs such as Prednisolone, widely used in ALL treatment [8] and previous studies demonstrated that the use of PI3K inhibitors can sensitize E/R-positive cells to GCs [14].

After verifying a lower activation levels of PI3K/Akt/mTOR pathway with the elimination of E/R expression, we aimed to test if these cells responded in the same way to PI3K inhibitors. For that, we used Copanlisib, a PI3K inhibitor with inhibitory activity predominantly against the PI3K-alpha and PI3K-delta isoforms [29,30]. Treatment with Copanlisib (10 mM) resulted in higher decrease of viability in E/R KO clones compared with REH cells and controls clones (Figure 5A). To verify if Copanlisib was actually inhibiting the PI3K/Akt/mTOR pathway, we measured the phosphorylation levels of Akt and mTOR by WB, before and after treatment. We observed that the phosphorylation levels of both proteins decreased after treatment (Figure 5B).

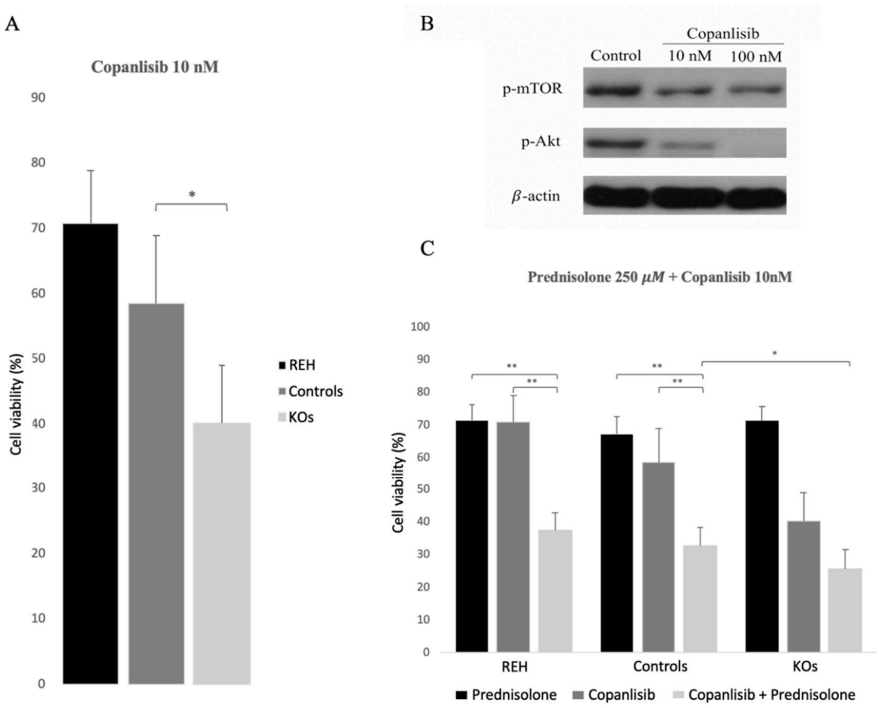

Figure 5. Cell viability and protein expression measured after Copanlisib/Prednisolone treatment. (**A**) Cell viability was measured by the 3-(4,5-Dimethyl-2-thiazolyl)-2,5-diphenyl-2H-tetrazolium bromide also named as Methylthiazolyldiphenyl-tetrazolium bromide (MTT) proliferation assay after treatment (192 h) with Copanlisib (10 nM). E/R KO clones (light grey square line) showed a higher sensitivity to Copanlisib than REH cells (black square line) and control clones (grey square line). This graph represents the average of three independent experiments and in turn the average of the 2 control clones and the 3 KO clones. (**B**) p-Akt (60 kDa) and p-mTOR (289 kDa) expression levels decreased after treatment with Copanlisib. (**C**) Prednisolone (black square line), Copanlisib (dark grey square line) and Copanlisib plus Prednisolone combination (grey square line) were tested in the different clones. The relative cell viability was calculated as the percentage of untreated cells. This experiment had three replicates. * $p \leq 0.05$; ** $p \leq 0.005$ (unpaired *t*-test).

On the other hand, treatment with Prednisolone (250 μM) was comparable to the effect of Copanlisib on E/R-positive cells. We did not observe a higher decrease of cell viability in E/R KO clones as compared with REH cells and control clones (Figure 5C). The combination of Copanlisib (10 nM) and Prednisolone (250 μM) showed a synergistic effect by decreasing the cell viability in REH and control clones expressing *E/R* fusion gene as compared with Prednisolone and Copanlisib alone. Furthermore, we also observed greater reduction of cell viability in E/R KO clones as compared with REH cells and control clones (Figure 5C).

3.5. E/R Repression Impairs the Tumourigenicity In vivo

In order to determine the effects of E/R expression abrogation in vivo, 16 NSG mice were subcutaneously injected with REH cells or control clone (left flank) and KO clones (right flank). Only 6 mice injected with KO clones developed tumour growth on the right flank (6/16), whereas all those injected with REH or control clone developed a tumour (16/16). In the first group (REH cells vs. KO2 clone), none of flanks injected with KO2 developed tumour (mean mass: 0 mg ± 0 vs. 4872.5 mg ± 1323; $p = 0.029$). In the second group (REH cells vs. KO3 clone), only one of flanks injected with KO3 developed a tumour (1/4). This tumour was significantly smaller than those generated from REH cells (mean mass: 40 mg ± 69.3 vs. 4212.5 mg ± 1663.9; $p = 0.029$). In the third group (control clone vs. KO1), we observed tumour growth in 2/4 flanks of mice injected with KO1. These tumours were significantly smaller than those generated from control clone (mean mass: 483 mg ± 354.4 vs. 2470 mg ± 872.5 vs. $p = 0.041$). In the same way, 3/4 mice develop tumours from KO2 in the group 4 (control clone vs. KO2), but these tumours were significantly smaller than those generated from control clone (mean mass: 355 mg ± 293.6 vs. 2255 mg ± 1215.6; $p = 0.029$) (Figure 6A and Figure S5). In general, subcutaneous tumours generated from E/R KO cells were significantly smaller than those produced by REH cells or control clone (mean mass 202 mg ± 298.9 vs. 4542.5 mg ± 1539, $p < 0.001$; 202 mg ± 298.9 vs. 2347.1 mg ± 1087.2, $p \leq 0.001$) (Figure 6B).

In addition, significant differences were observed in the time of appearance of the tumours. Those generated through the KO clones appeared around day 42 (mean: 46.5 ± 7.8), unlike those generated by the REH cells or the control clone, which appeared around day 29 (mean: 29 ± 4.2; $p = 0.001$) and day 36 (mean: 36.6 ± 5.34; $p = 0.03$) respectively (Figure 6C).

Histopathological analysis of representative tumours from each group of mice revealed a proliferation of immature cells with a diffuse pattern (emerging from the dermis) infiltrating the muscle tissue and subcutaneous tissue (dermis and hypodermis) in tumours from REH cells and control clones. These tumours were larger than E/R KO tumours, showing some areas of apoptosis and necrosis. They were composed by round-shaped monoform cells with round nuclei and nucleoli. E/R KO tumours were smaller showing a nodular-diffuse pattern. These tumours were composed of monomorphic and more mature-appearing cells. These cells did not show nucleoli.

Tumours from REH and control clones revealed a higher number of mitotic figures as compared to tumours from KOs clones (52 vs. 20, $p = 0.017$//62 vs. 20; $p = 0.006$). Interestingly in KOs tumours, but not in REH and control clone tumours, we observed the "starry skyő (macrophages containing dead apoptotic tumour cells) (Figure S6). No other morphological changes between tumours were observed.

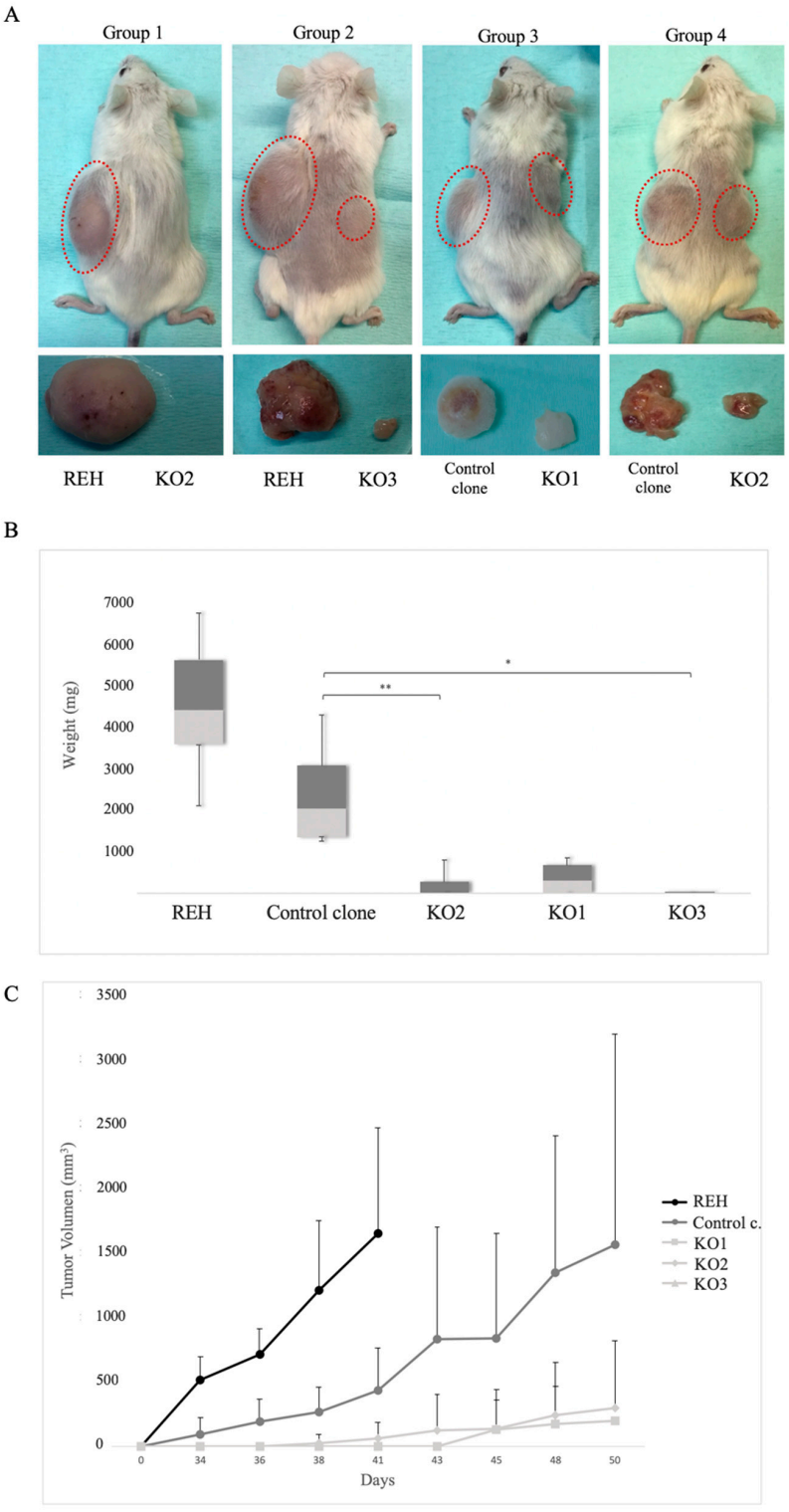

Figure 6. In vivo effects of CRISPR-mediated editing of the *E/R* oncogene. (**A**) External appearance of mice and developed tumours 48–62 days after subcutaneous cell injection. Tumours formed by KO clones (right flank) were smaller than those induced by REH cells or control clones (control c.) (left flank). Each group had four mice. (**B**) Evolution of tumour growth measured every 2–3 days until the moment in which mice were sacrificed. (**C**) Representation of the mean tumour size corresponding to each clone, independently of the group. * $p \leq 0.05$; ** $p \leq 0.005$ (unpaired *t*-test).

4. Discussion

In this study, we generated an E/R KO model in an ALL cell line carrying the t(12,21) in order to assess how the loss of fusion expression affects the tumour cells. Functional analysis by RNA-seq showed that the loss of fusion gene expression caused the deregulation of some genes involved in proliferation and apoptosis processes among others. In vitro, ALL cells showed a lower proliferation rate and a higher apoptosis sensitivity after *E/R* fusion gene abrogation. Furthermore, the loss of E/R expression was able to sensitize ALL cells to PI3K inhibitors. The xenograft model confirmed the results observed in vitro showing a lower oncogenicity of ALL cells after fusion gene suppression.

The recent evolution of genetic editing techniques with the CRISPR/Cas9 system has allowed, among others, the generation of KO gene models, helping us to better understanding the biology of diseases such as ALL [31]. We used CRISPR/Cas9 system to completely eliminate the expression of the E/R fusion protein.

The loss of fusion expression was checked, observing an absence of mRNA coding for E/R in the KO2 and KO3 clones and a leaky expression in KO1 clone. We hypothesize that this loss of mRNA was due to nonsense-mediated mRNA decay mechanism [32]. The design of the RT-qPCR oligonucleotides outside the editing region ruled out the expression of an aberrant form of the fusion protein between exon 5 of *ETV6* and exon 4 of *RUNX1*. Furthermore, the loss of E/R expression was observed by total RNA-seq in E/R KO clones. In this way we generated a powerful model on which to study the effect of the elimination of the fusion gene on leukemic cells. These cells maintain a series of secondary alterations that triggered the leukaemia, similar as occurs in patients.

Transcriptome analysis of different clones showed a huge number of genes significantly deregulated after *E/R* abrogation. Some of them have been previously described in E/R fusion protein silencing studies, such as *CXXC5*, *ARX* and *SORBS2*, which supports these results. Moreover, a high number of upregulated genes were observed after fusion protein abrogation which agrees with the repressive activity of the *E/R* fusion gene [33,34]. Some of these genes have been previously described to be directly regulated by *RUNX1* transcript factor [35]. The most of genes significantly deregulated are involved in different biological processes such as germinal centre formation, regulation of response to external stimulus, positive regulation of multicellular organism process, negative regulation of apoptotic/necroptotic process, regulation of GTPase activity, I-kappaB kinase/NF-kappaB signalling, cellular calcium ion homeostasis, regulation of protein localization, regulation of cell adhesion, cytoskeleton organization and actin filament-based process. These results are in agreement with previous studies, in which was demonstrated the implication of E/R in the cellular processes that may be maintaining the leukemic state of the tumour cells [14,28,33,36]. Furthermore, in our study we observed the downregulation of genes such as *VPS34*, *PTPKR*, *ARHGEF12*, *RGM* and *HAP1*. These findings are in agreement with previous studies by Ross E. and Yeoh E. in which they described the upregulation of these genes in E/R positive patients [25,26].

Within of the significantly deregulated genes we observed in our study the deregulation of genes involved in regulation of cell proliferation such as *RGS16* and *PTPRK* genes. *RGS16* who plays an antiproliferative role through inhibition of the PI3K/Akt/mTOR pathway [37–39] and inhibition of cell migration [40], was upregulated in E/R KO cells. Meanwhile *PTPRK* gene was downregulated after E/R fusion gene abrogation, in line with what was observed in E/R-ALL patients in which it was upregulated [25,26].

Very subtle changes were observed in cell proliferation and cell cycle distribution after *E/R* abrogation in vitro, in agreement with previous studies [12,14]. However, E/R KO clones showed a significantly lower proliferation rate when they were co-cultured with MSC. Mesenchymal cells have been shown to play a key role in the development and evolution of ALL [41,42] and MSCs induced greater cell adhesion, higher proliferation ratio and greater migration capacity to REH cells in a recent study [43]. Our data show that the *E/R* fusion gene therefore participates in the interaction of leukemic cells with the microenvironment and the loss of *E/R* fusion gene expression reverts the proliferative capacity that MSCs confer on leukemic cells.

The regulation of programmed death was another of the altered processes after the elimination of the fusion gene. In particular, an overexpression of the *mir-146* gene was observed. *miR-146* can regulate the expression of the apoptosis factor *STAT1*, and the anti-apoptosis factor *Bcl-xL*, thus promoting the apoptosis of ALL cells [44]. Furthermore, tumour protein P63 gene (*TP63* gene) was also upregulated in E/R KO clones as compared with control clones. This gene is involved in an antiapoptotic pathway that regulates the normal survival of B cells [45,46]. The decreased expression of antiapoptotic factors such as, Bcl-2 and Bcl-xL supported the observed results. E/R KO clones also showed a higher late apoptotic rate in vitro, demonstrating that the fusion gene regulates the expression of antiapoptotic factors that protect leukemic cells from apoptosis. Death levels were also higher in E/R KO clones after treatment with Vincristine.

Furthermore, we wanted to analyse whether the non-expression of E/R and consequently the loss of activation of the PI3K/Akt/mTOR pathway, was able to sensitize the cells to PI3K inhibitors. The use of PI3K inhibitors alone has shown to be an effective treatment in E/R-positive cells. In addition, the activity of these inhibitors in combination with Prednisolone, a GC widely used in the treatment of ALL, decreasing the resistance offered by E/R-positive cells to GCs. In our study, we observed that the use of Copanlisib, a PI3K inhibitor, achieved a significantly decrease of cell viability in E/R KO clones as compared with E/R-positive cells. We also observed that treatment with Copanlisib achieved the sensitization to Prednisolone in E/R-positive cells as recently described [14]. However, in our study, this sensitization was even higher in E/R KO cells. In this way, we can conclude that the fusion gene may be a good therapeutic target with which to improve the drug sensitivity of E/R-positive cells.

Finally, we wanted to check if E/R abrogation also decreased the tumour potential of cells in vivo. For that, a xenograft model was generated by injecting these cells into immunosuppressed mice, taking the injection of REH cells or a control clone on the opposite flank as control. Mice injected with KO clone cells did not generate tumours or generated smaller tumours than those generated by REH cells or control clone. The higher rate of mitotic activity in REH and control tumours observed through the histopathology analysis explains the greater growth of these tumours and reveals a greater tumoural capacity of these cells carrying *E/R* fusion gen in vivo.

Together these data show that by eliminating E/R expression, the cells lost tumourigenicity, decreasing its proliferative capacity, resistance to apoptosis and becoming more sensitive to PI3K inhibitors. Therefore, *E/R* fusion gene seems to play a key role in the maintenance of the leukemic phenotype, protecting cells from apoptosis and generating resistance to treatments. Furthermore, these data suggest that microenvironment confers a proliferative advantage to leukemic cells through E/R fusion gene. However, this study is based on a single E/R cell line, so it would be of great interest to reproduce these results in another cell line carrying the fusion gene to confirm these findings. In this way, although more studies are needed to elucidate the mechanism of action of the fusion gene and despite the good clinical course of these patients, this study suggests that the fusion gene could be a possible therapeutic target to design new drugs that prevent the expression of this protein, especially in those cases of relapse or lack of response to treatments.

Supplementary Materials: The following are available online at http://www.mdpi.com/2073-4409/9/1/215/s1. Table S1: sgRNA designed against E/R fusion sequence, Table S2: Possible off-targets of the sgRNAs, Table S3: Genes significantly deregulated after E/R fusion gene abrogation, Table S4: Enrichment of differentially expressed genes after E/R abrogation, Figure S1: Edited-REH sequences, Figure S2: Edited sequences of single cell derived-cell line, Figure S3: GO Enrichment Analysis, Figure S4: MTT proliferation assay, Figure S5: Measure of tumour growth, Figure S6: Tumour growth and histopathological findings.

Author Contributions: A.M., I.G.-T., R.B. and J.M.H.-R. designed the research. A.M. performed the experiments, compiled data and drafted the manuscript. J.L.O. and V.A.-P. were responsible for mouse experiments and drug tests. J.H.-S. and S.S. were responsible for sequencing experiments. R.B. and T.G. helped interpret the transcriptomic analysis. I.G.T. and J.M.H.-R. helped to interpret functional analysis. A.M. wrote the paper with input from all authors. All authors have read and agreed to the published version of the manuscript.

Funding: This work was financially supported in part by a grant from the Consejería de Educación, Junta de Castilla y León, Fondos FEDER (SA085U16, SA271P18), and the Regional Council of Castilla y León SACYL, (GRS 1847/A/18, GRS 2062/A/19), SYNtherapy. Synthetic Lethality for Personalized Therapy-based Stratification In Acute

Leukaemia (ERAPERMED2018-275); ISCIII (AC18/00093), co-funded by ERDF/ESF, "Investing in your future", Fundación Castellano Leonesa de Hematología y Hemoterapia (FUCALHH 2017), Proyectos de investigación en Biomedicina, gestión sanitaria y atención sociosanitaria del IBSAL (IBY17/00006), Fundación Memoria Don Samuel Solórzano Barruso, Centro de Investigación Biomédica en Red de Cáncer (CIBERONC CB16/12/00233).JMHS is supported by a research grant by FEHH ("Fundación Española de Hematología y Hemoterapia"), and JLO is supported by a grant from the University of Salamanca ("Contrato postdoctoral programa II 2017-18")., and AM by a grant from the Junta Provincial de Salamanca of the Asociación Española Contra el Cáncer (AECC).

Acknowledgments: We thank Sara González, Irene Rodríguez, Teresa González, Maribel Forero-Castro, Ana Marín-Quílez, María Herrero-García, Cristina Miguel, Alejandro Rodríguez, Teresa Prieto, María Ángeles Ramos, Filomena Corral, Almudena Martín, Ana Díaz, Ana Simón, María del Pozo, Isabel M Isidro, Vanesa Gutiérrez, Sandra Pujante and María Angeles Hernández from the Cancer Research Center of Salamanca, Spain, for their technical support. We are grateful to Ángel Prieto and Ana I García, María Luz Sánchez and María Carmen Macías from the Microscopy Unit, Cytometry Unit and Molecular Pathology Unit, respectively, from the Cancer Research Center of Salamanca for the technical assistance. We thank Luis Muñoz and all the members from the Animal Experimentation Research Center from the University of Salamanca.

Conflicts of Interest: The authors declare no conflict of interest.

References

1. Pui, C.H.; Relling, M.V.; Downing, J.R. Acute lymphoblastic leukemia. *N. Engl. J. Med.* **2004**, *350*, 1535–1548.
2. Shurtleff, S.A.; Buijs, A.; Behm, F.G.; Rubnitz, J.E.; Raimondi, S.C.; Hancock, M.L.; Chan, G.C.; Pui, C.H.; Grosveld, G.; Downing, J.R. TEL/AML1 fusion resulting from a cryptic t(12;21) is the most common genetic lesion in pediatric ALL and defines a subgroup of patients with an excellent prognosis. *Leukemia* **1995**, *9*, 1985–1989. [PubMed]
3. Conter, V.; Bartram, C.R.; Valsecchi, M.G.; Schrauder, A.; Panzer-Grumayer, R.; Moricke, A.; Arico, M.; Zimmermann, M.; Mann, G.; De Rossi, G.; et al. Molecular response to treatment redefines all prognostic factors in children and adolescents with B-cell precursor acute lymphoblastic leukemia: Results in 3184 patients of the AIEOP-BFM ALL 2000 study. *Blood* **2010**, *115*, 3206–3214. [CrossRef] [PubMed]
4. Moorman, A.V.; Ensor, H.M.; Richards, S.M.; Chilton, L.; Schwab, C.; Kinsey, S.E.; Vora, A.; Mitchell, C.D.; Harrison, C.J. Prognostic effect of chromosomal abnormalities in childhood B-cell precursor acute lymphoblastic leukaemia: Results from the UK Medical Research Council ALL97/99 randomised trial. *Lancet Oncol.* **2010**, *11*, 429–438. [CrossRef]
5. Pui, C.-H.; Robison, L.L.; Look, A.T. Acute lymphoblastic leukaemia. *Lancet* **2008**, *371*, 1030–1043. [CrossRef]
6. Rubnitz, J.E.; Downing, J.R.; Pui, C.H. Significance of the TEL-AML fusion gene in childhood AML. *Leukemia* **1999**, *13*, 1470–1471. [CrossRef] [PubMed]
7. Uckun, F.M.; Pallisgaard, N.; Hokland, P.; Navara, C.; Narla, R.; Gaynon, P.S.; Sather, H.; Heerema, N. Expression of TEL-AML1 fusion transcripts and response to induction therapy in standard risk acute lymphoblastic leukemia. *Leuk. Lymphoma* **2001**, *42*, 41–56. [CrossRef]
8. Bokemeyer, A.; Eckert, C.; Meyr, F.; Koerner, G.; von Stackelberg, A.; Ullmann, R.; Turkmen, S.; Henze, G.; Seeger, K. Copy number genome alterations are associated with treatment response and outcome in relapsed childhood ETV6/RUNX1-positive acute lymphoblastic leukemia. *Haematologica* **2014**, *99*, 706–714. [CrossRef]
9. Kuster, L.; Grausenburger, R.; Fuka, G.; Kaindl, U.; Krapf, G.; Inthal, A.; Mann, G.; Kauer, M.; Rainer, J.; Kofler, R.; et al. ETV6/RUNX1-positive relapses evolve from an ancestral clone and frequently acquire deletions of genes implicated in glucocorticoid signaling. *Blood* **2011**, *117*, 2658–2667. [CrossRef]
10. Raynaud, S.; Cave, H.; Baens, M.; Bastard, C.; Cacheux, V.; Grosgeorge, J.; Guidal-Giroux, C.; Guo, C.; Vilmer, E.; Marynen, P.; et al. The 12;21 translocation involving TEL and deletion of the other TEL allele: Two frequently associated alterations found in childhood acute lymphoblastic leukemia. *Blood* **1996**, *87*, 2891–2899. [CrossRef]
11. Sun, C.; Chang, L.; Zhu, X. Pathogenesis of ETV6/RUNX1-positive childhood acute lymphoblastic leukemia and mechanisms underlying its relapse. *Oncotarget* **2017**, *8*, 35445–35459. [CrossRef] [PubMed]
12. Zaliova, M.; Madzo, J.; Cario, G.; Trka, J. Revealing the role of TEL/AML1 for leukemic cell survival by RNAi-mediated silencing. *Leukemia* **2011**, *25*, 313–320. [CrossRef] [PubMed]
13. Diakos, C.; Krapf, G.; Gerner, C.; Inthal, A.; Lemberger, C.; Ban, J.; Dohnal, A.M.; Panzer-Grumayer, E.R. RNAi-mediated silencing of TEL/AML1 reveals a heat-shock protein and survivin-dependent mechanism for survival. *Blood* **2007**, *109*, 2607–2610. [CrossRef] [PubMed]

14. Fuka, G.; Kantner, H.P.; Grausenburger, R.; Inthal, A.; Bauer, E.; Krapf, G.; Kaindl, U.; Kauer, M.; Dworzak, M.N.; Stoiber, D.; et al. Silencing of ETV6/RUNX1 abrogates PI3K/AKT/mTOR signaling and impairs reconstitution of leukemia in xenografts. *Leukemia* **2012**, *26*, 927–933. [CrossRef] [PubMed]
15. Garcia-Tunon, I.; Hernandez-Sanchez, M.; Ordonez, J.L.; Alonso-Perez, V.; Alamo-Quijada, M.; Benito, R.; Guerrero, C.; Hernandez-Rivas, J.M.; Sanchez-Martin, M. The CRISPR/Cas9 system efficiently reverts the tumorigenic ability of BCR/ABL in vitro and in a xenograft model of chronic myeloid leukemia. *Oncotarget* **2017**, *8*, 26027–26040. [CrossRef]
16. Martinez, N.; Drescher, B.; Riehle, H.; Cullmann, C.; Vornlocher, H.P.; Ganser, A.; Heil, G.; Nordheim, A.; Krauter, J.; Heidenreich, O. The oncogenic fusion protein RUNX1–CBFA2T1 supports proliferation and inhibits senescence in t(8;21)-positive leukaemic cells. *BMC Cancer* **2004**, *4*, 44. [CrossRef]
17. Supek, F.; Bosnjak, M.; Skunca, N.; Smuc, T. REVIGO summarizes and visualizes long lists of gene ontology terms. *PLoS ONE* **2011**, *6*, e21800. [CrossRef]
18. Abramoff, M.D.; Magalhães, P.J.; Ram, S.J. Image Processing with ImageJ. *Biophotonics Int.* **2004**, *11*, 36–42.
19. Collins, T.J. ImageJ for microscopy. *Biotechniques* **2007**, *43*, 25–30. [CrossRef]
20. Ordonez, J.L.; Amaral, A.T.; Carcaboso, A.M.; Herrero-Martin, D.; del Carmen Garcia-Macias, M.; Sevillano, V.; Alonso, D.; Pascual-Pasto, G.; San-Segundo, L.; Vila-Ubach, M.; et al. The PARP inhibitor olaparib enhances the sensitivity of Ewing sarcoma to trabectedin. *Oncotarget* **2015**, *6*, 18875–18890. [CrossRef]
21. Brownlie, R.J.; Zamoyska, R. T cell receptor signalling networks: Branched, diversified and bounded. *Nat. Rev. Immunol.* **2013**, *13*, 257–269. [CrossRef]
22. Corthals, S.L.; Wynne, K.; She, K.; Shimizu, H.; Curman, D.; Garbutt, K.; Reid, G.S. Differential immune effects mediated by Toll-like receptors stimulation in precursor B-cell acute lymphoblastic leukaemia. *Br. J. Haematol.* **2006**, *132*, 452–458. [CrossRef]
23. Melo, R.C.C.; Longhini, A.L.; Bigarella, C.L.; Baratti, M.O.; Traina, F.; Favaro, P.; de Melo Campos, P.; Saad, S.T. CXCR7 is highly expressed in acute lymphoblastic leukemia and potentiates CXCR4 response to CXCL12. *PLoS ONE* **2014**, *9*, e85926. [CrossRef]
24. Polak, R.; Bierings, M.B.; van der Leije, C.S.; Sanders, M.A.; Roovers, O.; Marchante, J.R.M.; Boer, J.M.; Cornelissen, J.J.; Pieters, R.; den Boer, M.L.; et al. Autophagy inhibition as a potential future targeted therapy for ETV6-RUNX1-driven B-cell precursor acute lymphoblastic leukemia. *Haematologica* **2019**, *104*, 738–748. [CrossRef]
25. Ross, M.E.; Zhou, X.; Song, G.; Shurtleff, S.A.; Girtman, K.; Williams, W.K.; Liu, H.C.; Mahfouz, R.; Raimondi, S.C.; Lenny, N.; et al. Classification of pediatric acute lymphoblastic leukemia by gene expression profiling. *Blood* **2003**, *102*, 2951–2959. [CrossRef]
26. Yeoh, E.J.; Ross, M.E.; Shurtleff, S.A.; Williams, W.K.; Patel, D.; Mahfouz, R.; Behm, F.G.; Raimondi, S.C.; Relling, M.V.; Patel, A.; et al. Classification, subtype discovery, and prediction of outcome in pediatric acute lymphoblastic leukemia by gene expression profiling. *Cancer Cell* **2002**, *1*, 133–143. [CrossRef]
27. Bauer, E.; Schlederer, M.; Scheicher, R.; Horvath, J.; Aigner, P.; Schiefer, A.I.; Kain, R.; Regele, H.; Hoermann, G.; Steiner, G.; et al. Cooperation of ETV6/RUNX1 and BCL2 enhances immunoglobulin production and accelerates glomerulonephritis in transgenic mice. *Oncotarget* **2016**, *7*, 12191–12205. [CrossRef]
28. Torrano, V.; Procter, J.; Cardus, P.; Greaves, M.; Ford, A.M. ETV6-RUNX1 promotes survival of early B lineage progenitor cells via a dysregulated erythropoietin receptor. *Blood* **2011**, *118*, 4910–4918. [CrossRef]
29. Krause, G.; Hassenruck, F.; Hallek, M. Copanlisib for treatment of B-cell malignancies: The development of a PI3K inhibitor with considerable differences to idelalisib. *Drug Des. Dev. Therapy* **2018**, *12*, 2577–2590. [CrossRef]
30. Liu, N.; Rowley, B.R.; Bull, C.O.; Schneider, C.; Haegebarth, A.; Schatz, C.A.; Fracasso, P.R.; Wilkie, D.P.; Hentemann, M.; Wilhelm, S.M.; et al. BAY 80–6946 is a highly selective intravenous PI3K inhibitor with potent p110alpha and p110delta activities in tumor cell lines and xenograft models. *Mol. Cancer Ther.* **2013**, *12*, 2319–2330. [CrossRef]
31. Montano, A.; Forero-Castro, M.; Hernandez-Rivas, J.M.; Garcia-Tunon, I.; Benito, R. Targeted genome editing in acute lymphoblastic leukemia: A review. *BMC Biotechnol.* **2018**, *18*, 45. [CrossRef] [PubMed]
32. Culbertson, M.R.; Leeds, P.F. Looking at mRNA decay pathways through the window of molecular evolution. *Curr. Opin. Genet. Dev.* **2003**, *13*, 207–214. [CrossRef]

33. Fuka, G.; Kauer, M.; Kofler, R.; Haas, O.A.; Panzer-Grumayer, R. The leukemia-specific fusion gene ETV6/RUNX1 perturbs distinct key biological functions primarily by gene repression. *PLoS ONE* **2011**, *6*, e26348. [CrossRef] [PubMed]
34. Hiebert, S.W.; Sun, W.; Davis, J.N.; Golub, T.; Shurtleff, S.; Buijs, A.; Downing, J.R.; Grosveld, G.; Roussell, M.F.; Gilliland, D.G.; et al. The t(12;21) translocation converts AML-1B from an activator to a repressor of transcription. *Mol. Cell. Biol.* **1996**, *16*, 1349–1355. [CrossRef]
35. Tijssen, M.R.; Cvejic, A.; Joshi, A.; Hannah, R.L.; Ferreira, R.; Forrai, A.; Bellissimo, D.C.; Oram, S.H.; Smethurst, P.A.; Wilson, N.K.; et al. Genome-wide analysis of simultaneous GATA1/2, RUNX1, FLI1, and SCL binding in megakaryocytes identifies hematopoietic regulators. *Dev. Cell* **2011**, *20*, 597–609. [CrossRef]
36. Inthal, A.; Krapf, G.; Beck, D.; Joas, R.; Kauer, M.O.; Orel, L.; Fuka, G.; Mann, G.; Panzer-Grumayer, E.R. Role of the erythropoietin receptor in ETV6/RUNX1-positive acute lymphoblastic leukemia. *Clin. Cancer Res.* **2008**, *14*, 7196–7204. [CrossRef]
37. Liang, G.; Bansal, G.; Xie, Z.; Druey, K.M. RGS16 inhibits breast cancer cell growth by mitigating phosphatidylinositol 3-kinase signaling. *J. Biol. Chem.* **2009**, *284*, 21719–21727. [CrossRef]
38. Liu, T.; Bohlken, A.; Kuljaca, S.; Lee, M.; Nguyen, T.; Smith, S.; Cheung, B.; Norris, M.D.; Haber, M.; Holloway, A.J.; et al. The retinoid anticancer signal: Mechanisms of target gene regulation. *Br. J. Cancer* **2005**, *93*, 310–318. [CrossRef]
39. Vasilatos, S.N.; Katz, T.A.; Oesterreich, S.; Wan, Y.; Davidson, N.E.; Huang, Y. Crosstalk between lysine-specific demethylase 1 (LSD1) and histone deacetylases mediates antineoplastic efficacy of HDAC inhibitors in human breast cancer cells. *Carcinogenesis* **2013**, *34*, 1196–1207. [CrossRef]
40. Berthebaud, M.; Riviere, C.; Jarrier, P.; Foudi, A.; Zhang, Y.; Compagno, D.; Galy, A.; Vainchenker, W.; Louache, F. RGS16 is a negative regulator of SDF-1-CXCR4 signaling in megakaryocytes. *Blood* **2005**, *106*, 2962–2968. [CrossRef]
41. Genitsari, S.; Stiakaki, E.; Perdikogianni, C.; Martimianaki, G.; Pelagiadis, I.; Pesmatzoglou, M.; Kalmanti, M.; Dimitriou, H. Biological Features of Bone Marrow Mesenchymal Stromal Cells in Childhood Acute Lymphoblastic Leukemia. *Turk. J. Haematol. Off. J. Turk. Soc. Haematol.* **2018**, *35*, 19–26. [CrossRef]
42. Nwabo Kamdje, A.H.; Kamga, P.T.; Simo, R.T.; Vecchio, L.; Seke Etet, P.F.; Muller, J.M.; Bassi, G.; Lukong, E.; Goel, R.K.; Amvene, J.M.; et al. Mesenchymal stromal cells' role in tumor microenvironment: Involvement of signaling pathways. *Cancer Biol. Med.* **2017**, *14*, 129–141. [CrossRef]
43. Bonilla, X.; Vanegas, N.P.; Vernot, J.P. Acute Leukemia Induces Senescence and Impaired Osteogenic Differentiation in Mesenchymal Stem Cells Endowing Leukemic Cells with Functional Advantages. *Stem Cells Int.* **2019**, *2019*, 3864948. [CrossRef]
44. Yan, W.; Guo, H.; Suo, F.; Han, C.; Zheng, H.; Chen, T. The effect of miR-146a on STAT1 expression and apoptosis in acute lymphoblastic leukemia Jurkat cells. *Oncol. Lett.* **2017**, *13*, 151–154. [CrossRef]
45. Binsky, I.; Lantner, F.; Grabovsky, V.; Harpaz, N.; Shvidel, L.; Berrebi, A.; Goldenberg, D.M.; Leng, L.; Bucala, R.; Alon, R.; et al. TAp63 regulates VLA-4 expression and chronic lymphocytic leukemia cell migration to the bone marrow in a CD74-dependent manner. *J. Immunol.* **2010**, *184*, 4761–4769. [CrossRef]
46. Lantner, F.; Starlets, D.; Gore, Y.; Flaishon, L.; Yamit-Hezi, A.; Dikstein, R.; Leng, L.; Bucala, R.; Machluf, Y.; Oren, M.; et al. CD74 induces TAp63 expression leading to B-cell survival. *Blood* **2007**, *110*, 4303–4311. [CrossRef]

GENERAL DISCUSSION

"Live as if you were to die tomorrow. Learn as if you were to live forever"

Mahatma Gandhi

Acute lymphoblastic leukemia (ALL) is a hematological neoplasm that can affect both the B and T-lymphoid lineages. B-cell acute lymphoblastic leukemia (B-ALL) is the most common subtype and presents great heterogeneity both at a clinical and biological level. It is therefore essential to assess the clinical, biological and genetic factors at time of diagnosis, since these allow us to stratify patients according to risk and are also especially relevant in therapy decision-making. These factors include a series of clinical-biological parameters such as age, minimal residual disease (MRD) or the cytogenetic subgroup, this latter one defined by a series of genetic alterations that appear recurrently in these patients [6].

B-ALL presents a series of recurrent genetic alterations which are the basis of the current WHO classification, and considered one of the most important prognostic factors [27]. These anomalies mainly include aneuploidies and chromosomal rearrangements leading to fusion genes. Each of these recurrent alterations has also been associated with a specific prognostic risk, so patients can be classified into different genetic subtypes considered high, intermediate or low risk [65]. In fact, some of the large differences observed in survival rates in children and adults could mainly be due to the distribution of the different biological subtypes among the age groups. According to our results and previous studies, it can be observed that in children low-risk biological subgroups, such as high hyperdiploidy and rearranged *ETV6/RUNX1*, were more frequent, while in adults high-risk biological subgroups, such as the presence of Philadelphia chromosome, were more recurrent [65].

The application of high-throughput genomic methodologies such as array analysis and NGS to the study of B-ALL, allowing the identification of multiple new alterations helping to better understand the development and evolution of the disease [17,137,166,174]. These alterations include point mutations, copy number changes (CNVs), as well as new rearrangements. The latter were recently identified thanks to the integration of RNA-seq into the study of B-ALL [194,200]. Gene expression profile studies have even managed to establish new independent biological groups defined by the presence of some of these alterations, such as the rearrangements of *DUX4*, *ZNF384* and *NUMT1* genes, or anomalies in *PAX5* [174,194–200].

Although most of these new alterations are not yet taken into account in the clinical routine, they will probably be considered in the not too distant future. In fact, some of them already have an established prognostic value, as is the case of *IKZF1, CDKN2A/B* and *BTG1* losses or *TP53*, *JAK2* and *ABL1* mutations, all considered as poor prognostic factors [39,126,127,172,184,186,224]. Especially, previous studies in our group reported the importance of mutations in *TP53* and *JAK2*, both associated with lower overall survival, event-free survival and higher relapse rates. Mutations in *TP53* were maintained as an independent risk factor associated with a higher relapse rate in both children and adults, while *JAK2* mutations only in adults [126].

The detection of these secondary alterations with high prognostic value, such as mutations and CNVs, is very interesting since they help us to refine the stratification of patients, especially in the so called of B-other patients. This subgroup of patients constitutes approximately 30% of B-ALL patients and it is defined by the lack of some of the recurrent genetic alterations that allow their stratification in the different risk groups. Although the classification of these patients has been substantially refined, many of the new alterations described overlap with the different biological groups, so a correct genetic characterization and classification of these patients is necessary. Due to the lack of criteria for the classification of these patients, they are considered to be of uncertain risk, which constitutes a problem in clinical practice since many of them have been found to have a poor outcome. Our results showed that the loss of *IKZF1*, *CDKN2A/*B, and *PAX5* genes, as well as *CRLF2* rearrangements were frequently observed within this subgroup of patients, which is in agreement with previous studies [61]. Both the loss of *IKZF1* and *CDKN2A*, as well as *CRLF2* rearrangements have been associated with a poor prognosis in previous studies [39,170,186]. Therefore, the recurrence of these alterations with high prognostic value could be very useful in the risk re-stratification of these patients.

Some of these secondary alterations are also considered as possible therapeutic targets. In fact, specific targeted treatments have already been proposed. For example, the use of inhibitors or immunotherapy for the treatment of patients with *CRLF2* rearrangements, the use of ruxolitinib for patients with alterations in the JAK/STAT pathway, or the use of MEK molecule inhibitors for those with altered RAS/MAPK pathway [204,206–209]. Patients having these alterations could benefit from personalized therapy, which could result in an improvement in survival rates. Proof of this is the better survival rates achieved by Philadelphia+ patients thanks to the development and application of tyrosine kinase inhibitors (TKI). The use of TKIs has thus changed the outcome of these patients, who were historically considered to be a high-risk group and now have a better prognosis [58].

Genetic studies in B-ALL have also identified a series of gene variants and SNPs that are strongly related to the response to drugs already used in ALL treatment, and these genetic changes were detected in our series of patients. Among them, it is worth mentioning the polymorphisms identified in *TPMT* and *MTHFR* genes, implicated in the metabolism of 6-mercaptopurine and methotrexate, respectively [74,235]. The detection of SNPs associated with pharmacogenetics could lead a change in current therapeutic strategies or dose adjustment, and thus reducing treatment toxicity [236].

Therefore, the detection of these secondary alterations that include mutations, CNVs and SNPs during the diagnostic process of B-ALL patients could imply an improvement in the classification and risk stratification of patients and have a direct impact on therapy decision-making. Nowadays, the

detection of genetic alterations in B-ALL patients during the diagnosis is carried out through the use of conventional cytogenetic techniques (karyotyping and FISH), which mainly allows the detection of translocations and aneuploidies. The use of an array of different techniques is thus often required for the correct biological stratification of patients, resulting in higher costs and more time-consuming. Moreover, some of these previously mentioned techniques can report false negatives. For example, karyotyping can often be misleading either due to the absence of metaphases to analyze or the lack of growth of the malignant clone and, as a result, they cannot be analyzed [54,142]. On the other hand, FISH is limited by the number of known alterations to be studied. MLPA is also often prone to false positives and cannot detect alterations that are below 25% of the cells. This can make it difficult to detect alterations with high prognostic value such as the loss of *IKZF1*, although it has not yet been demonstrated whether subclonal alterations are also associated with a poor prognosis [237]. In addition, both MLPA and array approaches have limitations in recognizing point mutations, focal aberrations such as small insertions/deletions (INDEL) and chromosomal rearrangements [144].

The recent development of genomic techniques such as NGS has made it possible to facilitate the sequencing of genetic regions, proving to be able to detect a wide range of alterations including not only mutations, but also fusion genes and CNVs [238,239]. NGS approaches include the study of DNA and RNA (usually mRNA) and it can be based on the study of whole genome (WGS), whole exome (WES), or specific regions of interest through targeted panels. The sequencing of these targeted regions can also follow two main strategies, the capture hybridization-based sequencing, which offers a more homogeneous coverage between the different regions, and amplicon-based sequencing, which offers a higher depth although it is more prone to errors. Unlike WGS and WES, the targeted panels only provide information on the regions of interest for which they are designed. This avoids the analysis of a large number of variants of uncertain significance that are not useful for clinical management, and also greatly simplifies data analysis [151,152]. This is translated into a shorter turnaround time, which is essential when dealing with diseases such as B-ALL that must be treated quickly due to their rapid evolution. Targeted panels are also dynamic, allowing the integration of new described regions with prognostic value, making them the ideal candidate for clinical application, one that needs to be constantly updated. Nevertheless, the use of WGS and WES continue to be powerful tools, but more focused, in our view, to be used in research applications only by conducting new exploratory studies. RNA-seq studies, on the other hand, allow for expression analysis, which is of great interest in the study of diseases such as B-ALL in which a large number of gene fusions have been reported. Its application is particularly interesting in the detection of expression signatures that allow the identification of Ph-like patients. However, the main limitation

is the need to work with RNA which it is much less stable than DNA, making it more difficult to handle, transport and store.

Taking all of this into consideration, one of the objectives of this doctoral thesis was to develop a comprehensive DNA-based targeted panel that would make it possible to detect the main genetic alterations associated with B-ALL in a single assay and, thus, improve patient classification and stratification in the ALL diagnostic routine. These alterations include mutations (SNVs/INDELs), recurrent fusion genes (*ETV6/RUNX1*, *BCR/ABL1*, *MLL*r and *CRLF2*r), CNVs, aneuploidies and pharmacogenetic SNPs.

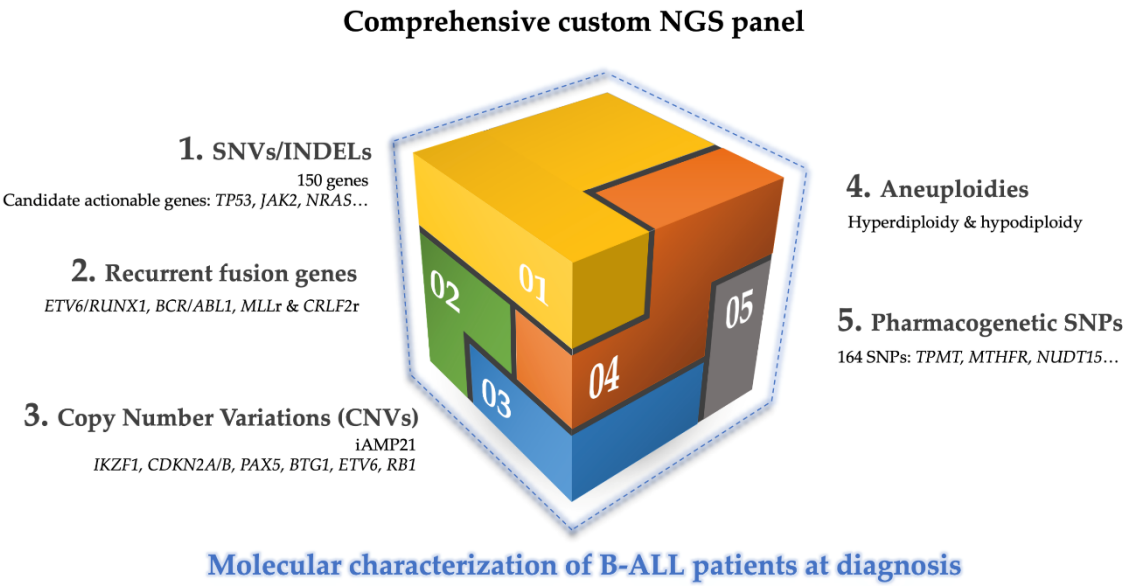

The results of our work show that the custom NGS panel successfully detected the genetic alterations included in the design. On the one hand, the NGS supported conventional cytogenetic techniques by detecting the recurrent genetic alterations included in the WHO classification. In particular, the NGS panel proved to be a powerful tool in the identification of high hyperdiploid patients, even detecting those cases that were not detected by karyotyping. In this sense, the combined application of the designed targeted NGS panel together with the standard diagnostic techniques (karyotype and FISH) allowed us to stratify a higher number of patients than with the standard diagnostic techniques alone.

On the other hand, the custom NGS panel proved to be also a robust tool in the detection of secondary alterations, reproducing faithfully the findings observed by other techniques such as MLPA and aCGH. Moreover, the NGS showed a higher sensitivity than aCGH in the detection of trisomies and allowed the detection of CNVs in much more genes than those included in the commercial MLPA panels. Thus, the NGS panel was able to overcome some of the limitations of the

techniques commonly used in the clinical routine, so that their use could replace that of additional techniques such as array and MLPA approaches. This could lead to a drastic cost reduction and, above all, a reduction in turnaround time.

Furthermore, the NGS panel was particularly interesting in the detection of potential Ph-like patients. The diagnosis of these patients is a real challenge since, unlike the rest of the subgroups, it is defined by the presence of a characteristic expression profile, thus lacking a specific genetic alteration that would help identify them [240,241]. However, the detection of a series of recurrent alterations in these patients, such as the loss of *IKZF1*, *PAX5* and *BTG1* genes, as well as mutations in the RAS pathway and *CRLF2* gene rearrangements, allowed the identification of possible Philadelphia like cases [173,184,242,243]. This is of great interest since these patients have been associated with poor prognosis and may benefit from specific therapies such as TKIs [244]. The detection of possible Ph-like patients through the NGS panel could serve as a first screening to avoid performing expression studies in all newly diagnosed patients, which would also help reduce time and costs.

The NGS panel was therefore able to identify the main genetic alterations that are clinically relevant in B-ALL, also allowing to improve and refine the classification and stratification of patients, as well as to detect possible therapeutic targets and treatment predictors such as pharmacogenetic SNPs. However, the panel presented in this study also has some limitations. Due to the current design of the panel where we prevailed the size and the starting material (just DNA), we could detect rearrangements only in the designed regions. For this reason, and even taking into account its limitations, we consider that the NGS panel could be a valuable tool to be translated into the clinical routine, in combination with conventional cytogenetic techniques, at least until the aforementioned NGS limitations are resolved. This idea is also defended by other groups, who propose the NGS as the most promising tool with which to achieve one of the most desired goals of today's medicine, personalized precision medicine [144,245]. In fact, the group of Inaba H et al. evaluated the use of NGS using RNA-seq in the clinical setting of ALL, concluding that it was a very valuable tool for the clinical management of patients because it allowed the identification of therapeutic targets and markers that help select a more appropriate treatment and, thus reduce toxicity [165]. Due to the high coverage of the genetic lesions this panel is now used in the Current Pethema Protocol for the treatment of ALL patients.

These results also propose that the use of the NGS panel would not only be useful in the diagnosis but could also be useful for monitoring patients during treatment. Optimistically, having the better understanding of the genomic heterogeneity at diagnosis and throughout treatment should allow us to recognize problematic and complex clones that may require targeted therapies to achieve deep and durable remission. In particular, the genetic study of patients who relapse could

help to understand how the disease evolves and to determine the impact of these genetic alterations which could become new risk factors for relapse. Relapsed B-ALL is a very complex process characterized by the presence of a great clonal heterogeneity and a genetically dynamic profile from diagnosis to relapse [128].

Despite efforts to intensify reintroduction strategies, a high percentage of patients continue to have relapses. Specifically, 40-50% of adults and 15-20% of children relapse [114–117]. In addition, the prognosis after the relapse is very adverse, so many of them end up succumbing to the disease [246].

In line with other studies, many of the alterations present in the relapse of B-ALL patients were also present from the moment of diagnosis. In fact, only 6% of relapsed cases of B-ALL are considered "new leukemias" because they do not present common alterations with the clone present at diagnosis [24,130,131]. Nevertheless, a greater number of studies are needed to determine whether these are really new leukemias or whether these alterations are not detected at diagnosis because they are present in a very low percentage of the cells and therefore the techniques used were not sufficiently sensitive to detect them. Furthermore, the results presented in this doctoral thesis show that patients presented a significantly higher number of alterations in relapse compared to the time of diagnosis. These facts suggest that the relapse process could be driven by the persistence of a series of genetic alterations that confer resistance to treatment and that these alterations can be present from the moment of diagnosis or can be acquired during treatment.

The integrative study of mutations and CNVs using NGS, aCGH and MLPA was able to identify a large number of alterations in the paired diagnostic-relapse samples. These findings suggest once again that B-ALL is a complex disease with diverse types of alterations and that these should be studied together and not independently. The focal and broad loss of the short arm of chromosome 9 (9p) and chromosome 7 (7p) were the two most recurrent events detected at diagnosis and/or relapse. Both events involve the loss of the *CDKN2A/B* and *IKZF1* genes respectively and are considered poor prognostic factors [39,172,186]. Indeed, the loss of *IKZF1* together with *TP53* mutations were the most frequently observed events in relapsed patients. These results are in agreement with previous studies in which these alterations are associated with a higher risk of relapse [39,124–126]. Although the presence of these alterations has been shown to be more frequent in adults, they have also demonstrated their prognostic value in the pediatric population [191].

In our study we also observed different patterns in the detected alterations. On the one hand, all cases with *TP53* mutations at diagnosis showed an increase in VAF at the time of relapse. In two patients a mutation in *TP53* gene was even detected “de novo” at relapse. On the other hand, one of

the patients showed the loss of a *PAX5* mutation at the time of relapse. This indicates that there are alterations that are sensitive to treatment and therefore are disappearing or even disappearing completely at the time of relapse.

These results once again highlight the importance of correct genetic characterization of patients at diagnosis and underline the importance of detecting even the small subclones that may be responsible for relapse [24,247,248]. In particular, the presence of alterations in *TP53* and *IKZF1* gene could contribute to the re-stratification of the risk of B-ALL patients and to propose timely therapeutic strategies, such as intensifying treatment and identifying transplant candidates or inclusion in clinical trials due to their high risk of a second relapse. In fact, these two events were included in the new "Pethema 2019" protocol established by the Spanish group, to be considered in therapy decision-making.

Thus, advances in genomic techniques have made it possible to identify a wide spectrum of new alterations, although many of them do not yet have an established prognostic value. In this sense, functional studies are required to help elucidate the role that these alterations play in the pathogenesis of the disease. The new approaches of genomic editing, such as the CRISPR/Cas9 system, used in this doctoral thesis, have shown to be a very powerful tool in the generation of *in vitro* and *in vivo* models that help to recapitulate the alterations described by genomic techniques and therefore study these at a functional level. In fact, a large number of studies have already been published in the area of ALL [232]. The generation of *in vitro* and *in vivo* models could thus help to elucidate the role of these alterations in leukemogenesis and also represents a fundamental step in the development of new drugs.

Most of these recurrent genetic alterations are considered to be the primary events that trigger the development of the disease, as is the case with *MLL* rearrangements. Previously published studies have shown that the presence of this alteration by itself is sufficient to initiate the development of leukemia [12]. Nevertheless, there is still controversy about whether other alterations, such as *ETV6/RUNX1* fusion gene, have a role in maintaining the disease once it has developed. The generation of murine models carrying the *ETV6/RUNX1* fusion gene revealed that the appearance of second events was necessary to trigger the leukemic process in these mice [13,14]. These findings made think that the *ETV6/RUNX1* fusion gene did not contribute therefore in the maintenance of the leukemic phenotype, even suggesting that the presence of the fusion gene was dispensable for the survival of the leukemic cells [249–251]. Conversely, other studies suggested that the fusion gene did participate in the maintenance of the leukemic phenotype through the deregulation of different pathways such as PI3K/Akt/mTOR, STAT3 and MDM2/TP53 pathways [26].

The results presented in this doctoral thesis shed light on the controversy thus generated, demonstrating through the generation of an *ETV6/RUNX1* KO model, that it contributes to the maintenance of the leukemic phenotype through the regulation of key processes for the survival of leukemic cells such as the control of apoptosis. In addition, the deregulation of other key processes was observed such as autophagy through the under-expression of the *Vps34* gene, which was also recently described by Polak et al's group [252]. The generation of xenograft models further showed that the oncogenic potential of leukemic cells was significantly lower when the expression of the fusion gene was eliminated. Our results thus show that the *ETV6/RUNX1* fusion gene could be driving the evolution of the disease and thus be partly responsible for the relapse of these patients. These findings suggest, therefore, that the *ETV6/RUNX1* fusion gene could be considered as a possible therapeutic target with which to treat these patients, who even considered to have a favorable prognosis continue to have a high rate of relapse [26,253,254].

Some studies already propose the use of specific therapies for these patients such as inhibitors of autophagy [252]. On the other hand, the group of Fuka G et al., observed that the use of PI3K inhibitors could be a potential and plausible therapeutic option for these patients, especially for those who presented resistance to prednisolone [251]. Furthermore, our results showed that the elimination of the fusion gene succeeded in sensitizing cells to the treatment, in particular to PI3K inhibitors, as well as to their combination with prednisolone. These findings therefore suggest that the use of inhibitors that block the activity of the fusion gene could reduce resistance to treatment and thus prevent the occurrence of relapses.

The presence of these recurrent alterations not only allows the stratification of patients according to risk but could also condition the choice of therapeutic regime. This suggests that, in the future, personalized therapies can be applied for the different biological subgroups. Especially, this would be of great interest in the subgroup of patients with *MLL* rearrangements, characterized by poor response to treatment and a high rate of early relapses [255]. However, currently only patients who are carriers of the Philadelphia chromosome benefit from specific therapy thanks to the development of TKIs.

The microenvironment could also play a key role in the relapse process, as we have observed in cells carrying the *ETV6/RUNX1* fusion gene. Our results showed that mesenchymal cells could be offering protection and proliferative advantage to cells carrying the fusion gene, which would make them more resistant to treatment. Several studies have already suggested the importance of the microenvironment in the pathogenesis of ALL, even proposing it as a target for a new therapeutic strategy [256,257].

In summary, the application of new available methodologies such as NGS techniques are useful to understand the molecular basis of the disease, and their use should not be limited exclusively to the field of research, having also proven to be very useful in the clinical setting. The data presented in this work show how the genetic study of B-ALL patients at the time of diagnosis is key not only to determine the risk of patients, but also to identify markers that allow predicting the evolution of the patients. On the one hand, the presence of established genetic alterations routinely detected by conventional techniques allows us to stratify patients according to prognostic risk, while the detection of the broad spectrum of new alterations associated with high risk, as well as the detection of predictors of response to treatments, help us in refining the stratification and in therapy decision-making. Clonal evolution studies, on the other hand, can help us to identify the alterations that may be driving the relapse process, and therefore be considered as possible targets or as risk predictors, which could also imply a modification of the therapeutic strategy. In our study we therefore consider that the integration of new methodologies such as NGS in the diagnostic process of LAL-B, as well as that of genetic editing systems, could help in the understanding of the biology of the disease and suppose in the long term a drastic improvement in survival rates.

CONCLUDING REMARKS

1. The integrated use of genomic techniques of NGS, aCGH and MLPA achieved a better molecular characterization of the genetic profile of B-ALL patients during the evolution of the disease, through the simultaneous study of mutations and copy number variations. A more exhaustive molecular analysis that includes the study of the main genetic alterations associated with the risk of B-ALL could be especially relevant during the clinical management of patients for the detection of prognostic markers and predictors of the risk of relapse.

2. The use of the comprehensive custom NGS panel, including mutations, copy number variations, gene fusions and pharmogenomic markers, is a feasible tool allowing a complete genetic characterization of B-ALL patients.

3. The integrated use of the custom NGS panel along with standard diagnostic techniques resulted in improved and refined classification and stratification of patients. The use of the NGS panel also provided clues for the detection of possible Ph-like patients.

4. The custom NGS panel faithfully reproduced the findings observed by aCGH and MLPA. The use of the panel could thus avoid the use of additional techniques during B-ALL diagnosis, reducing costs and response time.

5. The integration of NGS into the clinical practice could therefore be a valuable tool to assist in the clinical management of B-ALL patients, helping to reduce treatment toxicity and relapses.

6. Relapsing B-ALL is characterized by a genetically dynamic profile that could be driven by the presence of genetic alterations that are present from the moment of diagnosis or acquired during the evolution.

7. The loss of *IKZF1* gene, as well as mutations in *TP53* were especially recurrent in relapsed patients. An increase in the variant allele frequency at the time of relapse was observed in all patients with *TP53* mutations. Both genetic events could be considered as risk factors for relapse and contribute to the re-stratification of the risk of B-ALL patients.

8. *ETV6/RUNX1* fusion gene plays a key role in the maintenance of the leukemic phenotype through the regulation of key processes such as apoptosis control. The elimination of the expression of the fusion gene showed a reduction in the oncogenic potential of leukemic cells both *in vitro* and *in vivo*, suggesting that it could be considered as a possible therapeutic option for the treatment of these patients.

9. Genetic editing systems such as the CRISPR/Cas9 system have proven to be a powerful tool for the study of genetic alterations characteristic of B-ALL patients, helping to better understand the role of these alterations in the development and evolution of the disease.

RESUMEN EN CASTELLANO

Tesis doctoral

Caracterización molecular de la Leucemia Aguda Linfoblástica B (LAL-B):

Análisis genómico y funcional de la Leucemia Aguda Linfoblástica y un modelo *in vitro* de modificación genética dirigida

Promotor:
Prof. Dr. Jesús María Hernández Rivas

Supervisora:
Dra. M del Rocío Benito Sánchez
Dr. Teresa González Martínez

Adrián Montaño Brioso

Noviembre de 2020

“A veces sentimos que lo que hacemos es tan solo una gota en el mar, pero el mar sería mucho menos si le faltara una gota”

Madre Teresa de Calcuta

INTRODUCCIÓN

"El punto de partida de todo logro es el deseo"

Napoleon Hill

1. LEUCEMIA AGUDA LINFOBLÁSTICA (LAL)

La leucemia aguda linfoblástica (LAL) es una neoplasia hematológica de la médula ósea que puede afectar tanto al linaje linfoide B como al T, siendo la LAL-B la más frecuente.

En Europa, la incidencia de la LAL se estima en 1,28 por cada 100.000 personas al año, lo que supone casi el 12% de los casos de leucemia de todo el mundo y constituye el cáncer más común de la infancia: casi el 80% de las leucemias agudas que se dan en los niños y el 20% de las leucemias agudas en los adultos [2,3]. Alrededor del 60% de los pacientes con LAL son diagnosticados antes de los 20 años. El pico máximo de incidencia se encuentra entre 1 y 4 años, observándose un segundo aumento gradual de los casos a partir de los 45 años [4].

La LAL-B se origina a partir de la aparición de una serie de alteraciones que provocan el bloqueo de la diferenciación de los precursores linfoides, y como consecuencia, la maduración incorrecta y la proliferación incontrolada de estos precursores que alteran el proceso de hematopoyesis de la médula. La enfermedad afecta principalmente a la médula ósea, pudiendo invadir la sangre y sitios extramedulares, como los ganglios linfáticos, el bazo y el sistema nervioso central [5,6].

La etiología de LAL-B es desconocida. Sin embargo, la susceptibilidad genética junto con los factores de riesgo ambientales como la exposición a pesticidas, pinturas, o incluso los hábitos maternos durante el embarazo han sido considerados como los posibles responsables del desarrollo de la enfermedad [6–9]. En la mayoría de los pacientes se ha identificado un evento primario que podría ser el desencadenante del proceso leucémico. Este evento se define por una serie de alteraciones genéticas recurrentes características de estos pacientes, principalmente traslocaciones y aneuploidías, que en la mayoría de los casos, han mostrado estar presentes desde el útero [10,11]. Algunas de estas alteraciones, como los reordenamientos del gen *KMT2A* (*MLL*), han demostrado ser suficientes por si solas para iniciar el desarrollo de la leucemia [12]. Sin embargo, a veces se requiere de la aparición de segundos eventos [13,14]. Estas segundas alteraciones suelen afectar a vías clave en el desarrollo de la enfermedad como el la diferenciación de los linfocitos, la regulación del ciclo celular o la regulación de la transcripción [16,17].

Por otra parte, la leucemia aguda linfoblástica T (LAL-T) se caracteriza por la acumulación de alteraciones genéticas, que afectan a genes supresores de tumores y a las vías de desarrollo implicadas en el control del crecimiento, la diferenciación y la supervivencia de los linfocitos T [18]. Cabe destacar la presencia de mutaciones en la vía NOTCH como los genes *NOTCH1* y *FBXW7* [19,20].

Una vez que la leucemia se ha desarrollado, existe controversia sobre si las alteraciones secundarias o los eventos primarios son los responsables de la evolución de la enfermedad y, por lo tanto, del fenotipo leucémico. Este es el caso, por ejemplo, de la t(12;21), la traslocación más

frecuente en los niños pediátricos con LAL-B que provoca la fusión génica entre los genes *ETV6* y *RUNX1*. Este gen de fusión es un evento primario en la leucemogénesis que aparece desde el útero, pero por si solo no es capaz de desarrollar la leucemia, sino que requiere de segundos eventos genéticos postnatales [21].

1.1 Diagnóstico y sistemas de clasificación

El diagnóstico de una leucemia aguda linfoblástica se realiza mediante el análisis morfológico, molecular y citogenético del aspirado de la MO, teniendo en cuenta los criterios y las recomendaciones del actual sistema de clasificación establecido por la organización mundial de la salud (OMS) en 2016 [27].

En primer lugar, se realiza una evaluación morfológica mediante microscopía celular para identificar los linfoblastos y determinar el nivel de infiltración en la médula ósea y la sangre periférica. Por definición, la médula ósea debe tener al menos un 20% de linfoblastos, presentando éstos una morfología muy variable [28]. Por otro lado, la inmunofenotipificación mediante la citometría de flujo multiparámetrica (CFM) se ha convertido en el estándar de oro en el diagnóstico y la clasificación de la LAL-B, permitiendo la evaluación de los linajes B y T y la presencia de aneuploidías. La CFM también juega un papel fundamental en la detección y monitorización de la enfermedad mínima residual (EMR) [30,31]. El análisis genético mediante técnicas citogenéticas convencionales como el cariotipo y la FISH también es obligatorio en el manejo clínico de la LAL, lo que permite estratificar a los pacientes según la clasificación establecida por la OMS [27].

Los sistemas de clasificación de la LAL han cambiado en las últimas décadas, a medida que han evolucionado las técnicas disponibles en la rutina clínica. Actualmente, el sistema más ampliamente usado es el establecido por la OMS, que integra aspectos clínicos, morfológicos, inmunofenotípicos y genéticos, y que estratifica a los pacientes de LAL en diferentes entidades [36]. Siguiendo las directrices de la clasificación de la OMS de 2016, la LAL-B pertenece a la categoría de "leucemia/linfoma linfocítico B" y se clasifica en dos grupos principales: los pacientes de LAL-B con alteraciones genéticas recurrentes y los pacientes carentes de estas alteraciones. A su vez, los pacientes con alteraciones genéticas recurrentes son estratificados en los siguientes subgrupos: hiperdiploidía (>50 y <60 cromosomas), hipodiploidía (<45 cromosomas), t(12;21)(p13;q22) *TEL/AML1* (*ETV6/RUNX1*), t(v;11q23) *KMT2A* (*MLL*) reordenado, t(1;19)(q23;p13) *E2A/PBX1* (*TCF3/PBX1*), t(9;22)(q34;q11.2) *BCR/ABL1* y t(5;14)(q31;q32) *IL3/IGH*. La revisión de 2016 incluyó también dos nuevas entidades provisionales: los pacientes con amplificación intracromosómica del cromosoma 21 (iAMP21) y los pacientes *BCR/ABL1*-like o Ph-like [37–39].

1.2 Marcadores pronósticos

La edad es uno de los parámetros clínicos más relevantes en la estratificación del riesgo de los pacientes con LAL. Sin embargo, los marcadores genéticos en el momento del diagnóstico, así como alcanzar una EMR negativa después del tratamiento, son considerados también como factores pronósticos importantes en la LAL [6]. Otros factores, como el recuento de glóbulos blancos (WBC) en el momento del diagnóstico y la afectación del sistema nervioso central también nos ayudan a definir el riesgo [43–47].

Históricamente, la edad nos permite establecer dos grandes grupos pronósticos, los niños (<18 años) y los adultos, caracterizados por unas marcadas diferencias en las tasas de supervivencia. Mientras que los niños alcanzan tasas de supervivencia superiores al 90%, los adultos difícilmente superan el 40% [40]. En varios estudios se ha propuesto también subdividir esos grupos en diferentes grupos de edad, aunque no se ha llegado a un consenso. Por ejemplo, el Instituto Nacional del Cáncer definió un nuevo subgrupo compuesto por adolescentes y adultos jóvenes (AYA) (15-39 años), asociados con un pronóstico intermedio, mostrando tasas de supervivencia de alrededor del 60-70%[41,42].

En las últimas décadas, la detección de la EMR ha cobrado gran importancia, y se utiliza cada vez más en la práctica clínica como marcador independiente del pronóstico para la duración de la remisión completa [48,49].

Aunque los factores clínicos desempeñan un papel importante en la orientación de la terapia, los cambios genéticos son también fundamentales en la determinación del riesgo. De hecho, cada una de las alteraciones citogenéticas establecidas por la clasificación de la OMS ha sido asociadas con un riesgo pronóstico determinado. Mientras que la presencia de hiperdiploidía o el gen de fusión *ETV6/RUNX1* se asocian con bajo riesgo y un buen pronóstico, la presencia de hipodiploidía, el gen de fusión *BCR/ABL1*, los reordenamientos de *MLL*, la iAMP21 o el subgrupo *BCR/ABL1*-like se asocian con un alto riesgo y un pronóstico adverso [51–57]. Por otro lado, los pacientes portadores de la t(1;19) (*TCF3/PBX1*) y t(5;14) (*IL3/IGH*) se asocian a un riesgo intermedio y los pacientes que no presentan ninguna de las alteraciones genéticas recurrentes son considerados de riesgo incierto [58,59]. Este último subgrupo de pacientes se conocen como "B-others" [61].

En el caso de LAL-T, no se han descrito subgrupos citogenéticos con valor pronóstico. Sin embargo, se han detectado alteraciones recurrentes que podrían tener algún impacto en el curso clínico de estos pacientes [62,63].

1.3 Tratamiento

Los regímenes terapéuticos actuales han logrado mejorar significativamente la supervivencia de los pacientes con LAL, especialmente en los niños. Estos protocolos siguen principalmente dos estrategias, la quimioterapia y el trasplante alogénico de células madre hematopoyéticas (TCMH).

El régimen quimioterapéutico se divide en tres fases. La primera es la inducción de la remisión, que tiene como objetivo lograr la remisión completa mediante el restablecimiento de la hematopoyesis normal. Durante esta fase se utiliza generalmente la combinación de glucocorticoides, vincristina, L-asparaginasa y antraciclinas. Más tarde, una fase de intensificación o consolidación (de seis meses a un año), en la que se incluye el uso de glucocorticoides, vincristina, altas dosis de metotrexato (MTX), citarabina (citosina arabinosida, ara-C) y asparaginasa. Por último, la fase de mantenimiento, que se basa principalmente en la combinación de los fármacos utilizados durante las fases anteriores (administrados durante 2 o 3 años) y que incorpora también el uso de las mercaptopurinas (6-MP). La mayoría de estos fármacos se basan en la inducción de la apoptosis mediante la parada del ciclo celular, la inhibición de la síntesis de ADN o de la expresión de oncogenes.

Por otro lado, el TCMH alogénico ha demostrado ser un tratamiento muy efectivo para prevenir las recaídas. Sin embargo, el TCMH alogénico es un procedimiento terapéutico complejo condicionado por muchos factores que pueden afectar a la respuesta clínica, por lo que su uso está reservado para pacientes con EMR positiva persistente o grupos de muy alto riesgo [67].

Uno de los principales problemas de la quimioterapia son los efectos secundarios. De hecho, se ha demostrado una alta incidencia de efectos secundarios en los pacientes con LAL, que pueden ser incluso secuelas permanentes [68,69]. Los efectos secundarios más comunes incluyen reacciones de hipersensibilidad, neuro, cardio y hepatotoxicidad, toxicidad del tracto digestivo y del riñón, así como mielosupresión y osteonecrosis [70].

Los avances en las nuevas técnicas, como la secuenciación masiva (NGS), han permitido la detección de múltiples mutaciones y polimorfismos asociadas con la resistencia al tratamiento y la recaída. Estas alteraciones pueden estar presentes desde el momento del diagnóstico o incluso pueden aparecen durante el tratamiento [71,72]. Además, la identificación de nuevas alteraciones moleculares que afectan a las vías oncogénicas críticas en la evolución de la LAL, ha permitido también el desarrollo emergente de nuevos fármacos, que podrían ser combinados con los fármacos "clásicos" con el objetivo de mejorar las tasas de respuesta de los pacientes. Estos nuevos fármacos incluyen los inhibidores de la quinasa (inhibidores de la quinasa *ABL1*, inhibidores de la aurora quinasa, inhibidores de la quinasa janus y los inhibidores tirosina quinasa (TKI)), otros inhibidores moleculares o de señalización (proteasoma, rapamicina-mTOR, Farnesiltransferasa, γ -Secreatasa,

angiogénesis, inductores de apoptosis y antagonistas del receptor de quimiocinas-CXCR4), así como la terapia epigenética (metiltransferasa de ADN, metiltransferasa de histonas e inhibidores de la histona deacetilasa) [97,98,99–106,107]. La incorporación de estas nuevas terapias ha logrado mejorar las tasas de supervivencia de los pacientes, como se ha observado por ejemplo con el uso de los TKIs en el subgrupo Filadelfia positivo, históricamente considerado de alto riesgo y que ahora cuenta con un mejor pronóstico [58].

Por otro lado, la inmunoterapia y la terapia celular han tenido un gran desarrollo en los últimos años. De hecho, se han realizado un gran número de ensayos clínicos y muchos siguen en curso. Especialmente, el uso de las células T con receptores quiméricos de antígenos (células CAR-T) dirigidas contra CD19 y CD22 para la LAL-B, y contra CD38 para la LAL-T ha mostrado resultados prometedores, habiendo revolucionado el tratamiento de la LAL tanto en niños como en adultos [6].

1.4 Recaída y heterogeneidad clonal en la LAL

Los actuales regímenes terapéuticos han logrado aumentar las tasas de supervivencia de los enfermos en las últimas décadas. Sin embargo, entre el 15-20% de los niños y el 40-50% de los adultos siguen sufriendo recaídas [114–117]. Además, el pronóstico después de una recaída suele ser pobre, principalmente debido a que los pacientes suelen presentar una mayor resistencia a la quimioterapia en comparación con el momento del diagnóstico [118–120]. Esta resistencia es inducida por la persistencia de una serie de alteraciones genéticas como resultado de la selección clonal realizada durante el tratamiento [121]. La interacción con el microambiente podría desempeñar también un papel importante en la resistencia, protegiendo a las células leucémicas de la respuesta inmune y los agentes quimioterapéuticos [122]. La recaída, junto con la toxicidad, supone así uno de los principales problemas en el tratamiento clínico de los pacientes con LAL.

El desarrollo de las tecnologías de alto rendimiento ha permitido identificar un gran número de alteraciones frecuentes en los pacientes que recaen, incluyendo variaciones en el número de copias (CNVs), mutaciones y cambios en el perfil de expresión génica. Estas alteraciones podrían ser la base de los procesos biológicos responsables de la farmacorresistencia y de la recaída. Sin embargo, las bases clonales de la recaída han mostrado ser muy heterogéneas y aún no están completamente claras. Aproximadamente el 94% de las recaídas tienen su origen en clones leucémicos persistentes que ya estaban presentes en el momento del diagnóstico, aunque estas pueden aparecer también durante el transcurso de la enfermedad. [23, 128-130].

En resumen, la recaída de LAL es un proceso complejo y, aunque se han realizado muchos esfuerzos para caracterizar el paisaje genómico de las recaídas, queda mucho por descubrir y aprender. El uso integrado de las plataformas genéticas, así como el desarrollo de estudios

funcionales, serán esenciales para la identificación de posibles dianas o biomarcadores de la resistencia y la recaída.

2. GENÉTICA DE LA LEUCEMIA AGUDA LINFOBLÁSTICA

Las técnicas citogenéticas convencionales como el cariotipo y la FISH continúan siendo los "estándares de oro" para determinar el análisis genético de los pacientes en la práctica clínica. Además, otras técnicas también se aplican de forma rutinaria en la clínica como: I) estudios de arrays; II) ensayo de amplificación de sonda dependiente de la ligación múltiple (MLPA), tanto para evaluar CNVs pequeños como grandes pérdidas/ganancias; III) qPCR para la detección de reordenamientos y la determinación de la EMR; así como IV) la secuenciación de Sanger para la evaluación de variantes genéticas específicas.

En conjunto, la aplicación de los ensayos de arrays y MLPA al estudio de la LAL-B ha permitido identificar numerosas alteraciones que afectan a los genes implicados en el desarrollo normal de las células B y se han posicionado como poderosas herramientas que ayudan durante el proceso de diagnóstico de los pacientes [137,138]. Sin embargo, una de las principales limitaciones es que es necesario integrar todas estas metodologías para obtener un análisis molecular completo de los pacientes de LAL-B, resultando tedioso y aumentando el tiempo de respuesta [139–141]. Además, estas técnicas cuentan con limitaciones que dificultan la detección de algunas alteraciones específicas [142]. Sin embargo, el uso de técnicas de alto rendimiento como la NGS ha demostrado ser una herramienta valiosa en la identificación de las alteraciones genéticas al diagnóstico, lo que podría ser clave en la clasificación, la determinación del riesgo y en la selección de tratamiento en la LAL-B, mejorando incluso la sensibilidad de detección de las técnicas convencionales.

2.1 Secuenciación de alto rendimiento en el estudio de la LAL-B

La secuenciación de Sanger ha sido el método más utilizado durante más de dos décadas desde que se comercializó por primera vez en 1986. Sin embargo, en los últimos años, debido a los mayores niveles de cobertura que proporcionan las técnicas de NGS, se han identificado nuevas mutaciones en genes implicados en neoplasias hematológicas, especialmente en la LAL-B. Esta tecnología permite la realización de la secuenciación del genoma completo (WGS); la secuenciación del exoma completo (WES) y la secuenciación de regiones específicas mediante paneles de genes personalizados [144].

La aplicación de los paneles personalizados ha logrado identificar genes particularmente relevantes asociados con un mal pronóstico como las mutaciones en *TP53* y *JAK2* [126]. Además, los paneles de NGS están empezando a utilizarse en la práctica clínica para el estudio de enfermedades como las inmunodeficiencias hereditarias y varios tipos de cáncer hereditario, y su uso se está generalizando debido a la reducción de los costes y a la simplificación de los análisis [148–152].

El uso del WES y el WGS en los pacientes de LAL-B, ha permitido, por otro lado, el estudio de un mayor número de genes y con ello el estudio más completo de las diferentes rutas biológicas [153]. La aplicación de la WES en muestras de diagnóstico y recaída también permitió la identificación de mutaciones que podrían estar conduciendo el proceso de la recaída [154]. El uso de WES y WGS permitió además refinar la estratificación de los pacientes con hipodiploidía [156].

La secuenciación del ARN (RNA-seq) se ha convertido en el método de elección para el análisis de la expresión génica prevaleciendo así sobre los métodos convencionales de microarrays. La aplicación del RNA-seq es especialmente relevante para la identificación de nuevos transcritos y el análisis de genes desconocidos, lo que es de gran interés en la LAL-B debido a la alta recurrencia de reordenamientos genéticos reportada en estos enfermos [157,158]. La integración de los análisis transcriptómicos al estudio de la LAL-B ha permitido así la identificación de nuevas entidades mediante la detección de nuevos genes de fusión y firmas de expresión génica, como el subgrupo Ph-like, recientemente incorporado como una nueva entidad provisional en la última revisión de la clasificación de la OMS [27].

Aunque los estudios de NGS se han centrado en el desarrollo de nuevos estudios exploratorios y se han limitado casi exclusivamente al área de la investigación, el uso de la NGS en la práctica clínica se está incorporando cada vez más gracias al desarrollo de nuevas metodologías que han permitido reducir sustancialmente los costes y el tiempo de respuesta, así como simplificar el análisis de los datos.

2.2 Eventos genéticos asociados con los Pacientes de LAL-B

La integración de las diferentes técnicas como los análisis del perfil de expresión génica, SNP arrays y, actualmente, la NGS, ha permitido definir mejor el paisaje molecular de la LAL y la identificación de un amplio espectro de mutaciones. Estas mutaciones afectan a vías clave en el desarrollo de la LAL, como la diferenciación y el desarrollo linfoide (ej. *PAX5*, *IKZF1*, *EBF1*), la ruta de JAK/STAT (ej. *JAK1*, *JAK2*, *IL7R*, *CRLF2*), la ruta de RAS (ej. *NRAS*, *KRAS*, *PTPN11*, *FLT3*, *NF1*), la regulación del ciclo celular y genes supresores de tumores (ej. *TP53*, *RB1*, *CDKN2A/B*), la ruta Wnt/β-catenina (ej. *Wnt*, *FAT1*), la ruta de NOTCH (ej. *NOTCH1*, *NOTCH2*, *NOTCH3*, *FBXW7*, *HES1*, *JAG1*, *JAG2*), modificadores de la estructura de la cromatina y reguladores epigenéticos (ej, *PHF6*, *EZH2*, *DNMT3A*),

y vías no canónicas u otros genes desconocidos (ej., *CREBBP*, *NT5C2*, *TBL1XR1*) [16,17]. Estas alteraciones pueden ayudar a identificar nuevas dianas terapéuticas y a establecer nuevos marcadores pronósticos, lo que resulta especialmente interesante para los pacientes de riesgo incierto "B others".

Además de las mutaciones somáticas, se han detectado CNVs recurrentes en las vías asociadas a la patogénesis de la LAL-B. Estos incluyen los genes involucrados en el desarrollo de las células B (ej. *IKZF1*, *EBF1*, *PAX5*, *ETV6*), el ciclo y la proliferación celular (ej. *CDKN2A*, *CDKN2B*, *RB1*, *BTG1*), y los receptores de citoquinas (ej. *CRLF2*) [137,171].

La pérdida *IKZF1* ha sido reportada en aproximadamente el 15% de los niños y el 40% de los pacientes adultos con LAL-B y ha sido establecido como un marcador poderoso e independiente asociado con un mal pronóstico y con la resistencia a los tratamientos [38,171,173–175,178,179]. La pérdida de *IKZF1* también se ha asociado fuertemente con la pérdida de otros genes como *PAX5*, *EBF1* y *BTG1*, así como con la presencia de reordenamientos de *CRLF2*. Esto sugiere un efecto cooperativo de estas alteraciones en la leucemogénesis [173].

La pérdida de *EBF1* es muy poco frecuente, aunque suele aparecer en un porcentaje mayor en pacientes en recaída (~25%), lo que justifica su fuerte asociación con una menor supervivencia libre de recaída [183,184]. La alteración de *PAX5*, en cambio, se ha observado en aproximadamente el 30% de los pacientes, ya sea por deleciones, reordenamientos o mutaciones específicas [185].

Otro CNV recurrente es la pérdida del gen *ETV6*, especialmente enriquecido en el subgrupo de pacientes *ETV6/RUNX1* positivos (~70%). La pérdida de este gen no se ha asociado con un pronóstico determinado [185].

CDKN2A y *CDKN2B* son dos genes supresores de tumores y su pérdida ha demostrado ser un importante marcador pronóstico [186].

El gen *RB1* es un regulador del ciclo celular, cuya pérdida ha sido reportada en ~7% de los pacientes. La pérdida de este gen parece estar asociada con una peor respuesta al tratamiento, aunque su verdadero valor pronóstico no está del todo claro. En casi la mitad de los casos, la pérdida de *RB1* está asociada con la pérdida del brazo largo del cromosoma 13 [185,187].

El gen 1 de translocación de células B (*BTG1*) desempeña un papel en varios procesos celulares cruciales, como la proliferación y la apoptosis. Su pérdida se ha asociado con una respuesta deficiente a los glucocorticoides [188]. La pérdida de *BTG1* se ha observado en alrededor del 8% de los pacientes con LAL-B, aunque con una incidencia mucho mayor en los pacientes con síndrome de Down [189].

La sobreexpresión del gen *CRFL2* ha sido también reportada de forma recurrente en los pacientes de LAL-B, principalmente debido a la presencia de mutaciones o reordenamientos que

afectan a este gen [190]. La sobreexpresión de CRLF2 ha sido asociada con un pronóstico desfavorable, aunque esto se debe probablemente a la alta frecuencia de estas alteraciones detectadas en el grupo de mal pronóstico, los pacientes de tipo Ph-like [170,177].

En conjunto, la detección de estas alteraciones genera un gran interés en el manejo de los pacientes de LAL-B, pero especialmente en el subgrupo de pacientes Ph-like. El diagnóstico de estos pacientes suele estar determinado por el perfil de expresión génica, aunque sigue siendo un reto debido a la falta de una alteración genética recurrente que permita su identificación inequívoca. Sin embargo, se ha establecido una firma genética específica para estos pacientes, caracterizada por los reordenamientos de *CRFL2*, alteraciones en la vía JAK/STAT (incluyendo mutaciones y reordenamientos), fusiones de genes de la familia de ABL, alteraciones de la ruta de RAS/MAPK, así como la pérdida recurrente de los genes *IKZF1*, *PAX5*, *EBF1* y *BTG1* [137,191–193].

La integración de los análisis transcriptómicos permitió también la identificación de nuevos subgrupos genéticos (<10% de los pacientes), como los portadores de los reordenamientos afectando a *DUX4*, *ZNF384* y *NUMT1* o el subgrupo *ETV6/RUNX1*-like [174,194–200]. El grupo de investigación infantil del hospital St Jude ha publicado recientemente la identificación de dos nuevos subgrupos de LAL-B a través del perfil de expresión, uno de ellos caracterizado por alteraciones en *PAX5* (reordenamientos, amplificaciones o mutaciones intragénicas) y el otro por la mutación puntual p.Pro80Arg (P80R) en *PAX5* [201].

Muchas de las alteraciones identificadas por la aplicación de los estudios de NGS en la LAL también han sido establecidas como objetivos terapéuticos prometedores. Por ejemplo, las alteraciones en la ruta RAS/MAPK, gracias al desarrollo de múltiples compuestos que inhiben las moléculas de esta vía (inhibidores de la MEK) o los de la ruta de JAK/STAT con el uso del ruxolitinib [203,205] Además, se han identificado posibles estrategias de tratamiento adaptadas a los pacientes con reordenamiento de *CRLF2*, como los inhibidores USP9X, el inhibidor de la histona deacetilasa "givinostat", los anticuerpos anti-TSLPR/CRLF2 y la inmunoterapia celular con células CAR-T dirigidas frente el receptor de la linfopoyetina estromal tímica [207–209].

Por otra parte, con el desarrollo de la farmacogenética y la farmacogenómica, se han establecido asociaciones entre las diferentes alteraciones genéticas y la respuesta al tratamiento [191,192]. De hecho, numerosos polimorfismos y mutaciones se han asociado a la respuesta a los fármacos, estando ambos relacionados con la susceptibilidad y la resistencia, especialmente en aquellos genes que median en el transporte y el metabolismo de los fármacos [202,203].

Por lo tanto, la LAL-B es una enfermedad muy heterogénea a nivel biológico con un gran número de alteraciones genéticas recurrentes que pueden ayudar en la clasificación, la estratificación del

riesgo y el manejo clínico de los pacientes. No obstante, se necesitan más estudios para establecer el verdadero valor pronóstico de muchas de estas alteraciones.

3. ESTUDIOS FUNCIONALES

Con el desarrollo de las técnicas de NGS, surgió la necesidad de interpretar, a nivel funcional, el gran número de nuevas alteraciones identificadas, extendiéndose el uso de los modelos *in vitro* e *in vivo* generados mediante técnicas de edición genética. Estos modelos ayudan a dilucidar los mecanismos de acción de las diferentes alteraciones, establecer qué vías podrían verse afectadas y, por tanto, identificar nuevas dianas y diseñar nuevos fármacos. Además, permiten evaluar el efecto de los fármacos nuevos o ya establecidos en presencia o ausencia de estas alteraciones.

3.1 Sistemas de edición genética en el estudio de la LAL-B

Los sistemas de edición genética han ido evolucionando desde las nucleasas de dedos de zinc (ZNF) y las nucleasas efectoras activadoras de la transcripción (TALEN), hasta el sistema más utilizado, el sistema CRISPR "repeticiones palindrómicas cortas intercaladas con intervalos regulares", que se ha posicionado como el sistema más rápido, simple y barato [230]. Este sistema se basa en el uso de nucleasas, siendo la Cas9 la más utilizada, que es guiada por una molécula de ARN de 20 nucleótidos de cadena simple para producir el corte deseado en el ADN [231].

Los sistemas CRISPR/Cas9 han sido utilizados en el estudio de varias neoplasias hematológicas, incluyendo la LAL-B. La mayoría de estos estudios se centraron en la generación de modelos de knock-out para determinar la función de los factores de transcripción (ej. *IZKF1*, *PAX5*); genes de fusión (ej. *MLL/AF4*, *ETV6/RUNX1*) o posibles dianas terapéuticas, entre otros. De manera interesante, el uso de los sistemas de edición genética en el estudio de LAL-B ha permitido avanzar en el conocimiento de estas alteraciones implicadas no sólo en la evolución de la enfermedad, sino también en su desarrollo. Los sistemas de edición genética juegan también un papel clave en el proceso de desarrollo de nuevas terapias, especialmente durante la generación de la inmunoterapia basada en células CAR-T [234].

HIPÓTESIS

Los pacientes con leucemia aguda linfoblástica se caracterizan por la presencia de una serie de alteraciones genéticas que marcan el curso de la enfermedad. Estas alteraciones son la base de los actuales sistemas de clasificación y algunas de ellas han sido establecidas como importantes marcadores pronósticos. La identificación de estas alteraciones, entre otros factores, permite predecir así el pronóstico de los pacientes. La correcta y rápida detección de estas alteraciones es por ello fundamental durante el proceso diagnóstico. Una estratificación errónea podría conducir a una selección de tratamiento inapropiada, a una dosis incorrecta y, en consecuencia, a problemas de refractariedad, así como de toxicidad del tratamiento.

El reciente desarrollo de las técnicas ómicas, como la secuenciación masiva y los ensayos de arrays, han posibilitado el estudio de un gran número de alteraciones genéticas con gran sensibilidad y precisión. Su aplicación en el estudio de LAL-B ha permitido así identificar una serie de nuevas alteraciones recurrentes que a menudo se correlacionan con resultados clínicos como la reducción de la supervivencia, el aumento de las tasas de recaída o las toxicidades del tratamiento. Estas alteraciones incluyen un amplio espectro de eventos genéticos como mutaciones, CNVs y traslocaciones. La mayoría de estas alteraciones todavía no se han incorporado en la práctica clínica. Sin embargo, estos biomarcadores podrían establecerse como nuevos marcadores de pronóstico en un futuro próximo. Así pues, el estudio integrativo del amplio espectro de alteraciones genéticas presentes en los pacientes de LAL-B podría ayudar a establecer nuevos y mejores marcadores pronósticos, que se aplicarían en la práctica clínica para la clasificación y estratificación del riesgo de los pacientes y para identificar marcadores pronósticos y predictores de la respuesta al tratamiento. En consecuencia, podríamos lograr una reducción de las tasas de recaída, uno de los principales problemas en el tratamiento clínico de los pacientes con LAL.

La integración de la NGS en la práctica clínica podría permitir la detección, en un solo ensayo, de las principales alteraciones asociadas al riesgo de LAL-B, convirtiéndose así en una poderosa herramienta para el diagnóstico de estos pacientes. Por lo tanto, el diseño de un amplio panel dirigido de NGS que pueda detectar simultáneamente las principales alteraciones presentes en LAL-B, además de las alteraciones cooperantes que tienen algún impacto en el curso clínico de los pacientes, podría ser de gran interés y muy útil para mejorar la clasificación y estratificación del riesgo de LAL-B y para la toma de decisiones de la terapia.

La recaída de la LAL-B se caracteriza por una gran heterogeneidad clonal, compuesta por un amplio número de alteraciones que podrían estar impulsando el proceso de recaída. El uso integrado de diferentes técnicas genómicas puede ser útil para evaluar el perfil genético de los pacientes en recaída y determinar así los factores que podrían predecir el riesgo de recaída.

Los estudios funcionales, mediante la generación de modelos *in vitro* e *in vitro*, son también cruciales para determinar el posible impacto biológico (mecanismos de acción) de las diferentes alteraciones genéticas, así como para poder evaluarlas como posibles dianas terapéuticas mediante el desarrollo de ensayos farmacológicos. La t(12;21), la translocación más frecuente en la LAL-B pediátrica, juega un importante papel en el desarrollo de la leucemia. Sin embargo, requiere de la aparición de alteraciones secundarias para que se produzca el desarrollo clínico de la enfermedad. En este sentido, el papel del gen de fusión *ETV6/RUNX1* es controvertido. Mientras que algunos estudios sugieren que el gen de fusión actúa exclusivamente en las primeras etapas de la enfermedad, otros afirman que también desempeña un papel clave en el mantenimiento de la leucemia. La generación de un modelo *ETV6/RUNX1* knock-out podría ayudar a demostrar que el gen de fusión interviene en el mantenimiento del potencial oncogénico de las células tumorales, convirtiéndola así en una posible diana terapéutica que potencialmente podría reducir la tasa de recaída de estos pacientes.

En resumen, la combinación de las nuevas tecnologías ómicas y el sistema de edición genética CRISPR/cas9 nos ayudará a alcanzar una mayor comprensión de las anomalías genéticas de la LAL-B tanto en el diagnóstico como en la recaída. Además, el uso del sistema CRISPR/Cas9 proporcionará nuevos conocimientos sobre los mecanismos moleculares de las translocaciones involucradas en LAL-B, abriendo nuevas vías para el manejo de la enfermedad.

OBJETIVOS

Objetivos específicos:

I. Diseñar y validar un panel de NGS personalizado para la detección de las principales alteraciones genéticas asociadas al riesgo de la LAL-B en el diagnóstico.

II. Estudiar el perfil genético asociado a la recaída de los pacientes de LAL-B a través del estudio integrativo de mutaciones y CNVs mediante el uso de la NGS, MLPA y aCGH.

III. Evaluar el papel del gen de fusión *ETV6/RUNX1* en el mantenimiento del fenotipo leucémico mediante la generación de un modelo *in vitro* y un modelo de xenoinjerto.

RESULTADOS – RESÚMENES

Resumen capítulo I. **Comprehensive custom NGS panel validation for the improvement of the stratification of B-Acute Lymphoblastic Leukemia patients.**

Adrián Montaño[1], Jesús Hernández-Sánchez[1], Maribel Forero-Castro[2], María Matorra-Miguel[1], Eva Lumbreras[1], Cristina Miguel[1], Sandra Santos[1], Valentina Ramírez-Maldonado[1], Jose Luís Fuster[3], Natalia de Las Heras[4], Alfonso García-de Coca[5], Magdalena Sierra[6], Julio Dávila[7], Ignacio de la Fuente[8], Carmen Olivier[9], Juan Olazabal[10], Joaquín Martínez[11], Nerea Vega-García[12], Teresa González[7], Jesús María Hernández-Rivas*[1,7] Rocío Benito[1].
**Correspondence.*

[1]IBSAL, IBMCC, Universidad de Salamanca, CSIC, Centro de Investigación del Cáncer (CIC), Salamanca, España. [2]Colegio de ciencias biológicas (GICBUPTC grupo de investigación), Universidad pedagógica y tecnológica de Colombia (UPTC), Colombia. [3]Sección de oncohematología pediátrica, Hospital Clínico Universitario Virgen de la Arrixaca; Instituto Murciano de Investigación Biosanitaria (IMIB), Murcia, España. [4]Departamento de Hematología - Hospital Virgen Blanca, León, España. [5]Departamento de Hematología - Hospital Clínico de Valladolid, Valladolid, España. [6]Complejo Sanitario de Zamora, Zamora, España. [7]Departamento de Hematología - Hospital Universitario de Salamanca, Salamanca, España. [8]Departamento de Hematología - Hospital Rio Hortega, Valladolid, España. [9]Servicio de Hematología y Hemoterapia - Complejo Sanitario de Segovia, Segovia, España. [10]Departamento de Hematología - Hospital Universitario de Burgos, Burgos, España. [11]Departamento de Hematología - Hospital Universitario 12 de Octubre, Madrid, España. [12]Laboratorio de Hematología, Instituto de Investigación, Hospital Sant Joan de Déu, Barcelona, España.

J. Pers. Med. 2020, 10, 0137; doi:10.3390/jpm10030137.

Introducción: La LAL-B es una neoplasia hematológica de la célula madre linfoide de linaje B, caracterizada por la presencia de alteraciones genéticas que determinan el curso de la enfermedad. Su detección es esencial en el diagnóstico para la correcta clasificación y estratificación de los pacientes. El cariotipo y la FISH se utilizan convencionalmente para analizar los cambios numéricos/estructurales y la aCGH o MLPA para las alteraciones del número de copias (CNVs) y las grandes pérdidas/ganancias. Sin embargo, se está implementando el uso de técnicas como la secuenciación masiva (NGS) que permiten además de la detección de mutaciones puntuales, la identificación de un amplio espectro de diferentes tipos de alteraciones. La optimización de un panel de NGS que permita detectar el mayor número de alteraciones en un solo experimento aceleraría el diagnóstico y mejoraría la estratificación de los enfermos.

Objetivos: Diseño y validación de un panel personalizado de NGS basado en ADN para la detección de las principales alteraciones genéticas asociadas a LAL-B.

Métodos: Para el diseño del panel personalizado se utilizó el software SureDesign, incluyéndose regiones para la detección de: mutaciones somáticas en 150 genes; CNVs (ej. *IKZF1*del e iAMP21); reordenamientos génicos (ej. *CRLF2*r) y SNPs farmacogenéticos. A partir de ADN se realizó la secuenciación masiva con SureSelectQXT-Target-Enrichment (Agilent) en un NextSeq (Illumina). El análisis de los datos se realizó con un pipeline propio, así como la detección de CNVs y aneuploidías. Para la detección de reordenamientos se usó el software MANTA (Illumina). Para la validación técnica se seleccionaron y analizaron un total de 75 muestras de pacientes de LAL-B al diagnóstico que fueron previamente caracterizadas genéticamente por cariotipo/FISH. De algunas de ellas se disponía además información genética de aCGH, MLPA y otras técnicas de secuenciación.

Resultados: Se obtuvo un promedio de $3x10^6$ lecturas/muestra. Debido al diseño, las regiones correspondientes a las mutaciones alcanzaron una profundidad media de cobertura de 342 lecturas, permitiendo así evaluar la presencia de subclones. Las regiones de CNVs y de los genes de fusión obtuvieron una cobertura media de 355 y 570 lecturas, respectivamente. El análisis mutacional mostró que el 81% de los pacientes presentaban al menos una mutación en alguno de los genes estudiados. *NRAS* fue el gen más recurrentemente mutado (30%), seguido por *KRAS*, *JAK2*, *PAX5* e *IKZF1*. El 100% de los casos con alta hiperdiploidía fueron detectados en los cromosomas 4, 8, 10 y 21, así como el 67% de los casos con hipodiploidía. Además, también se detectaron todos los casos con iAMP21. En cuanto a los genes de fusión, se detectó el 100% de los casos Philadelphia, el 90% de

los casos *ETV6/RUNX1*, el 70% de los casos con reordenamiento de *MLL*, así como el 100% de los pacientes con reordenamiento de *CRLF2*. También se detectaron el 100% de las deleciones del gen *IKZF1* observadas por aCGH/MLPA/PCR, así como la pérdida de *CDKN2A/B* (92,3%), *PAX5* (92,3%), *ETV6* (83,3%), *RB1* (100%) y *BTG1* (85,7%). La integración del panel de NGS-LAL B junto con las técnicas clásicas de diagnóstico (cariotipo/FISH) permitió además mejorar la estratificación de los pacientes, logrando identificar alteraciones "de novo" y recurrentes (>80% y 12% de los pacientes respectivamente) que no habían sido detectadas por técnicas convencionales.

Conclusiones: El uso de este panel personalizado de NGS permite detectar de forma rápida y eficaz las principales alteraciones genéticas presentes en LAL-B en un solo experimento (mutaciones, CNVs, aneuploidías y translocaciones). La aplicación del panel nos permitiría así acelerar el proceso de diagnóstico molecular de los pacientes, ayudando en la clasificación y estratificación de los enfermos, así como en la toma de decisiones terapéuticas.

Resumen capítulo II. Integrated genomic analysis of chromosomal alterations and mutations in B-cell acute lymphoblastic leukemia reveals distinct genetic profiles at relapse

Maribel Forero-Castro[1,†], Adrián Montaño[2,†], Cristina Robledo[2], Alfonso García de Coca[3], José Luis Fuster[4], Natalia de las Heras[5], José Antonio Queizán[6], María Hernández-Sánchez[2], Luis A. Corchete-Sánchez[2,7], Marta Martín-Izquierdo[2], Jordi Ribera[8], José-María Ribera[9], Rocío Benito[2,*,‡] and Jesús M. Hernández-Rivas[2,7,10,*,‡]

*†These authors contributed equally to this work. ‡Sharing senior authorship. *Correspondence.*

[1]Escuela de Ciencias Biológicas, Universidad Pedagógica y Tecnológica de Colombia. Avenida Central del Norte 39-115, Tunja 150003, Boyacá, Colombia. [2]IBSAL, IBMCC, Universidad de Salamanca-CSIC, Cancer Research Center, Campus Miguel de Unamuno, 37007 Salamanca, Spain. [3]Servicio de Hematología, Hospital Clínico de Valladolid, Av. Ramón y Cajal, 3, 47003 Valladolid, Spain. [4]Servicio de Oncohematología Pediátrica, Hospital Universitario Virgen de la Arrixaca, Murcia, Ctra. Madrid-Cartagena, s/n, 30120 Murcia, El Palmar, Spain. [5]Servicio de Hematología, Hospital Virgen Blanca, Altos de Nava s/n, 24071 León, Spain. [6]Servicio de Hematología, Hospital General de Segovia, C/Luis Erik Clavería Neurólogo S/N, 40002 Segovia, Spain. [7]Servicio de Hematología, Hospital Universitario de Salamanca, Paseo de San Vicente, 88-182, 37007 Salamanca, Spain. [8]Acute Lymphoblastic Leukemia Group, Josep Carreras Leukaemia Research Institute, Carretera de Canyet, s/n, Barcelona, 08916 Badalona, Spain. [9]Servicio de Hematología Clínica, Institut Català d'Oncologia, Hospital Germans Trias i Pujol, Josep Carreras Research Institute, Universitat Autònoma de Barcelona, Carretera de Canyet, s/n, Barcelona, 08916 Badalona, Spain. [10]Departamento de Medicina, Universidad de Salamanca, Campus Miguel de Unamuno. C/Alfonso X El Sabio s/n, 37007 Salamanca, Spain.

Diagnostics 2020, 10(7), 455. doi:10.3390/diagnostics10070455

Introducción: La recaída junto con la toxicidad a los tratamientos supone una de las principales complicaciones en la clínica de la LAL-B. La aplicación de las técnicas de alto rendimiento al estudio de la LAL-B ha permitido la identificación de una serie de alteraciones genéticas asociadas con la resistencia a los fármacos, el fracaso del tratamiento o con un mayor riesgo de recaída. Aunque se sabe que los pacientes en recaída muestran una gran heterogeneidad clonal, la base clonal de dicha recaída es compleja y aún no se comprende plenamente. Un análisis combinado de las mutaciones genéticas y las alteraciones del número de copias (CNVs) podría proporcionar una valiosa información para la identificación de los patrones de evolución clonal y biomarcadores que ayuden a predecir el riesgo de sufrir una recaída en la LAL-B.

Objetivo: Realizar un análisis genómico integrativo combinando el uso de la secuenciación masiva (NGS), la hibridación genómica comparativa de arrays (aCGH) y la amplificación con sonda dependiente de ligadura múltiple (MLPA), con el fin de identificar los patrones de evolución genética que podrían explicar los cambios fenotípicos asociados con la recaída de la enfermedad.

Métodos: Se analizó un total de trece muestras pareadas de pacientes con LAL-B en el momento del diagnóstico y en la recaída (cuatro niños y nueve adultos), mediante el uso de la NGS, aCGH y MLPA. El análisis por NGS se realizó aplicando la tecnología de amplicones de Junior 454 (Roche), lo que permitió determinar el estado mutacional de los genes *TP53* (E4-E11), *JAK2* (E12-E16), *PAX5* (E2-E3), *LEF1* (E2-E3), *CRLF2* (E6) y *IL7R* (E5). Todas las muestras fueron también analizadas en una plataforma de aCGH 12X135K (Roche NimbleGen, EE. UU.). Además, se realizó MLPA usando el kit SALSA MLPA P335-B1 ALL-IKZF1-probemix (MRC-Holanda, Países Bajos), que contiene sondas para los genes *IKZF1*, *CDKN2A/B*, *PAX5*, *EBF1*, *ETV6*, *BTG1*, *RB1*, así como genes de la región PAR1 (*CRLF2*, *CSF2RA*, *IL3RA* y *P2RY8*).

Resultados: El análisis genómico integrativo mediante el uso de aCGH, MLPA y NGS reveló que el 100% de los pacientes con LAL-B presentaba al menos una alteración genética en alguno de los momentos estudiados. Además, se observó un aumento significativo en la frecuencia de los CNVs en el momento de la recaída en comparación con el diagnóstico (mediana, 47 vs 6 alteraciones por muestra) (p=0,019). Según la aCGH, los CNVs más recurrentemente observados en el diagnóstico y/o recaída fueron: del(7p) (77%) y del(9p) (62%) seguidos de dup(X)(31%), dup(7q)(31%), del(13q)(23%), dup(1q)(23%), dup(21)(15%), del(12p)(15%) y del(17p)(15%). Además, el análisis integrativo MLPA-aCGH mostró la pérdida concreta de los siguientes genes, entre los que no se observaron diferencias comparando el momento del diagnóstico y la recaída: *IKZF1* (54% vs. 62%),

CDKN2A/B (54% vs. 23%), *PAX5* (38% vs. 23%), *EBF1* (23% vs. 15%), *BTG1* (23% vs. 23%), *ETV6* (15% vs. 15%), *RB1* (8% vs. 15%) y PAR1(15% vs. 8%). Por otro lado, se observó un patrón muy heterogéneo entre los distintos pacientes. Algunos de ellos solo adquirieron nuevas alteraciones en el momento de la recaída (8%), otros pacientes adquirieron y perdieron también alteraciones presentes en el diagnóstico (38%), mientras que, en la mayoría de ellos se observó la adquisición de nuevas alteraciones, junto con la pérdida y mantenimiento de otras presentes en el diagnóstico (54%). De manera interesante, el 71% de los pacientes con *IKZF1*del en el momento del diagnóstico retuvieron esta alteración en la recaída. El análisis de NGS reveló, además, la presencia de 6 mutaciones (5 en el gen *TP53* y 1 en el gen *PAX5*) en 4 de los 13 pacientes (31%) en el momento del diagnóstico y/o la recaída. Especialmente, todas las mutaciones en *TP53* mostraron un mayor VAF en el momento de la recaída (53% vs 71%, 11% vs 21% y 3,5% vs 26% respectivamente). Dos de ellas aparecieron incluso de manera exclusiva en la muestra de la recaída.

Conclusión: El presente estudio proporciona pruebas adicionales de que la clonalidad de la LAL-B es genéticamente dinámica desde el diagnóstico hasta la recaída. La combinación de análisis de NGS, aCGH y MLPA permitió además una mejor caracterización molecular del perfil genético en los pacientes con LAL-B en recaída.

Resumen capítulo III. *ETV6/RUNX1* Fusion Gene Abrogation Decreases the Oncogenicity of Tumour Cells in a Preclinical Model of Acute Lymphoblastic Leukaemia.

Adrián Montaño[1], Jose Luis Ordoñez[2], Verónica Alonso-Pérez[2], Jesús Hernández-Sánchez[1], Sandra Santos[1], Teresa González[3], Rocío Benito[1], Ignacio García-Tuñón[*2] and Jesús María Hernández-Rivas[1,2,3,4*]
**Correspondence.*

[1]IBSAL, IBMCC, Universidad de Salamanca-CSIC, Cancer Research Center; Salamanca; Spain. [2]Unidad de Diagnóstico Molecular y Celular del Cáncer, Centro de Investigación del Cáncer-IBMCC (USAL-CSIC), Salamanca, Spain. [3]Dept of Hematology, Hospital Universitario de Salamanca; Salamanca; Spain. [4]Dept of Medicine, Universidad de Salamanca, Spain.

Cells 2020, 9(1), 215. doi: 10.3390/cells9010215

Introducción: La fusión génica entre los genes *ETV6* y *RUNX1* generada por t(12;21)(p13; q22), es la translocación cromosómica más frecuente en los niños con LAL-B. Los pacientes portadores de esta translocación están asociados con un buen pronóstico y una excelente respuesta molecular al tratamiento. Sin embargo, hasta el 20% de los casos recaen. Además, la respuesta al tratamiento de algunos casos que recaen se asocia a la resistencia a tratamientos como los glucocorticoides, y estos pacientes deben ser tratados con un trasplante de médula ósea. Estudios recientes sugieren que el gen de fusión *ETV6/RUNX1* (*E/R*) desempeña un papel no solo en la iniciación de la leucemia si no también en la progresión y el mantenimiento de la enfermedad, mediante la desregulación de diferentes vías moleculares que contribuyen a la leucemogénesis, como la sobreexpresión de la ruta de PI3K/AKT/mTOR.

Objetivo: En este estudio utilizamos el sistema CRISPR/Cas9 para eliminar la fusión oncogénica *E/R* en una línea celular de LAL para evaluar de manera *in vitro* e *in vivo* su contribución a la leucemogénesis.

Métodos: Basados en el sistema CRISPR/Cas9, se diseñaron dos sgRNAs dirigidos hacia el gen de fusión para producir indels que modificaran el ORF del oncogen y, así, truncar la expresión de la proteína. Las células tumorales (línea celular REH que expresan el gen de fusión *E/R*) fueron electroporadas (nucleofector Amaxa, Basilea, Suiza) y sorteadas por citometría de flujo, generando así tres clones *E/R* KO y dos clones control. qPCR y Western Blot se utilizaron para comprobar la expresión del ARNm de E/R y la expresión de los genes regulados por la proteína de fusión. El RNA-seq total fue realizado para determinar el perfil de expresión génica de los distintos clones. La viabilidad celular y la distribución en las fases del ciclo celular se midió mediante citometría de flujo basadas en el marcaje con yoduro de propidio (PI). Se empleó el uso de células estromales mesenquimales humanas HS-5 (MSC) para el cocultivo de los distintos clones. Para medir la proliferación, se utilizaron los ensayos de MTT y el etiquetado de las células con el Kit de Proliferación Celular CellTrace CFSE (Thermo Fisher). Para los ensayos farmacológicos las células fueron tratadas con copanlisib, un inhibidor de PI3K, (10nM) y prednisolona (250 μM). La viabilidad celular se midió mediante ensayo de MTT. Para el modelo de xenoinjerto, se inyectaron por vía subcutánea células *E/R* positivas (flanco derecho) y células *E/R* KO (flanco izquierdo) en 16 ratones nulos de cadena gamma de receptores NOD/SCID/IL2. Los tumores extirpados fueron muestreados justo después del sacrificio y teñidos con hematoxilina y eosina.

Resultados: Los clones E/R KO generados mediante el sistema CRISPR/Cas9 mostraron la pérdida total de los niveles de expresión de la proteína de fusión E/R. El análisis transcriptómico mostró además la desregulación de genes involucrados en procesos biológicos que afectaban a la supervivencia, como a la resistencia a la apoptosis y la capacidad de proliferación celular, tras la eliminación de la expresión de E/R. Confirmando estos hallazgos, los clones E/R KO mostraron una disminución de los factores antiapoptóticos Bcl-2 (60%) y Bcl-xL (47%) medidos mediante WB. En consecuencia, las células carentes de la fusión mostraron mayores niveles de apoptosis en comparación con los controles. Estos niveles de apoptosis fueron aún mayores en las células E/R KO cuando se indujo la apoptosis celular mediante la administración de Vincristina. No se observaron diferencias en cuanto a la distribución del ciclo celular y a la capacidad de proliferación entre los distintos clones. Sin embargo, cuando las células fueron cocultivadas con células mesenquimales, los clones E/R KO mostraron una capacidad proliferativa reducida respecto a los controles. Por otro lado, las células E/R KO mostraron una mayor sensibilidad al tratamiento con Copanlisib, un inhibidor de la ruta de PI3K, así como a su combinación con Prednisolona. La eliminación del gen de fusión *E/R* mostró también una disminución significativa del potencial oncogénico *in vivo*. Los ratones inyectados con células E/R KO no generaron tumores o generaron tumores significativamente más pequeños que los generados por los controles. Además, se observó una mayor tasa de actividad mitótica en los tumores de las células E/R positivas.

Conclusión: La eliminación del gen de fusión *E/R* reduce significativamente el potencial oncogénico de las células leucémicas (REH, E/R positivas) tanto *in vivo* como *in vitro*. Las células E/R KO también mostraron una mayor sensibilidad a los fármacos (copanlisib solo y en combinación con prednisolona), lo que sugiere que la expresión E/R podría estar implicada en la resistencia a la prednisolona observada en algunos pacientes. Estos resultados sugieren que el gen de fusión *E/R* juega un papel importante en el mantenimiento del fenotipo leucémico. Por consiguiente, el gen de fusión podría convertirse en una posible diana terapéutica específica para estos pacientes con la que se obtendrían mejores tasas de respuesta.

DISCUSIÓN GENERAL

"Vive como si fueras a morir mañana. Aprende como si fueras a vivir para siempre"

Mahatma Gandhi

La leucemia aguda linfoblástica (LAL) es una neoplasia hematológica de la médula ósea que puede afectar a los linfocitos B y T. La leucemia aguda linfoblástica de células B (LAL-B) es el subtipo más común y se caracteriza por una gran heterogeneidad tanto a nivel clínico como biológico. Es fundamental la detección de una serie de factores clínicos, biológicos y genéticos en el momento del diagnóstico, ya que éstos nos permiten clasificar y estratificar a los pacientes según el riesgo y también son especialmente relevantes en la toma de decisiones terapéuticas. Entre estos factores se encuentran una serie de parámetros clínico-biológicos como la edad, la enfermedad mínima residual o el subgrupo citogenético, este último definido por una serie de alteraciones genéticas que aparecen de manera recurrente en estos pacientes [6].

Estas alteraciones genéticas incluyen principalmente aneuploidías y reordenamientos cromosómicos y constituyen la base del actual sistema de clasificación establecido por la OMS. Además, son consideradas como uno de los factores pronósticos más importantes [27]. Cada una de estas alteraciones han sido asociadas a un riesgo pronóstico específico, pudiéndose clasificar a los pacientes en diferentes subtipos genéticos considerados de riesgo alto, intermedio o bajo [65]. De hecho, algunas de las grandes diferencias observadas en las tasas de supervivencia de niños y adultos podrían deberse principalmente a la distribución de los diferentes subtipos biológicos entre los grupos de edad. De acuerdo con nuestros resultados y con estudios previos, se pudo observar que en los niños fueron más frecuentes los subgrupos biológicos asociados con un bajo riesgo, mientras que en los adultos fueron más recurrentes los subgrupos biológicos de alto riesgo [65].

La aplicación de las técnicas genómicas de alto rendimiento, como los estudios de arrays y la NGS al estudio de LAL-B ha permitido la identificación de nuevas alteraciones que ayudan a comprender mejor el desarrollo y la evolución de la enfermedad [17,137,166,174]. Estas alteraciones incluyen mutaciones puntuales, cambios en el número de copias (CNVs), así como nuevos reordenamientos. Estas últimas identificadas recientemente gracias a la integración del RNA-seq al estudio de LAL-B [194,200]. Aunque la mayoría de estas nuevas alteraciones no se tienen aún en cuenta en la rutina clínica, probablemente sean incluidas en un futuro próximo. De hecho, algunas de ellas ya tienen un valor pronóstico establecido, como es el caso de las pérdidas de *IKZF1*, *CDKN2A/B* y *BTG1* o las mutaciones en *TP53*, *JAK2* y *ABL1*, todas ellas consideradas como factores de mal pronóstico [39,126,127,172,184,186,224]. Estudios publicados por nuestro grupo mostraron la relevancia de las mutaciones en *TP53* y *JAK2*, ambas asociadas con una reducción de la supervivencia global y libre de evento, así como con mayores tasas de recaída [126].

La detección de estas alteraciones secundarias de alto valor pronóstico nos ayuda a mejorar la estratificación, especialmente en los pacientes "B-others". Este subgrupo constituye aproximadamente el 30% de los pacientes LAL-B y se define por la ausencia de algunas de las

alteraciones genéticas recurrentes que permiten su estratificación en los diferentes grupos de riesgo. Nuestros resultados mostraron que la pérdida de los genes *IKZF1*, *CDKN2A/B* y *PAX5*, así como los reordenamientos *CRLF2* se observaron con frecuencia dentro de este subgrupo de pacientes, lo que concuerda con estudios previos [61]. Tanto la pérdida de *IKZF1* y *CDKN2A*, como los reordenamientos *CRLF2* se han asociado con un mal pronóstico [39,170,186].

Algunas de estas alteraciones secundarias también se consideran como posibles dianas terapéuticas. De hecho, ya se han propuesto tratamientos específicos dirigidos. Por ejemplo, el uso de inhibidores o inmunoterapia para el tratamiento de pacientes con reordenamientos de *CRLF2*, el uso de ruxolitinib para pacientes con alteraciones en la vía JAK/STAT, o el uso de inhibidores de la molécula MEK para aquellos con la vía RAS/MAPK alterada [204,206–209].

Los estudios genéticos en la LAL-B han logrado también la identificación de una serie de variantes genéticas y SNPs fuertemente relacionados con la respuesta a los tratamientos empleados en la LAL. Entre ellos, cabe mencionar los polimorfismos identificados en los genes *TPMT* y *MTHFR*, implicados en el metabolismo de la 6-mercaptopurina y el metotrexato, respectivamente [74,235]. La detección de SNPs asociados a la farmacogenética podría conducir a un cambio en las estrategias terapéuticas actuales o al ajuste de las dosis, y por lo tanto a la reducción de la toxicidad del tratamiento [236].

En la actualidad, la detección de alteraciones genéticas en los pacientes de LAL-B durante el diagnóstico se realiza mediante el uso de técnicas citogenéticas convencionales (cariotipo y FISH), que permiten la detección de translocaciones y aneuploidías. Así pues, para la correcta estratificación biológica de los pacientes suele ser necesario el uso de una serie de técnicas adicionales como MLPA o los estudios de arrays, lo que supone un aumento de los costes y del tiempo. Además, algunas de estas técnicas mencionadas anteriormente cuentan con grandes limitaciones en cuanto a la sensibilidad y el número de genes a estudiar [53,141,143].

El reciente desarrollo de las técnicas genómicas como la NGS ha permitido detectar un amplio espectro de nuevas alteraciones que incluyen no sólo las mutaciones, sino también genes de fusión y CNVs [238,239]. La NGS puede seguir varias estrategias como el estudio del genoma completo (WGS), el exoma completo (WES) o de regiones específicas a través de los paneles personalizados. A diferencia de la WGS y la WES, los paneles personalizados sólo proporcionan información sobre las regiones de interés para las que están diseñados. Esto evita el análisis de un gran número de variantes de significado incierto que no son útiles para la gestión clínica, y también simplifica en gran medida el análisis de los datos [151,152]. Además, se traduce en un menor tiempo de respuesta, que es esencial cuando se trata de enfermedades como la LAL-B, que deben ser tratadas rápidamente debido a su rápida evolución.

Uno de los objetivos de esta tesis doctoral fue desarrollar un panel de ADN personalizado que permitiera detectar las principales alteraciones genéticas asociadas con la LAL-B en un solo ensayo y, de este modo, mejorar la clasificación y estratificación de los pacientes durante el proceso diagnóstico. Estas alteraciones incluyen mutaciones (SNV/INDEL), genes de fusión recurrentes (*ETV6/RUNX1*, *BCR/ABL1*, *MLL*r y *CRLF2*r), CNVs, aneuploidías y SNPs farmacogenéticos.

Los resultados de nuestro trabajo mostraron que el panel de NGS detectó con éxito las diferentes alteraciones genéticas incluidas en el diseño. Por un lado, la NGS sirvió de apoyo a las técnicas citogenéticas convencionales detectando las alteraciones genéticas recurrentes incluidas en la clasificación de la OMS. Por otra parte, el panel personalizado de NGS demostró ser también un instrumento robusto en la detección de alteraciones secundarias, logrando incluso superar algunas de las limitaciones de las técnicas convencionales. Además, el panel de NGS resultó ser particularmente interesante en la identificación de posibles pacientes Ph-like, mediante la detección de una serie de alteraciones frecuentemente reportadas en estos pacientes [173,184,242,243]. El panel de NGS podría servir así como un primer cribado para evitar realizar estudios de expresión en todos los pacientes recién diagnosticados, lo que también ayudaría a reducir el tiempo y los costes.

El panel de NGS permitió identificar las principales alteraciones genéticas que son clínicamente relevantes en la LAL-B, mejorando y refinando la estratificación de los pacientes, así como detectar posibles dianas terapéuticas y predictores de tratamiento como los SNPs farmacogenéticos.

Estos resultados revelan además que el uso del panel no sólo sería útil para el diagnóstico, sino también para el seguimiento de los pacientes durante el tratamiento. Una mejor comprensión de la heterogeneidad genómica en el diagnóstico y a lo largo del tratamiento debería permitirnos reconocer los clones problemáticos y complejos que pueden requerir terapias específicas para lograr una remisión profunda y duradera. En particular, el estudio genético de los pacientes que sufren una recaída podría ayudar a comprender cómo evoluciona la enfermedad y a determinar la repercusión de esas alteraciones genéticas que podrían convertirse en nuevos factores predictores del riesgo de recaída.

A pesar de los esfuerzos por intensificar las estrategias terapéuticas, un alto porcentaje de pacientes sigue teniendo recaídas. En concreto, el 40-50% de los adultos y el 15-20% de los niños recaen [114–117]. Además, el pronóstico después de la recaída es muy adverso, por lo que muchos de ellos acaban sucumbiendo a la enfermedad [246].

En línea con otros estudios, en nuestros resultados observamos que muchas de las alteraciones presentes en la recaída de los pacientes de LAL-B estaban ya presentes en el momento del diagnóstico [24,130,131]. Los resultados presentados en esta tesis doctoral mostraron que el número de alteraciones presentes en el momento de la recaída fue significativamente mayor que las observadas

en el diagnóstico. Estos hechos sugieren que el proceso de recaída podría estar impulsado por la persistencia de una serie de alteraciones genéticas que confieren resistencia al tratamiento y que estas alteraciones pueden estar presentes desde el momento del diagnóstico o pueden adquirirse durante el tratamiento.

El estudio integrativo de mutaciones y CNVs mediante el uso de la NGS, aCGH y MLPA logró identificar un gran número de alteraciones en las muestras pareadas de diagnóstico y recaída. Estos hallazgos sugieren una vez más que la LAL-B es una enfermedad compleja con diversos tipos de alteraciones y que éstas deben estudiarse conjuntamente y no de forma independiente. La pérdida focal y amplia del brazo corto del cromosoma 9 (9p) y del cromosoma 7 (7p) fueron los dos eventos más recurrentes detectados en el diagnóstico y/o la recaída. Ambos eventos implican la pérdida de los genes *CDKN2A/B* e *IKZF1*, respectivamente. De hecho, la pérdida de *IKZF1* junto con las mutaciones en *TP53* fueron los eventos más frecuentes observados en los pacientes en el momento de la recaída. La presencia de estas alteraciones podría contribuir a la reestratificación del riesgo de los pacientes de LAL-B y a proponer estrategias terapéuticas oportunas, como la intensificación del tratamiento y la identificación de candidatos a trasplantes o la inclusión en ensayos clínicos debido a su alto riesgo de una segunda recaída.

En nuestro estudio también observamos diferentes patrones en las alteraciones detectadas debido probablemente a la sensibilidad o resistencia que estas ofrecen a las células leucémicas. Así, pudimos detectar mutaciones que aumentaron el VAF en el momento de la recaída como las de *TP53*, y mutaciones que llegaban incluso a desaparecer como la detectada en *PAX5*.

Muchas de las alteraciones genéticas descritas por las técnicas genómicas no cuentan aún con un valor pronóstico establecido. En este sentido, se requieren estudios funcionales que ayuden a dilucidar el papel que desempeñan esas alteraciones en la patogénesis de la enfermedad. Los nuevos enfoques de edición genómica, como el sistema CRISPR/Cas9, utilizado en esta tesis doctoral, han demostrado ser una herramienta muy poderosa en la generación de modelos *in vitro* e *in vivo* que ayudan a recapitular las alteraciones descritas por las técnicas genómicas y por tanto a estudiarlas a nivel funcional. La generación de estos modelos podría ayudar así a dilucidar el papel de estas alteraciones en la leucemogénesis y en el desarrollo de nuevos fármacos.

La generación de modelos murinos portadores del gen de fusión *ETV6/RUNX1* reveló que la aparición de segundos eventos era necesaria para desencadenar el proceso leucémico en estos ratones [13,14]. Estos hallazgos hicieron pensar que el gen de fusión *ETV6/RUNX1* no contribuía por tanto al mantenimiento del fenotipo leucémico, sugiriendo incluso que la presencia del gen de fusión era prescindible para la supervivencia de las células leucémicas [249–251]. Por el contrario, otros estudios sugirieron que el gen de fusión sí participaba en el mantenimiento del fenotipo leucémico

mediante la desregulación de diferentes vías como las vías PI3K/Akt/mTOR, STAT3 y MDM2/TP53 [26].

Los resultados presentados en esta tesis doctoral arrojan luz sobre la controversia así generada, demostrando a través de la generación de un modelo *ETV6/RUNX1* KO, que el gen de fusión contribuye al mantenimiento del fenotipo leucémico a través de la regulación de procesos clave para la supervivencia de las células leucémicas como el control de la apoptosis. Además, se observó la desregulación de otros procesos clave como la autofagia mediante la infraexpresión del gen *Vps34*, que fue también recientemente descrito por el grupo de Polak [252]. La generación de modelos de xenoinjerto mostró además que el potencial oncogénico de las células leucémicas fue significativamente menor cuando se eliminó la expresión del gen de fusión. Así pues, nuestros resultados demuestran que el gen de fusión *ETV6/RUNX1* podría estar impulsando la evolución de la enfermedad y, por lo tanto, ser en parte responsable de la recaída de estos pacientes. Estos hallazgos sugieren que el gen de fusión *ETV6/RUNX1* podría ser considerado como una posible diana terapéutica con la que tratar a estos pacientes [26,253,254]. La eliminación del gen de fusión logró además sensibilizar a las células al tratamiento, en particular a los inhibidores de PI3K, así como a su combinación con la prednisolona, lo que sugiere que el uso de inhibidores que bloqueen la actividad del gen de fusión podría reducir la resistencia al tratamiento y, por lo tanto, evitar la aparición de recaídas. La presencia de estas alteraciones recurrentes no sólo permite así la estratificación de los pacientes según el riesgo, sino que también podría condicionar la elección del régimen terapéutico.

El microambiente también podría desempeñar un papel clave en el proceso de recaída, como hemos observado en las células portadoras del gen de fusión *ETV6/RUNX1*. Nuestros resultados mostraron que las células mesenquimales podrían estar ofreciendo protección y ventaja proliferativa a las células portadoras del gen de fusión, lo que las haría más resistentes al tratamiento.

En resumen, la aplicación de las nuevas metodologías disponibles, como las técnicas de NGS, son útiles para comprender la base molecular de la enfermedad, y su uso no debe limitarse exclusivamente al área de la investigación, habiendo demostrado ser también muy útil en la clínica. Los datos presentados en este trabajo muestran cómo el estudio genético de los pacientes de LAL-B en el momento del diagnóstico es clave no sólo para determinar el riesgo de los pacientes, sino también para identificar los marcadores que permitan predecir la evolución de los pacientes. Por un lado, la presencia de alteraciones genéticas establecidas y detectadas de forma rutinaria por las técnicas convencionales nos permite estratificar a los pacientes en función del riesgo pronóstico, mientras que la detección del amplio espectro de nuevas alteraciones asociadas a un alto riesgo, así como la detección de predictores de respuesta a los tratamientos, nos ayudan a afinar la estratificación y a la toma de decisiones terapéuticas. Los estudios de evolución clonal, por su parte,

pueden ayudarnos a identificar las alteraciones que pueden estar impulsando el proceso de recaída, y por lo tanto ser considerados como posibles dianas o como predictores de riesgo, lo que también podría implicar una modificación de la estrategia terapéutica. La generación de modelos funcionales mediante el uso de las técnicas de edición como CRISPR/Cas9 han demostrado ser también fundamentales para el estudio de las alteraciones detectadas con las técnicas genómicas, así como para la identificación de posibles dianas. Por ello, en nuestro estudio consideramos que la integración de las nuevas metodologías como la NGS en el proceso diagnóstico de la LAL-B, así como la utilización de los sistemas de edición genética, podrían ayudar a la comprensión de la biología de la enfermedad y suponer a largo plazo una mejora en el manejo clínico del paciente con LAL-B.

CONCLUSIONES

1. El uso integrativo de las técnicas genómicas de NGS, aCGH y MLPA logró una mejor caracterización molecular del perfil genético de los pacientes de LAL-B durante la evolución de la enfermedad, mediante el estudio simultáneo de mutaciones y variaciones del número de copias. Un análisis molecular más exhaustivo, que incluya el estudio de las principales alteraciones genéticas asociadas al riesgo de la LAL-B, podría ser especialmente relevante durante el manejo clínico de los pacientes para la detección de marcadores pronósticos y predictores del riesgo de recaída.

2. El uso del panel personalizado de NGS, que incluye mutaciones, variaciones del número de copias, genes de fusión y marcadores farmacogenómicos, es una herramienta viable que permite una caracterización genética completa de los pacientes de LAL-B.

3. El uso integrado del panel de NGS junto con las técnicas de diagnóstico estándar dio lugar a una clasificación y estratificación mejorada de los pacientes. El uso del panel de NGS también permitió la detección de posibles pacientes Ph-like.

4. El panel de NGS personalizado reprodujo fielmente los resultados observados por aCGH y MLPA. De este modo, el uso del panel pudo evitar el uso de técnicas adicionales durante el diagnóstico de la LAL-B, reduciendo los costes y el tiempo de respuesta.

5. Por consiguiente, la integración de la NGS en la práctica clínica podría ser un instrumento valioso para orientar en el tratamiento clínico de los pacientes de LAL-B, contribuyendo a reducir la toxicidad del tratamiento y las recaídas.

6. La recaída de LAL-B se caracteriza por un perfil genético dinámico que podría estar impulsado por la presencia de alteraciones genéticas presentes desde el momento del diagnóstico o adquiridas durante la evolución.

7. La pérdida del gen *IKZF1*, así como las mutaciones en *TP53* fueron especialmente recurrentes en los pacientes en recaída. Se observó un aumento de la frecuencia alélica en el momento de la recaída en todos los pacientes con mutaciones en *TP53*. Ambos eventos genéticos podrían considerarse como factores de riesgo de recaída y contribuir a la reestratificación del riesgo de los pacientes de LAL-B.

8. El gen de fusión *ETV6/RUNX1* desempeña un papel fundamental en el mantenimiento del fenotipo leucémico mediante la regulación de procesos clave como el control de la apoptosis. La eliminación de la expresión del gen de fusión mostró una reducción del potencial oncogénico de las células leucémicas tanto *in vitro* como *in vivo*, lo que sugiere que podría considerarse como una posible opción terapéutica para el tratamiento de esos pacientes.

9. Los sistemas de edición genética como el sistema CRISPR/Cas9 han demostrado ser una herramienta poderosa para el estudio de las alteraciones genéticas características de los pacientes de la LAL-B, ayudando a comprender mejor el papel de estas alteraciones en el desarrollo y evolución de la enfermedad.

REFERENCES

1. Terwilliger, T.; Abdul-Hay, M. Acute lymphoblastic leukemia: a comprehensive review and 2017 update. *Blood Cancer J.* **2017**, *7*, e577, doi:10.1038/bcj.2017.53.
2. Sant, M.; Allemani, C.; Tereanu, C.; De Angelis, R.; Capocaccia, R.; Visser, O.; Marcos-Gragera, R.; Maynadié, M.; Simonetti, A.; Lutz, J.M.; et al. Incidence of hematologic malignancies in Europe by morphologic subtype: Results of the HAEMACARE project. *Blood* **2010**, *116*, 3724–3734, doi:10.1182/blood-2010-05-282632.
3. Redaelli, A.; Laskin, B.L.; Stephens, J.M.; Botteman, M.F.; Pashos, C.L. A systematic literature review of the clinical and epidemiological burden of acute lymphoblastic leukaemia (ALL). *Eur. J. Cancer Care* **2005**, *14*, 53–62, doi:10.1111/j.1365-2354.2005.00513.x.
4. Howlader, N.; Noone, A.M.; Krapcho, M.; Miller, D.; Brest, A.; Yu, M.; Ruhl, J.; Tatalovich, Z.; Mariotto, A.; Lewis, D.R.; et al. SEER Cancer Statistics Review (CSR) 1975-**2017** Available online: https://seer.cancer.gov/csr/1975_2017/.
5. Hunger, S.P.; Mullighan, C.G. Acute lymphoblastic leukemia in children. *N. Engl. J. Med.* **2015**, *373*, 1541–1552, doi:10.1056/NEJMra1400972.
6. Malard, F.; Mohty, M. Acute lymphoblastic leukaemia. *Lancet* **2020**, *395*, 1146–1162, doi:10.1016/S0140-6736(19)33018-1.
7. Bailey, H.D.; Fritschi, L.; Infante-Rivard, C.; Glass, D.C.; Miligi, L.; Dockerty, J.D.; Lightfoot, T.; Clavel, J.; Roman, E.; Spector, L.G.; et al. Parental occupational pesticide exposure and the risk of childhood leukemia in the offspring: Findings from the childhood leukemia international consortium. *Int. J. Cancer* **2014**, *135*, 2157–2172, doi:10.1002/ijc.28854.
8. Turner, M.C.; Wigle, D.T.; Krewski, D. Residential pesticides and childhood leukemia: A systematic review and meta-analysis. *Environ. Health Perspect.* **2010**, *118*, 33–41, doi:10.1289/ehp.0900966.
9. Chunxia, D.; Meifang, W.; Jianhua, Z.; Ruijuan, Z.; Xiue, L.; Zhuanzhen, Z.; Linhua, Y.; Gutti, R.K. Tobacco smoke exposure and the risk of childhood acute lymphoblastic leukemia and acute myeloid leukemia: A meta-Analysis. *Med.* **2019**, *98*.
10. Gale, K.B.; Ford, A.M.; Repp, R.; Borkhardt, A.; Keller, C.; Eden, O.B.; Greaves, M.F. Backtracking leukemia to birth: Identification of clonotypic gene fusion sequences in neonatal blood spots. *Proc. Natl. Acad. Sci.* **1997**, *94*, 13950–13954, doi:10.1073/pnas.94.25.13950.
11. Greaves, M.F.; Maia, A.T.; Wiemels, J.L.; Ford, A.M. Review article Leukemia in twins : lessons in natural history. *Blood* **2003**, *102*, 2321–2333, doi:10.1182/blood-2002-12-3817.Supported.
12. Reimer, J.; Knöß, S.; Labuhn, M.; Charpentier, E.M.; Göhring, G.; Schlegelberger, B.; Klusmann, J.H.; Heckl, D. CRISPR-Cas9-induced t(11;19)/MLL-ENL translocations initiate leukemia in human hematopoietic progenitor cells in vivo. *Haematologica* **2017**, *102*, 1558–1566, doi:10.3324/haematol.2017.164046.
13. Tsuzuki, S.; Seto, M.; Greaves, M.; Enver, T. Modeling first-hit functions of the t(12;21) TEL-AML1 translocation in mice. *Proc. Natl. Acad. Sci.* **2004**, *101*, 8443–8448, doi:10.1073/pnas.0402063101.
14. Li, M.; Jones, L.; Gaillard, C.; Binnewies, M.; Ochoa, R.; Garcia, E.; Lam, V.; Wei, G.; Yang, W.; Lobe, C.; et al. Initially disadvantaged, TEL-AML1 cells expand and initiate leukemia in response to irradiation and cooperating mutations. *Leukemia* **2013**, *27*, 1570–1573, doi:10.1038/leu.2013.15.
15. Williams, L.A.; Yang, J.J.; Hirsch, B.A.; Marcotte, E.L.; Spector, L.G. Is there etiologic heterogeneity between subtypes of childhood acute lymphoblastic leukemia? A review of variation in risk by subtype. *Cancer Epidemiol. Biomarkers Prev.* **2019**, *28*, 846–856, doi:10.1158/1055-9965.EPI-18-0801.
16. Schwab, C.; Harrison, C.J. Advances in B-cell precursor acute lymphoblastic leukemia genomics. *HemaSphere* **2018**, *2*.
17. Harrison, C.J. Targeting signaling pathways in acute lymphoblastic leukemia: new insights. *Hematology Am. Soc. Hematol. Educ. Program* **2013**, *2013*, 118–125, doi:10.1182/asheducation-2013.1.118.
18. Belver, L.; Ferrando, A. The genetics and mechanisms of T cell acute lymphoblastic leukaemia. *Nat. Rev. Cancer* **2016**, *16*, 494–507, doi:10.1038/nrc.2016.63.
19. Weng, A.P.; Ferrando, A.A.; Lee, W.; Morris IV, J.P.; Silverman, L.B.; Sanchez-Irizarry, C.; Blacklow, S.C.; Look, A.T.; Aster, J.C. Activating mutations of NOTCH1 in human T cell acute lymphoblastic leukemia. *Science* **2004**, *306*, 269–271, doi:10.1126/science.1102160.
20. Tosello, V.; Ferrando, A.A. The NOTCH signaling pathway: Role in the pathogenesis of T-cell acute lymphoblastic leukemia and implication for therapy. *Ther. Adv. Hematol.* **2013**, *4*, 199–210.
21. Raynaud, B.S.; Cave, H.; Baens, M.; Bastard, C.; Cacheux, V.; Grosgeorge, J.; Guidal-giroux, C.; Guo, C.; Vilmer, E.; Marynen, P.; et al. Allele : Two Frequently Associated Alterations Found in Childhood. *Blood* **1996**, *87*, 2891–2899.

22. Bokemeyer, A.; Eckert, C.; Meyr, F.; Koerner, G.; von Stackelberg, A.; Ullmann, R.; Türkmen, S.; Henze, G.; Seeger, K. Copy number genome alterations are associated with treatment response and outcome in relapsed childhood ETV6/RUNX1-positive acute lymphoblastic leukemia. *Haematologica* **2014**, *99*, 706 LP – 714, doi:10.3324/haematol.2012.072470.
23. Konrad, M.; Metzler, M.; Panzer, S.; Östreicher, I.; Peham, M.; Repp, R.; Haas, O.A.; Gadner, H.; Panzer-Grümayer, E.R. Late relapses evolve from slow-responding subclones in t(12;21)-positive acute lymphoblastic leukemia: Evidence for the persistence of a preleukemic clone. *Blood* **2003**, *101*, 3635–3640, doi:10.1182/blood-2002-10-3252.
24. Mullighan, C.G.; Phillips, L.A.; Su, X.; Ma, J.; Miller, C.B.; Shurtleff, S.A.; Downing, J.R. Genomic Analysis of the Clonal Origins of Relapsed Acute Lymphoblastic Leukemia. *Science.* **2008**, *322*, 1377–1380, doi:10.1126/science.1164266.
25. Panzer-Grümayer, E.R.; Cazzaniga, G.; Van Der Velden, V.H.J.; Del Giudice, L.; Peham, M.; Mann, G.; Eckert, C.; Schrauder, A.; Germano, G.; Harbott, J.; et al. Immunogenotype changes prevail in relapses of young children with TEL-AML1-positive acute lymphoblastic leukemia and derive mainly from clonal selection. *Clin. Cancer Res.* **2005**, *11*, 7720–7727, doi:10.1158/1078-0432.CCR-05-1239.
26. Sun, C.; Chang, L.; Zhu, X. Pathogenesis of ETV6/RUNX1-positive childhood acute lymphoblastic leukemia and mechanisms underlying its relapse. *Oncotarget* **2017**, *8*, 35445–35459, doi:10.18632/oncotarget.16367.
27. Arber, D.A.; Orazi, A.; Hasserjian, R.; Thiele, J.; Borowitz, M.J.; Le Beau, M.M.; Bloomfield, C.D.; Cazzola, M.; Vardiman, J.W. The 2016 revision to the World Health Organization classification of myeloid neoplasms and acute leukemia. *Blood* **2016**, *127*, 2391–2405.
28. d'Onofrio, G.; Zini, G. *Morphology of Blood Disorders, 2nd Edition | Wiley*; **2014**; ISBN 978-1-118-44260-9.
29. Teachey, D.T.; Pui, C.H. Comparative features and outcomes between paediatric T-cell and B-cell acute lymphoblastic leukaemia. *Lancet Oncol.* **2019**, *20*, e142–e154.
30. Tembhare, P.; Badrinath, Y.; Ghogale, S.; Patkar, N.; Dhole, N.; Dalavi, P.; Kunder, N.; Kumar, A.; Gujral, S.; Subramanian, P.G. A novel and easy FxCycle™ violet based flow cytometric method for simultaneous assessment of DNA ploidy and six-color immunophenotyping. *Cytom. Part A* **2016**, *89*, 281–291, doi:10.1002/cyto.a.22803.
31. Theunissen, P.; Mejstrikova, E.; Sedek, L.; Van Der Sluijs-Gelling, A.J.; Gaipa, G.; Bartels, M.; Sobral da Costa, E.; Kotrová, M.; Novakova, M.; Sonneveld, E.; et al. Standardized flow cytometry for highly sensitive MRD measurements in B-cell acute lymphoblastic leukemia. *Blood* **2017**, *129*, 347–357, doi:10.1182/blood-2016-07-726307.
32. Bene, M.C.; Castoldi, G.; Knapp, W.; Ludwig, W.D.; Matutes, E.; Orfao, A.; van't, V.M. Proposals for the immunological classification of acute leukemias. *Leukemia* **1995**, *9*, 1783–1786.
33. Hayhoe, F.G.J. Classification of acute leukaemias. *Blood Rev.* **1988**, *2*, 186–193, doi:10.1016/0268-960X(88)90024-0.
34. Dworzak, M.N.; Buldini, B.; Gaipa, G.; Ratei, R.; Hrusak, O.; Luria, D.; Rosenthal, E.; Bourquin, J.-P.; Sartor, M.; Schumich, A.; et al. AIEOP-BFM Consensus Guidelines 2016 for Flow Cytometric Immunophenotyping of Pediatric Acute Lymphoblastic Leukemia. *Cytom. Part B Clin. Cytom.* **2018**, *94*, 82–93, doi:10.1002/cyto.b.21518.
35. Bennett, J.M.; Catovsky, D.; Daniel, M. -T; Flandrin, G.; Galton, D.A.G.; Gralnick, H.R.; Sultan, C. Proposals for the Classification of the Acute Leukaemias French-American-British (FAB) Co-operative Group. *Br. J. Haematol.* **1976**, *33*, 451–458, doi:10.1111/j.1365-2141.1976.tb03563.x.
36. Harris, N.L.; Jaffe, E.S.; Diebold, J.; Flandrin, G.; Muller-Hermelink, H.K.; Vardiman, J.; Lister, T.A.; Bloomfield, C.D. World health organization classification of neoplastic diseases of the hematopoietic and lymphoid tissues: Report of the clinical advisory committee meeting - Airlie house, Virginia, November 1997. *J. Clin. Oncol.* **1999**, *17*, 3835–3849.
37. Harrison, C.J.; Moorman, A. V.; Barber, K.E.; Broadfield, Z.J.; Cheung, K.L.; Harris, R.L.; Jalali, G.R.; Robinson, H.M.; Strefford, J.C.; Stewart, A.; et al. Interphase molecular cytogenetic screening for chromosomal abnormalities of prognostic significance in childhood acute lymphoblastic leukaemia: A UK Cancer Cytogenetics Group Study. *Br. J. Haematol.* **2005**, *129*, 520–530, doi:10.1111/j.1365-2141.2005.05497.x.
38. Den Boer, M.L.; van Slegtenhorst, M.; De Menezes, R.X.; Cheok, M.H.; Buijs-Gladdines, J.G.; Peters, S.T.; Van Zutven, L.J.; Beverloo, H.B.; Van der Spek, P.J.; Escherich, G.; et al. A subtype of childhood acute lymphoblastic leukaemia with poor treatment outcome: a genome-wide classification study.

Lancet Oncol. **2009**, *10*, 125–134, doi:10.1016/S1470-2045(08)70339-5.

39. Mullighan, C.G.; Su, X.; Zhang, J.; Radtke, I.; Phillips, L.A.A.; Miller, C.B.; Ma, J.; Liu, W.; Cheng, C.; Schulman, B.A.; et al. Deletion of IKZF1 and Prognosis in Acute Lymphoblastic Leukemia. *N. Engl. J. Med.* **2009**, *360*, 470–480, doi:10.1056/NEJMoa0808253.
40. Roberts, K.G. Genetics and prognosis of ALL in children vs adults. *Hematol.* **2018**, *2018*, 137–145, doi:10.1182/asheducation-2018.1.137.
41. Siegel, S.E.; Stock, W.; Johnson, R.H.; Advani, A.; Muffly, L.; Douer, D.; Reed, D.; Lewis, M.; Freyer, D.R.; Shah, B.; et al. Pediatric-inspired treatment regimens for adolescents and young adults with philadelphia chromosome–negative acute lymphoblastic leukemia: A review. *JAMA Oncol.* **2018**, *4*, 725–734, doi:10.1001/jamaoncol.2017.5305.
42. Stock, W.; Luger, S.M.; Advani, A.S.; Yin, J.; Harvey, R.C.; Mullighan, C.G.; Willman, C.L.; Fulton, N.; Laumann, K.M.; Malnassy, G.; et al. A pediatric regimen for older adolescents and young adults with acute lymphoblastic leukemia: Results of CALGB 10403. *Blood* **2019**, *133*, 1548–1559, doi:10.1182/blood-2018-10-881961.
43. Hoelzer, D.; Thiel, E.; Loffler, H.; Buchner, T.; Ganser, A.; Heil, G.; Koch, P.; Freund, M.; Diedrich, H.; Ruhl, H.; et al. Prognostic factors in a multicenter study for treatment of acute lymphoblastic leukemia in adults. *Blood* **1988**, *71*, 123–131, doi:10.1182/blood.v71.1.123.bloodjournal711123.
44. Hunault, M.; Harousseau, J.L.; Delain, M.; Truchan-Graczyk, M.; Cahn, J.Y.; Witz, F.; Lamy, T.; Pignon, B.; Jouet, J.P.; Garidi, R.; et al. Better outcome of adult acute lymphoblastic leukemia after early genoidentical allogeneic bone marrow transplantation (BMT) than after late high-dose therapy and autologous BMT: A GOELAMS trial. *Blood* **2004**, *104*, 3028–3037, doi:10.1182/blood-2003-10-3560.
45. Pui, C.H.; Howard, S.C. Current management and challenges of malignant disease in the CNS in paediatric leukaemia. *Lancet Oncol.* **2008**, *9*, 257–268, doi:10.1016/S1470-2045(08)70070-6.
46. Frishman-Levy, L.; Izraeli, S. Advances in understanding the pathogenesis of CNS acute lymphoblastic leukaemia and potential for therapy. *Br. J. Haematol.* **2017**, *176*, 157–167, doi:10.1111/bjh.14411.
47. Lenk, L.; Alsadeq, A.; Schewe, D.M. Involvement of the central nervous system in acute lymphoblastic leukemia: opinions on molecular mechanisms and clinical implications based on recent data. *Cancer Metastasis Rev.* **2020**, *39*, 173–187.
48. Scheuring, U.J.; Pfeifer, H.; Wassmann, B.; Brück, P.; Gehrke, B.; Petershofen, E.K.; Gschaidmeier, H.; Hoelzer, D.; Ottmann, O.G. Serial minimal residual disease (MRD) analysis as a predictor of response duration in Philadelphia-positive acute lymphoblastic leukemia (Ph+ALL) during imatinib treatment. *Leukemia* **2003**, *17*, 1700–1706, doi:10.1038/sj.leu.2403062.
49. Pieters, R.; De Groot-Kruseman, H.; Van Der Velden, V.; Fiocco, M.; Van Den Berg, H.; De Bont, E.; Egeler, R.M.; Hoogerbrugge, P.; Kaspers, G.; Van Der Schoot, E.; et al. Successful therapy reduction and intensification for childhood acute lymphoblastic leukemia based on minimal residual disease monitoring: Study ALL10 from the Dutch Childhood Oncology Group. *J. Clin. Oncol.* **2016**, *34*, 2591–2601, doi:10.1200/JCO.2015.64.6364.
50. Gökbuget, N.; Dombret, H.; Giebel, S.; Bruggemann, M.; Doubek, M.; Foà, R.; Hoelzer, D.; Kim, C.; Martinelli, G.; Parovichnikova, E.; et al. Minimal residual disease level predicts outcome in adults with Ph-negative B-precursor acute lymphoblastic leukemia. *Hematol.* **2019**, *24*, 337–348, doi:10.1080/16078454.2019.1567654.
51. Chilton, L.; Buck, G.; Harrison, C.J.; Ketterling, R.P.; Rowe, J.M.; Tallman, M.S.; Goldstone, A.H.; Fielding, A.K.; Moorman, A. V. High hyperdiploidy among adolescents and adults with acute lymphoblastic leukaemia (ALL): Cytogenetic features, clinical characteristics and outcome. *Leukemia* **2014**, *28*, 1511–1518, doi:10.1038/leu.2013.379.
52. Bhojwani, D.; Pei, D.; Sandlund, J.T.; Jeha, S.; Onciu, M.; Cheng, C.; Coustan-smith, E.; Paul, W. ETV6-RUNX1-positive childhood acute lymphoblastic leukemia: improved outcome with contemporary therapy. *Leukemia* **2012**, *26*, 265–270, doi:10.1038/leu.2011.227.
53. Nachman, J.B.; Heerema, N.A.; Sather, H.; Camitta, B.; Forestier, E.; Harrison, C.J.; Dastugue, N.; Schrappe, M.; Pui, C.H.; Basso, G.; et al. Outcome of treatment in children with hypodiploid acute lymphoblastic leukemia. *Blood* **2007**, *110*, 1112–1115, doi:10.1182/blood-2006-07-038299.
54. Pullarkat, V.; Slovak, M.L.; Kopecky, K.J.; Forman, S.J.; Appelbaum, F.R. Impact of cytogenetics on the outcome of adult acute lymphoblastic leukemia: Results of Southwest Oncology Group 9400 study. *Blood* **2008**, *111*, 2563–2572, doi:10.1182/blood-2007-10-116186.
55. Pui, C.H.; Gaynon, P.S.; Boyett, J.M.; Chessells, J.M.; Baruchel, A.; Kamps, W.; Silverman, L.B.;

Biondi, A.; Harms, D.O.; Vilmer, E.; et al. Outcome of treatment in childhood acute lymphoblastic leukaemia with rearrangements of the 11q23 chromosomal region. *Lancet* **2002**, *359*, 1909–1915, doi:10.1016/S0140-6736(02)08782-2.

56. Heerema, N.A.; Carroll, A.J.; Devidas, M.; Loh, M.L.; Borowitz, M.J.; Gastier-Foster, J.M.; Larsen, E.C.; Mattano, L.A.; Maloney, K.W.; Willman, C.L.; et al. Intrachromosomal amplification of chromosome 21 is associated with inferior outcomes in children with acute lymphoblastic leukemia treated in contemporary standard-risk children's oncology group studies: A report from the children's oncology group. *J. Clin. Oncol.* **2013**, *31*, 3397–3402, doi:10.1200/JCO.2013.49.1308.
57. Van Der Veer, A.; Waanders, E.; Pieters, R.; Willemse, M.E.; Van Reijmersdal, S. V.; Russell, L.J.; Harrison, C.J.; Evans, W.E.; Van Der Velden, V.H.J.; Hoogerbrugge, P.M.; et al. Independent prognostic value of BCR-ABL1-like signature and IKZF1 deletion, but not high CRLF2 expression, in children with B-cell precursor ALL. *Blood* **2013**, *122*, 2622–2629, doi:10.1182/blood-2012-10-462358.
58. Byun, J.M.; Koh, Y.; Shin, D.-Y.; Kim, I.; Yoon, S.-S.; Lee, J.-O.; Bang, S.-M.; Kim, K.H.; Jung, S.-H.; Lee, W.S.; et al. BCR-ABL translocation as a favorable prognostic factor in elderly patients with acute lymphoblastic leukemia in the era of potent tyrosine kinase inhibitors. *Haematologica* **2017**, *102*, e187–e190, doi:10.3324/haematol.2016.159988.
59. Andersen, M.K.; Autio, K.; Barbany, G.; Borgström, G.; Cavelier, L.; Golovleva, I.; Heim, S.; Heinonen, K.; Hovland, R.; Johannsson, J.H.; et al. Paediatric B-cell precursor acute lymphoblastic leukaemia with t(1;19)(q23;p13): Clinical and cytogenetic characteristics of 47 cases from the Nordic countries treated according to NOPHO protocols. *Br. J. Haematol.* **2011**, *155*, 235–243, doi:10.1111/j.1365-2141.2011.08824.x.
60. Fournier, B.; Balducci, E.; Duployez, N.; Clappier, E.; Cuccuini, W.; Arfeuille, C.; Caye-Eude, A.; Delabesse, E.; Bottollier-Lemallaz Colomb, E.; Nebral, K.; et al. B-ALL With t(5;14)(q31;q32); IGH-IL3 Rearrangement and Eosinophilia: A Comprehensive Analysis of a Peculiar IGH-Rearranged B-ALL. *Front. Oncol.* **2019**, *9*, 1–8, doi:10.3389/fonc.2019.01374.
61. Zaliova, M.; Stuchly, J.; Winkowska, L.; Musilova, A.; Fiser, K.; Slamova, M.; Starkova, J.; Vaskova, M.; Hrusak, O.; Sramkova, L.; et al. Genomic landscape of pediatric B-other acute lymphoblastic leukemia in a consecutive European cohort. *Haematologica* **2019**, *104*, 1396–1406, doi:10.3324/haematol.2018.204974.
62. Chiaretti, S.; Li, X.; Gentleman, R.; Vitale, A.; Vignetti, M.; Mandelli, F.; Ritz, J.; Foa, R. Gene expression profile of adult T-cell acute lymphocytic leukemia identifies distinct subsets of patients with different response to therapy and survival. *Blood* **2004**, *103*, 2771–2778, doi:10.1182/blood-2003-09-3243.
63. Cauwelier, B.; Dastugue, N.; Cools, J.; Poppe, B.; Herens, C.; De Paepe, A.; Hagemeijer, A.; Speleman, F. Molecular cytogenetic study of 126 unselected T-ALL cases reveals high incidence of TCRβ locus rearrangements and putative new T-cell oncogenes. *Leukemia* **2006**, *20*, 1238–1244, doi:10.1038/sj.leu.2404243.
64. Van Vlierberghe, P.; Ferrando, A. The molecular basis of T cell acute lymphoblastic leukemia Find the latest version : Review series The molecular basis of T cell acute lymphoblastic leukemia. *J. Clin. Invest.* **2012**, *122*, 3398–3406, doi:10.1172/JCI61269.3398.
65. Moorman, A. V. New and emerging prognostic and predictive genetic biomarkers in B-cell precursor acute lymphoblastic leukemia. *Haematologica* **2016**, *101*, 407–416, doi:10.3324/haematol.2015.141101.
66. Ribera, J.M.; Morgades, M.; Montesinos, P.; Tormo, M.; Martínez-Carballeira, D.; González-Campos, J.; Gil, C.; Barba, P.; García-Boyero, R.; Coll, R.; et al. A pediatric regimen for adolescents and young adults with Philadelphia chromosome-negative acute lymphoblastic leukemia: Results of the ALLRE08 PETHEMA trial. *Cancer Med.* **2020**, *9*, 2317–2329, doi:10.1002/cam4.2814.
67. Ribera, J.M.; Genescà, E.; Ribera, J. Who Should Receive an Allogeneic Transplant in First Complete Remission? *Clin. Lymphoma, Myeloma Leuk.* **2020**, *20*, S48–S51, doi:10.1016/S2152-2650(20)30459-6.
68. Alvarez, J.A.; Scully, R.E.; Miller, T.L.; Armstrong, F.D.; Constine, L.S.; Friedman, D.L.; Lipshultz, S.E. Long-term effects of treatments for childhood cancers. *Curr. Opin. Pediatr.* **2007**, *19*, 23–31, doi:10.1097/MOP.0b013e328013c89e.
69. Kızılocak, H.; Okcu, F. Late Effects of Therapy in Childhood Acute Lymphoblastic Leukemia Survivors. *Turkish J. Haematol. Off. J. Turkish Soc. Haematol.* **2019**, *36*, 1–11, doi:10.4274/tjh.galenos.2018.2018.0150.
70. Gervasini, G.; Vagace, J.M. Impact of genetic polymorphisms on chemotherapy toxicity in childhood acute lymphoblastic leukemia. *Front. Genet.* **2012**, *3*, 1–11, doi:10.3389/fgene.2012.00249.

71. Li, B.; Brady, S.W.; Ma, X.; Shen, S.; Zhang, Y.; Li, Y.; Szlachta, K.; Dong, L.; Liu, Y.; Yang, F.; et al. Therapy-induced mutations drive the genomic landscape of relapsed acute lymphoblastic leukemia. *Blood* **2020**, *135*, 41–55, doi:10.1182/blood.2019002220.
72. Pavlovic, S.; Kotur, N.; Stankovic, B.; Zukic, B.; Gasic, V.; Dokmanovic, L. Pharmacogenomic and pharmacotranscriptomic profiling of childhood acute lymphoblastic leukemia: Paving the way to personalized treatment. *Genes* **2019**, *10*, doi:10.3390/genes10030191.
73. Yang, J.J.; Cheng, C.; Devidas, M.; Cao, X.; Campana, D.; Yang, W.; Fan, Y.; Neale, G.; Cox, N.; Scheet, P.; et al. Genome-wide association study identifies germline polymorphisms associated with relapse of childhood acute lymphoblastic leukemia. *Blood* **2012**, *120*, 4197–4204, doi:10.1182/blood-2012-07-440107.
74. Abaji, R.; Krajinovic, M. Thiopurine S-methyltransferase polymorphisms in acute lymphoblastic leukemia, inflammatory bowel disease and autoimmune disorders: Influence on treatment response. *Pharmgenomics. Pers. Med.* **2017**, *10*, 143–156, doi:10.2147/PGPM.S108123.
75. Pottier, N.; Yang, W.; Assem, M.; Panetta, J.C.; Pei, D.; Paugh, S.W.; Cheng, C.; Den Boer, M.L.; Relling, M. V.; Pieters, R.; et al. The SWI/SNF chromatin-remodeling complex and glucocorticoid resistance in acute lymphoblastic leukemia. *J. Natl. Cancer Inst.* **2008**, *100*, 1792–1803, doi:10.1093/jnci/djn416.
76. Kutszegi, N.; Semsei, Á.F.; Gézsi, A.; Sági, J.C.; Nagy, V.; Csordás, K.; Jakab, Z.; Lautner-Csorba, O.; Gábor, K.M.; Kovács, G.T.; et al. Subgroups of paediatric acute lymphoblastic leukaemia might differ significantly in genetic predisposition to asparaginase hypersensitivity. *PLoS One* **2015**, *10*, 1–12, doi:10.1371/journal.pone.0140136.
77. Lopez-Santillan, M.; Iparraguirre, L.; Martin-Guerrero, I.; Gutierrez-Camino, A.; Garcia-Orad, A. Review of pharmacogenetics studies of L-asparaginase hypersensitivity in acute lymphoblastic leukemia points to variants in the GRIA1 gene. *Drug Metab. Pers. Ther.* **2017**, *32*, 1–9, doi:10.1515/dmpt-2016-0033.
78. Chen, S.-H; Pei, D.; Yang, W.; Cheng, C.; Jeha, S.; Cox, N.J.; Evans, W.E.; Pui, C.-H.; Relling, M. V. Genetic variations in GRIA1 on chromosome 5q33 related to asparaginase hypersensitivity. *Clin. Pharmacol. Ther.* **2010**, *88*, 191–196, doi:10.1038/clpt.2010.94.
79. Kantar, M.; Kosova, B.; Cetingul, N.; Gumus, S.; Toroslu, E.; Zafer, N.; Topcuoglu, N.; Aksoylar, S.; Cinar, M.; Tetik, A.; et al. Methylenetetrahydrofolate reductase C677T and A1298C gene polymorphisms and therapy-related toxicity in children treated for acute lymphoblastic leukemia and non-Hodgkin lymphoma. *Leuk. Lymphoma* **2009**, *50*, 912–917, doi:10.1080/10428190902893819.
80. Li, J.; Wang, X.R.; Zhai, X.W.; Wang, H.S.; Qian, X.W.; Miao, H.; Zhu, X.H. Association of SLCO1B1 gene polymorphisms with toxicity response of high dose methotrexate chemotherapy in childhood acute lymphoblastic leukemia. *Int. J. Clin. Exp. Med.* **2015**, *8*, 6109–6113.
81. Csordas, K.; Lautner-Csorba, O.; Semsei, A.F.; Harnos, A.; Hegyi, M.; Erdelyi, D.J.; Eipel, O.T.; Szalai, C.; Kovacs, G.T. Associations of novel genetic variations in the folate-related and ARID5B genes with the pharmacokinetics and toxicity of high-dose methotrexate in paediatric acute lymphoblastic leukaemia. *Br. J. Haematol.* **2014**, *166*, 410–420, doi:10.1111/bjh.12886.
82. Lopez-Lopez, E.; Ballesteros, J.; Piñan, M.A.; Sanchez De Toledo, J.; Garcia De Andoin, N.; Garcia-Miguel, P.; Navajas, A.; Garcia-Orad, A. Polymorphisms in the methotrexate transport pathway: A new tool for MTX plasma level prediction in pediatric acute lymphoblastic leukemia. *Pharmacogenet. Genomics* **2013**, *23*, 53–61, doi:10.1097/FPC.0b013e32835c3b24.
83. Liu, Y.; Yin, Y.; Sheng, Q.; Lu, X.; Wang, F.; Lin, Z.; Tian, H.; Xu, A.; Zhang, J. Association of ABCC2 −24C>T Polymorphism with High-Dose Methotrexate Plasma Concentrations and Toxicities in Childhood Acute Lymphoblastic Leukemia. *PLoS One* **2014**, *9*, e82681, doi:10.1371/journal.pone.0082681.
84. Ankathil, R. ABCB1 genetic variants in leukemias: Current insights into treatment outcomes. *Pharmgenomics. Pers. Med.* **2017**, *10*, 169–181, doi:10.2147/PGPM.S105208.
85. Matimba, A.; Li, F.; Livshits, A.; Cartwright, C.S.; Scully, S.; Brooke, L.; Jenkins, G.; Batzler, A.; Wang, L.; Weinshilboum, R.; et al. Clinical Response and Functional Validation of Candidate Genes. *Pharmacogenomics* **2014**, *15*, 433–447, doi:10.2217/pgs.13.226.
86. Moriyama, T.; Nishii, R.; Lin, T.-N.; Kihira, K.; Toyoda, H.; Nersting, J.; Kato, M.; Koh, K.; Inaba H.; Manabe, A.; et al. The Effects of Inherited NUDT15 Polymorphisms on Thiopurine Active Metabolites in Japanese Children with Acute Lymphoblastic Leukemia. *Pharmacogenet. Genomics* **2017**, *27*, 236–239, doi:10.1097/FPC.0000000000000282. The.
87. Khera, S.; Trehan, A.; Bhatia, P.; Singh, M.; Bansal, D.; Varma, N. Prevalence of TPMT, ITPA and

NUDT 15 genetic polymorphisms and their relation to 6MP toxicity in north Indian children with acute lymphoblastic leukemia. *Cancer Chemother. Pharmacol.* **2019**, *83*, 341–348, doi:10.1007/s00280-018-3732-3.

88. Cargnin, S.; Genazzani, A.A.; Canonico, P.L.; Terrazzino, S. Diagnostic accuracy of NUDT15 gene variants for thiopurine-induced leukopenia: a systematic review and meta-analysis. *Pharmacol. Res.* **2018**, *135*, 102–111, doi:10.1016/j.phrs.2018.07.021.
89. Wang, L.; Pelleymounter, L.; Weinshilboum, R.; Johnson, J.A.; Hebert, J.M.; Altman, R.B.; Klein, T.E. Very important pharmacogene summary: thiopurine S-methyltransferase. *Pharmacogenet. Genomics* **2010**, *20*, 401–405, doi:10.1097/FPC.0b013e3283352860.
90. Weinshilboum, R. Thiopurine pharmacogenetics: Clinical and molecular studies of thiopurine methyltransferase. *Drug Metab. Dispos.* **2001**, *29*, 601–605.
91. Kim, H.; Seo, H.; Park, Y.; Min, B.J.; Seo, M.E.; Park, K.D.; Shin, H.Y.; Kim, J.H.; Kang, H.J. APEX1 polymorphism and mercaptopurine-related early onset neutropenia in pediatric acute lymphoblastic leukemia. *Cancer Res. Treat.* **2018**, *50*, 823–834, doi:10.4143/crt.2017.351.
92. Stocco, G.; Cheok, M.H.; Crews, K.R.; Dervieux, T.; French, D.; Pei, D.; Yang, W.; Cheng, C.; Pui, C.H.; Relling, M. V.; et al. Genetic polymorphism of inosine triphosphate pyrophosphatase is a determinant of mercaptopurine metabolism and toxicity during treatment for acute lymphoblastic leukemia. *Clin. Pharmacol. Ther.* **2009**, *85*, 164–172, doi:10.1038/clpt.2008.154.
93. Hawwa, A.F.; Collier, P.S.; Millership, J.S.; McCarthy, A.; Dempsey, S.; Cairns, C.; McElnay, J.C. Population pharmacokinetic and pharmacogenetic analysis of 6-mercaptopurine in paediatric patients with acute lymphoblastic leukaemia. *Br. J. Clin. Pharmacol.* **2008**, *66*, 826–837, doi:10.1111/j.1365-2125.2008.03281.x.
94. Renbarger, J.L.; McCammack, K.C.; Rouse, C.E.; Hall, S.D. Effect of race on vincristine-associated neurotoxicity in pediatric acute lymphoblastic leukemia patients. *Pediatr. Blood Cancer* **2008**, *50*, 769–771, doi:10.1002/pbc.21435.
95. Hartford, C.M.; Duan, S.; Delaney, S.M.; Mi, S.; Kistner, E.O.; Lamba, J.K.; Huang, R.S.; Dolan, M.E. Population-specific genetic variants important in susceptibility to cytarabine arabinoside cytotoxicity. *Blood* **2009**, *113*, 2145–2153, doi:10.1182/blood-2008-05-154302.
96. Huang, R.S.; Duan, S.; Kistner, E.O.; Bleibel, W.K.; Delaney, S.M.; Fackenthal, D.L.; Das, S.; Dolan, M.E. Genetic variants contributing to daunorubicin-induced cytotoxicity. *Cancer Res.* **2008**, *68*, 3161–3168, doi:10.1158/0008-5472.CAN-07-6381.
97. Senkevitch, E.; Li, W.; Hixon, J.A.; Andrews, C.; Cramer, S.D.; Pauly, G.T.; Back, T.; Czarra, K.; Durum, S.K. Inhibiting Janus Kinase 1 and BCL-2 to treat T cell acute lymphoblastic leukemia with IL7-Rα mutations. *Oncotarget* **2018**, *9*, 22605–22617, doi:10.18632/oncotarget.25194.
98. Ling, Y.; Xie, Q.; Zhang, Z.; Zhang, H. Protein kinase inhibitors for acute leukemia. *Biomark. Res.* **2018**, *6*, 1–7, doi:10.1186/s40364-018-0123-1.
99. Evangelisti, C.; Chiarini, F.; McCubrey, J.A.; Martelli, A.M. Therapeutic targeting of mTOR in T-cell acute lymphoblastic leukemia: An update. *Int. J. Mol. Sci.* **2018**, *19*, doi:10.3390/ijms19071878.
100. Cloos, J.; Roeten, M.S.; Franke, N.E.; van Meerloo, J.; Zweegman, S.; Kaspers, G.J.; Jansen, G. (Immuno)proteasomes as therapeutic target in acute leukemia. *Cancer Metastasis Rev.* **2017**, *36*, 599–615, doi:10.1007/s10555-017-9699-4.
101. Costa, C.B.; Casalta-Lopes, Joa.; Andrade, C.; Moreira, D.; Oliveira, A.C.; Gonçalves, A.C.; Alves, V.; Silva, T.; Dourado, M.; Nascimento-Costa, J.M.; et al. Farnesyltransferase inhibitors: Molecular evidence of therapeutic efficacy in acute lymphoblastic leukemia through cyclin D1 inhibition. *Anticancer Res.* **2012**, *32*, 831–838.
102. Baratta, M.G. Adjusting the focus on γ-secretase inhibition. *Nat. Rev. Cancer* **2019**, *19*, 419, doi:10.1038/s41568-019-0174-0.
103. Han, Y.; Wang, X.; Wang, B.; Jiang, G. The progress of angiogenic factors in the development of leukemias. *Intractable Rare Dis. Res.* **2016**, *5*, 6–16, doi:10.5582/irdr.2015.01048.
104. Juarez, J.; Bradstock, K.F.; Gottlieb, D.J.; Bendall, L.J. Effects of inhibitors of the chemokine receptor CXCR4 on acute lymphoblastic leukemia cells in vitro. *Leukemia* **2003**, *17*, 1294–1300, doi:10.1038/sj.leu.2402998.
105. Garcia-Manero, G.; Yang, H.; Kuang, S.-Q.; O'Brien, S.; Thomas, D.; Kantarjian, H. Epigenetics of Acute Lymphocytic Leukemia. *Semin. Hematol.* **2009**, *46*, 24–32, doi:10.1053/j.seminhematol.2008.09.008.
106. Greenblatt, S.M.; Numer, S.D. Chromatin modifiers and the promise of epigenetic therapy in acute leukemia. *Leukemia* **2014**, *28*, 1396–1406, doi:10.1038/leu.2014.94.

107. Hartsink-Segers, S.A.; Zwaan, C.M.; Exalto, C.; Luijendijk, M.W.J.; Calvert, V.S.; Petricoin, E.F.; Evans, W.E.; Reinhardt, D.; De Haas, V.; Hedtjärn, M.; et al. Aurora kinases in childhood acute leukemia: The promise of aurora B as therapeutic target. *Leukemia* **2013**, *27*, 560–568, doi:10.1038/leu.2012.256.
108. De Labarthe, A.; Rousselot, P.; Huguet-Rigal, F.; Delabesse, E.; Witz, F.; Maury, S.; Réa, D.; Cayuela, J.M.; Vekemans, M.C.; Reman, O.; et al. Imatinib combined with induction or consolidation chemotherapy in patients with de novo Philadelphia chromosome-positive acute lymphoblastic leukemia: Results of the GRAAPH-2003 study. *Blood* **2007**, *109*, 1408–1413, doi:10.1182/blood-2006-03-011908.
109. Porkka, K.; Koskenvesa, P.; Lundán, T.; Rimpiläinen, J.; Mustjoki, S.; Smykla, R.; Wild, R.; Luo, R.; Arnan, M.; Brethon, B.; et al. Dasatinib crosses the blood-brain barrier and is an efficient therapy for central nervous system philadelphia chromosome positive leukemia. *Blood* **2008**, *112*, 1005–1012, doi:10.1182/blood-2008-02-140665.
110. Foà, R.; Vitale, A.; Vignetti, M.; Meloni, G.; Guarini, A.; De Propris, M.S.; Elia, L.; Paoloni, F.; Fazi, P.; Cimino, G.; et al. Dasatinib as first-line treatment for adult patients with Philadelphia chromosome-positive acute lymphoblastic leukemia. *Blood* **2011**, *118*, 6521–6528, doi:10.1182/blood-2011-05-351403.
111. Cortes, J.E.; Kim, D.W.; Pinilla-Ibarz, J.; Le Coutre, P.; Paquette, R.; Chuah, C.; Nicolini, F.E.; Apperley, J.F.; Khoury, H.J.; Talpaz, M.; et al. A phase 2 trial of ponatinib in Philadelphia chromosome-positive leukemias. *N. Engl. J. Med.* **2013**, *369*, 1783–1796, doi:10.1056/NEJMoa1306494.
112. Sasaki, K.; Jabbour, E.; Ravandi, F.; Short, N.J.; Thomas, D.; Garcia-manero, G.; Daver, N.; Kadia, T.; Konopleva, M.; Ph, D.; et al. therapy for Ph-positive ALL : a propensity score analysis. *Cancer* **2016**, *122*, 3650–3656, doi:10.1002/cncr.30231.Hyper-CVAD.
113. Dai, H.; Wang, Y.; Lu, X.; Han, W. Chimeric antigen receptors modified T-cells for cancer therapy. *J. Natl. Cancer Inst.* **2016**, *108*.
114. Schmiegelow, K.; Forestier, E.; Hellebostad, M.; Heyman, M.; Kristinsson, J.; Söderhäll, S.; Taskinen, M. Long-term results of NOPHO ALL-92 and ALL-2000 studies of childhood acute lymphoblastic leukemia. *Leukemia* **2010**, *24*, 345–354, doi:10.1038/leu.2009.251.
115. Stary, J.; Zimmermann, M.; Campbell, M.; Castillo, L.; Dibar, E.; Donska, S.; Gonzalez, A.; Izraeli, S.; Janic, D.; Jazbec, J.; et al. Intensive chemotherapy for childhood acute lymphoblastic leukemia: Results of the randomized intercontinental trial ALL IC-BFM 2002. *J. Clin. Oncol.* **2014**, *32*, 174–184, doi:10.1200/JCO.2013.48.6522.
116. Jabbour, E.; Ravandi, F.; Kebriaei, P.; Huang, X.; Short, N.J.; Thomas, D.; Sasaki, K.; Rytting, M.; Jain, N.; Konopleva, M.; et al. Salvage chemoimmunotherapy with inotuzumab ozogamicin combined with mini-hyper-CVD for patients with relapsed or refractory philadelphia chromosome-negative acute lymphoblastic leukemia: A phase 2 clinical trial. *JAMA Oncol.* **2018**, *4*, 230–234, doi:10.1001/jamaoncol.2017.2380.
117. Kantarjian, H.M.; Thomas, D.; Ravandi, F.; Faderl, S.; Jabbour, E.; Garcia-Manero, G.; Pierce, S.; Shan, J.; Cortes, J.; O'Brien, S. Defining the course and prognosis of adults with acute lymphocytic leukemia in first salvage after induction failure or short first remission duration. *Cancer* **2010**, *116*, 5568–5574.
118. Raetz, E.A.; Borowitz, M.J.; Devidas, M.; Linda, S.B.; Hunger, S.P.; Winick, N.J.; Camitta, B.M.; Gaynon, P.S.; Carroll, W.L. Reinduction platform for children with first marrow relapse in acute lymphoblastic lymphoma. *J. Clin. Oncol.* **2008**, *26*, 3971–3978, doi:10.1200/JCO.2008.16.1414.
119. Eckert, C.; Henze, G.; Seeger, K.; Hagedorn, N.; Mann, G.; Panzer-Grümayer, R.; Peters, C.; Klingebiel, T.; Borkhardt, A.; Schrappe, M.; et al. Use of allogeneic hematopoietic stem-cell transplantation based on minimal residual disease response improves outcomes for children with relapsed acute lymphoblastic leukemia in the intermediate-risk group. *J. Clin. Oncol.* **2013**, *31*, 2736–2742, doi:10.1200/JCO.2012.48.5680.
120. Borowitz, M.J.; Devidas, M.; Hunger, S.P.; Bowman, W.P.; Carroll, A.J.; Carroll, W.L.; Linda, S.; Martin, P.L.; Pullen, D.J.; Viswanatha, D.; et al. Clinical significance of minimal residual disease in childhood acute lymphoblastic leukemia and its relationship to other prognostic factors: A Children's Oncology Group study. *Blood* **2008**, *111*, 5477–5485, doi:10.1182/blood-2008-01-132837.
121. Goto, H. Childhood relapsed acute lymphoblastic leukemia: Biology and recent treatment progress. *Pediatr. Int.* **2015**, *57*, 1059–1066, doi:10.1111/ped.12837.
122. Mcmillin, D.W.; Negri, J.M.; Mitsiades, C.S. The role of tumour-stromal interactions in modifying drug response: Challenges and opportunities. *Nat. Rev. Drug Discov.* **2013**, *12*, 217–228,

doi:10.1038/nrd3870.

123. Forestier, E.; Heyman, M.; Andersen, M.K.; Autio, K.; Blennow, E.; Borgström, G.; Golovleva, I.; Heim, S.; Heinonen, K.; Hovland, R.; et al. Outcome of ETV6/RUNX1-positive childhood acute lymphoblastic leukaemia in the NOPHO-ALL-1992 protocol: Frequent late relapses but good overall survival. *Br. J. Haematol.* **2008**, *140*, 665–672, doi:10.1111/j.1365-2141.2008.06980.x.
124. Salmoiraghi, S.; Guinea M., Marie L.; Ubiali, G.; Tosi, M.; Peruta, B.; Zanghi, P.; Oldani, E.; Boschini, C.; Kohlmann, A.; et al. Mutations of TP53 gene in adult acute lymphoblastic leukemia at diagnosis do not affect the achievement of hematologic response but correlate with early relapse and very poor survival. *Haematologica* **2016**, *101*, 245–248, doi:10.3324/haematol.2015.137059.
125. Yu, C.H.; Chang, W.T.; Jou, S.T.; Lin, T.K.; Chang, Y.H.; Lin, C.Y.; Lin, K.H.; Lu, M.Y.; Chen, S.H.; Wu, K.H.; et al. TP53 alterations in relapsed childhood acute lymphoblastic leukemia. *Cancer Sci.* **2020**, *111*, 229–238, doi:10.1111/cas.14238.
126. Forero-Castro, M.; Robledo, C.; Benito, R.; Bodega-Mayor, I.; Rapado, I.; Hernández-Sánchez, M.; Abáigar, M.; Maria Hernández-Sánchez, J.; Quijada-Álamo, M.; María Sánchez-Pina, J.; et al. Mutations in TP53 and JAK2 are independent prognostic biomarkers in B-cell precursor acute lymphoblastic leukaemia. *Br. J. Cancer* **2017**, *117*, 256–265, doi:10.1038/bjc.2017.152.
127. Stengel, A.; Kern, W.; Haferlach, T.; Meggendorfer, M.; Fasan, A.; Haferlach, C. The impact of TP53 mutations and TP53 deletions on survival varies between AML, ALL, MDS and CLL: An analysis of 3307 cases. *Leukemia* **2017**, *31*, 705–711, doi:10.1038/leu.2016.263.
128. Hogan, L.E.; Meyer, J.A.; Yang, J.; Wang, J.; Wong, N.; Yang, W.; Condos, G.; Hunger, S.P.; Raetz, E.; Saffery, R.; et al. Integrated genomic analysis of relapsed childhood acute lymphoblastic leukemia reveals therapeutic strategies. *Blood* **2011**, *118*, 5218–5226, doi:10.1182/blood-2011-04-345595.
129. Pierro, J.; Hogan, L.E.; Bhatla, T.; Carroll, W.L. New targeted therapies for relapsed pediatric acute lymphoblastic leukemia. *Expert Rev. Anticancer Ther.* **2017**, *17*, 725–736, doi:10.1080/14737140.2017.1347507.
130. Inaba, H.; Greaves, M.; Mullighan, C.G. Acute lymphoblastic leukaemia. *Lancet* **2013**, *381*, 1943–1955, doi:10.1016/S0140-6736(12)62187-4.
131. Bhojwani, D.; Yang, J.J.; Pui, C.-H. Biology of Childhood Acute Lymphoblastic Leukemia Deepa. *Pediatr. Clin. North Am.* **2015**, *62*, 47–60, doi:10.1016/j.pcl.2014.09.004.
132. De Ravel, T.J.L.; Devriendt, K.; Fryns, J.P.; Vermeesch, J.R. What's new in karyotyping? The move towards array comparative genomic hybridisation (CGH). *Eur. J. Pediatr.* **2007**, *166*, 637–643, doi:10.1007/s00431-007-0463-6.
133. Maciejewski, J.P.; Mufti, G.J. Whole genome scanning as a cytogenetic tool in hematologic malignancies. *Blood* **2008**, *112*, 965–974, doi:10.1182/blood-2008-02-130435.
134. Song, J.; Shao, H. SNP Array in Hematopoietic Neoplasms: A Review. *Microarrays* **2015**, *5*, 1, doi:10.3390/microarrays5010001.
135. Stuppia, L.; Antonucci, I.; Palka, G.; Gatta, V. Use of the MLPA assay in the molecular diagnosis of gene copy number alterations in human genetic diseases. *Int. J. Mol. Sci.* **2012**, *13*, 3245–3276, doi:10.3390/ijms13033245.
136. Bashton, M.; Hollis, R.; Ryan, S.; Schwab, C.J.; Moppett, J.; Harrison, C.J.; Moorman, A. V.; Enshaei, A. Concordance of copy number abnormality detection using SNP arrays and Multiplex Ligation-dependent Probe Amplification (MLPA) in acute lymphoblastic leukaemia. *Sci. Rep.* **2020**, *10*, 1–11, doi:10.1038/s41598-019-56972-0.
137. Mullighan, C.G.; Goorha, S.; Radtke, I.; Miller, C.B.; Coustan-Smith, E.; Dalton, J.D.; Girtman, K.; Mathew, S.; Ma, J.; Pounds, S.B.; et al. Genome-wide analysis of genetic alterations in acute lymphoblastic leukaemia. *Nature* **2007**, *446*, 758–764, doi:10.1038/nature05690.
138. Mullighan, C.G.; Downing, J.R. Global Genomic Characterization of Acute Lymphoblastic Leukemia. *Semin. Hematol.* **2009**, *46*, 3–15, doi:10.1053/j.seminhematol.2008.09.005.
139. Harrison, C.J.; Haas, O.; Harbott, J.; Biondi, A.; Stanulla, M.; Trka, J.; Izraeli, S. Detection of prognostically relevant genetic abnormalities in childhood B-cell precursor acute lymphoblastic leukaemia: Recommendations from the Biology and Diagnosis Committee of the International Berlin-Frankfürt-Münster study group. *Br. J. Haematol.* **2010**, *151*, 132–142, doi:10.1111/j.1365-2141.2010.08314.x.
140. Rack, K.A.; van den Berg, E.; Haferlach, C.; Beverloo, H.B.; Costa, D.; Espinet, B.; Foot, N.; Jeffries, S.; Martin, K.; O'Connor, S.; et al. European recommendations and quality assurance for cytogenomic analysis of haematological neoplasms. *Leukemia* **2019**, *33*, 1851–1867,

doi:10.1038/s41375-019-0378-z.
141. Usvasalo, A.; Elonen, E.; Saarinen-Pihkala, U.M.; Räty, R.; Harila-Saari, A.; Koistinen, P.; Savolainen, E.R.; Knuutila, S.; Hollmén, J. Prognostic classification of patients with acute lymphoblastic leukemia by using gene copy number profiles identified from array-based comparative genomic hybridization data. *Leuk. Res.* **2010**, *34*, 1476–1482, doi:10.1016/j.leukres.2010.02.031.
142. Mrózek, K.; Harper, D.P.; Aplan, P.D. Cytogenetics and Molecular Genetics of Acute Lymphoblastic Leukemia. *Hematol. Oncol. Clin. North Am.* **2009**, *23*, 991–1010, doi:10.1016/j.hoc.2009.07.001.
143. Voelkerding, K. V; Dames, S.A.; Durtschi, J.D. Next-Generation Sequencing: From Basic Research to Diagnostics. *Clin. Chem.* **2009**, *55*, 641–658, doi:10.1373/clinchem.2008.112789.
144. Coccaro, N.; Anelli, L.; Zagaria, A.; Specchia, G.; Albano, F. Next-generation sequencing in acute lymphoblastic Leukemia. *Int. J. Mol. Sci.* **2019**, *20*.
145. Rothberg, J.M.; Leamon, J.H. The development and impact of 454 sequencing. *Nat. Biotechnol.* **2008**, *26*, 1117–1124, doi:10.1038/nbt1485.
146. Samorodnitsky, E.; Jewell, B.M.; Hagopian, R.; Miya, J.; Wing, M.R.; Lyon, E.; Damodaran, S.; Bhatt, D.; Reeser, J.W.; Datta, J.; et al. Evaluation of Hybridization Capture Versus Amplicon-Based Methods for Whole-Exome Sequencing. *Hum. Mutat.* **2015**, *36*, 903–914, doi:10.1002/humu.22825.
147. Zhang, H.; Wang, H.; Qian, X.; Gao, S.; Xia, J.; Liu, J.; Cheng, Y.; Man, J.; Zhai, X. Genetic mutational analysis of pediatric acute lymphoblastic leukemia from a single center in China using exon sequencing. *BMC Cancer* **2020**, *20*, 211, doi:10.1186/s12885-020-6709-7.
148. Nijman, I.J.; Van Montfrans, J.M.; Hoogstraat, M.; Boes, M.L.; Van De Corput, L.; Renner, E.D.; Van Zon, P.; Van Lieshout, S.; Elferink, M.G.; Van Der Burg, M.; et al. Targeted next-generation sequencing: A novel diagnostic tool for primary immunodeficiencies. *J. Allergy Clin. Immunol.* **2014**, *133*, 529-534.e1, doi:10.1016/j.jaci.2013.08.032.
149. Strom, S.P. Current practices and guidelines for clinical next-generation sequencing oncology testing. *Cancer Biol. Med.* **2016**, *13*, 3–11, doi:10.28092/j.issn.2095-3941.2016.0004.
150. Kamps, R.; Brandão, R.D.; van den Bosch, B.J.; Paulussen, A.D.C.; Xanthoulea, S.; Blok, M.J.; Romano, A. Next-generation sequencing in oncology: Genetic diagnosis, risk prediction and cancer classification. *Int. J. Mol. Sci.* **2017**, *18*, doi:10.3390/ijms18020308.
151. Miller, E.M.; Patterson, N.E.; Zechmeister, J.M.; Bejerano-Sagie, M.; Delio, M.; Patel, K.; Ravi, N.; Quispe-Tintaya, W.; Maslov, A.; Simmons, N.; et al. Development and validation of a targeted next generation DNA sequencing panel outperforming whole exome sequencing for the identification of clinically relevant genetic variants. *Oncotarget* **2017**, *8*, 102033–102045, doi:10.18632/oncotarget.22116.
152. Lionel, A.C.; Costain, G.; Monfared, N.; Walker, S.; Reuter, M.S.; Hosseini, S.M.; Thiruvahindrapuram, B.; Merico, D.; Jobling, R.; Nalpathamkalam, T.; et al. Improved diagnostic yield compared with targeted gene sequencing panels suggests a role for whole-genome sequencing as a first-tier genetic test. *Genet. Med.* **2018**, *20*, 435–443, doi:10.1038/gim.2017.119.
153. Loh, M.L.; Zhang, J.; Pei, D.; Dai, Y.; Ma, X.; Devidas, M.; Edmondson, M.; Rusch, M.; Carroll, A.J.; Chen, I.-M.; et al. Whole Exome Sequencing of Pediatric Acute Lymphoblastic Leukemia Patients Identify Mutations in 11 Pathways: A Report from the Children's Oncology Group. *Blood* **2016**, *128*, 455–455, doi:10.1182/blood.v128.22.455.455.
154. Malinowska-Ozdowy, K.; Frech, C.; Schönegger, A.; Eckert, C.; Cazzaniga, G.; Stanulla, M.; Zur Stadt, U.; Mecklenbräuker, A.; Schuster, M.; Kneidinger, D.; et al. KRAS and CREBBP mutations: A relapse-linked malicious liaison in childhood high hyperdiploid acute lymphoblastic leukemia. *Leukemia* **2015**, *29*, 1656–1667, doi:10.1038/leu.2015.107.
155. Paulsson, K.; Lilljebjörn, H.; Biloglav, A.; Olsson, L.; Rissler, M.; Castor, A.; Barbany, G.; Fogelstrand, L.; Nordgren, A.; Sjögren, H.; et al. The genomic landscape of high hyperdiploid childhood acute lymphoblastic leukemia. *Nat. Genet.* **2015**, *47*, 672–676, doi:10.1038/ng.3301.
156. Holmfeldt, L.; Wei, L.; Diaz-Flores, E.; Walsh, M.; Zhang, J.; Ding, L.; Payne-Turner, D.; Churchman, M.; Andersson, A.; Chen, S.C.; et al. The genomic landscape of hypodiploid acute lymphoblastic leukemia. *Nat. Genet.* **2013**, *45*, 242–252, doi:10.1038/ng.2532.
157. Stark, R.; Grzelak, M.; Hadfield, J. RNA sequencing: the teenage years. *Nat. Rev. Genet.* 2019, *20*, 631–656.
158. Hrdlickova, R.; Toloue, M.; Tian, B. RNA-Seq methods for transcriptome analysis. *Wiley Interdiscip. Rev. RNA* **2017**, *8*.
159. Wang, Y.; Wu, N.; Liu, D.; Jin, Y. Recurrent Fusion Genes in Leukemia: An Attractive Target for Diagnosis and Treatment. *Curr. Genomics* **2017**, *18*, 378–384,

doi:10.2174/1389202918666170329110349.
160. Afrin, S.; Zhang, C.R.C.; Meyer, C.; Stinson, C.L.; Pham, T.; Bruxner, T.J.C.; Venn, N.C.; Trahair, T.N.; Sutton, R.; Marschalek, R.; et al. Targeted Next-Generation Sequencing for Detecting MLL Gene Fusions in Leukemia. *Mol. Cancer Res.* **2018**, *16*, 279–285, doi:10.1158/1541-7786.MCR-17-0569.
161. Koch, C.M.; Chiu, S.F.; Akbarpour, M.; Bharat, A.; Ridge, K.M.; Bartom, E.T.; Winter, D.R. A beginner's guide to analysis of RNA sequencing data. *Am. J. Respir. Cell Mol. Biol.* **2018**, *59*, 145–157, doi:10.1165/rcmb.2017-0430TR.
162. Pulsipher, M.A.; Carlson, C.; Langholz, B.; Wall, D.A.; Schultz, K.R.; Bunin, N.; Kirsch, I.; Gastier-Foster, J.M.; Borowitz, M.; Desmarais, C.; et al. IgH-V(D)J NGS-MRD measurement pre-and early post-allotransplant defines very low-and very high-risk ALL patients. *Blood* **2015**, *125*, 3501–3508, doi:10.1182/blood-2014-12-615757.
163. Faham, M.; Zheng, J.; Moorhead, M.; Carlton, V.E.H.; Stow, P.; Coustan-Smith, E.; Pui, C.H.; Campana, D. Deep-sequencing approach for minimal residual disease detection in acute lymphoblastic leukemia. *Blood* **2012**, *120*, 5173–5180, doi:10.1182/blood-2012-07-444042.
164. Wu, D.; Emerson, R.O.; Sherwood, A.; Loh, M.L.; Angiolillo, A.; Howie, B.; Vogt, J.; Rieder, M.; Kirsch, I.; Carlson, C.; et al. Detection of minimal residual disease in B lymphoblastic leukemia by high-throughput sequencing of IGH. *Clin. Cancer Res.* **2014**, *20*, 4540–4548, doi:10.1158/1078-0432.CCR-13-3231.
165. Inaba, H.; Azzato, E.M.; Mullighan, C.G. Integration of next-generation sequencing to treat acute lymphoblastic leukemia with targetable lesions: The St. Jude Children's Research Hospital approach. *Front. Pediatr.* **2017**, *5*, 1–5, doi:10.3389/fped.2017.00258.
166. Montaño, A.; Forero-Castro, M.; Marchena-Mendoza, D.; Benito, R.; Hernández-Rivas, J.M. New challenges in targeting signaling pathways in acute lymphoblastic leukemia by NGS approaches: An update. *Cancers.* **2018**, *10*.
167. Safavi, S.; Olsson, L.; Biloglav, A.; Veerla, S.; Blendberg, M.; Tayebwa, J.; Behrendtz, M.; Castor, A.; Hansson, M.; Johansson, B.; et al. Genetic and epigenetic characterization of hypodiploid acute lymphoblastic leukemia. *Oncotarget* **2015**, *6*, 42793–42802, doi:10.18632/oncotarget.6000.
168. Andersson, A.K.; Ma, J.; Wang, J.; Chen, X.; Gedman, A.L.; Kriwacki, R.; Rusch, M.; Wu, G.; Li, Y.; Mulder, H.; et al. The landscape of somatic mutations in Infant MLL rearranged acute lymphoblastic leukemias. *Nat. Genet.* **2015**, *47*, 330–337, doi:10.1038/ng.3230.
169. Fischer, U.; Forster, M.; Rinaldi, A.; Risch, T.; Sungalee, S.; Warnatz, H.-J.; Bornhauser, B.; Gombert, M.; Kratsch, C.; Stütz, A.M.; et al. Genomics and drug profiling of fatal TCF3-HLF−positive acute lymphoblastic leukemia identifies recurrent mutation patterns and therapeutic options. *Nat. Genet.* **2015**, *47*, 1020–1029, doi:10.1038/ng.3362.
170. Chiaretti, S.; Brugnoletti, F.; Messina, M.; Paoloni, F.; Fedullo, A.L.; Piciocchi, A.; Elia, L.; Vitale, A.; Mauro, E.; Ferrara, F.; et al. CRLF2 overexpression identifies an unfavourable subgroup of adult B-cell precursor acute lymphoblastic leukemia lacking recurrent genetic abnormalities. *Leuk. Res.* **2016**, *41*, 36–42, doi:10.1016/j.leukres.2015.11.018.
171. Forero-Castro, M.; Robledo, C.; Benito, R.; Abáigar, M.; África Martín, A.; Arefi, M.; Fuster, J.L.; de las Heras, N.; Rodríguez, J.N.; Quintero, J.; et al. Genome-Wide DNA Copy Number Analysis of Acute Lymphoblastic Leukemia Identifies New Genetic Markers Associated with Clinical Outcome. *PLoS One* **2016**, *11*, e0148972, doi:10.1371/journal.pone.0148972.
172. Kuiper, R.P.; Waanders, E.; Van Der Velden, V.H.J.; Van Reijmersdal, S. V.; Venkatachalam, R.; Scheijen, B.; Sonneveld, E.; Van Dongen, J.J.M.; Veerman, A.J.P.; Van Leeuwen, F.N.; et al. IKZF1 deletions predict relapse in uniformly treated pediatric precursor B-ALL. *Leukemia* **2010**, *24*, 1258–1264, doi:10.1038/leu.2010.87.
173. Marke, R.; Van Leeuwen, F.N.; Scheijen, B. The many faces of IKZF1 in B-cell precursor acute lymphoblastic leukemia. *Haematologica* **2018**, *103*, 565–574, doi:10.3324/haematol.2017.185603.
174. Iacobucci, I.; Mullighan, C.G. Genetic basis of acute lymphoblastic leukemia. *J. Clin. Oncol.* **2017**, *35*, 975–983, doi:10.1200/JCO.2016.70.7836.
175. Chiaretti, S.; Gianfelici, V.; O'Brien, S.M.; Mullighan, C.G. Advances in the Genetics and Therapy of Acute Lymphoblastic Leukemia. *Am. Soc. Clin. Oncol. Educ. B.* **2016**, *36*, e314–e322, doi:10.14694/edbk_156628.
176. Iacobucci, I.; Storlazzi, C.T.; Cilloni, D.; Lonetti, A.; Ottaviani, E.; Soverini, S.; Astolfi, A.; Chiaretti, S.; Vitale, A.; Messa, F.; et al. Identification and molecular characterization of recurrent genomic deletions on 7p12 in the IKZF1 gene in a large cohort of BCR-ABL1-positive acute lymphoblastic leukemia patients: On behalf of Gruppo Italiano Malattie Ematologiche dell'Adulto Acute Leukemia

Working Party (GIMEMA AL WP). *Blood* **2009**, *114*, 2159–2167, doi:10.1182/blood-2008-08-173963.
177. Roberts, K.G.; Li, Y.; Payne-Turner, D.; Harvey, R.C.; Yang, Y.L.; Pei, D.; McCastlain, K.; Ding, L.; Lu, C.; Song, G.; et al. Targetable kinase-activating lesions in Ph-like acute lymphoblastic leukemia. *N. Engl. J. Med.* **2014**, *371*, 1005–1015, doi:10.1056/NEJMoa1403088.
178. Mullighan, C.G.; Miller, C.B.; Radtke, I.; Phillips, L.A.; Dalton, J.; Ma, J.; White, D.; Hughes, T.P.; Le Beau, M.M.; Pui, C.H.; et al. BCR-ABL1 lymphoblastic leukaemia is characterized by the deletion of Ikaros. *Nature* **2008**, *453*, 110–114, doi:10.1038/nature06866.
179. Marke, R.; Havinga, J.; Cloos, J.; Demkes, M.; Poelmans, G.; Yuniati, L.; Van Ingen Schenau, D.; Sonneveld, E.; Waanders, E.; Pieters, R.; et al. Tumor suppressor IKZF1 mediates glucocorticoid resistance in B-cell precursor acute lymphoblastic leukemia. *Leukemia* **2016**, *30*, 1599–1603, doi:10.1038/leu.2015.359.
180. Imamura, T.; Yano, M.; Asai, D.; Moriya-Saito, A.; Suenobu, S.I.; Hasegawa, D.; Deguchi, T.; Hashii, Y.; Kawasaki, H.; Hori, H.; et al. IKZF1 deletion is enriched in pediatric B-cell precursor acute lymphoblastic leukemia patients showing prednisolone resistance. *Leukemia* **2016**, *30*, 1801–1803, doi:10.1038/leu.2016.128.
181. Ribera, J.; Morgades, M.; Zamora, L.; Montesinos, P.; Gõmez-Seguí, I.; Pratcorona, M.; Sarrà, J.; Guàrdia, R.; Nomdedeu, J.; Tormo, M.; et al. Prognostic significance of copy number alterations in adolescent and adult patients with precursor B acute lymphoblastic leukemia enrolled in PETHEMA protocols. *Cancer* **2015**, *121*, 3809–3817, doi:10.1002/cncr.29579.
182. Kobitzsch, B.; Gökbuget, N.; Schwartz, S.; Reinhardt, R.; Brüggemann, M.; Viardot, A.; Wäsch, R.; Starck, M.; Thiel, E.; Hoelzer, D.; et al. Loss-of-function but not dominant-negative intragenic IKZF1 deletions are associated with an adverse prognosis in adult BCR-ABL-negative acute lymphoblastic leukemia. *Haematologica* **2017**, *102*, 1739–1747, doi:10.3324/haematol.2016.161273.
183. Yang, J.J.; Bhojwani, D.; Yang, W.; Cai, X.; Stocco, G.; Crews, K.; Wang, J.; Morrison, D.; Devidas, M.; Hunger, S.P.; et al. Genome-wide copy number profiling reveals molecular evolution from diagnosis to relapse in childhood acute lymphoblastic leukemia. *Blood* **2008**, *112*, 4178–4183, doi:10.1182/blood-2008-06-165027.
184. Harvey, R.C.; Mullighan, C.G.; Wang, X.; Dobbin, K.K.; Davidson, G.S.; Bedrick, E.J.; Chen, I.M.; Atlas, S.R.; Kang, H.; Ar, K.; et al. Identification of novel cluster groups in pediatric high-risk B-precursor acute lymphoblastic leukemia with gene expression profiling: Correlation with genome-wide DNA copy number alterations, clinical characteristics, and outcome. *Blood* **2010**, *116*, 4874–4884, doi:10.1182/blood-2009-08-239681.
185. Steeghs, E.M.P.; Boer, J.M.; Hoogkamer, A.Q.; Boeree, A.; de Haas, V.; de Groot-Kruseman, H.A.; Horstmann, M.A.; Escherich, G.; Pieters, R.; den Boer, M.L. Copy number alterations in B-cell development genes, drug resistance, and clinical outcome in pediatric B-cell precursor acute lymphoblastic leukemia. *Sci. Rep.* **2019**, *9*, 1–11, doi:10.1038/s41598-019-41078-4.
186. Zhang, W.; Kuang, P.; Liu, T. Prognostic significance of CDKN2A/B deletions in acute lymphoblastic leukaemia: a meta-analysis. *Ann. Med*. **2019**; Vol. 51; ISBN 8613980562.
187. Schwab, C.J.; Chilton, L.; Morrison, H.; Jones, L.; Al-Shehhi, H.; Erhorn, A.; Russell, L.J.; Moorman, A. V.; Harrison, C.J. Genes commonly deleted in childhood B-cell precursor acute lymphoblastic leukemia: Association with cytogenetics and clinical features. *Haematologica* **2013**, *98*, 1081–1088, doi:10.3324/haematol.2013.085175.
188. Van Galen, J.C.; Kuiper, R.P.; Van Emst, L.; Levers, M.; Tijchon, E.; Scheijen, B.; Waanders, E.; Van Reijmersdal, S. V.; Gilissen, C.; Van Kessel, A.G.; et al. BTG1 regulates glucocorticoid receptor autoinduction in acute lymphoblastic leukemia. *Blood* **2010**, *115*, 4810–4819, doi:10.1182/blood-2009-05-223081.
189. Buitenkamp, T.D.; Pieters, R.; Zimmermann, M.; De Haas, V.; Richards, S.M.; Vora, A.J.; Mitchell, C.D.; Schwab, C.; Harrison, C.J.; Moorman, A. V.; et al. BTG1 deletions do not predict outcome in Down syndrome acute lymphoblastic leukemia. *Leukemia* **2013**, *27*, 251–252, doi:10.1038/leu.2012.199.
190. Russell, L.J.; Capasso, M.; Vater, I.; Akasaka, T.; Bernard, O.A.; Calasanz, M.J.; Chandrasekaran, T.; Chapiro, E.; Gesk, S.; Griffiths, M.; et al. Deregulated expression of cytokine receptor gene, CRLF2, is involved in lymphoid transformation in B-cell precursor acute lymphoblastic leukemia. *Blood* **2009**, *114*, 2688–2698, doi:10.1182/blood-2009-03-208397.
191. Stanulla, M.; Dagdan, E.; Zaliova, M.; Möricke, A.; Palmi, C.; Cazzaniga, G.; Eckert, C.; Te Kronnie, G.; Bourquin, J.P.; Bornhauser, B.; et al. IKZF1 plus defines a new minimal residual disease-dependent very-poor prognostic profile in pediatric b-cell precursor acute lymphoblastic leukemia.

J. Clin. Oncol. **2018**, *36*, 1240–1249, doi:10.1200/JCO.2017.74.3617.

192. Moorman, A. V.; Enshaei, A.; Schwab, C.; Wade, R.; Chilton, L.; Elliott, A.; Richardson, S.; Hancock, J.; Kinsey, S.E.; Mitchell, C.D.; et al. A novel integrated cytogenetic and genomic classification refines risk stratification in pediatric acute lymphoblastic leukemia. *Blood* **2014**, *124*, 1434–1444, doi:10.1182/blood-2014-03-562918.
193. Scheijen, B.; Boer, J.M.; Marke, R.; Tijchon, E.; van Ingen Schenau, D.; Waanders, E.; van Emst, L.; van der Meer, L.T.; Pieters, R.; Escherich, G.; et al. Tumor suppressors BTG1 and IKZF1 cooperate during mouse leukemia development and increase relapse risk in B-cell precursor acute lymphoblastic leukemia patients. *Haematologica* **2017**, *102*, 541–551, doi:10.3324/haematol.2016.153023.
194. Liu, Y.F.; Wang, B.Y.; Zhang, W.N.; Huang, J.Y.; Li, B.S.; Zhang, M.; Jiang, L.; Li, J.F.; Wang, M.J.; Dai, Y.J.; et al. Genomic Profiling of Adult and Pediatric B-cell Acute Lymphoblastic Leukemia. *EBioMedicine* **2016**, *8*, 173–183, doi:10.1016/j.ebiom.2016.04.038.
195. Lilljebjörn, H.; Henningsson, R.; Hyrenius-Wittsten, A.; Olsson, L.; Orsmark-Pietras, C.; Von Palffy, S.; Askmyr, M.; Rissler, M.; Schrappe, M.; Cario, G.; et al. Identification of ETV6-RUNX1-like and DUX4-rearranged subtypes in paediatric B-cell precursor acute lymphoblastic leukaemia. *Nat. Commun.* **2016**, *7*, doi:10.1038/ncomms11790.
196. Gu, Z.; Churchman, M.; Roberts, K.; Li, Y.; Liu, Y.; Harvey, R.C.; McCastlain, K.; Reshmi, S.C.; Payne-Turner, D.; Iacobucci, I.; et al. Genomic analyses identify recurrent MEF2D fusions in acute lymphoblastic leukaemia. *Nat. Commun.* **2016**, *7*, 1–10, doi:10.1038/ncomms13331.
197. Zhang, Jinghui; McCastlain, Kelly; Yoshihara, Hiroki; Xu, Beisi; Chang, Yunchao; Churchman, Michelle L.; Wu, G. Deregulation of DUX4 and ERG in acute lymphoblastic leukemia. *Nat. Genet.* **2016**, *48*, 1481–1489, doi:10.1038/ng.3691.
198. Yasuda, T.; Tsuzuki, S.; Kawazu, M.; Hayakawa, F.; Kojima, S.; Ueno, T.; Imoto, N.; Kohsaka, S.; Kunita, A.; Doi, K.; et al. Recurrent DUX4 fusions in B cell acute lymphoblastic leukemia of adolescents and young adults. *Nat. Genet.* **2016**, *48*, 569–574, doi:10.1038/ng.3535.
199. Qian, M.; Zhang, H.; Kham, S.K.Y.; Liu, S.; Jiang, C.; Zhao, X.; Lu, Y.; Goodings, C.; Lin, T.N.; Zhang, R.; et al. Whole-transcriptome sequencing identifies a distinct subtype of acute lymphoblastic leukemia with predominant genomic abnormalities of EP300 and CREBBP. *Genome Res.* **2017**, *27*, 185–195, doi:10.1101/gr.209163.116.
200. Li, J.F.; Dai, Y.T.; Lilljebjörn, H.; Shen, S.H.; Cui, B.W.; Bai, L.; Liu, Y.F.; Qian, M.X.; Kubota, Y.; Kiyoi, H.; et al. Transcriptional landscape of B cell precursor acute lymphoblastic leukemia based on an international study of 1,223 cases. *Proc. Natl. Acad. Sci.* **2018**, *115*, E11711–E11720, doi:10.1073/pnas.1814397115.
201. Gu, Z.; Churchman, M.L.; Roberts, K.G.; Moore, I.; Zhou, X.; Nakitandwe, J.; Hagiwara, K.; Pelletier, S.; Gingras, S.; Berns, H.; et al. PAX5-driven subtypes of B-progenitor acute lymphoblastic leukemia. *Nat. Genet.* **2019**, *51*, 296–307, doi:10.1038/s41588-018-0315-5.
202. Zhang, H.; He, X.; Ni, D.; Mou, L.; Chen, X.; Lu, S. How does the novel T315L mutation of breakpoint cluster region-abelson (BCR-ABL) kinase confer resistance to ponatinib: a comparative molecular dynamics simulation study. *J. Biomol. Struct. Dyn.* **2020**, *38*, 89–100, doi:10.1080/07391102.2019.1567390.
203. Meyer, J.A.; Wang, J.; Hogan, L.E.; Yang, J.J.; Dandekar, S.; Patel, J.P.; Tang, Z.; Zumbo, P.; Li, S.; Zavadil, J.; et al. Relapse specific mutations in NT5C2 in childhood acute lymphoblastic leukemia. *Nat. Genet.* **2013**, *45*, 290–294, doi:10.1038/ng.2558.
204. Jerchel, I.S.; Hoogkamer, A.Q.; Ariës, I.M.; Steeghs, E.M.P.; Boer, J.M.; Besselink, N.J.M.; Boeree, A.; Van De Ven, C.; De Groot-Kruseman, H.A.; De Haas, V.; et al. RAS pathway mutations as a predictive biomarker for treatment adaptation in pediatric B-cell precursor acute lymphoblastic leukemia. *Leukemia* **2018**, *32*, 931–940, doi:10.1038/leu.2017.303.
205. Cheng, Y.; Tian, H. Current development status of MEK inhibitors. *Molecules* **2017**, *22*, doi:10.3390/molecules22101551.
206. Schwartzman, O.; Savino, A.M.; Gombert, M.; Palmi, C.; Cario, G.; Schrappe, M.; Eckert, C.; Stackelberg, A. Von; Huang, J.Y.; Hameiri-Grossman, M.; et al. Suppressors and activators of JAK-STAT signaling at diagnosis and relapse of acute lymphoblastic leukemia in Down syndrome. *Proc. Natl. Acad. Sci.* **2017**, *114*, E4030–E4039, doi:10.1073/pnas.1702489114.
207. Qin, H.; Cho, M.; Haso, W.; Zhang, L.; Tasian, S.K.; Oo, H.Z.; Negri, G.L.; Lin, Y.; Zou, J.; Mallon, B.S.; et al. Eradication of B-ALL using chimeric antigen receptor-expressing T cells targeting the TSLPR oncoprotein. *Blood* **2015**, *126*, 629–639, doi:10.1182/blood-2014-11-612903.

208. Savino, A.M.; Sarno, J.; Trentin, L.; Vieri, M.; Fazio, G.; Bardini, M.; Bugarin, C.; Fossati, G.; Davis, K.L.; Gaipa, G.; et al. The histone deacetylase inhibitor givinostat (ITF2357) exhibits potent anti-tumor activity against CRLF2-rearranged BCP-ALL. *Leukemia* **2017**, *31*, 2365–2375, doi:10.1038/leu.2017.93.
209. Verstraete, K.; Peelman, F.; Braun, H.; Lopez, J.; Van Rompaey, D.; Dansercoer, A.; Vandenberghe, I.; Pauwels, K.; Tavernier, J.; Lambrecht, B.N.; et al. Structure and antagonism of the receptor complex mediated by human TSLP in allergy and asthma. *Nat. Commun.* **2017**, *8*, doi:10.1038/ncomms14937.
210. Churchman, M.L.; Evans, K.; Richmond, J.; Robbins, A.; Jones, L.; Shapiro, I.M.; Pachter, J.A.; Weaver, D.T.; Houghton, P.J.; Smith, M.A.; et al. Synergism of FAK and tyrosine kinase inhibition in Ph+ B-ALL. *JCI Insight* **2016**, *1*, doi:10.1172/jci.insight.86082.
211. Churchman, M.L.; Low, J.; Qu, C.; Paietta, E.M.; Lawryn, H.; Chang, Y.; Payne-turner, D.; Althoff, M.J.; Song, G.; Chen, S.; et al. Efficacy of Retinoids in IKZF1-Mutated BCR-ABL1 Acute Lymphoblastic Leukemia. *Cancer Cell* **2015**, *28*, 343–356, doi:10.1016/j.ccell.2015.07.016.
212. Roberts, K.G.; Gu, Z.; Payne-Turner, D.; McCastlain, K.; Harvey, R.C.; Chen, I.M.; Pei, D.; Iacobucci, I.; Valentine, M.; Pounds, S.B.; et al. High Frequency and Poor Outcome of Philadelphia Chromosome-Like Acute Lymphoblastic Leukemia in Adults. *J. Clin. Oncol.* **2017**, *35*, 394–401, doi:10.1200/JCO.2016.69.0073.
213. Fischer, U.; Forster, M.; Rinaldi, A.; Risch, T.; Sungalee, S.; Warnatz, H.J.; Bornhauser, B.; Gombert, M.; Kratsch, C.; Stütz, A.M.; et al. Genomics and drug profiling of fatal TCF3-HLFâ ’positive acute lymphoblastic leukemia identifies recurrent mutation patterns and therapeutic options. *Nat. Genet.* **2015**, *47*, 1020–1029, doi:10.1038/ng.3362.
214. Suzuki, K.; Okuno, Y.; Kawashima, N.; Muramatsu, H.; Okuno, T.; Wang, X.; Kataoka, S.; Sekiya, Y.; Hamada, M.; Murakami, N.; et al. MEF2D-BCL9 fusion gene is associated with high-risk acute B-cell precursor lymphoblastic leukemia in adolescents. *J. Clin. Oncol.* **2016**, *34*, 3451–3459, doi:10.1200/JCO.2016.66.5547.
215. Shago, M.; Abla, O.; Hitzler, J.; Weitzman, S.; Abdelhaleem, M. Frequency and outcome of pediatric acute lymphoblastic leukemia with ZNF384 gene rearrangements including a novel translocation resulting in an ARID1B/ZNF384 gene fusion. *Pediatr. Blood Cancer* **2016**, *63*, 1915–1921, doi:10.1002/pbc.26116.
216. Hormann, F.M.; Hoogkamer, A.Q.; Beverloo, H.B.; Boeree, A.; Dingjan, I.; Wattel, M.M.; Stam, R.W.; Escherich, G.; Pieters, R.; den Boer, M.L.; et al. NUTM1 is a recurrent fusion gene partner in B-cell precursor acute lymphoblastic leukemia associated with increased expression of genes on chromosome band 10p12.31-12.2. *Haematologica* **2019**, *104*, e455–e459, doi:10.3324/haematol.2018.206961.
217. Stanulla, M.; Dagdan, E.; Zaliova, M.; Anja, M.; Palmi, C.; Cazzaniga, G.; Kronnie, G.; Bourquin, J.; Bornhauser, B.; Koehler, R.; et al. IKZF1 plus De fi nes a New Minimal Residual Disease – Dependent Very-Poor Prognostic Pro fi le in Pediatric B-Cell Precursor Acute Lymphoblastic Leukemia. *J. Clin. Oncol.* **2020**, *36*.
218. Familiades, J.; Bousquet, M.; Lafage-Pochitaloff, M.; Béné, M.C.; Beldjord, K.; De Vos, J.; Dastugue, N.; Coyaud, E.; Struski, S.; Quelen, C.; et al. PAX5 mutations occur frequently in adult B-cell progenitor acute lymphoblastic leukemia and PAX5 haploinsufficiency is associated with BCR-ABL1 and TCF3-PBX1 fusion genes: A GRAALL study. *Leukemia* **2009**, *23*, 1989–1998, doi:10.1038/leu.2009.135.
219. Mangum, D.S.; Downie, J.; Mason, C.C.; Jahromi, M.S.; Joshi, D.; Rodic, V.; Müschen, M.; Meeker, N.; Trede, N.; Frazer, J.K.; et al. VPREB1 deletions occur independent of lambda light chain rearrangement in childhood acute lymphoblastic leukemia. *Leukemia* **2014**, *28*, 216–220, doi:10.1038/leu.2013.223.
220. Ivanov Öfverholm, I.; Zachariadis, V.; Taylan, F.; Marincevic-Zuniga, Y.; Tran, A.N.; Saft, L.; Nilsson, D.; Syvänen, A.C.; Lönnerholm, G.; Harila-Saari, A.; et al. Overexpression of chromatin remodeling and tyrosine kinase genes in iAMP21-positive acute lymphoblastic leukemia. *Leuk. Lymphoma* **2020**, *61*, 604–613, doi:10.1080/10428194.2019.1678153.
221. Robinson, H.M.; Broadfield, Z.J.; Cheung, K.L.; Harewood, L.; Harris, R.L.; Jalali, G.R.; Martineau, M.; Moorman, A. V.; Taylor, K.E.; Richards, S.; et al. Amplification of AML1 in acute lymphoblastic leukemia is associated with a poor outcome. *Leukemia* **2003**, *17*, 2249–2250.
222. Safavi, S.; Paulsson, K. Near-haploid and low-hypodiploid acute lymphoblastic leukemia: Two distinct subtypes with consistently poor prognosis. *Blood* **2017**, *129*, 420–423, doi:10.1182/blood-2016-

10-743765.
223. Tasian, S.K.; Loh, M.L.; Hunger, S.P. Philadelphia chromosome–like acute lymphoblastic leukemia. *Blood* **2017**, *130*, 2064–2072, doi:10.1182/blood-2017-06-743252.
224. Ting, S.; Mixue, X.; Lixia, Z.; Xueying, L.; Wanzhuo, X.; Xiujin, Y. T315I mutation exerts a dismal prognosis on adult BCR-ABL1-positive acute lymphoblastic leukemia, and salvage therapy with ponatinib or CAR-T cell and bridging to allogeneic hematopoietic stem cell transplantation can improve clinical outcomes. *Ann. Hematol.* **2020**, *99*, 829–834, doi:10.1007/s00277-020-03949-z.
225. Armstrong, S.A.; Staunton, J.E.; Silverman, L.B.; Pieters, R.; Den Boer, M.L.; Minden, M.D.; Sallan, S.E.; Lander, E.S.; Golub, T.R.; Korsmeyer, S.J. MLL translocations specify a distinct gene expression profile that distinguishes a unique leukemia. *Nat. Genet.* **2002**, *30*, 41–47, doi:10.1038/ng765.
226. Armstrong, S.A.; Mabon, M.E.; Silverman, L.B.; Li, A.; Gribben, J.G.; Fox, E.A.; Sallan, S.E.; Korsmeyer, S.J. FLT3 mutations in childhood acute lymphoblastic leukemia. *Blood* **2004**, *103*, 3544–3546, doi:10.1182/blood-2003-07-2441.
227. Wyman, C.; Kanaar, R. DNA double-strand break repair: All's well that ends well. *Annu. Rev. Genet.* **2006**, *40*, 363–383, doi:10.1146/annurev.genet.40.110405.090451.
228. Jasin, M.; Haber, J.E. The democratization of gene editing: Insights from site-specific cleavage and double-strand break repair. *DNA Repair* **2016**, *44*, 6–16, doi:10.1016/j.dnarep.2016.05.001.
229. Chiruvella, K.K.; Liang, Z.; Wilson, T.E. Repair of double-strand breaks by end joining. *Cold Spring Harb. Perspect. Biol.* **2013**, *5*, 1–21, doi:10.1101/cshperspect.a012757.
230. Gaj, T.; Gersbach, C.A.; Barbas, C.F. ZFN, TALEN, and CRISPR/Cas-based methods for genome engineering. *Trends Biotechnol.* **2013**, *31*, 397–405, doi:10.1016/j.tibtech.2013.04.004.
231. Cong, L.; Ran, F.A.; Cox, D.; Lin, S.; Barretto, R.; Habib, N.; Hsu, P.D.; Wu, X.; Jiang, W.; Marraffini, L.A.; et al. Multiplex genome engineering using CRISPR/Cas systems. *Science* **2013**, *339*, 819–823, doi:10.1126/science.1231143.
232. Montaño, A.; Forero-Castro, M.; Hernández-Rivas, J.M.; García-Tuñón, I.; Benito, R. Targeted genome editing in acute lymphoblastic leukemia: A review. *BMC Biotechnol.* **2018**, *18*, 1–10, doi:10.1186/s12896-018-0455-9.
233. Böiers, C.; Richardson, S.E.; Laycock, E.; Zriwil, A.; Turati, V.A.; Brown, J.; Wray, J.P.; Wang, D.; James, C.; Herrero, J.; et al. A Human IPS Model Implicates Embryonic B-Myeloid Fate Restriction as Developmental Susceptibility to B Acute Lymphoblastic Leukemia-Associated ETV6-RUNX1. *Dev. Cell* **2018**, *44*, 362-377.e7, doi:10.1016/j.devcel.2017.12.005.
234. Eyquem, J.; Mansilla-Soto, J.; Giavridis, T.; van der Stegen, S.J.C.; Hamieh, M.; Cunanan, K.M.; Odak, A.; Gönen, M.; Sadelain, M. Targeting a CAR to the TRAC locus with CRISPR/Cas9 enhances tumour rejection. *Nature* **2017**, *543*, 113–117, doi:10.1038/nature21405.
235. Umerez, M.; Gutierrez-Camino, Á.; Muñoz-Maldonado, C.; Martin-Guerrero, I.; Garcia-Orad, A. MTHFR polymorphisms in childhood acute lymphoblastic leukemia: Influence on methotrexate therapy. *Pharmgenomics. Pers. Med.* **2017**, *10*, 69–78.
236. Rudin, S.; Marable, M.; Huang, R.S. The Promise of Pharmacogenomics in Reducing Toxicity During Acute Lymphoblastic Leukemia Maintenance Treatment. *Genomics, Proteomics Bioinforma.* **2017**, *15*, 82–93.
237. Stanulla, M.; Cavé, H.; Moorman, A. V. IKZF1 deletions in pediatric acute lymphoblastic leukemia: Still a poor prognostic marker? *Blood* **2020**, *135*, 252–260, doi:10.1182/blood.2019000813.
238. Xu, H.; Wu, X.; Sun, D.; Li, S.; Zhang, S.; Teng, M.; Bu, J.; Zhang, X.; Meng, B.; Wang, W.; et al. SEGF: A novel method for gene fusion detection from single-end next-generation sequencing data. *Genes* **2018**, *9*, doi:10.3390/genes9070331.
239. Moreno-Cabrera, J.M.; del Valle, J.; Castellanos, E.; Feliubadaló, L.; Pineda, M.; Brunet, J.; Serra, E.; Capellà, G.; Lázaro, C.; Gel, B. Evaluation of CNV detection tools for NGS panel data in genetic diagnostics. *Eur. J. Hum. Genet.* **2020**, 1–11, doi:10.1038/s41431-020-0675-z.
240. Chiaretti, S.; Messina, M.; Foà, R. *BCR/ABL1* -like acute lymphoblastic leukemia: How to diagnose and treat? *Cancer* **2019**, *125*, 194–204, doi:10.1002/cncr.31848.
241. Frisch, A.; Ofran, Y. How i diagnose and manage Philadelphia chromosome-like acute lymphoblastic leukemia. *Haematologica* **2019**, *104*, 2135–2143.
242. Cario, G.; Zimmermann, M.; Romey, R.; Gesk, S.; Vater, I.; Harbott, J.; Schrauder, A.; Moericke, A.; Izraeli, S.; Akasaka, T.; et al. Presence of the P2RY8-CRLF2 rearrangement is associated with a poor prognosis in non-high-risk precursor B-cell acute lymphoblastic leukemia in children treated according to the ALL-BFM 2000 protocol. *Blood* **2010**, *115*, 5393–5397, doi:10.1182/blood-2009-11-256131.

243. Meyer, L.K.; Delgado-Martin, C.; Maude, S.L.; Shannon, K.M.; Teachey, D.T.; Hermiston Id, M.L. CRLF2 rearrangement in Ph-like acute lymphoblastic leukemia predicts relative glucocorticoid resistance that is overcome with MEK or Akt inhibition. **2019**, doi:10.1371/journal.pone.0220026.
244. Tanasi, I.; Ba, I.; Sirvent, N.; Braun, T.; Cuccuini, W.; Ballerini, P.; Duployez, N.; Tanguy-Schmidt, A.; Tamburini, J.; Maury, S.; et al. Efficacy of tyrosine kinase inhibitors in Ph-like acute lymphoblastic leukemia harboring ABL-class rearrangements. *Blood* **2019**, *134*, 1351–1355.
245. Brown, L.M.; Lonsdale, A.; Zhu, A.; Davidson, N.M.; Schmidt, B.; Hawkins, A.; Wallach, E.; Martin, M.; Mechinaud, F.M.; Khaw, S.L.; et al. The application of RNA sequencing for the diagnosis and genomic classification of pediatric acute lymphoblastic leukemia. *Blood Adv.* **2020**, *4*, 930–942, doi:10.1182/bloodadvances.2019001008.
246. Raetz, E.A.; Bhatla, T. Where do we stand in the treatment of relapsed acute lymphoblastic leukemia? *Hematol. Am. Soc. Hematol. Educ. Progr.* **2012**, *2012*, doi:10.1182/ASHEDUCATION-2012.1.129.
247. Ma, X.; Edmonson, M.; Yergeau, D.; Muzny, D.M.; Hampton, O.A.; Rusch, M.; Song, G.; Easton, J.; Harvey, R.C.; Wheeler, D.A.; et al. Rise and fall of subclones from diagnosis to relapse in pediatric B-acute lymphoblastic leukaemia. *Nat. Commun.* **2015**, *6*, 1–12, doi:10.1038/ncomms7604.
248. Oshima, K.; Khiabanian, H.; Da Silva-Almeida, A.C.; Tzoneva, G.; Abate, F.; Ambesi-Impiombato, A.; Sanchez-Martin, M.; Carpenter, Z.; Penson, A.; Perez-Garcia, A.; et al. Mutational landscape, clonal evolution patterns, and role of RAS mutations in relapsed acute lymphoblastic leukemia. *Proc. Natl. Acad. Sci.* **2016**, *113*, 11306–11311, doi:10.1073/pnas.1608420113.
249. Zaliova, M.; Madzo, J.; Cario, G.; Trka, J. Revealing the role of TEL/AML1 for leukemic cell survival by RNAi-mediated silencing. *Leukemia* **2011**, *25*, 313–320, doi:10.1038/leu.2010.277.
250. Diakos, C.; Krapf, G.; Gerner, C.; Inthal, A.; Lemberger, C.; Ban, J.; Dohnal, A.M.; Panzer-Gruemayer, E.R. RNAi-mediated silencing of TEL/AML1 reveals a heat-shock protein- and survivin-dependent mechanism for survival. *Blood* **2007**, *109*, 2607–2610, doi:10.1182/blood-2006-04-019612.
251. Fuka, G.; Kantner, H.P.; Grausenburger, R.; Inthal, A.; Bauer, E.; Krapf, G.; Kaindl, U.; Kauer, M.; Dworzak, M.N.; Stoiber, D.; et al. Silencing of ETV6/RUNX1 abrogates PI3K/AKT/mTOR signaling and impairs reconstitution of leukemia in xenografts. *Leukemia* **2012**, *26*, 927–933, doi:10.1038/leu.2011.322.
252. Polak, R.; Bierings, M.B.; van der Leije, C.S.; Sanders, M.A.; Roovers, O.; Marchante, J.R.M.; Boer, J.M.; Cornelissen, J.J.; Pieters, R.; Den Boer, M.L.; et al. Autophagy inhibition as a potential future targeted therapy for ETV6-RUNX1-driven B-cell precursor acute lymphoblastic leukemia. *Haematologica* **2019**, *104*, 738–748, doi:10.3324/haematol.2018.193631.
253. J Harbott, S.V.A.B.G.H.F.L. Incidence of TEL/AML1 fusion gene analyzed consecutively in children with acute lymphoblastic leukemia in relapse. *Blood* **1997**, *90*, 4933–4937.
254. K Seeger, H.P.A.D.B.B.B.B.K.C.N.J.R.D.S.D.H.M.S.G.H. TEL-AML1 fusion transcript in relapsed childhood acute lymphoblastic leukemia. The Berlin-Frankfurt-Münster Study Group. *Blood* **1998**, *91*, 1716–1722.
255. Meyer, C.; Burmeister, T.; Gröger, D.; Tsaur, G.; Fechina, L.; Renneville, A.; Sutton, R.; Venn, N.C.; Emerenciano, M.; Pombo-De-Oliveira, M.S.; et al. The MLL recombinome of acute leukemias in 2017. *Leukemia* **2018**, *32*, 273–284, doi:10.1038/leu.2017.213.
256. Kotecha, R.S.; Cheung, L.C. Targeting the bone marrow microenvironment: A novel therapeutic strategy for pre-B acute lymphoblastic leukemia. *Oncotarget* **2019**, *10*, 1756–1757.
257. Chiarini, F.; Lonetti, A.; Evangelisti, C.; Buontempo, F.; Orsini, E.; Evangelisti, C.; Cappellini, A.; Neri, L.M.; McCubrey, J.A.; Martelli, A.M. Advances in understanding the acute lymphoblastic leukemia bone marrow microenvironment: From biology to therapeutic targeting. *Biochim. Biophys. Acta - Mol. Cell Res.* **2016**, *1863*, 449–463.

SUPPLEMENTARY APENDIX

Annex I

Supplemental material of Chapter I. Comprehensive custom NGS panel validation for the improvement of the stratification of B-Acute Lymphoblastic Leukemia patients.

Supplementary information

Comprehensive Custom NGS Panel Validation for the Improvement of the Stratification of B-Acute Lymphoblastic Leukemia Patients

Adrián Montaño [1], Jesús Hernández-Sánchez [1], Maribel Forero-Castro [2], María Matorra-Miguel [1], Eva Lumbreras [1], Cristina Miguel [1], Sandra Santos [1], Valentina Ramírez-Maldonado [1], José Luís Fuster [3], Natalia de Las Heras [4], Alfonso García-de Coca [5], Magdalena Sierra [6], Julio Dávila [7], Ignacio de la Fuente [8], Carmen Olivier [9], Juan Olazabal [10], Joaquín Martínez [11], Nerea Vega-García [12], Teresa González [7], Jesús María Hernández-Rivas [1,7,*] and Rocío Benito [1,*]

[1] IBSAL, IBMCC, Universidad de Salamanca, CSIC, Centro de Investigación del Cáncer (CIC), Salamanca, 37007, Spain; adrianmo18@gmail.com (A.M.); jesus807@gmail.com (J.H.-S.); mariammzamora@gmail.com (M.M.-M.); a21093@usal.es (E.L.); cristinamiguelgarcia@gmail.com (C.M.); sandruskism90@gmail.com (S.S.); vramirem@gmail.com (V.R.);

[2] Escuela de Ciencias Biológicas (Grupo de investigación GICBUPTC), Universidad Pedagógica y Tecnológica de Colombia, Tunja, 150003, Colombia; maribel.forero@uptc.edu.co

[3] Sección de Oncohematología Pediátrica, Hospital Clínico Universitario Virgen de la Arrixaca; Instituto Murciano de Investigación Biosanitaria (IMIB), Murcia, 30120, Spain; josel.fuster@carm.es

[4] Departamento de Hematología—Hospital Virgen Blanca, León, 24008, Spain; nherasr@saludcastillayleon.es

[5] Departamento de Hematología—Hospital Clínico de Valladolid, Valladolid, 47003, Spain; agarciaco@saludcastillayleon.es

[6] Complejo Sanitario de Zamora, Zamora, 49022, Spain; msierrap@saludcastillayleon.es

[7] Departamento de Hematología—Hospital Universitario de Salamanca, Salamanca, 37007, Spain; juldaval@hotmail.com, teresa.gonzalez.mart@gmail.com

[8] Departamento de Hematología—Hospital Rio Hortega, Valladolid, 47012, Spain; ifuentegr@saludcastillayleon.es

[9] Servicio de Hematología y Hemoterapia—Complejo Sanitario de Segovia, Segovia, 40002, Spain; colivierco@gmail.com

[10] Departamento de Hematología—Hospital Universitario de Burgos, Burgos, 09006, Spain; jolazabal@saludcastillayleon.es

[11] Departamento de Hematología—Hospital Universitario 12 de Octubre, Madrid, 28041, Spain; jmarti01@med.ucm.es

[12] Laboratorio de Hematología, Instituto de Investigación, Hospital Sant Joan de Déu, Barcelona, 08950, Spain; nvega@fsjd.org

* Correspondence: jmhr@usal.es (J.M.H.-R.); beniroc@usal.es (R.B.)

Table S1. Genetic characteristics of the patients. This table shows the genetic characteristics of the B-ALL patients included in the study. In the first column the genetic subtype, followed by the patient identifier, the karyotype, the FISH, the findings observed by MLPA and changes greater than 5Mb detected by aCGH. Not done or Not data (ND), Male (M), Female (F).

Genetic subtype	ID	Sex/ Age (years)	Karyotype	FISH	MLPA	aCGH >5Mb
BCR/ABL1	ID1	M/70	Karyotype failure	LSI BCR/ABL1 fusion (54%)	*IKZF1*	+19
	ID2	M/76	55-60,XY,+Y,+4,+5,+7,+8,t(9;22)(q34;q11),+9,+11,add(12)(p12)[15]	LSI BCR/ABL1 Clonal - 9q34/ABL1 gain (89%), BCR/ABL1 fusion (89%), LSI MLL-r clonal - 11q23/MLL gain (28%)	ND	+4, +18, +X, -19
	ID3	M/34	46,XY,t(9;22)(q34;q11)[7]/46,XY[5]	ND	*IKZF1*	+17, +X
	ID4	M/50	46,XY,t(9;22)(q14;q11)[10]/46,XY[5]	LSI BCR/ABL1 fusion (97%)	ND	ND
	ID5	M/47	46,XY,t(9;22)(q34;q11)[7]/47,XY,+8,t(9;22)(q34;q11)[2]/46,XY[5]	LSI BCR/ABL1 fusion (65%)	Normal	+8
	ID6	M/ND	46,XY[6]	LSI BCR/ABL1 fusion (82.5%)	*IKZF1, CDKN2A, PAX5*	-9
	ID7	M/70	46,XY,t(9;22)(q34;q11)[8]/46,XY[2]	LSI BCR/ABL1 fusion (87%)	*CDKN2A*	Normal
	ID8	F/72	46,XX,t(9;22)(q34;q11)[2]/46,XX[10]	LSI BCR/ABL1 fusion (26%)	ND	ND
	ID9	M/70	46,XY,t(9;22)(q34;q11)[13]/46,XY[8]	LSI BCR/ABL1 fusion (93%)	*IKZF1*	Normal
	ID10	F/45	Karyotype failure	LSI BCR/ABL1 fusion (98%)	*BTG1*	+2, +4, +6, +10, +14, +21, -12p
ETV6/RUNX1	ID11	M/14	46,XY[15]	LSI ETV6/RUNX1 fusion (80%), LSI 12p13/ETV6 gain (33%), 21q22/RUNX1 gain (76%), LSI 11q23/MLL gain (26%), LSI 9q34/ABL1 gain (48%), 22q11.2/BCR gain (60%)	*CDKN2A, PARP1*	+21

	ID12	F/3	46,XX[12]	ETV6/RUNX1 fusion (12%), LSI - 21q22/RUNX1 gain (63%)	*PAX5, ETV6*	+21
	ID13	F/5	Karyotype failure	LSI ETV6/RUNX1 fusion (81%)	*PARP1*	-X
	ID14	M/3	46,XY[10]	LSI ETV6/RUNX1 fusion (95,5%)	Normal	Normal
	ID15	M/2	48,XY,+11,+17[3]/44,XY,-13,-15[2]/46,XY[14]	Normal. ETV6/RUNX1 fusion positive by RT-PCR	*ETV6*	+X, -12p
	ID16	M/2	46,XY[10]	LSI ETV6/RUNX1 fusion (94%)	Normal	Normal
	ID17	F/5	46,XX[10]	LSI ETV6/RUNX1 fusion (96%)	*BTG1, ETV6*	+19
	ID18	M/2	Karyotype failure	LSI ETV6/RUNX1 fusion (90%)	ND	ND
	ID19	F/15	47,XX,+21c[15]/46,XX[3]	LSI ETV6/RUNX1 fusion (88,5%), LSI 21q22/RUNX1 gain (100%)	Normal	Normal
	ID20	F/14	Karyotype failure	LSI ETV6/RUNX1 fusion (96%)	*PAX5, ETV6*	+21, -6q
	ID21	F/47	46,XX,t(4;11)(q21;q23)[14]	Normal	Normal	Normal
	ID22	M/46	Karyotype failure	LSI MLL-r (95,5%)	Normal	Normal
	ID23	F/0	46,XX,inv(11)(q12q23),del(12)(p13)[7]/46,XX[13]	LSI MLL-r (93%)	Normal	Normal
	ID24	M/60	Karyotype failure	LSI MLL-r (73%)	*PARP1*	+6
MLLr	ID25	F/31	46,XX,t(4;11)(q21;q23)[10]	Normal	Normal	Normal
	ID26	M/16	46,XY,t(4;11)(q21;q23)[7]/46,XY[3]	LSI MLL-r (83%)	*IKZF1, PAX5*	-17, -19, -22
	ID27	M/55	46,XY,t(4;11)(q21;q23)[3]/46,XY[10]	LSI MLL-r (75%)	*CDKN2A*	Normal
	ID28	F/0	47,XX,t(4;11)(q21;q23),+mar[23]	LSI MLL-r (83%)	Normal	Normal
	ID29	F/0	40-42,XX[6]/46,XX[6]	LSI MLL-r (18%)	Normal	Normal
	ID30	M/0	ND	LSI MLL-r (65%)	ND	ND

High hyperdiploid	ID31	F/5	51-58,XX,+5,+6,+9,+10,+21[14]/46,XX[6]	LSI 21q22/RUNX1 gain (89%)	Normal	+4, +6, +14, +17q, +18, +21, +X, -17p
	ID32	F/4	48-52,XX,+2,+6,+8,+10,+12,+21 [12]/46,XX[3]	ND	ND	ND
	ID33	F/3	51,XX,+21,4mar[4]/46,XX[17]	LSI 21q22/RUNX1 gain (94%), LSI 9q34/ABL1 gain (51%), LSI 11q23/MLL gain (25,5%)	Normal	+10, +18, +21
	ID34	F/4	50-52,XX,+10,+17,+18,+21,+mar[3]/46,XX[8]	LSI 21q22/RUNX1 gain (48.5%)	*IKZF1*	+10, +14, +21
	ID35	F/2	Karyotype failure	LSI 12p13.2/ETV6 gain (16%), LSI 21q22.12/RUNX1 gain (55%)	Normal	+4, +5, +6, +8, +10, +14, +21, +X, -19, -20, -22
	ID36	F/47	46,XX[10]	LSI 2p13.2/ETV6 gain (90%), LSI 21q22.12/RUNX1 gain (90%), LSI MYC gain (62%), LSI IGH gain (60%)	Normal	+6, +8, +13, +14, +19, +21, -17q, -X
	ID37	F/4	46,XX[10]	Normal	*IKZF1*	+1q, +4, +6, +7q, +9, +10, +14, +17, +21, -7p
	ID38	F/6	46,XX [6]/46,XX,add(3)(q)(21)[2]	ND	*IKZF1, ETV6*	+10, +14, +17, +21
	ID39	M/16	46,XY [10]	Normal	Normal	+10q, +14, +17, +18, +21, +22, +X
	ID40	F/4	60,XY,+X,+4,+5,+6,+8,+10,+10,+16,+17,+18,+21,.MOB+22,+mar[14]	ND	ND	ND
Hypodiploid	ID41	M/34	39-42,XY[cp12]	Normal	Normal	Normal
	ID42	ND	39,XX,-3,-7,-13,-15,-16,-17,-20[18]/46,XX[2]	Normal	ND	ND
	ID43	F/71	33-40,XX,add(4)(q33)[9]/46,XX[1]	ND	*CDKN2A*	Normal
iAMP21	ID44	M/13	Karyotype failure	LSI 21q22/RUNX1 gain (98%)	ND	ND
	ID45	F/8	Karyotype failure	LSI 21q22/RUNX1 gain (90%)	ND	ND

	ID46	F/11	Karyotype failure	LSI 21q22/RUNX1 gain (55%)	ND	ND
B-Other	ID47	ND	47,XX,t(X;14)(p22;q32),+der(X)t(X;14),inc[6]/47,idem,i(17)(q10)[1]	LSI CRFL2/IGH fusion (90%)	ND	ND
	ID48	F/58	46,XX[20]	LSI CRFL2/IGH fusion (87%)	ND	ND
	ID49	M/3	Karyotype failure	LSI 21q22/RUNX1 gain (82%)	Normal	X+
	ID50	F/6	Karyotype failure	Normal	Normal	Normal
	ID51	F/39	46,XX[22]	Normal	*CDKN2A*	+1q, +10p, +19p, -9p, -17p
	ID52	F/7	46,XX[4]/46,XX,del(6)(q15q23) [6]	ND	*CDKN2A, ETV6*	-9p
	ID53	M/16	46,XX[12]	Normal	*IKZF1*	+14
	ID54	F/10	46,XX[8]	Normal	*BTG1*	Normal
	ID55	F/6	46,XX[22]	Normal	*ETV6*	-13
	ID56	M/4	46,XY[20]	Normal	*RB1*	Normal
	ID57	M/7	46,XY[22]	Normal	*CDKN2A, PAX5*	-9p
	ID58	F/1	46,XX[14]	Normal	*PAX5*	+1q
	ID59	M/4	Karyotype failure	Normal	*IKZF1, CDKN2A, PAX5*	-9p, -20q
	ID60	M/61	46,XY[13]	Normal	*IKZF1*	ND
	ID61	M/5	46,XY,add(12)(q22)[16]/46,XY[4]	ND	*BTG1*	Normal
	ID62	F/1	46,XX[5]/46,XX[15]	Normal	*PAX5*	-7p
	ID63	M/8	46,XY[11]	ND	ND	ND
	ID64	F/2	46,XX[10]	ND	Normal	-X
	ID65	F/15	46,XX[2]/46,XX,t(3;17)(q13;p13)[10]	ND	Normal	-X
	ID66	F/6	46,XX[10]	Normal	Normal	Normal
	ID67	M/1	47,XY,+21[3]/46,XY[18]	Normal	Normal	Normal

	ID68	M/25	46,XY [17]/46,XY,del(14)(q12)[8]	Normal	*IKZF1, BTG1*	-8p
	ID69	F/5	46,XY[8]	ND	Normal	Normal
	ID70	M/5	Karyotype failure	Normal	ND	ND
	ID71	F/ND	Karyotype failure	Normal	*CDKN2A*	ND
	ID72	M/1	46,XY[12]	ND	*IKZF1, JAK2, CDKN2A, PAX5*	-9p, -X
	ID73	M/20	Karyotype failure	Normal	*IKZF1, CDKN2A, BTG1, ETV6*	+X
	ID74	M/3	47,XY,+21c	ND	ND	ND
	ID75	F/4	49,XX,+10,+19,+20[7]/46,XX[3]	Normal	Normal	Normal

Table S2. Clinical and demographic characteristics of the patient cohort.

Parameter	**N**	**%**	**Median** (range)
Gender (n=73)			
Male	35	47.9	
Female	38	52.1	
Age (years)			7 (0 - 76)
Age <18	50	66.7	
Age >18	25	33.3	
Biochemical data			
Hb (g/L)			84 (26 - 144)
Platelets (x 10^9/L)			55 (7 - 580)
WBC >30 (x10^9/L) (n=55)	28	50.1	
Blast in BM			85 (10 - 98.3)
MRD >0.01% (n=59)	27	45.8	

Table S3. List of genes included in panel design for mutation analysis.

ID gene	Exon	Transcript
ABL1	4 - 10	NM_005157.5
ABL2	Full CDS	NM_001136000
ADARB2	5 - 7	NM_018702.3
AFF3	14, 17	NM_002285.2
ASMTL	4, 7, 10 - 12	NM_004192.3
ASXL1	13	NM_015338.5
ATM	3	NM_000051.3
ATP10A	10	NM_024490.3
ATRX	8, 17, 22, 30	NM_138270.3
BCOR	4, 13	NM_017745.5
BIRC3	4	NM_001165.4
BLNK	17	NM_013314.3
BRAF	1, 3, 10, 11, 15, 17, 18	NM_004333.5
CBL	8, 9	NM_005188.3
CCT6B	4, 8	NM_006584.3
CDCP1	3	NM_022842.4
CDH17	16	NM_004063.3
CDKN2A	1, 2	NM_000077.4
CDX2	3	NM_001265.5
CENPE	24	NM_001813.2
CLCA4	6	NM_012128.3
CREBBP	1, 4, 6, 10, 14, 16 - 19, 21, 24 - 28, 30, 31	NM_004380.2
CRLF2	Full CDS	NM_022148
CSF3R	14	NM_000760.3
CTCF	6	NM_006565.3
DCK	2, 3	NM_000788.2
DIS3	Full CDS	NM_014953
DNAH2	71	NM_020877.3
DNM2	Full CDS	NM_004945

DNMT3A	13 - 23	NM_022552.4
DOT1L	5, 15	NM_032482.2
DRD3	2, 3	NM_000796.5
DTX1	6	NM_004416.2
EBF1	3, 13	NM_024007.4
ECT2	20	NM_018098.5
ECT2L	Full CDS	NM_001077706
EED	8, 12	NM_003797.4
EP300	2, 11, 12, 14, 30	NM_001429.3
EPOR	2, 3	NM_000121.3
ERG	11	NM_004449.4
ETV6	Full CDS	NM_001987
EZH2	1, 3, 5, 7, 13 - 19	NM_152998.2
FANCD2	6	NM_033084.4
FAT1	2, 8	NM_005245.3
FAT3	6, 23	NM_001008781.2
FBL	2	NM_001436.3
FBXW7	Full CDS	NM_033632
FLT3	5, 8, 9, 12 - 16, 19 - 21	NM_004119.2
FOXO4	1	NM_005938.3
GATA2	3	NM_032638.4
GATA3	5, 6	NM_002051.2
GATA4	6	NM_002052.4
GSTM1	Full CDS	NM_000561
GSTP1	5	NM_000852.3
HDAC2	6	NM_001527.3
HES1	3	NM_005524.3
HPRT1	7	NM_000194.2
HRAS	2	NM_005343.2
IDH1	4, 7	NM_005896.3
IDH2	4	NM_002168.3
IKZF3	Full CDS	NM_012481

IL7R	3, 5, 6	NM_002185.4
IRF8	7, 8	NM_002163.2
JAK1	9, 10, 12 - 23	NM_002227.3
JAK2	14, 16, 20, 21, 24	NM_004972.3
JAK3	2, 4, 5, 10 - 13, 16, 18, 19	NM_00215.3
KLHL6	6	NM_130446.3
KMD6A	15, 16, 24, 26, 28	NM_021140.3
KMT2C	7, 14, 18, 53	NM_170606.2
KMT2D	11, 28, 38, 43, 53	NM_003482.3
KRAS	1 - 4	NM_004985.4
LEF1	3, 4	NM_016269.4
LLGL1	14	NM_004140.3
MAPK1	4, 9	NM_002745.4
MDM4	3	NM_002393.4
MOV10L1	18	NM_018995.2
MPL	10, 12	NM_005373.2
MST1	14	NM_020998.3
MYBL2	6, 7	NM_002466.3
MYC	2	NM_002467.5
NANOG	3	NM_024865.3
NBN	6	NM_002485.4
NCOR1	5, 15	NM_006311.3
NF1	9, 10, 12, 18, 19, 21, 23, 25 - 29, 31, 33, 34, 36 - 38, 41, 42, 44, 49, 52	NM_00267.3
NOTCH1	7, 11, 17, 25 - 28, 33, 34	NM_017617.4
NOTCH2	11, 34	NM_024408.3
NOTCH3	33	NM_00435.2
NR3C1	2, 6 - 8	NM_000176.2
NR3C2	2	NM_000901.4
NRAS	1- 3	NM_002524.4
NSD2	4 - 20	NM_133335.3
NT5C2	4, 11, 15	NM_012229.4

NTRK3	3, 13	NM_002530.3
NUDT15	1, 3	NM_018283.3
OBSCN	37	NM_052843.3
PAG1	7	NM_018440.3
PAX5	2 - 5, 7 - 9	NM_016734.2
PDGFRA	10	NM_006206.5
PDGFRB	3, 18	NM_002609.3
PHF6	Full CDS	NM_032458
PLEKHG1	2	NM_001329801.1
PMS2	2, 9, 14	NM_000535.6
PRF1	3	NM_005041.5
PRKD1	6	NM_002742.2
PRKN	9	NM_004562.2
PRPS1	2 - 5, 7	NM_002764.3
PTEN	2, 5, 7	NM_000314.6
PTPN11	3, 4, 7, 8, 11, 13	NM_080601.2
PTPN14	10	NM_05401.4
RAG1	Full CDS	NM_000448
RAG2	Full CDS	NM_001243786
RANBP2	27	NM_006267.4
RB1	4, 8, 9, 13, 16, 19, 20, 23	NM_00321.2
RELN	29, 33, 40, 55, 59	NM_005045.3
RFPL4B	3	NM_001013734.2
RHOBTB2	3	NM_015178.2
RHOH	3	NM_004310.4
RIT1	5	NM_006912.5
RUNX1	3 - 9	NM_001754.4
SAE1	3	NM_005500.2
SBNO2	17, 20	NM_014963.2
SETD2	1 - 17, 19, 20	NM_014159.6
SF1	Full CDS	NM_201995
SF3A1	13	NM_005877.5

SH2B3	2 - 8	NM_005475.2
SLC25A6	4	NM_001636.3
SMAD5	8	NM_005903.6
SMARCA1	22	NM_003069.4
SOS1	6	NM_005633.3
SOX3	1	NM_005634.2
SP140	16	NM_007237.4
SPI1	3	NM_003120.2
SPRED1	3	NM_152594.2
STAG2	Full CDS	NM_001042749
STIM2	7	NM_020860.3
SUZ12	14, 15	NM_015355.3
SYNE1	14, 16, 35, 41, 62	NM_033071.3
TBL1XR1	5 - 9	NM_024665.5
TCF12	8	NM_207040.1
TCF3	Full CDS	NM_003200
TET2	Full CDS	NM_001127208
TP53	2 - 11	NM_000546.5
TRAPP	61	NM_003496.3
TRIM13	3	NM_052811.3
TYK2	8, 20, 22	NM_003331.4
WDR72	14	NM_182758.3
WEE1	5	NM_003390.3
WNK3	2	NM_020922.4
WT1	5 - 9	NM_00378.5
XPO1	15	NM_003400.3

Table S4. Chromosomic regions for fusion genes detection.

Fusion gene	Exon/Intron	Genomic position GRCh38/hg38
ETV6/*RUNX1* t(12;21)(p13;q22)	Intron 5 of *ETV6*	chr12: 11869929 - 11884409
BCR/*ABL1* t(9;22) (q34;q11)	Intron 1 of *BCR*	chr22: 23182170 - 23253663
BCR/ABL1 t(9;22)(p24;q11.2)	Exon 12-16 of *BCR*	chr22: 23288058 - 23295133
*MLL*r (*KMT2A*r)	Intron 9 to exon 12 of *MLL*	chr11: 118484173 - 118489862
TCF3/*PBX1* t(1;19)(q23;p13)and *TCF3*/*HLF* t(17;19)(q22;p13)	Intron 16 of *TCF3*	chr19: 1619457 - 1620958
CRLF2/*IGH* t(X;14)(p22; q32)	Upstream region of *CRLF2* exon 1	chrX: 1228511 - 1228820

Table S5. Chromosomes mapped to aneuploidy detection.

Aneuploidy	Chromosome
High hyperdiploidy	4
High hyperdiploidy	8
High hyperdiploidy	10
High hyperdiploidy	21
Low hypodiploidy	7
Low hypodiploidy	17

Table S6. Genes for CNVs detection.

ID gene	Exon	Transcript
IKZF1	Full CDS	NM_006060.6
CDKN2A	Full CDS	NM_000077.4
PAX5	2 - 9	NM_016734.2
ETV6	Full CDS	NM_001987
RB1	*4, 8, 9, 13, 16, 19, 20, 23*	NM_00321.2
BTG1	Full CDS	NM_001731.3
ERG	Full CDS	NM_004449.4

Table S7. Pharmacogenomic SNPs included.

ID gene	rs number or AA change
A2BP1	rs9924075
ABCB1	rs3770102, rs4728709, rs1128503, rs10264856
ABCC1	rs246240
ABCC2	rs3740065, rs3740066, rs717620
ABCC3	rs9895420
ABCC4	rs9516519, rs17268122, rs9556455
ACTG1	rs1135989
ADORA2A	rs2236624
APEX1	rs2307486
ARID5B	rs4948502, rs4948496, rs4948487, rs6479778, rs2893881, rs4948488, rs2393782, rs10821938, rs7923074, rs6479779, rs17215180
ATP6AP2	rs5917990
BCL2L11 (BIM)	rs724710
C3orf6	rs13358399
C5orf3, MFAP3	rs707184, rs1438588
CCDC24	rs368182
CDH12	rs10473594
CTLA-4	rs3087243, rs231775
CYP2C19	rs4244285, rs1057910
CYP3A5	rs776746
CYP4F2	rs2108622
DPYD	rs3918290
DROSHA	rs639174
FAM8A6P	rs1040637
FCHSD1	rs251177, rs6773449, rs6007758, rs41488548
FRMD4B	rs11707515, rs6549198
G6PD	rs5030868

GALNT10	rs11167667, rs12523441, rs7737215, rs10875583, rs6890748, rs6863455
GART	rs2070388
GATA3	rs3824662
GIT1	rs17808412
GNG2	rs12886319
GRIA1	rs2055083
	rs707176, rs17356099, rs13354399, rs10072570, rs11167640, rs6889909, rs4958676, rs6890057, rs10070447, rs4958351, rs4424038, rs7711124, rs7708391
HIVEP2, AIG1	rs200148
IMPDH1	rs4731448
ITPA	94C >A, rs41320251, rs1127354, rs7270101
KCNMA1	rs11001976, rs17480656, rs12765834, rs17389791, rs11001997
KIF13A	rs73726531
LOC642340	rs10170236
MAPK4	rs11662176, rs9953685
MCL1	rs3738485, 256G>C , 194T>G
MOCOS	rs3744900
MTHFR	rs786204016, rs1801131, rs1801133
MYRIP	rs17079534
NBN	1197A>G
NFATC2	rs6021191
NME1	rs2215290
NME1, NME2	rs3760467, rs1558254
NUDT15	rs746071566, rs766023281, 103A > G, rs116855232, rs186364861, rs147390019, rs554405994
P2RX1	rs17795186
PACSIN2	rs2413739
PAG1	rs877419
PDE4B	rs6683977, rs1402612, rs7578361, rs524770, rs641262, rs4265132, rs16965335, rs7141601, rs2613079,rs12751530
PTPRS	rs17763463, rs7600852

PYGL	rs7142143
RAD51AP2	rs424827, rs665312, rs7017705, rs13273490
SLC24A3	rs3748483
SLC25A37	rs2775139, rs2775134, rs1332944, rs2585498, rs2585499
SLC28A3	rs17428030, rs4588940, rs4305983, rs7043257, rs7035753, rs17087144
SLC36A3	rs7717132
SLCO1B1	rs11045879, rs4149081, rs4149056, rs2306283
SMARCB1	228G>T
SOD2	rs4880
TPMT	rs1800462, rs1800460, rs1142345, rs1800584, rs115106679, rs144041067, rs12201199, rs1142345, rs75543815, rs144041067, rs115106679
VKORC1	rs9923231
VSNL1	rs2710688
XDH	rs494852
XRCC1	26304C>T
XRCC3	rs1799794
ZP4	rs1565430

Table S8. Genes include in targeted TruSeqCustom Amplicon (TSCA) panel for ALL (pre-beta Test Plan for Illumina)

Genes			
ABL1	*EZH2*	*KRAS*	*RELN*
ADARB2	*FBXW7*	*LEF1*	*RUNX1*
ASMTL	*FLT3*	*MAPK1*	*SAE1*
BRAF	*GATA3*	*MYBL2*	*SETD2*
CDKN2A	*IDH1*	*NF1*	*SH2B3*
CREBBP	*IDH2*	*NOTCH1*	*SLC25A6*
CRLF2	*IKZF3*	*NR3C1*	*STAG2*
DNM2	*IL7R*	*NRAS*	*SUZ12*
DNMT3A	*JAK1*	*PAX5*	*TBL1XR1*
ECT2L	*JAK2*	*PHF6*	*TCF3*
EED	*JAK3*	*PTEN*	*TP53*
EP300	*KDM6A*	*PTPN11*	*WHSC1*
ETV6	*KMT2D*	*RB1*	*WT1*

Table S9. Oligonucleotide pair for fusion gene detection. Oligonucleotide pairs used in the PCR to confirm the presence of the fusion gene in the different samples. ID52, forward: intron 5 of *ETV6* (NM_001987.5) and reverse: intron 3 *RUNX1* (NM_001754.4). ID61, forward: intron 5 of *ETV6* (NM_001987.5) and reverse: intron 2 *RUNX1* (NM_001754.4). ID63, forward: intron 1 *BCR* (NM_004327.4) and reverse: intron 1 *ABL1* (NM_007313.2).

	Fusion gene	**Forward 5′-3′**	**Reverse 5′-3′**
ID52	*ETV6*/*RUNX1*	TGTGTGCAGCAGTACTTGACA (I.5 *ETV6*)	AAACGTTCTGGTTCTGCGGAT (I.3 *RUNX1*)
ID61	*ETV6*/*RUNX1*	TTCATGTAAAATAACCCTGGGG (I.5 *ETV6*)	GGCTCATATTTCAGCTCTAGAT (I.2 *RUNX1*)
ID63	*BCR*/*ABL1*	ATGTTGGTTCCACGTCCAAAC (I.1 *BCR*)	TGTTGCAGCATCCAGTTCATC (I.1 *ABL1*)

Table S10. List of variants detected in duplicate sequenced samples. VAF obtained in the sequencing of each of the samples (VAF1) and the one obtained the second time they were sequenced (VAF2).

Sample	*Gene*	**Exon, AA change & Transcript**	**VAF 1 (%)**	**VAF 2 (%)**
S1	*PAX5*	exon5:c.589_590insACTACCC:p.R197fs	37.66	37.55
S2	*PAX5*	exon6:c.748_749insCT:p.F250fs	39.89	35.69
	PAX5	exon3:c.T395C:p.V132A	10.99	6.86
	KCNE2	exon2:c.T170C:p.I57T	47.22	38.46
S3	*TCF3*	exon11:c.C923T:p.T308M	52.57	46.99
	NOTCH1	exon34:c.T7328G:p.V2443G	20.35	20.99

Table S11. Sensitivity and specificity of detection of different types of alterations. Sensitivity = true positives / (true positives + false negatives) x100 (%), specificity = true negatives / (true negatives + false positives) x100 (%).

Type of alteration	**Sensitivity** (%)	**Specificity** (%)
SNV/INDELS	96.3	90
CNVs	95.5	100
Aneuploidies	93.3	100
Fusion genes	89.7	100

Table S12. List of detected mutations. In the first column the sample identifier (ID), followed by the gene, VAF, function, exonic consequence, exon and AA change, cosmic82 identifier and avsnp144 identifier.

ID	Gene	VAF (%)	Function	Exonic consequence	Exon and AA change	cosmic82	avsnp144
ID1	*EP300*	49.25	exonic	nonsynonymous SNV	exon14:c.C2773A:p.P925T	COSM88779	rs148884710
	IKZF1	74.63	exonic	nonsynonymous SNV	exon5:c.G468C:p.Q156H	NA	NA
	PHF6	21.43	exonic	frameshift deletion	exon7:c.586_587del:p.R196fs	NA	NA
	PHF6	51.52	exonic	nonframeshift insertion	exon9:c.901_902insCGGGGG:p.Y301delinsSGD	NA	NA
ID2	*CBL*	69.58	exonic	nonsynonymous SNV	exon9:c.C1298T:p.P433L	COSM4669519	rs140627020
	RFPL4B	65.1	exonic	nonsynonymous SNV	exon3:c.G679A:p.V227I	NA	NA
	TCF12	49.6	exonic	nonsynonymous SNV	exon8:c.T860C:p.V287A,TCF12	NA	NA
ID3	*IKZF3*	31.11	exonic	nonsynonymous SNV	exon8:c.G1516A:p.A506T	COSM5972169	rs749495184
	SF1	45.17	exonic	nonsynonymous SNV	exon6:c.G582C:p.Q194H	NA	NA
	TCF3	42.73	exonic	nonsynonymous SNV	exon7:c.C472T:p.R158W	NA	rs749247091
ID5	*RUNX1*	40.76	exonic	nonsynonymous SNV	exon4:c.G320A:p.R107H	COSM4385193	NA
ID8	*IKZF1*	17.18	exonic	frameshift insertion	exon7:c.732dupT:p.T244fs	NA	NA
ID9	*TET2*	50	exonic	nonsynonymous SNV	exon7:c.C3813G:p.C1271W	COSM120176	NA
ID10	*TET2*	35.6	exonic	nonsynonymous SNV	exon3:c.G1909A:p.E637K	NA	NA
ID11	*KMT2C*	41.61	exonic	nonsynonymous SNV	exon14:c.A2233G:p.I745V	NA	rs769543160
	NF1	19.67	exonic	frameshift insertion	exon18:c.2027dupC:p.T676fs	COSM1235317	rs587781807
	NRAS	2.02	exonic	nonsynonymous SNV	exon2:c.G35T:p.G12V	COSM566	rs121913237
	NRAS	6.14	exonic	nonsynonymous SNV	exon2:c.G38A:p.G13D	COSM573	rs121434596
ID13	*RB1*	36.51	exonic	nonsynonymous SNV	exon9:c.C920T:p.T307I	NA	rs183898408

ID14	*CREBBP*	19.54	exonic	nonsynonymous SNV	exon30:c.T5050C:p.S1684P	NA	rs587783503
	NRAS	21.58	exonic	nonsynonymous SNV	exon2:c.G35A:p.G12D	COSM564	rs121913237
ID15	*NR3C2*	28.14	exonic	stopgain	exon2:c.C785G:p.S262X	NA	NA
ID16	*PAX5*	37.66	exonic	frameshift insertion	exon5:c.589_590insACTACCC:p.R197fs	NA	NA
ID18	*BRAF*	29.35	exonic	nonsynonymous SNV	exon15:c.G1780A:p.D594N	COSM27639	rs397516896
ID20	*NRAS*	4.49	exonic	nonsynonymous SNV	exon2:c.G35A:p.G12D	COSM564	rs121913237
ID21	*CDKN2A*	3.63	exonic	stopgain	exon2:c.C216A:p.C72X	COSM13567	NA
	KRAS	1.97	exonic	nonsynonymous SNV	exon4:c.A351T:p.K117N	COSM1562192	NA
	KRAS	16.87	exonic	nonsynonymous SNV	exon2:c.G35T:p.G12V	COSM1140133	rs121913529
	SLC25A6	41.01	exonic	nonsynonymous SNV	exon4:c.T856A:p.F286I	NA	NA
ID22	*CRLF2*	62.96	exonic	nonsynonymous SNV	exon5:c.C485A:p.S162Y	NA	NA
	NR3C1	48.75	exonic	nonsynonymous SNV	exon2:c.A695G:p.D232G	NA	NA
	NRAS	5.11	exonic	nonsynonymous SNV	exon2:c.G38A:p.G13D	COSM573	rs121434596
	TET2	44.56	exonic	nonsynonymous SNV	exon3:c.A2580T:p.Q860H	NA	NA
ID23	*FLT3*	12.86	exonic	nonsynonymous SNV	exon20:c.G2503T:p.D835Y	COSM783	rs121913488
	FLT3	41.24	exonic	nonsynonymous SNV	exon19:c.G2329A:p.E777K	NA	NA
	JAK3	41.18	exonic	nonsynonymous SNV	exon2:c.C23T:p.T8M	NA	rs145500023
	KRAS	14.68	exonic	nonsynonymous SNV	exon2:c.G35T:p.G12V	COSM1140133	rs121913529
ID25	*PAX5*	23.08	exonic	nonsynonymous SNV	exon3:c.T399A:p.S133R	NA	NA
ID26	*SH2B3*	51.58	exonic	nonsynonymous SNV	exon2:c.C464T:p.P155L	COSM1685385	rs531156627
ID27	*BCOR*	99.46	exonic	nonsynonymous SNV	exon4:c.G1780A:p.V594I	COSM5030822	rs764515953
	CDKN2A	56.94	exonic	frameshift insertion	exon2:c.225dupC:p.A76fs	NA	NA
	NRAS	6.79	exonic	nonsynonymous SNV	exon2:c.G35A:p.G12D	COSM564	rs121913237
	RANBP2	52.4	exonic	nonsynonymous SNV	exon27:c.T8800C:p.F2934L	NA	NA
ID28	*CDKN2A*	51.67	exonic	nonsynonymous SNV	exon2:c.G397A:p.A133T	NA	NA

	RUNX1	49.09	exonic	nonsynonymous SNV	exon8:c.G849C:p.Q283H	NA	NA
ID29	*NOTCH2*	50	exonic	nonsynonymous SNV	exon34:c.C6094A:p.H2032N	COSM1581340	rs143236410
	NRAS	5.13	exonic	nonsynonymous SNV	exon2:c.G35A:p.G12D	COSM564	rs121913237
ID30	*FLT3*	10.25	exonic	nonsynonymous SNV	exon20:c.A2504T:p.D835V	COSM784	rs121909646
ID31	*ASXL1*	45.98	exonic	nonsynonymous SNV	exon12:c.A2957G:p.N986S	COSM96383	rs145132837
	KRAS	39.7	exonic	nonsynonymous SNV	exon4:c.A351C:p.K117N	COSM1256061	rs770248150
	TET2	61.75	exonic	nonsynonymous SNV	exon3:c.G1285A:p.G429R	COSM5095018	rs201642693
ID32	*NRAS*	1.9	exonic	nonsynonymous SNV	exon2:c.G35C:p.G12A	COSM565	rs121913237
	NRAS	5.95	exonic	nonsynonymous SNV	exon2:c.G38A:p.G13D	COSM573	rs121434596
	PTPN11	33.76	exonic	nonsynonymous SNV	exon3:c.G226A:p.E76K	COSM13000	rs121918464
ID33	*KRAS*	5.85	exonic	nonsynonymous SNV	exon2:c.G38A:p.G13D	COSM1140132	rs112445441
ID34	*KRAS*	13.39	exonic	nonsynonymous SNV	exon2:c.G35T:p.G12V	COSM1140133	rs121913529
	PAX5	48.12	exonic	nonsynonymous SNV	exon9:c.T1032A:p.S344R	NA	NA
ID35	*DIS3*	20.49	splicing	NA	NA	NA	rs750580353
	NRAS	3.62	exonic	nonsynonymous SNV	exon3:c.C181A:p.Q61K	COSM580	rs121913254
ID36	*CREBBP*	68.71	exonic	nonsynonymous SNV	exon26:c.C4336T:p.R1446C	COSM88749	rs398124146
	IKZF1	7.77	exonic	nonsynonymous SNV	exon8:c.G1381C:p.V461L	NA	NA
	NRAS	10.2	exonic	nonsynonymous SNV	exon3:c.A183C:p.Q61H	COSM586	NA
	SETD2	74.13	exonic	stopgain	exon3:c.A1126T:p.K376X	NA	NA
ID37	*FLT3*	30.59	exonic	nonframeshift deletion	exon20:c.2508_2510del:p.836_837del	COSM19836	rs121913490
	PTPN11	2.96	exonic	nonsynonymous SNV	exon3:c.G226C:p.E76Q	COSM13016	rs121918464
ID38	*SH2B3*	48.11	exonic	nonsynonymous SNV	exon2:c.C639A:p.S213R	COSM1685386	rs111360561
ID39	*ETV6*	19.07	exonic	nonsynonymous SNV	exon6:c.G1080C:p.W360C	NA	NA
	IRF8	48.95	exonic	nonsynonymous SNV	exon7:c.T895G:p.C299G	NA	NA

	KRAS	16.67	exonic	nonsynonymous SNV	exon4:c.G436A:p.A146T	COSM1165198	rs121913527
	KRAS	21.86	exonic	nonsynonymous SNV	exon2:c.G35T:p.G12V	COSM1140133	rs121913529
ID40	*ETV6*	35.19	exonic	frameshift deletion	exon7:c.1165_1166del:p.M389fs	NA	NA
	FLT3	36.51	exonic	nonsynonymous SNV	exon14:c.T1733C:p.M578T	COSM5945297	NA
ID41	*PAX5*	44.13	exonic	nonsynonymous SNV	exon3:c.C239G:p.P80R	COSM85953	NA
	PAX5	50.66	exonic	nonsynonymous SNV	exon3:c.A215G:p.Y72C	COSM455949	NA
	PTPN11	4.86	exonic	nonsynonymous SNV	NM_080601:exon3:c.G181T:p.D61Y	COSM13011	NA
	PTPN11	30.87	exonic	nonsynonymous SNV	NM_080601:exon3:c.A227G:p.E76G	COSM13017	rs121918465
	IKZF1	41.93	exonic	frameshift insertion	exon3:c.97_98insTCGC:p.I33fs	NA	NA
ID42	*NF1*	69.35	exonic	stopgain	exon34:c.C4537T:p.R1513X	COSM24466	rs760703505
	SH2B3	49.28	exonic	nonsynonymous SNV	exon2:c.G622C:p.E208Q	COSM1235390	rs202080221
	TP53	88.82	exonic	nonsynonymous SNV	exon6:c.G638A:p.R213Q	COSM131469	rs587778720
ID43	*ANKRD11*	26.24	exonic	nonsynonymous SNV	exon9:c.G6076A:p.A2026T	NA	rs752781169
	SETD2	27.67	exonic	nonsynonymous SNV	exon15:c.A6472G:p.N2158D	NA	NA
	TP53	42.27	splicing	NA	NA	COSM18655	NA
ID44	*EP300*	53.17	exonic	nonsynonymous SNV	exon14:c.C2773A:p.P925T	ICOSM88779	rs148884710
	IKZF1	6.42	exonic	nonsynonymous SNV	exon5:c.G472A:p.G158S	COSM303844	NA
	KMT2C	9.54	exonic	nonsynonymous SNV	exon18:c.G2926A:p.A976T	COSM3304323	rs779599464
	NRAS	35.68	exonic	nonsynonymous SNV	exon2:c.G35A:p.G12D	ICOSM564	rs121913237
	PAX5	35.29	exonic	nonsynonymous SNV	exon3:c.C224T:p.T75I	COSM4993960	NA
	SH2B3	38.41	exonic	stopgain	exon6:c.1200_1201insTAGGGGT:p.E400_Y401delinsEX	NA	NA
ID45	*ABL2*	46.67	exonic	nonsynonymous SNV	exon12:c.A1945T:p.T649S	NA	rs141450341
	NRAS	39.82	exonic	nonsynonymous SNV	exon2:c.G38A:p.G13D	COSM573	rs121434596
ID46	*EP300*	51.46	exonic	nonsynonymous SNV	exon14:c.C2773A:p.P925T	COSM88779	rs148884710
	IKZF1	10	exonic	nonsynonymous SNV	exon5:c.G472A:p.G158S	COSM303844	NA

ID47	*ETV6*	41.37	exonic	frameshift insertion	exon5:c.479_480insGA:p.R160fs	NA	NA
	JAK2	6.74	exonic	nonsynonymous SNV	exon16:c.A2044T:p.I682F	COSM303887	NA
	JAK2	10.06	exonic	nonsynonymous SNV	exon20:c.G2617A:p.D873N	COSM303882	NA
	NRAS	12.27	exonic	nonsynonymous SNV	exon3:c.C181A:p.Q61K	COSM580	rs121913254
	NRAS	16.22	exonic	nonsynonymous SNV	exon3:c.A182T:p.Q61L	COSM583	rs11554290
ID48	*JAK2*	3.04	exonic	nonsynonymous SNV	exon16:c.A2049T:p.R683S	COSM29302	NA
	JAK2	12.13	exonic	nonsynonymous SNV	exon16:c.T2081C:p.F694S	NA	NA
	JAK2	29.87	exonic	nonsynonymous SNV	exon16:c.A2047G:p.R683G	COSM29300	NA
	NRAS	4.22	exonic	nonsynonymous SNV	exon2:c.G35A:p.G12D	COSM564	rs121913237
ID49	*JAK2*	25.97	exonic	nonsynonymous SNV	exon20:c.C2624A:p.T875N	COSM23940	NA
	MPL	42.68	exonic	nonsynonymous SNV	exon9:c.T1432A:p.S478T	NA	rs781129632
ID51	*NRAS*	7.58	exonic	nonsynonymous SNV	exon2:c.G35A:p.G12D	COSM564	rs121913237
ID52	*KRAS*	9.02	exonic	nonsynonymous SNV	exon2:c.G34C:p.G12R	COSM518	rs121913530
ID53	*PEAK1*	53.49	exonic	nonsynonymous SNV	exon5:c.A2689G:p.T897A	NA	NA
ID54	*FAT1*	49.12	exonic	nonsynonymous SNV	exon2:c.G1555A:p.V519M	NA	NA
ID55	*ASXL1*	48.55	exonic	nonsynonymous SNV	exon12:c.G1831A:p.A611T	COSM2889263	rs372418554
	KMT2C	10.71	exonic	nonsynonymous SNV	exon18:c.G2914A:p.G972R	NA	rs746739227
	NRAS	21.83	exonic	nonsynonymous SNV	exon2:c.G38A:p.G13D	COSM573	rs121434596
ID57	*NRAS*	45.12	exonic	nonsynonymous SNV	exon2:c.G35A:p.G12D	COSM564	rs121913237
	XPO1	51.52	exonic	nonsynonymous SNV	exon15:c.G1711A:p.E571K	COSM96797	NA
ID58	*SPI1*	31.92	exonic	frameshift insertion	exon3:c.186_187insTCCCTCC:p.E63fs	NA	NA
ID59	*KRAS*	23.36	exonic	nonsynonymous SNV	exon2:c.G34A:p.G12S	COSM1152506	rs121913530
	NRAS	8.03	exonic	nonsynonymous SNV	exon2:c.G35A:p.G12D	COSM564	rs121913237
	PTPN11	4.93	exonic	nonsynonymous SNV	NM_080601:exon3:c.C215A:p.A72D	COSM13035	NA
ID60	*CRLF2*	2.84	exonic	nonsynonymous SNV	exon6:c.T695G:p.F232C	COSM41268	NA

	DNMT3A	2.91	exonic	nonsynonymous SNV	exon23:c.C2711T:p.P904L	COSM87007	rs149095705
	JAK2	6.67	exonic	nonsynonymous SNV	exon16:c.A2047G:p.R683G	COSM29300	NA
	JAK2	16.85	exonic	nonsynonymous SNV	exon20:c.C2624A:p.T875N	COSM23940	NA
ID61	*EZH2*	3.2	exonic	nonsynonymous SNV	exon17:c.C1948T:p.H650Y	COSM53040	rs193921147
	SETD2	5.11	exonic	nonsynonymous SNV	exon3:c.G1369A:p.E457K	NA	NA
	SETD2	5.17	exonic	frameshift insertion	exon3:c.1367dupG:p.R456fs	NA	NA
	SETD2	18.45	exonic	stopgain	exon3:c.C995G:p.S332X	NA	NA
	SETD2	19.49	exonic	nonsynonymous SNV	exon3:c.C805G:p.Q269E	COSM5986197	NA
ID63	*ZNF384*	44.84	exonic	nonsynonymous SNV	exon8:c.T1007A:p.L336H	NA	NA
ID64	*FLT3*	43.79	exonic	nonsynonymous SNV	exon5:c.G580A:p.V194M	COSM28039	rs146030737
ID65	*CSF2RA*	25	splicing	NA	NA	NA	NA
	IL7R	25.71	exonic	nonsynonymous SNV	exon3:c.G291T:p.K97N	COSM1067537	NA
	NRAS	3.64	exonic	nonsynonymous SNV	exon2:c.G35A:p.G12D	COSM564	rs121913237
ID66	*COG1*	37.93	exonic	nonsynonymous SNV	exon7:c.A1741G:p.I581V	NA	rs757072904
ID67	*NRAS*	26.62	exonic	nonsynonymous SNV	exon2:c.G38A:p.G13D	COSM573	rs121434596
	PTPN11	2.24	exonic	nonsynonymous SNV	exon3:c.T211C:p.F71L	COSM13039	rs397507512
ID68	*CREBBP*	42.81	exonic	nonsynonymous SNV	exon31:c.A5617G:p.N1873D	NA	NA
	ETV6	35.39	exonic	nonsynonymous SNV	exon7:c.G1223C:p.R408T	NA	NA
	NRAS	31.07	exonic	nonsynonymous SNV	exon2:c.G38A:p.G13D	COSM573	rs121434596
	RAG1	31.27	exonic	nonframeshift insertion	exon2:c.775_776insGCT:p.S259delinsSC	NA	NA
ID69	*KMT2D*	50	exonic	nonsynonymous SNV	exon11:c.C3793T:p.P1265S	NA	NA
	NOTCH1	48.37	exonic	nonsynonymous SNV	exon34:c.G6392A:p.G2131D	NA	NA
	PAX5	33.51	exonic	stopgain	exon5:c.601_602insCTT:p.E201delinsAX	NA	NA
	PAX5	36.04	exonic	nonsynonymous SNV	exon5:c.G601C:p.E201Q	NA	NA

ID70	*JAK2*	15.84	exonic	nonsynonymous SNV	exon16:c.A2049T:p.R683S	COSM29302	NA
ID71	*GRM1*	42	exonic	nonsynonymous SNV	exon8:c.C2756T:p.T919I	NA	rs536808733
	PHF6	18.42	exonic	stopgain	exon5:c.C385T:p.R129X	COSM4775093	NA
	RUNX1	48.68	exonic	nonsynonymous SNV	exon4:c.G136A:p.A46T	NA	NA
ID72	*EP300*	42.98	exonic	nonsynonymous SNV	exon14:c.C2773A:p.P925T	COSM88779	rs148884710
	NRAS	3.97	exonic	nonsynonymous SNV	exon2:c.G35A:p.G12D	COSM564	rs121913237
ID73	*CRLF2*	25.69	exonic	nonsynonymous SNV	exon6:c.T695G:p.F232C	COSM41268	NA
	JAK2	14.96	exonic	nonsynonymous SNV	exon16:c.A2049T:p.R683S	COSM29302	NA
	PAX5	17.27	exonic	frameshift insertion	exon6:c.621_622insCTGGCGCCTTGGCCTG:p.V208fs	NA	NA
ID74	*JAK2*	41.1	exonic	nonsynonymous SNV	exon16:c.A2047G:p.R683G	COSM29300	NA
ID75	*NRAS*	34	exonic	nonsynonymous SNV	exon2:c.G34A:p.G12S	COSM563	rs121913250

Table S13. Mutations described in REH cell line. The following table shows a number of mutations detected in the REH cell line and two clones established from it. In the first column the gene, altered nucleotide (CDS mutation), altered amino acid (AA mutation) and variant allele frequency (VAF) detected in REH cells, clon 1 and clon 2.

Gene	CDS mutation	AA mutation	VAF (%)		
			REH	Clon 1	Clon 2
TBLX1R1	c.G497A	p.R166Q	53.3	62.36	48.94
IKZF1	c.G1079A	p.R360H	44.14	46.96	49.76
NOTCH1	c.C7568T	p.S2523L	26	0	0
IL27	c.G100A	p.G34R	32.32	29.9	34.43
TP53	c.C541T	p.R181C	29.3	0	0
GATA3	c.C953T	p.A318V	41.85	47.19	50.78
BCL11B	c.G1251A	p.T417T	40.71	44.01	42.41
BCL11B	c.C915T	p.F305F	52.26	46.63	45.93

Table S14. Frequency of pharmacogenetic SNPs detected in the patient cohort.

rs number	Gene	Heterozygosis frequency (%)	Homozygosis frequency (%)	Total frequency (%)
rs1128503	*ABCB1*	18.7	8.0	29.3
rs4728709	*ABCB1*	1.3	0.0	1.3
rs3740066	*ABCC2*	17.3	2.7	20.0
rs3740065	*ABCC2*	13.3	0.0	13.3
rs717620	*ABCC2*	12.0	0.0	12.0
rs17216310	*ABCC2*	1.3	0.0	1.3
rs4793665	*ABCC3*	21.3	10.7	32.0
rs9895420	*ABCC3*	4.0	1.3	5.3
rs9516519	*ABCC4*	6.7	0.0	6.7
rs9556455	*ABCC4*	4.0	1.3	5.3
rs1139405	*ACTG1*	13.3	20.0	33.3
rs1135989	*ACTG1*	16.0	5.3	21.3
rs1048945	*APEX1*	6.7	0.0	6.7
rs2307486	*APEX1*	1.3	0.0	1.3
rs10821936	*ARID5B*	40.0	18.7	58.7
rs7073837	*ARID5B*	36.0	18.7	54.7
rs10994982	*ARID5B*	38.7	10.7	49.3
rs10740055	*ARID5B*	37.3	10.7	48.0
rs10821935	*ARID5B*	36.0	10.7	46.7
rs7089424	*ARID5B*	38.7	5.3	44.0
rs6479778	*ARID5B*	12.0	22.7	34.7
rs4614389	*ARID5B*	12.0	22.7	34.7
rs2893881	*ARID5B*	12.0	22.7	34.7
rs2393782	*ARID5B*	13.3	18.7	32.0
rs4948496	*ARID5B*	22.7	8.0	30.7
rs7923074	*ARID5B*	14.7	14.7	29.3
rs10821938	*ARID5B*	14.7	14.7	29.3
rs4948488	*ARID5B*	12.0	16.0	28.0
rs17215180	*ARID5B*	21.3	5.3	26.7
rs6479779	*ARID5B*	16.0	9.3	25.3
rs4948502	*ARID5B*	16.0	4.0	20.0
rs7075591	*ARID5B*	14.7	4.0	18.7
rs4948487	*ARID5B*	12.0	4.0	16.0

rs2393783	*ARID5B*	8.0	6.7	14.7
rs77918077	*ARID5B*	5.3	0.0	5.3
rs10994973	*ARID5B*	2.7	0.0	2.7
rs77708105	*ARID5B*	1.3	0.0	1.3
rs188676594	*ARID5B*	1.3	0.0	1.3
rs149113357	*ARID5B*	1.3	0.0	1.3
rs776746	*CYP3A5*	4.0	26.7	30.7
rs2108622	*CYP4F2*	13.3	4.0	17.3
rs17376848	*DPYD*	2.7	0.0	2.7
rs3918290	*DPYD*	1.3	0.0	1.3
rs3918289	*DPYD*	1.3	0.0	1.3
rs639174	*DROSHA*	1.3	0.0	1.3
rs251177	*FCHSD1*	18.7	0.0	18.7
rs11707515	*FRMD4B*	9.3	1.3	10.7
rs7737215	*GALNT10*	16.0	12.0	28.0
rs6890748	*GALNT10*	17.3	9.3	26.7
rs12523441	*GALNT10*	13.3	9.3	22.7
rs11167667	*GALNT10*	13.3	8.0	21.3
rs10875583	*GALNT10*	13.3	8.0	21.3
rs153440	*GALNT10*	8.0	0.0	8.0
rs139021674	*GALNT10*	1.3	0.0	1.3
rs422628	*GATA3*	34.7	61.3	96.0
rs3839918	*GATA3*	20.0	40.0	60.0
rs1058240	*GATA3*	20.0	40.0	60.0
rs9746	*GATA3*	22.7	4.0	26.7
rs3824662	*GATA3*	17.3	5.3	22.7
rs11567941	*GATA3*	9.3	1.3	10.7
rs552157419	*GATA3*	1.3	0.0	1.3
rs12886319	*GNG2*	9.3	24.0	33.3
rs707176	*GRIA1*	16.0	2.7	18.7
rs6889794	*GRIA1*	12.0	5.3	17.3
rs4958351	*GRIA1*	13.3	0.0	13.3
rs10070447	*GRIA1*	13.3	0.0	13.3
rs6890057	*GRIA1*	10.7	0.0	10.7
rs6889909	*GRIA1*	10.7	0.0	10.7
rs4958676	*GRIA1*	10.7	0.0	10.7
rs13354399	*GRIA1*	10.7	0.0	10.7

rs10072570	*GRIA1*	10.7	0.0	10.7
rs7711124	*GRIA1*	9.3	0.0	9.3
rs4424038	*GRIA1*	8.0	1.3	9.3
rs7708391	*GRIA1*	8.0	0.0	8.0
rs67708322	*GRIA1*	6.7	0.0	6.7
rs2055083	*GRIA1*	5.3	1.3	6.7
rs17356099	*GRIA1*	5.3	0.0	5.3
rs11167640	*GRIA1*	4.0	0.0	4.0
rs11743325	*GRIA1*	2.7	0.0	2.7
rs72804610	*GRIA1*	1.3	0.0	1.3
rs10954184	*IMPDH1*	40.0	17.3	57.3
rs10954183	*IMPDH1*	37.3	17.3	54.7
rs4731448	*IMPDH1*	9.3	21.3	30.7
rs7270101	*ITPA*	10.7	1.3	12.0
rs1127354	*ITPA*	5.3	0.0	5.3
rs10762752	*KCNMA1*	44.0	4.0	48.0
rs17480264	*KCNMA1*	9.3	0.0	9.3
rs17480656	*KCNMA1*	6.7	0.0	6.7
rs17389791	*KCNMA1*	6.7	0.0	6.7
rs12765834	*KCNMA1*	6.7	0.0	6.7
rs11001997	*KCNMA1*	6.7	0.0	6.7
rs11001976	*KCNMA1*	6.7	0.0	6.7
rs11662176	*MAPK4*	13.3	2.7	16.0
rs9953685	*MAPK4*	13.3	1.3	14.7
rs3738485	*MCL1*	14.7	10.7	25.3
rs34645101	*MCL1*	1.3	0.0	1.3
rs376254012	*MOCOS*	1.3	0.0	1.3
rs3744900	*MOCOS*	1.3	0.0	1.3
rs4846051	*MTHFR*	1.3	34.7	36.0
rs1801133	*MTHFR*	20.0	2.7	22.7
rs1801131	*MTHFR*	14.7	2.7	17.3
rs709816	*NBN*	20.0	0.0	20.0
rs34767364	*NBN*	4.0	0.0	4.0
rs61973267	*NUDT15*	9.3	0.0	9.3
rs138959770	*NUDT15*	1.3	0.0	1.3
rs2413739	*PACSIN2*	18.7	5.3	24.0
rs117008677	*PACSIN2*	1.3	1.3	1.3

rs7006101	*PAG1*	13.3	1.3	14.7
rs1866275	*PAG1*	1.3	0.0	1.3
rs140643833	*PAG1*	1.3	0.0	1.3
rs641262	*PDE4B*	12.0	13.3	25.3
rs524770	*PDE4B*	9.3	16.0	25.3
rs12137115	*PDE4B*	10.7	13.3	24.0
rs12137080	*PDE4B*	10.7	2.7	13.3
rs71121613	*PYGL*	10.7	5.3	16.0
rs882860	*PYGL*	12.0	1.3	13.3
rs665312	*RAD51AP2*	9.3	1.3	10.7
rs7043257	*SLC28A3*	12.0	21.3	33.3
rs7035753	*SLC28A3*	13.3	18.7	32.0
rs4588940	*SLC28A3*	18.7	12.0	30.7
rs17087144	*SLC28A3*	14.7	5.3	20.0
rs17428030	*SLC28A3*	4.0	1.3	5.3
rs75316220	*SLC28A3*	2.7	0.0	2.7
rs4149057	*SLCO1B1*	17.3	9.3	25.3
rs4149056	*SLCO1B1*	13.3	1.3	14.7
rs11045879	*SLCO1B1*	12.0	1.3	13.3
rs4149081	*SLCO1B1*	4.0	0.0	4.0
rs4880	*SOD2*	21.3	6.7	28.0
rs2842949	*TPMT*	8.0	8.0	16.0
rs2842934	*TPMT*	2.7	1.3	4.0
rs12201199	*TPMT*	1.3	0.0	1.3
rs494852	*XDH*	4.0	4.0	8.0
rs1799782	*XRCC1*	5.3	0.0	5.3
rs2307170	*XRCC1*	1.3	0.0	1.3
rs1799779	*XRCC1*	1.3	0.0	1.3
rs861529	*XRCC3*	2.7	33.3	36.0
rs1799794	*XRCC3*	14.7	2.7	17.3

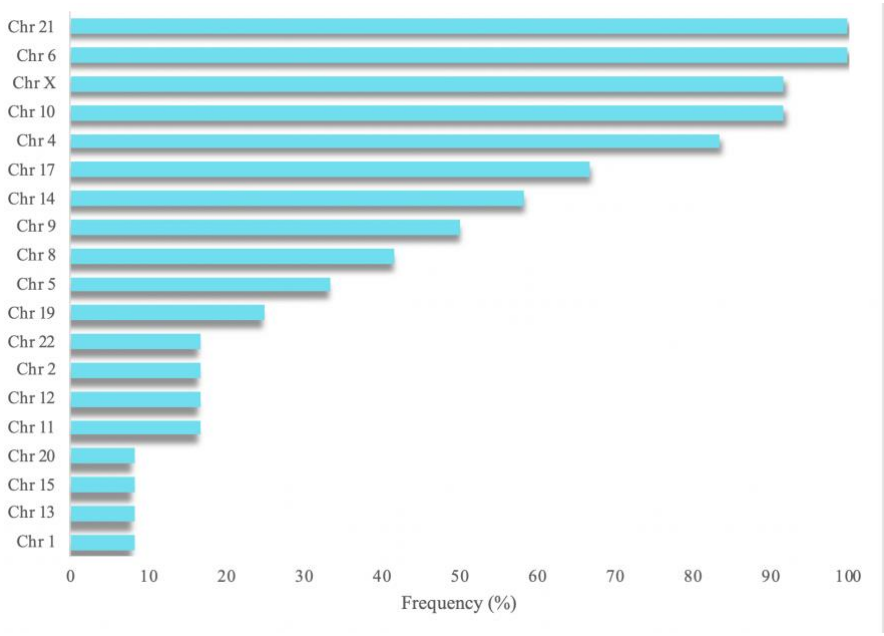

Figure S1. Frequency of trisomies in high hyperdiploidy cases. The following figure shows the frequency of trisomies observed in high hyperdiploidy patients included in this study in decreasing order.

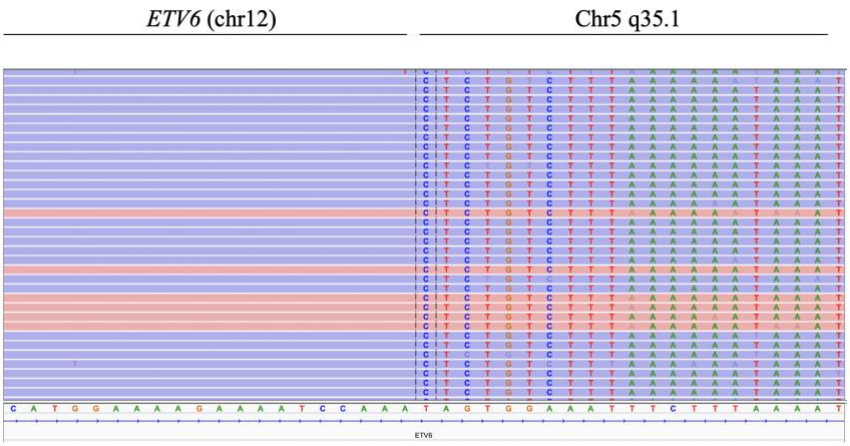

Figure S2. t(5;12)(q35;p13) visualized with IGV. t(5;12)(q35;p13) observed in (sample ID13). In the left region the reads aligned with intron 5 of *ETV6* and to the right the reads aligned with chromosome 5 q35.1.

Annex II

Supplemental material of Chapter II. Integrated genomic analysis of chromosomal alterations and mutations in B-cell acute lymphoblastic leukemia reveals distinct genetic profiles at relapse.

Supplementary File 1

Article

Integrated genomic analysis of chromosomal alterations and mutations in B-cell acute lymphoblastic leukemia reveals distinct genetic profiles at relapse

Maribel Forero-Castro [1†], Adrián Montaño [2†], Cristina Robledo [2], Alfonso García de Coca [3], José Luis Fuster [4], Natalia de las Heras [5], José Antonio Queizán [6], María Hernández-Sánchez [2], Luis A. Corchete-Sánchez [2,7], Marta Martín-Izquierdo [2], Jordi Ribera [8], José-María Ribera [9], Rocío Benito [2*], Jesús M. Hernández-Rivas [2,7,10*]

[1]Escuela de Ciencias Biológicas, Universidad Pedagógica y Tecnológica de Colombia. Avenida Central del Norte 39-115, 150003, Tunja, Boyacá, Colombia; maribel.forero@uptc.edu.co

[2]IBSAL, IBMCC, Universidad de Salamanca-CSIC, Cancer Research Center, Campus Miguel de Unamuno, 37007 Salamanca, Spain; adrianmo18@gmail.com (A.M.); crisrmontero@hotmail.com (C.R.); mahesa2504@hotmail.com (M.H.S); lacorsan@hotmail.com (L.A.C.S); marta.martini@usal.es (M.M.I); beniroc@usal.es (R.B.); jmhr@usal.es (J.M.H.R)

[3]Servicio de Hematología, Hospital Clínico de Valladolid, Av. Ramón y Cajal, 3, 47003 Valladolid, Spain; agarciaco@saludcastillayleon.es

[4]Servicio de Oncohematología Pediátrica, Hospital Universitario Virgen de la Arrixaca, Murcia, Ctra. Madrid-Cartagena, s/n, 30120 El Palmar, Murcia, Spain; josel.fuster@carm.es

[5]Servicio de Hematología, Hospital Virgen Blanca, Altos de Nava s/n, 24071 León, Spain; ndelasheras22@hotmail.com

[6]Servicio de Hematología, Hospital General de Segovia, C/ Luis Erik Clavería Neurólogo S/N, 40002 Segovia, Spain; jqueizan@saludcastillayleon.es

[7]Servicio de Hematología, Hospital Universitario de Salamanca, Paseo de San Vicente, 88-182, 37007 Salamanca, Spain; lacorsan@hotmail.com (L.A.C.S); jmhr@usal.es (J.M.H.R)

[8]Acute Lymphoblastic Leukemia Group, Josep Carreras Leukaemia Research Institute, Carretera de Canyet, s/n, 08916 Badalona, Barcelona, Spain; jribera@carrerasresearch.org

[9]Servicio de Hematología Clínica, Institut Català d'Oncologia, Hospital Germans Trias i Pujol, Josep Carreras Research Institute, Universitat Autònoma de Barcelona, Carretera de Canyet, s/n, 08916 Badalona, Barcelona, Spain; jribera@iconcologia.net

[10]Departamento de Medicina, Universidad de Salamanca, Campus Miguel de Unamuno. C/ Alfonso X El Sabio s/n. 37007-Salamanca; jmhr@usal.es (J.M.H.R)

† M.F.-C. and A.M. contributed equally to this work.

*Sharing senior authorship

*Correspondence: jmhr@usal.es (J.M.H.R.) and beniroc@usal.es (R.B.); Tel.: Phone: + 34 923291384 (J.M.H.R.) and + 34 923294812 (R.B.).

Table of contents of supplementary patients and methods

List of supplementary tables

List of supplementary figures

References for supplementary information

Supplementary patients and methods

DNA isolation

Genomic DNA was extracted from frozen bone marrow or peripheral blood fixed cell samples using a QIAamp DNA Mini Kit (Qiagen, Valencia, CA, USA) following the manufacturer's instructions. DNA quality was assessed as the A260/A280 ratio with a NanoDrop ND-1000 spectrophotometer (NanoDrop Technologies, Wilmington, DE, USA) and by 1% agarose gel electrophoresis. A260/A280 ≥ 1.8 and A260/A230 ≥ 1.9 ratios were required for optimal labeling of DNA samples.

Oligonucleotide array comparative genomic hybridizations

In brief, patient DNA and normal control DNA (Human Genomic DNA: Male/Female, Promega, Madison, WI, USA) samples were denatured and labeled in parallel with Cy3 for the test group and Cy5 for the control group, each through a random priming method, using Klenow fragments (NimbleGen Dual-Color DNA Labeling Kit, Roche NimbleGen, Inc., Madison, WI, USA). Following cleanup and quantification, the test and sex-matched reference DNA samples were combined in equimolar amounts and loaded into one of the twelve filled ports on the microarray slide. Hybridization was carried out in a NimbleGen Hybridization Chamber for 16-20 hours at 42°C. Subsequently, the microarray slide was washed, dried and scanned at 2-μm resolution using a NimbleGen MS 200 microarray scanner. To avoid slide batch spotting bias, samples were hybridized in random order.

Array-CGH data analysis methods

Array image files (532.tif and 635.tif) generated by the MS 200 Data Collection Software were imported into Nexus Copy Number software (version 4.1) (Biodiscovery, Inc., Hawthorne, CA, USA) for analysis. Log_2 values of the raw data were normalized using the loess algorithm implemented in the affy R package (version 1.50.0). Quality control measures involved checking the consistency of signal distributions across samples; unsupervised clustering was performed to check outlier samples using SIMFIT statistical software (www.simfit.org.uk) (data not shown). Each genomic region exhibiting a copy number change was examined using the University of California at Santa Cruz Genome Browser (http://genome.cse.ucsc.edu) tool to determine the location and significance of the change. Normalized log_2 ratios were processed for outlier removal though winsorization and segmented by piecewise constant segmentation (PCF) using the copynumber R package (version 1.20.0). Statistically significant regions in common between cases were assessed by Genomic Identification of Significant Targets in Cancer (GISTIC) analysis [1] with a confidence level of 0.90. The statistical significance of the aberrations was displayed as the FDR (false-discovery rate) q-values obtained for each region. The method accounts for multiple-hypothesis testing using the FDR framework and assigns a value of q to each result, reflecting the probability that the event is due to chance [1]. Values of $q < 0.05$ were considered to represent statistically significant amplification and deletion peaks in children and adult patients. The Database of Genomic Variants from Toronto (DGV, http://dgv.tcag.ca/dgv/app/home) was used to exclude DNA variations located in regions with defined copy number variations. Thus, all copy number changes with more than 50% overlap with respect to those reported in DGV were excluded. Sex chromosomes were included from array-CGH data analysis. CNAs ≥ 0.5 Mb and detected by at least five consecutive aCGH probes were retained for copy number analysis. Large-scale or broad copy number alterations corresponded to regions larger than 50% of a chromosome arm. All genome-based data reported in this manuscript correspond to NCBI build 36 (hg18- Mar. 2006).

Amplicon library preparation

A sensitive next-generation amplicon deep-sequencing assay (NGS) was applied, using the Titanium amplicon chemistry (454 Life Sciences, Branford, CT, USA). For this approach, two preconfigured 96-well primer plates containing lyophilized primer pairs (Roche, Branford, CT, USA) were used to prepare the amplicon library following the procedures used in the IRON-II Study (European Leukemia Network group). The first PCR plate (termed B-ALL SeqPlate) was designed to amplify *JAK2* (exons 12 to 16), *PAX5* (exons 2 and 3), *LEF1* (exons 2 and 3), *CRLF2* (exon 6) and *IL7R* (exon 5) genes, while the second plate (*TP53* SeqPlate) was designed to amplify the *TP53* (exons 4 to E11) gene. Thus, in total, 19 amplicon

preparations across 26 samples, involving 494 individual PCR reactions, were carried out. The B-ALL SeqPlate was used to generate 11 amplicons from up to eight individual samples while the *TP53* SeqPlate was used to generate eight amplicons from up to 11 individual samples, thus 88 amplicons per run were obtained of each plate. In *TP53* SeqPlate the size range of the amplified products was 404-431bp including the adaptor sequences, while in the B-ALL SeqPlate the size range was 304-427bp. The above-mentioned genes were selected due to their well-defined role as mutational hot spots in BCP-ALL [2-12].

Amplicon library pooling and purification

After generating the amplicons, amplicon library pooling in equivalent amounts was carried out. The pooled libraries could be either different amplicons of the same sample, of the same amplicon in different samples, or any combination of these. The pooled libraries were purified with Agencourt AMPure magnetic beads (Beckman Coulter, Krefeld, Germany) in order to remove small amplicons (< 100 bp) and separating only those amplicons with optimal size for high-throughput sequencing. The purified amplicon pooling was quantified by dsDNA HS Qubit® Fluorometric Quantitation Assay Kit (Life Technologies). The quality of the amplicon pool was evaluated with an Agilent 2100 Bioanalyzer.

Emulsion PCR and sequencing

The amplicon library pooling was subsequently diluted to a concentration of $2x10^6$ molecules per µl and subjected to emulsion PCR using GS Junior Titanium emPCR Kit (Lib-A) (Roche Applied Science). Forward (A beads) and reverse (B beads) reactions were carried out using 2 000 000 beads per emulsion oil tube. The copy per bead ratio used was 1:1. The diluted PCR amplicons were mixed with beads under conditions that favored one fragment per bead. The amplification reaction, breaking of the emulsions and enrichment of beads carrying amplified DNA was performed using the workflow as recommended by the manufacturer (Roche Applied Science, M Penzberg, Germany). The bidirectional sequencing was carried out for 200 cycles using full processing mode for amplicons on a GS Junior platform (454 Life Sciences, Branford, CT, USA).

Data processing and analysis

Sequencing reads in SFF (standard flowgram format) file format obtained from the 454 GS Junior sequencing run were analyzed using the GS Variant Analyzer Software 2.5.3 (454 Life Sciences, Roche Applied Science) and Sequence Pilot version 3.4.2 (JSI Medical Systems, Kippenheim, Germany) software. Sequence alignment and variant detection were performed using the following reference sequences: *JAK2:* Transcript-ID: ENST00000381652, *PAX5*:ENST00000358127, *LEF1*:ENST00000265165,*CRLF2*:ENST00000400841, *IL7R:* ENST00000303115 and *TP53*: ENST00000269305. Quality control (QC) was included to provide coverage of more than 140 reads per amplicon (70 minimum reads in both forward and reverse directions). The variants were filtered to display sequence variants occurring in more than 2% of bidirectional reads per amplicon in at least one patient [13-15]. All somatic mutations were searched in the online COSMIC database (http://cancer.sanger.ac.uk/cancergenome/projects/cosmic) and the IARC *TP53* database (http://p53.iarc.fr/p53Sequences.aspx) [16]. Variants previously reported as germline polymorphisms in the Single Nucleotide Polymorphism database (dbSNP build 138) were excluded. Sequence variations identified by NGS were independently validated using conventional Sanger sequencing from a second PCR using the original DNA and/or a separate setup of NGS PCR, emPCR and re-sequencing run.

MLPA

Variable quantities of sample DNA (50-250 ng) were subjected to MLPA reactions using SALSA MLPA P335-B1 ALL-IKZF1 probemix (MRC-Holland, Amsterdam, Netherlands) according to the manufacturer's instructions. DNA from three healthy donors was used as control samples. The P335-B1 probemix contains probes for the following genes: *IKZF1* (8 probes at 7p12.2), *CDKN2A/B* (3 probes at 9p21.3), *PAX5* (7 probes at 9p13.2), *EBF1* (4 probes at 5q33.3), *ETV6* (6 probes at 12p13.2), 4 probes for *BTG1* and the *BTG1* downstream region (at 12q21.33), *RB1* (5 probes at 13q14.2), as well as genes from the X/Y PAR1 region (*CRLF2, CSF2RA, IL3RA* and *P2RY8*) (5 probes at Xp22.33). Additionally, one probe at Yp11.31 (*ZFY*) and one at 9p24.1 (*JAK2*) were included to facilitate the determination of the extent of a deletion/duplication detected in patient samples. Finally, 13 reference probes were included targeting chromosomal regions that are relatively stable in ALL. The design of this MLPA-kit allows the identification of deletions and

duplications of one or more chromosomal regions in each DNA sample. MLPA amplification products were analyzed on a ABI 3130xl Genetic Analyzer (Applied Biosystems/Hitachi) with the GeneMapper software V.3.7, using the Genescan 500LIZ internal size standard (Applied Biosystems). Each peak in the electropherogram corresponded to the amplification product of a specific amplicon. Each patient's electropherogram was compared with three controls. Coffalyzer MLPA DAT (MRC-Holland) software was used to analyze MLPA data. The copy number at each locus was estimated according to method of Schwab et al. [17], whereby values above 1.3, between 1.3 and 0.75, between 0.75 and 0.25, and below 0.25 were considered as gain, normal, hemizygous loss, and homozygous loss, respectively.

Supplementary tables

Table S1. Frontline risk-adapted protocols, outcome, clinical status, karyotype, FISH, NGS, aCGH and MLPA analysis in matched diagnosis-relapse B-ALL patients.

Patient ID	Sex/age [1](years)	Moment evaluated	aCGH findings			Gene deletions (MLPA-aCGH)	Positive *NGS* results	Genetic subtype at diagnosis	Karyotype	Positive *FISH* results	Positive molecular biology results	Risk group	Frontline therapy	Outcome	Clinical status
			aCGH[2]	Broad gains (≥5Mb)	Broad losses (≥5Mb)										
ID1	F/4	Diagnosis	A	1q 4 6 7q* 9 10 14 17 21	7p*	*IKZF1, ETV6*		Normal	46,XX[10]	N	ND	IR	PETHEMA LAL-RI/96	CR	Rel-D
		Relapse	A		7 X	*IKZF1, PAR1*		NA	54,XX,+X,5,+17,+21,+4 mar[4]/46,XX[6]	N	UNKN	NA		NA	
ID2	F/12	Diagnosis	A	1q	9p 17p	*CDKN2A/B, PAX5*	*TP53*mut	*TCF3(E2A)-PBX1*	46,XX[15]	*TCF3* loss-89% *TCF3/PBX1* 89%	ND	HR	PETHEMA LAL-AR/2003	CR	Rel-D
		Relapse	A	1q	9p	*CDKN2A*	*TP53*mu	*NA*	F		UNKN	NA		NA	

					17p	*/B, PAX5*	t			*TCF3/PBX1* 75%					
ID3	F/14	Diagnosis	A	18 21 X		*CDKN2A /B*		Hyper (47-50)	F	*RUNX1* gain-85%	UNKN	LR	PETHEMA LAL-BR-01	CR	Rel-D
		Relapse	N				*TP53*mut	*NA*	F	*ETV6* loss-62% *KMT2A(MLL)* loss-82% *ABL* loss-88% *BCR* loss-88%	UNKN	NA		NA	
ID4	F/15	Diagnosis	A	7q**	7p** 19	*EBF1, IKZF1, PAR1*	*TP53*mut	Others	46,XX,t(7;15)(p13;q12)[3] /46,XX[7]	N	ND	IR	PETHEMA LAL-RI/96	CR	Rel-D
		Relapse	A	7q* 19 22	7p*	*IKZF1*	*TP53*mut	*NA*	47,XX,der(7)t(7;?)(p13;?),+mar[10]/ 46,XX[7]	N	UNKN	NA		NA	
ID5	F/23	Diagnosis	A	5p 9q***	9p***	*CDKN2A /B, PAX5*		Others	46,XX,del(1)(q21),i(9)(q10)[15] /46,XX[5]	*ABL* gain-29%	N	IR	PETHEMA LAL-RI/2008	CR	Rel-CR-A
		Relapse	A	9p21	14q23.3			*NA*	ND	ND	UNKN	NA		NA	
ID6	M/29	Diagnosis	A		7p12.2***	*IKZF1*		*BCR-ABL1*	46,XY,t(9;22)(q34;q11)[10]	*BCR/ABL* 91%	Major BCR/ABL Positive	HR	PETHEMA LAL-Ph/2000/ Imatinib	CR	Rel-D
		Relapse	A	Focal CNAs	Focal CNAs	*IKZF1*		*NA*	F	*BCR/ABL* 51%	UNKN	NA		NA	

ID7	F/31	Diagnosis	A	Focal CNAs	Focal CNAs		*TP53*mut/ *PAX5*mut	*KMT2A(MLL)-R*	46,XX,t(4;11)(q21;q23)[10]	N	UNKN	HR	GMALL	CR	Rel-D
		Relapse	A	7q* 17 19 22	4 7p*	*IKZF1*	*TP53*mut/ *TP53*mut	*NA*	F	*KMT2A(MLL)-R* 90%	UNKN	NA		NA	
ID8	M/32	Diagnosis	A	21 X		*CDKN2A/B, PAX5, IKZF1, BTG1, RB1*		Normal	46,XY[19]	N	ND	HR	FLAGIDA	PR (CR later on)	Rel-CR-D
		Relapse	A	21				*NA*	46,XY[10]/48,XY,+7,+21[2]	ND	UNKN	NA		NA	
ID9	F/34	Diagnosis	A		17 19	*EBF1, CDKN2A/B, PAX5, IKZF1, BTG1, PAR1*		*BCR-ABL1*	46,XX,t(9;22)(q34;q11)[8]/46,XX[2]	*BCR/ABL* 82%	Minor BCR/ABL Positive	HR	PETHEMA LAL-Ph/2000/ Imatinib	PR (CR later on)	Rel-D
		Relapse	A	22	4	*EBF1, PAX5, IKZF1, ETV6, BTG1, RB1*		*NA*	F	*BCR/ABL* 81%	UNKN	NA		NA	
ID10	M/36	Diagnosis	A		9p21.3***	*CDKN2A/B*		Hypo (<44)	34-44,XY[8]/46,XY[9]	ND	UNKN	HR	PETHEMA LAL-	PR (CR later on)	Rel-D

		Relapse	A	19 22 X	7p	*IKZF1*		*NA*	48,XY,+3,del(5)(p13p15),+18[8]/46,XY[11]	ND	UNKN	NA	AR/93	NA	
ID11	F/38	Diagnosis	A		7p12.2***	*EBF1, IKZF1*		Hyper (47-50)	46,XX[10]	*ABL* gain-30%	N	HR	PETHEMA LAL-AR/2003	CR	Rel-CR-D
		Relapse	A	1q21	7p15			*NA*	ND	N	UNKN	NA		NA	
ID12	F/52	Diagnosis	A		9p	*CDKN2A/B, PAX5, IKZF1, ETV6, BTG1*		Hypo (<44)	39-42,XX,add(12)(p13)[5]/46,XX,add(12)(p13)[2]/46,XX[9]	ND	ND	HR	UNKN	CR	Rel-D
		Relapse	A	X	9p 12p	*CDKN2A/B, PAX5, IKZF1, ETV6, BTG1*		*NA*	ND	*BCR/ABL* 94%	ND	NA		NA	
ID13	F/80	Diagnosis	N					*KMT2A(MLL)-R*	46,XX[15]	*KMT2A(MLL)-R* 93%	UNKN	HR	PETHEMA LAL/OLD-FRA	CR	Rel-D
		Relapse	A	7q* 19 22	4 7p* 13 X	*EBF1, CDKN2A/B, IKZF1, BTG1, RB1*		*NA*	ND	ND	UNKN	NA		NA	

[1]At diagnosis. [2]Not all CNAs <0.5 Mb are shown in this table. *Consistent with an isochromosome 7q, i(7q). **Consistent with pseudodiploid karyotype with unbalanced translocation involving gain of 7q and loss of 7p. ***Consistent with an isochromosome 9q, i(9q). **** Focal loss (CNA <0.5 Mb). **Abbreviations**: A: aCGH altered, N: aCGH normal, UNKN: unknown, NA: not applicable, CR: complete remission, D: dead, LR: low risk, IR: intermediate risk, HR: high risk, ND: Not done, Hyper (47-50), low hyperdiploid (47-50 chromosomes), Hypo (<44), FISH, fluorescence in situ hybridization; F: failed, NA: not applicable.

Table S2. Description of somatic mutations observed in diagnosis-relapse BCP-ALL patients. All three *TP53* mutations retained at relapse increased their mutational burden to relapse (c.818G>C from 3.5% to 26%, c.832C>T from 11% to 21% and 817_821delinsGACCC from 53% to 71%)

Patient ID	Gene	Type of mutation	Mutation	AA change	Database	Moment	Mutational burden
ID2	*TP53-E08*	Indel	c.817_821delinsGACCC	p.R273_V274delinsDP	Undescribed	Diagnosis	53%
						Relapse	71%
ID4	*TP53-E08*	Missense	c.832C>T	p.P278S	COSM10939/*TP53* website http p53.fr	Diagnosis	11%
						Relapse	21%
ID7	*PAX5-E03*	Missense	c.399T>A	p.S133R	Undescribed	Diagnosis only	20%
	TP53-E08	Missense	c.818G> C	p.R273P	COSM165077/*TP53* website http://p53.fr	Diagnosis	3.5%
						Relapse	26%
	TP53-E05	Splicing	c.-8_4del12	Splice_Intron 5 SA	*TP53* website http://p53.fr	Relapse only	15%
ID3	*TP53-E05*	Missense	c.829_842delins14	p.C277_D281delinsGPQG	Undescribed	Relapse only	90%

Table S3. Regions of significant recurrent amplification and deletion retained at relapse (*q-value* <0.05). This table shows the MCR identified at diagnosis (part a) that were retained at relapse (part b).

a) Diagnosis MCRs							
MCR	**Cytoband**	**Wide peak limits**	**Probes**	**q values**	**Frequency**	**Overlap_CNV**	**Genes associated with BCP-ALL**
Amplification Peak 1	10q26.13	chr10:125287308-125627394	13	0.0029798	69.2	49.9	
Amplification Peak 2	15q11.2	chr15:1-20387217	30	0.00152	30.8	10.4	
Deletion Peak 1	1p36.32	chr1:1-3740335	82	0.043017	30.8	61.9	
Deletion Peak 2	5p15.33	chr5:1-2809848	80	0.019729	23.1	43.0	
Deletion Peak 3	9p21.3	chr9:19775843-21252803	55	0.0011035	53.8	42.7	*PTPLAD2, MLLT3*
Deletion Peak 4	9p21.2	chr9:21943224-32382231	306	0.04103	38.5	38.8	*CDKN2B, CDKN2A, DMRTA1*
Deletion Peak 5	10q26.3	chr10:133639221-135374737	57	0.039672	23.1	61.2	
b) Relapse MCRs							
MCR	**Cytoband**	**Wide peak limits**	**Probes**	**q values**	**Frequency**	**Overlap_CNV**	**Genes associated with BCP-ALL**
Amplification Peak 1	10q26.13	chr10:125596091-126882537	71	0.016885	46.2	24.1	*FAM53B*
Amplification Peak 2	15q11.2	chr15:1-20387217	30	0.016885	30.8	10.4	
Deletion Peak 1	1p36.33	chr1:1804656-3559849	38	0.0010206	38.5	41.6	
Deletion Peak 2	5p15.33	chr5:1-2809848	80	0.0015214	38.5	43.0	
Deletion Peak 3	9p21.3	chr9:19775843-22441867	95	0.00015622	46.2	68.3	*CDKN2A, IFN, MLLT3, PTPLAD2, MTAP, DCKN2B, DMRTA1*
Deletion Peak 5	10q26.3	chr10:133821131-135374737	54	0.000211	53.8	68.4	

Table S4. Regions of significant recurrent deletion lost at relapse (*q-value* < 0.05).

MCR	Cytoband	Wide peak limits	Probes	q values	Frequency	Overlap_CNV	Genes associated with BCP-ALL
Deletion Peak 1	8q24.3	chr8:142063749-146274826	130	0.04103	23.0769231	33.8	
Deletion Peak 2	19p13.3	chr19:1-5585748	160	0.04103	30.7692308	36.8	*TCF3, E2A*

Table S5. Regions of significant recurrent amplification and deletion acquired at relapse (*q-value* < 0.05).

MCR	Cytoband	Wide peak limits	Probes	q values	Frequency	Overlap_CNV	Genes associated with BCP-ALL
Amplification Peak 1	1p36.22	chr1:8732967-9911979	49	0.016885	46.2	27	
Amplification Peak 2	1p36.22	chr1:11285557-12240632	39	0.016885	53.8	17	
Amplification Peak 3	1p36.13	chr1:14909013-18795097	196	0.045783	53.8	23	
Amplification Peak 4	1q21.1	chr1:120280136-144113553	86	0.016885	38.5	6	
Amplification Peak 5	1q23.2	chr1:158012327-158639152	42	0.032569	46.2	28	
Amplification Peak 6	2p24.3	chr2:15588842-16322114	34	0.016885	46.2	32	
Amplification Peak 7	2p23.3	chr2:26490879-27444893	44	0.016885	53.8	13	
Amplification Peak 8	2p13.3	chr2:69882623-72233418	112	0.024079	38.5	24	*DYSF*
Amplification Peak 9	2p11.2	chr2:85070707-85828746	44	0.016885	46.2	23	
Amplification Peak 10	2q13	chr2:108663875-109679153	47	0.016885	46.2	36	
Amplification Peak 11	2q14.2	chr2:120938348-121845814	60	0.016885	46.2	23	
Amplification Peak 12	3p25.1	chr3:13051957-13690735	25	0.016885	46.2	29	
Amplification Peak 13	3p22.1	chr3:42663872-43126699	35	0.016885	46.2	40	
Amplification Peak 14	3q21.1	chr3:124029509-124945325	63	0.016885	46.2	24	
Amplification Peak 15	3q21.3	chr3:127842173-130850454	151	0.016885	46.2	21	
Amplification Peak 16	4p16.1	chr4:5720583-7875973	106	0.016885	46.2	34	
Amplification Peak 17	5p15.1	chr5:16664587-31286811	323	0.045783	46.2	16	
Amplification Peak 18	5q31.1	chr5:133804535-134997254	66	0.016885	53.8	18	
Amplification Peak 19	5q31.3	chr5:140903053-142072612	89	0.019505	46.2	19	
Amplification Peak 20	5q33.1	chr5:149355702-150078235	38	0.016885	46.2	9	*PDGFRB*
Amplification Peak 21	5q35.1	chr5:167592461-168387411	92	0.045783	46.2	6	
Amplification Peak 22	5q35.1	chr5:171673733-172302393	41	0.016885	46.2	42	
Amplification Peak 23	6p25.3	chr6:1-1931210	121	0.032569	46.2	43	
Amplification Peak 24	6p21.1	chr6:43423545-44935974	78	0.019505	46.2	11	
Amplification Peak 25	7q22.1	chr7:100780141-101605221	61	0.016885	46.2	40	
Amplification Peak 26	7q22.2	chr7:104673282-105652483	63	0.045783	46.2	44	

Amplification Peak 27	7q32.3	chr7:131338179-131860908	54	0.024079	38.5	29	
Amplification Peak 28	7q36.1	chr7:148179407-148764908	28	0.019505	38.5	17	*EZH2*
Amplification Peak 29	8p21.3	chr8:21548589-23589751	121	0.016885	46.2	43	
Amplification Peak 30	8q24.22	chr8:133912051-134874122	63	0.045783	38.5	12	
Amplification Peak 31	8q24.3	chr8:140615440-141545165	56	0.016885	46.2	49	
Amplification Peak 32	9p13.1	chr9:38917771-70176099	315	0.016885	76.9	26	
Amplification Peak 33	9q22.2	chr9:91245647-91827350	32	0.016885	46.2	49	
Amplification Peak 34	9q32	chr9:114501990-116298659	113	0.032569	46.2	30	
Amplification Peak 35	9q33.3	chr9:127799231-128430649	53	0.016885	46.2	27	
Amplification Peak 36	10q23.2	chr10:87804465-88565173	33	0.016885	53.8	40	
Amplification Peak 37	10q24.1	chr10:98172138-100219092	109	0.016885	46.2	10	
Amplification Peak 38	10q25.2	chr10:111864227-112971515	62	0.045783	46.2	30	*ADD3*
Amplification Peak 39	10q26.11	chr10:120677309-121344955	37	0.016885	46.2	45	
Amplification Peak 40	11q12.1	chr11:56825293-57330723	33	0.024079	38.5	39	
Amplification Peak 41	11q13.4	chr11:74529331-74983324	25	0.016885	46.2	27	
Amplification Peak 42	11q24.2	chr11:124371528-124803387	28	0.016885	46.2	46	
Amplification Peak 43	11q24.2	chr11:125641427-126000192	27	0.016885	53.8	4	
Amplification Peak 44	12p13.33	chr12:2160004-3171873	69	0.016885	46.2	39	
Amplification Peak 45	12q13.13	chr12:52730714-53122322	27	0.019505	46.2	48	
Amplification Peak 46	12q24.13	chr12:111975073-112921584	58	0.024079	46.2	50	
Amplification Peak 47	12q24.22	chr12:115309409-116481375	87	0.016885	46.2	18	
Amplification Peak 48	13q14.3	chr13:48683941-49337754	39	0.024079	38.5	12	
Amplification Peak 49	14q32.31	chr14:98479480-103750044	282	0.016885	46.2	14	*BCL11B*
Amplification Peak 50	16q13	chr16:55439274-56721225	51	0.016885	46.2	14	
Amplification Peak 51	20q13.32	chr20:54421157-56041849	101	0.016885	46.2	45	
Deletion Peak 1	7p14.2	chr7:36428531-37756111	80	0.0011851	53.8	17	
Deletion Peak 2	9q34.2	chr9:135102408-136431045	24	0.0015593	38.5	34	
Deletion Peak 3	13q34	chr13:112554650-114142980	70	0.028348	30.8	25	

Supplementary figures

Figure S1. Location of the probes on X/Y PAR1 region provided in the MLPA probemix and NimbleGen High density microarray platform. X/Y PAR1 region (*CRLF2, CSF2RA, IL3RA* and *P2RY8*) (5 probes at Xp22.33).

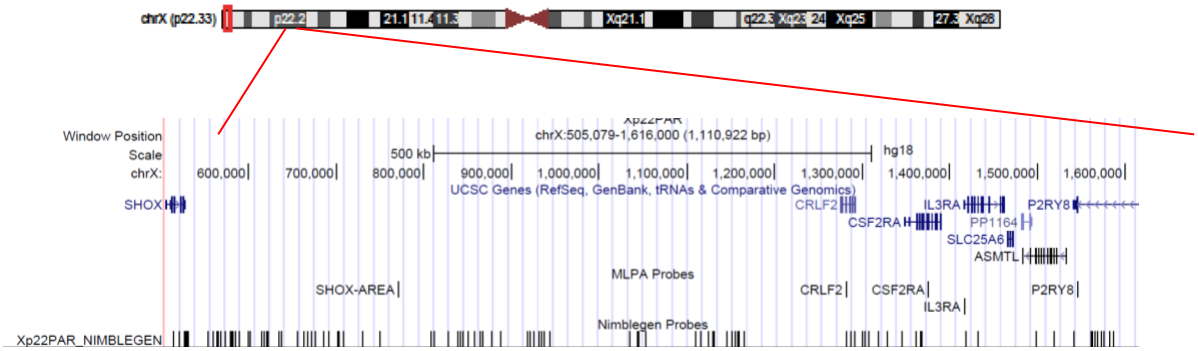

Figure S2. Patterns and frequencies of DNA copy alterations observed in 13 paired diagnostic/relapse samples. A. Frequency of CNAs observed in all samples at diagnosis, B. Frequency of CNAs observed in all samples at relapse. Gains in red and losses in blue.

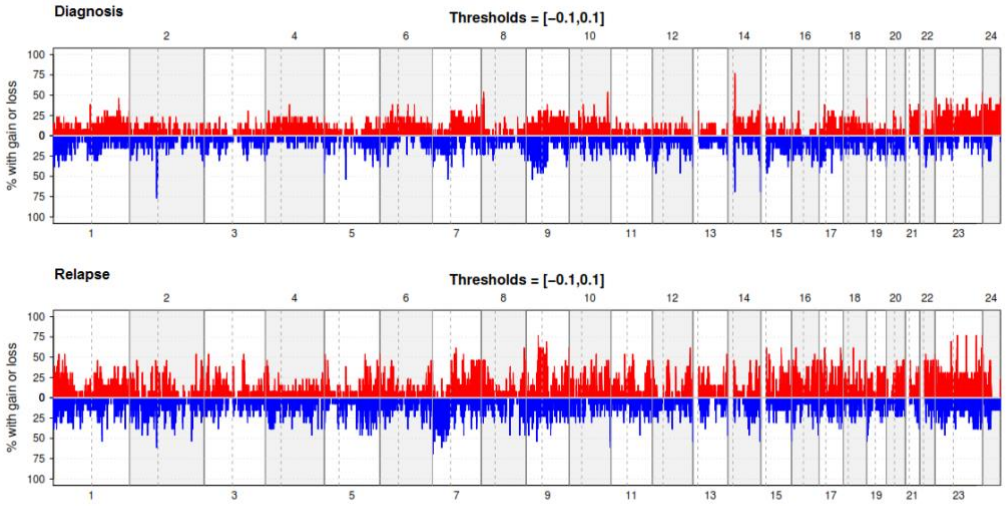

Figure S3. Gene deletions identified by integrative MLPA-aCGH analysis.

Patient ID	ID1		ID2		ID3		ID4		ID5		ID6		ID7		ID8		ID9		ID10		ID11		ID12		ID13	
Genes**	D	R	D	R	D	R	D	R	D	R	D	R	D	R	D	R	D	R	D	R	D	R	D	R	D	R
IKZF1	*	+					*	*			*	&		*	*		+	&		+	+		&	*		*
CDKN2A/B			*	*	+				*						*		*		+				*	*		+
PAX5			*	*					*						+		*	&					*	*		
EBF1							+										*	*			*					+
BTG1															*		*	+					*	&		+
ETV6	&																	*					*	*		
RB1															*			+								+
PAR1 region		+					+										+									

Abbreviations: D: diagnosis; R: relapse; *: Gene deletions identified by MLPA and aCGH analysis: +: Gene deletions identified by aCGH analysis only; &: Gene deletions identified by MLPA analysis only

** The P335-B1 probemix contains probes for the following genes: *IKZF1* (8 probes at 7p12.2), *CDKN2A/B* (3 probes at 9p21.3), *PAX5* (7 probes at 9p13.2), *EBF1* (4 probes at 5q33.3), *ETV6* (6 probes at 12p13.2), 4 probes for *BTG1* and the *BTG1* downstream region (at 12q21.33), *RB1* (5 probes at 13q14.2), as well as genes from the X/Y *PAR1* region (*CRLF2, CSF2RA, IL3RA* and *P2RY8*) (5 probes at Xp22.33). Additionally, there is one probe at Yp11.31 (*ZFY*) and one at 9p24.1

Figure S4. Mutations identified by NGS showed patterns of genetic evolution in paired diagnostic/relapse samples. Patient ID2 (red line) and Patient ID4 (black line): retained mutations in the *TP53* gene. Patient ID7 (green line): retained one mutation in the *TP53* gene, acquired a new mutation in the *TP53* gene and lost one mutation in the *PAX5* gene at relapse. Patient ID3 (blue line): acquired a new mutation in the *TP53* gene at relapse.

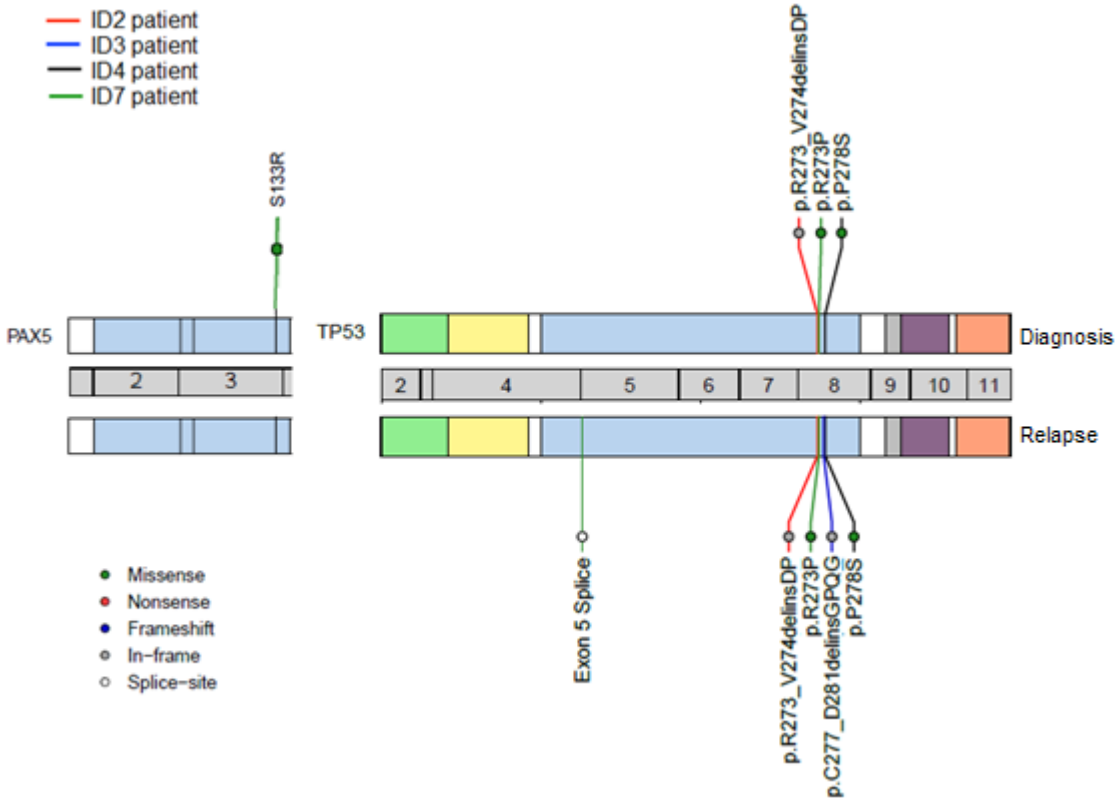

References for supplementary information

1. Beroukhim, R.; Getz, G.; Nghiemphu, L.; Barretina, J.; Hsueh, T.; Linhart, D.; Vivanco, I.; Lee, J.C.; Huang, J.H.; Alexander, S., et al. Assessing the significance of chromosomal aberrations in cancer: methodology and application to glioma. *Proc Natl Acad Sci U S A* **2007**, *104*, 20007-20012, doi:10.1073/pnas.0710052104.
2. Harrison, C.J. Key pathways as therapeutic targets. *Blood* **2011**, *118*, 2935-2936, doi:118/11/2935 [pii]10.1182/blood-2011-07-362723.
3. Chiaretti, S.; Zini, G.; Bassan, R. Diagnosis and subclassification of acute lymphoblastic leukemia. *Mediterranean journal of hematology and infectious diseases* **2014**, *6*, e2014073, doi:10.4084/MJHID.2014.073.
4. Chiaretti, S.; Gianfelici, V.; Ceglie, G.; Foa, R. Genomic characterization of acute leukemias. *Medical principles and practice : international journal of the Kuwait University, Health Science Centre* **2014**, *23*, 487-506, doi:10.1159/000362793.
5. Gowda, C.; Dovat, S. Genetic targets in pediatric acute lymphoblastic leukemia. *Adv Exp Med Biol* **2013**, *779*, 327-340, doi:10.1007/978-1-4614-6176-0_15.
6. Iacobucci, I.; Papayannidis, C.; Lonetti, A.; Ferrari, A.; Baccarani, M.; Martinelli, G. Cytogenetic and molecular predictors of outcome in acute lymphocytic leukemia: recent developments. *Curr Hematol Malig Rep* **2012**, *7*, 133-143, doi:10.1007/s11899-012-0122-5.
7. Loh, M.L.; Mullighan, C.G. Advances in the genetics of high-risk childhood B-progenitor acute lymphoblastic leukemia and juvenile myelomonocytic leukemia: implications for therapy. *Clin Cancer Res* **2012**, *18*, 2754-2767, doi:10.1158/1078-0432.CCR-11-1936.
8. Mullighan, C.G. Genomic profiling of B-progenitor acute lymphoblastic leukemia. *Best Pract Res Clin Haematol* **2011**, *24*, 489-503, doi:S1521-6926(11)00084-3 [pii]10.1016/j.beha.2011.09.004.
9. Roberts, K.G.; Mullighan, C.G. How new advances in genetic analysis are influencing the understanding and treatment of childhood acute leukemia. *Curr Opin Pediatr* **2011**, *23*, 34-40, doi:10.1097/MOP.0b013e3283426260.
10. Woo, J.S.; Alberti, M.O.; Tirado, C.A. Childhood B-acute lymphoblastic leukemia: a genetic update. *Experimental hematology & oncology* **2014**, *3*, 16, doi:10.1186/2162-3619-3-16.
11. Inaba, H.; Greaves, M.; Mullighan, C.G. Acute lymphoblastic leukaemia. *Lancet* **2013**, *381*, 1943-1955, doi:10.1016/S0140-6736(12)62187-4.
12. Pui, C.H.; Carroll, W.L.; Meshinchi, S.; Arceci, R.J. Biology, risk stratification, and therapy of pediatric acute leukemias: an update. *J Clin Oncol* **2011**, *29*, 551-565, doi:JCO.2010.30.7405 [pii]10.1200/JCO.2010.30.7405.
13. Weissmann, S.; Roller, A.; Jeromin, S.; Hernandez, M.; Abaigar, M.; Hernandez-Rivas, J.M.; Grossmann, V.; Haferlach, C.; Kern, W.; Haferlach, T., et al. Prognostic impact and landscape of NOTCH1 mutations in chronic lymphocytic leukemia (CLL): a study on 852 patients. *Leukemia* **2013**, *27*, 2393-2396, doi:10.1038/leu.2013.218.
14. Kohlmann, A.; Klein, H.U.; Weissmann, S.; Bresolin, S.; Chaplin, T.; Cuppens, H.; Haschke-Becher, E.; Garicochea, B.; Grossmann, V.; Hanczaruk, B., et al. The Interlaboratory RObustness of Next-generation sequencing (IRON) study: a deep sequencing investigation of TET2, CBL and KRAS mutations by an international consortium involving 10 laboratories. *Leukemia* **2011**, *25*, 1840-1848, doi:10.1038/leu.2011.155.
15. Grossmann, V.; Roller, A.; Klein, H.U.; Weissmann, S.; Kern, W.; Haferlach, C.; Dugas, M.; Haferlach, T.; Schnittger, S.; Kohlmann, A. Robustness of amplicon deep sequencing underlines its utility in clinical applications. *The Journal of molecular diagnostics : JMD* **2013**, *15*, 473-484, doi:10.1016/j.jmoldx.2013.03.003.
16. Leroy, B.; Anderson, M.; Soussi, T. TP53 mutations in human cancer: database reassessment and prospects for the next decade. *Human mutation* **2014**, *35*, 672-688, doi:10.1002/humu.22552.
17. Schwab, C.J.; Jones, L.R.; Morrison, H.; Ryan, S.L.; Yigittop, H.; Schouten, J.P.; Harrison, C.J. Evaluation of multiplex ligation-dependent probe amplification as a method for the detection of copy number abnormalities in B-cell precursor acute lymphoblastic leukemia. *Genes Chromosomes Cancer* **2010**, *49*, 1104-1113, doi:10.1002/gcc.20818.

Annex III

Supplemental material of Chapter III. *ETV6/RUNX1*

Fusion Gene Abrogation Decreases the Oncogenicity of Tumour Cells in a Preclinical Model of Acute Lymphoblastic Leukaemia

Supplementary information

ETV6/RUNX1 FUSION GENE ABROGATION DECREASE THE ONCOGENICITY OF TUMORS CELLS IN A PRECLINICAL MODEL OF ACUTE LYMPHOBLASTIC LEUKEMIA.

Adrián Montaño[1], Jose Luis Ordoñez[2], Verónica Alonso-Pérez[2], Jesús Hernández-Sánchez[1], Sandra Santos[1], Teresa González[3], Rocío Benito[1], Ignacio García-Tuñón*[2], Jesús María Hernández-Rivas[1,2,3,4]*

[1]IBSAL, IBMCC, Universidad de Salamanca-CSIC, Cancer Research Center; Salamanca; Spain.

[2]Unidad de Diagnóstico Molecular y Celular del Cáncer, Centro de Investigación del Cáncer-IBMCC (USAL-CSIC), Salamanca, Spain.

[3]Dept of Hematology, Hospital Universitario de Salamanca; Salamanca; Spain.

[4]Dept of Medicine, Universidad de Salamanca, Spain.

*These authors share senior authorship.

Corresponding author:

Jesús-María Hernández-Rivas

IBMCC, CIC Universidad de Salamanca-CSIC, Hospital Universitario de Salamanca

Paseo de San Vicente 58

37007 Salamanca

Spain

Phone: + 34 923291384 // Fax: +34 923294624

e-mail: jmhr@usal.es

Keywords

Acute lymphoblastic leukemia, ETV6/RUNX1, CRISPR/Cas9, Genome edition.

Supplementary tables and figures

Table S1. sgRNA designed against *E/R* fusion sequence. Two custom-designed single guide RNAs (sgRNAs) were designed to genetically inactivate the *E/R* oncogene. These specific sgRNAs direct Cas9 to the *E/R* fusion sequence. G1 sgRNA, directed at the end of exon 5 of *ETV6* and G2 directed to intronic region before the fusion point between *ETV6* and *RUNX1*.

	Forward	*Reverse*
G 1	caccgGCCTAATTGGGAATGGTGCG	aaacCGCACCATTCCCAATTAGGCc
G 2	caccgAAGAGCACGCCATGCCCATT	aaacAATGGGCATGGCGTGCTCTTc

Table S2. Possible off-targets of the sgRNAs. The possible off-targets of the sgRNAs used obtained from "Breaking Cas" website (http://bioinfogp.cnb.csic.es/tools/breakingcas/) were checked by PCR and sanger sequencing. Two pairs of oligonucleotides were designed for each off-target region.

Gen	*Score*	*Forward*	*Reverse*
PTPN21	0	AGTGTAATTTGGGAAACAGCCCT	TTGGGGCTTTTCCCACCTCAA
BCL9L	0.3	AGAGAATGGATCTGGGAGGGA	AGGCGAGGCAGTTGCAGTGTA
BEND4	0.1	GGCATCAGGTAGCCAACGTTC	CAGGATCAATGGATTTGTCACAG
VSIR	0	AAAGGGTCCAGAGAAGAGAGG	CTGGGGACGGAGCAAAACTTT

Table S3. Genes significantly deregulated after *E/R* fusion gene abrogation. List of 342 genes significantly deregulated after *E/R* fusion gene abrogation sorted according to the decreasing value of the FC. The TP50 of deregulated genes are shaded in grey. In the following columns from left to right, the mean of normalized counts of all samples (baseMean); log2-Fold Change (log2FC); log2FC unshrunk, P-value and adjusted P value.

Gene	baseMean	log2FC	log2FCunshrunk	Pvalue	Padj
DRD5	154.4	-2.34959	-3.92883	0	0
ATP10A	231.1	-2.07428	-3.35631	0	0
SGIP1	70.3	-2.0645	-3.86631	0	0
BIRC3	80.1	1.98755	4.09318	0	0
ACKR3	66.8	-1.98193	-3.84476	0	0
EMR2	80.4	1.97712	3.98976	0	0
FAM189A1	55.5	-1.80486	-4.18028	0	1.97E-13
MIR146A	278.6	1.77216	2.54174	0	1E-15
OPTN	315.4	1.7413	2.24832	0	0
LHX6	127.2	1.72519	3.8055	4E-15	3.17E-12

NBPF3	35.4	-1.67532	-4.9272	1.6E-14	1.23E-11
GCSAM	1072	-1.67221	-1.90226	0	0
PGPEP1	94.7	-1.66199	-3.62221	3.7E-14	2.72E-11
KCNA2	143.1	-1.65663	-2.17481	0	1E-15
RP11-622K12.1	367.2	1.59169	2.28594	2E-15	1.94E-12
RASD2	209.2	-1.47352	-2.0491	6.1E-14	4.04E-11
CDH23	265.2	-1.44672	-1.96584	6E-14	4.04E-11
ALOX5	89.6	1.37691	2.54469	2.65E-10	1.38E-07
SORBS2	882	-1.364	-1.63045	0	4.4E-14
HYDIN	83.6	1.36022	3.17093	5.3E-10	2.67E-07
GPR17	119.4	-1.33855	-2.68649	1.05E-09	4.79E-07
MOXD1	162.7	1.33314	3.05082	1.17E-09	5.15E-07
ARX	64.4	-1.30499	-2.44801	2.28E-09	9.76E-07
KCNE3	249.5	-1.30368	-1.95828	2.64E-10	1.38E-07
HOXA13	234.3	1.29849	1.52883	0	1.13E-13
LCK	214.4	-1.29552	-2.04607	7.9E-10	3.84E-07
RELB	271.2	1.28523	1.51994	0	4.11E-13
DDR1	207.4	1.23577	1.58447	9.25E-12	5.62E-09
SCN3A	361.8	1.23448	1.91793	3.86E-09	1.52E-06
FRMD4B	807.8	-1.22731	-1.62866	8.07E-11	4.52E-08
LIMS2	495.1	-1.20713	-2.10548	2.5E-08	7.02E-06
RGS1	221.1	-1.19302	-1.85261	1.24E-08	4.03E-06
CALML6	75.1	1.19083	1.84701	1.21E-08	4E-06
FZD3	83	1.179	2.86812	6.42E-08	1.49E-05
ARHGAP42P2	187.8	-1.17718	-2.04583	5.34E-08	1.25E-05
RP11-251M1.1	558.7	1.1701	1.89706	3.88E-08	9.91E-06
RXRA	695.7	1.16993	1.68558	6.77E-09	2.47E-06
RGS16	431.5	1.16993	4.27179	1.85E-08	5.52E-06
HOTTIP	40.8	1.16894	2.4038	1.01E-07	2.26E-05
FBN3	196.1	-1.16298	-1.45832	3.86E-11	2.25E-08
RP11-16L9.4	439.2	1.15288	1.66285	1.14E-08	3.86E-06
HLX	101.3	1.14724	1.59611	5.25E-09	1.97E-06
TP63	318.4	1.1262	1.88183	1.55E-07	3.14E-05
TLR7	61.4	1.12406	2.8608	2.25E-07	4.37E-05
PTPRG-AS1	73.4	-1.11862	-3.58436	1.17E-07	2.44E-05
FAM78A	548.8	1.11483	1.43424	9.77E-10	4.59E-07
BCAS1	210.8	-1.11072	-1.8555	2.28E-07	4.38E-05
PLS1	62.8	1.10389	2.20117	4.87E-07	8.16E-05
AQP5	229.5	1.09449	1.83256	3.47E-07	6.1E-05
PDE10A	95.9	-1.08807	-2.11786	6.94E-07	0.000109
CSF1	29.6	1.07667	3.30357	4.18E-07	7.16E-05
TTC28	422.8	-1.06872	-1.42756	1.9E-08	5.53E-06
EPHB6	332.1	1.05097	1.40655	3.42E-08	8.9E-06
GIMAP6	104.7	-1.04917	-2.08309	1.74E-06	0.000237
CNR2	151.2	-1.04836	-1.46725	1.15E-07	2.43E-05
SGK1	203.2	1.04539	1.4315	7.51E-08	1.71E-05

TRPM2	307.5	1.04389	1.56381	4.22E-07	7.16E-05
SLC25A4	375.9	-1.04233	-1.35587	1.71E-08	5.4E-06
SERPINB1	449.6	-1.03395	-1.48499	2.89E-07	5.4E-05
ADCY7	789.1	1.02767	1.67585	1.47E-06	0.000206
EPN2	211.7	-1.02564	-2.01505	2.94E-06	0.000382
NPL	61.1	1.01372	1.61799	1.64E-06	0.000226
RP11-1055B8.4	129.1	1.00869	1.41433	3.47E-07	6.1E-05
CD52	5748.7	-1.00638	-1.07155	0	0
C10orf10	193.8	-1.00598	-1.707	3.06E-06	0.000394
MYO7B	130	-1.00505	-2.57867	3.37E-06	0.000419
N4BP3	1631.4	1.0044	1.34839	1.49E-07	3.05E-05
TRNP1	843.7	-1.00257	-1.36303	2.17E-07	4.27E-05
RP11-443A13.5	571.4	1.00152	1.21962	2.54E-09	1.06E-06
LRP4	64.7	0.99177	2.46045	4.97E-06	0.000603
TSPAN9	526.5	-0.99105	-1.11836	1.14E-12	7.23E-10
TMEM64	260.3	0.98891	1.45127	1.27E-06	0.000182
TCF7	151	-0.98381	-1.32807	2.96E-07	5.46E-05
MMP14	192.5	0.98032	1.80139	7.14E-06	0.000846
FAM107B	10387.3	-0.97505	-1.19805	1.14E-08	3.86E-06
PLEK	1078.2	0.96863	1.28742	3.1E-07	5.65E-05
NOL4	214.5	0.96397	1.17625	1.07E-08	3.8E-06
CAV1	297	-0.95749	-1.27142	4.08E-07	7.08E-05
AGR2	38.8	0.95646	5.4769	9.71E-07	0.000149
RGMA	1017.8	-0.95634	-1.18978	4.04E-08	1.02E-05
RASSF4	289	-0.95437	-1.75826	1.25E-05	0.001381
LCN6	249.8	0.95321	1.81714	1.36E-05	0.001474
RP11-1055B8.7	6983	0.94416	1.00376	0	0
PTMS	72.4	0.94242	1.9579	1.77E-05	0.001864
CYTH4	524.2	0.9396	1.24137	5.87E-07	9.41E-05
KLHDC7B	22.2	0.93929	2.83172	9.63E-06	0.001105
HAP1	3579.1	-0.936	-1.13741	2.31E-08	6.59E-06
RHOH	1146.9	-0.9267	-1.23334	1.02E-06	0.000153
IRF8	803.1	-0.92338	-1.25995	1.95E-06	0.000263
LARGE	415.8	-0.91806	-1.3959	1.02E-05	0.001156
LAMB4	79.9	-0.9156	-1.67425	2.72E-05	0.002662
AK7	1333.1	-0.91269	-1.0905	1.8E-08	5.52E-06
TBXAS1	369.3	0.9111	1.09726	3.12E-08	8.26E-06
PLEKHB1	67.2	0.90934	1.81052	3.42E-05	0.00322
SPTBN4	89.6	-0.90781	-1.24563	3.11E-06	0.000397
CXXC5	1769.6	0.90625	1.05615	3.28E-09	1.33E-06
GUCY1A3	222.9	-0.89857	-1.50261	2.9E-05	0.00282
GPR142	27.8	-0.89415	-2.85582	1.96E-05	0.001998
ZNF264	134.7	0.89389	1.26566	7.45E-06	0.000869
SNTA1	325.1	-0.88594	-1.09918	3.25E-07	5.86E-05
SV2A	972.4	0.88563	1.08285	1.7E-07	3.39E-05
ZNF469	158.6	0.88264	1.58403	5.07E-05	0.004447

PIGM	310.8	0.88148	1.10151	4.97E-07	8.23E-05
AC090044.2	95.8	0.87855	1.7981	6.3E-05	0.005364
SEMA7A	122.3	0.87808	1.47324	4.44E-05	0.004041
NTN3	154.2	0.87613	1.09977	6.78E-07	0.000107
LINC01013	150	-0.87602	-1.36521	3.06E-05	0.002955
CROCC	298.9	0.87521	1.03825	4.13E-08	1.02E-05
MMP15	449.3	-0.8698	-1.13171	2.58E-06	0.000344
RP11-1055B8.6	283	0.86919	1.226	1.27E-05	0.001392
EMP2	378.1	0.86759	1.09257	9.99E-07	0.000152
RP11-431N15.2	20.1	0.86663	5.26703	6.26E-06	0.000747
ZNF528	133.8	0.8636	1.48223	6.46E-05	0.005392
FCGR2A	66.4	0.86013	1.72152	8.92E-05	0.006923
NEIL1	67.7	0.85161	1.49228	8.63E-05	0.006797
SIT1	183.8	0.85063	1.50487	9.1E-05	0.006981
NT5E	323.3	-0.85004	-1.0867	2.66E-06	0.000352
CECR2	268.9	0.84865	1.17241	1.5E-05	0.001603
SERPINB6	560.5	-0.84378	-1.0843	3.67E-06	0.000453
SIDT1	263.9	-0.84107	-1.39962	8.96E-05	0.006923
AFF2	979.3	0.83909	1.10828	8.18E-06	0.000947
TEAD3	73	0.83854	1.4096	9.67E-05	0.007272
CD302	207.1	0.83694	1.39459	9.73E-05	0.007272
C1QTNF4	454.5	-0.83462	-1.02567	1.03E-06	0.000153
PTPN7	496.1	-0.83337	-1.42407	0.000115	0.008254
LBH	1252.6	-0.8326	-1.02589	1.22E-06	0.000178
RIC3	24	0.83244	4.0662	1.94E-05	0.001998
SEMA4A	185.8	0.83085	1.17682	3.18E-05	0.003026
NRBP2	246.9	0.82947	1.18658	3.71E-05	0.00344
TSKU	93.4	0.82585	1.35517	0.000112	0.008122
CD40	168.6	0.82537	1.01695	1.47E-06	0.000206
DBNDD1	403.2	-0.82471	-1.16418	3.51E-05	0.00328
KCNJ4	36.7	-0.82267	-1.86593	0.000169	0.011166
SORBS1	27.8	0.81941	2.04647	0.000157	0.010539
IL4I1	31.7	0.81657	2.62006	8.98E-05	0.006923
RP11-469H8.6	67.9	0.81609	2.12138	0.000151	0.010331
GNG11	1694.7	-0.81545	-1.06571	1.16E-05	0.001309
CAP2	128.4	-0.81443	-1.23333	8.73E-05	0.006837
PLEC	410.6	0.80672	1.04502	1.17E-05	0.001309
PDZD7	100.6	0.80051	1.19706	0.000104	0.007603
TMEM52	235.2	0.79981	1.61531	0.00027	0.016797
AC090044.1	372.3	0.79949	1.33198	0.000198	0.01259
ATP13A2	773.7	0.79809	0.98318	3.28E-06	0.000412
NPY	354.1	0.79767	1.1838	0.000104	0.007611
SLC51A	923.8	-0.79604	-1.11872	6.19E-05	0.005302
PSD2	32.5	0.78983	1.91702	0.000279	0.017214
CAST	535.9	0.78854	1.09765	6.42E-05	0.005392
PRR5L	357.9	-0.785	-0.9029	1.1E-07	2.39E-05

ARHGEF12	926.6	-0.78172	-0.87228	5.27E-09	1.97E-06
C20orf197	21.9	0.78168	2.91678	0.000115	0.008254
ZNF704	1650.9	-0.78124	-0.89744	1.15E-07	2.43E-05
DAB2IP	529.9	0.77986	0.99995	1.79E-05	0.001872
TMEM173	173.5	0.77921	1.1944	0.00019	0.012234
IGHD	430.3	0.77753	1.17758	0.000182	0.011865
ACTN1	1971.1	0.7764	0.88027	4.2E-08	1.02E-05
RP3-455J7.4	112.6	0.7684	1.51577	0.000463	0.025573
TMEM229B	179.1	0.76807	1.38713	0.000428	0.024342
NAT8L	59	0.7666	1.47598	0.000471	0.02581
RBMS2	105.9	0.76601	1.02433	5.69E-05	0.004937
SPNS2	96.1	-0.76441	-1.13302	0.000197	0.01259
FAM65B	1931.9	-0.76332	-1.03087	7.24E-05	0.005959
KCTD12	44.2	0.7633	1.79551	0.00046	0.025497
LOXHD1	82	-0.76287	-2.05591	0.000363	0.021387
ARL4C	117.7	-0.7613	-1.60277	0.000521	0.027621
PDLIM1	3779.7	-0.75931	-1.07166	0.00014	0.009802
ZNF169	102.5	0.75727	1.06339	0.000135	0.009626
TPM2	503.6	0.75349	0.95242	2.39E-05	0.002421
PFN2	420.2	0.75328	1.19692	0.000376	0.022024
WFS1	101.5	0.75075	1.18653	0.000381	0.022203
LCN10	42.8	0.74986	1.967	0.000486	0.026329
LILRB4	30.2	-0.74518	-2.02167	0.000494	0.02656
NCALD	46.4	-0.74335	-1.48403	0.000709	0.034244
ID2	152.8	0.74327	1.53331	0.00071	0.034244
CAMK4	217.7	0.74297	0.96783	6.03E-05	0.0052
PDGFA	327.7	0.74222	1.18772	0.000473	0.025829
TEX14	53.7	0.74155	2.36737	0.000355	0.02103
SPRY1	230.1	-0.73794	-0.92144	2.53E-05	0.002512
STIM1	473.7	-0.73641	-0.97332	9.19E-05	0.00701
SPARC	101.2	0.7362	2.12186	0.000497	0.026604
CACNA2D1	75.1	0.73588	1.23955	0.000631	0.031553
ITGB2	713.9	0.73385	0.972	0.000101	0.007414
CTD-3018O17.3	68.5	0.73343	2.08948	0.000537	0.028172
ANO1	25.8	-0.73342	-1.94635	0.000632	0.031553
C20orf194	216.2	0.73325	0.93779	5.16E-05	0.004504
MS4A4A	134.3	0.73223	0.95342	7.59E-05	0.006175
GARNL3	45.5	0.73071	1.25472	0.000723	0.034641
CARD9	84.4	0.72843	1.27716	0.000792	0.037227
LINC00114	50.9	0.72708	1.56987	0.000912	0.041384
GALNT10	153.9	0.72678	1.17004	0.000634	0.031553
C1orf222	60.1	0.7267	3.38097	0.00016	0.010692
RASGRP2	5671	0.72471	0.80094	1.86E-08	5.52E-06
RP11-830F9.7	568.5	0.72421	0.97573	0.000161	0.0107
MAP3K15	84	0.7234	2.14555	0.000581	0.030165
TACC2	14.2	-0.7217	-2.80884	0.000312	0.018838

CORO2A	263.9	-0.72125	-1.07485	0.000465	0.025585
TNFAIP8	784.8	-0.72046	-0.80155	5.25E-08	1.25E-05
PKIG	180.6	0.7152	1.42286	0.001122	0.048384
TLR3	112	0.71488	1.14196	0.000752	0.035921
LMNA	28	0.71359	1.78526	0.000974	0.043658
TMPRSS15	176.6	-0.71246	-1.40711	0.001171	0.049885
FAM132B	448.9	-0.71207	-0.93437	0.000138	0.009751
LACC1	65.3	0.71038	1.2899	0.00113	0.048557
BRINP2	106.2	-0.70892	-1.81139	0.000999	0.044262
HNRNPA1P37	148.6	-0.70868	-1.18719	0.000988	0.04402
FAIM3	190.7	-0.70773	-1.18642	0.001006	0.044414
ZNF641	98.1	0.70696	1.05068	0.000587	0.030165
TTC9	223.9	-0.7064	-1.07029	0.000674	0.032979
ABLIM1	225.1	-0.70592	-1.07602	0.000704	0.034244
C10orf128	142.5	0.70535	1.8123	0.00105	0.045788
BTN2A3P	99.4	0.69936	1.01969	0.000588	0.030165
PTPN3	66.8	-0.69834	-1.16774	0.001161	0.049594
SERINC5	435.8	-0.69699	-0.97851	0.000449	0.02528
SLC38A1	6284.3	-0.69645	-0.87412	8.05E-05	0.006483
DAPK2	666.3	-0.69437	-0.83711	2.59E-05	0.002554
GIMAP8	19.7	-0.69337	-2.63213	0.000536	0.028172
BMP2K	1727.1	-0.69233	-0.75947	2.78E-08	7.64E-06
HIP1R	570	-0.6917	-0.84738	4.71E-05	0.004258
HTRA3	17.2	0.6915	2.51822	0.000634	0.031553
DSTYK	220	0.6907	0.87977	0.000126	0.009033
BCL11B	316.1	0.68927	0.99353	0.000652	0.03221
PLXNC1	284.8	0.68588	0.78584	2.71E-06	0.000356
ORAI2	1167.4	-0.68344	-0.88109	0.000189	0.012234
XBP1	5123.5	-0.68319	-0.93619	0.000456	0.025497
CDH24	1294	0.68212	0.84292	7.64E-05	0.006185
CD72	1662	0.68122	0.88181	0.000213	0.013462
PCDHGC4	364.2	-0.68111	-0.82387	4.12E-05	0.0038
GREB1	1076	-0.68088	-0.95199	0.000586	0.030165
KCNQ1OT1	78.4	0.67777	1.03449	0.001142	0.048945
MBOAT1	104.5	0.67352	1.00355	0.001076	0.046676
ZFHX3	434.9	0.67246	0.91572	0.00052	0.027621
NEAT1	2886.8	0.67221	0.95417	0.000787	0.037215
PCCA	700.6	-0.67141	-0.84344	0.000147	0.010087
LRRC4	495.5	-0.6704	-0.79996	3.38E-05	0.003202
BCL6	2112.8	-0.66649	-0.72574	2.96E-08	7.98E-06
PTPRK	5372.9	-0.66494	-0.75968	4.57E-06	0.000559
ALDH3A2	645	-0.66287	-0.85065	0.000271	0.016797
METRNL	199.1	-0.6628	-0.81304	9.94E-05	0.007392
RP11-715J22.6	155.9	0.66094	0.85659	0.000331	0.019844
FMO4	18.3	0.65854	2.85429	0.000706	0.034244
MFI2	975.1	0.65699	0.78398	4.86E-05	0.004367

CBR3-AS1	468.6	-0.65573	-0.7299	7.64E-07	0.000118
GALNT12	180.5	0.65362	0.79167	8.6E-05	0.006797
MECOM	542.8	-0.64174	-0.83026	0.000482	0.02623
GIPC1	309.8	0.6412	0.80317	0.000271	0.016797
SIKE1	1347.5	-0.63951	-0.85494	0.00079	0.037227
TAGLN3	209.4	-0.63932	-0.79078	0.000213	0.013462
AC002454.1	1316.6	-0.63931	-0.76796	9.63E-05	0.007272
AATK	11.4	-0.6371	-3.43338	0.000604	0.03067
ZC3H12A	275.7	0.63261	0.82339	0.000632	0.031553
MYOM2	241.4	0.63191	0.82335	0.000651	0.03221
LAX1	250.8	-0.61615	-0.79876	0.000827	0.038338
RMND5B	689.1	0.61304	0.75966	0.000402	0.023211
GPSM1	5511.7	0.60465	0.71777	0.000157	0.010539
SSH1	1022.2	-0.60434	-0.66309	1.27E-06	0.000182
DPEP1	659.7	0.59957	3.82265	0.000718	0.034544
PECR	528.8	-0.5978	-0.66384	5.37E-06	0.000646
AVEN	268.8	-0.59717	-0.75211	0.000767	0.036418
LIG4	1424.3	-0.59515	-0.76201	0.001043	0.045721
JAM2	167.8	0.59361	0.74641	0.000798	0.037408
C12orf23	3429.3	-0.59254	-0.63665	1.07E-07	2.36E-05
HLA-F	1579	0.59166	0.72213	0.00046	0.025497
TMEM169	243.2	-0.58601	-0.73804	0.00096	0.043177
PPM1L	569	0.58504	0.69388	0.000247	0.015533
GRAMD1B	666.5	-0.58441	-0.72068	0.000674	0.032979
TCL1A	14125.8	-0.58379	-0.7102	0.000508	0.027111
LTBP4	1986	-0.58366	-0.70366	0.000408	0.023403
GABRA3	600.3	0.58365	0.73228	0.000946	0.042792
CLSTN3	436.5	0.58028	0.65011	1.96E-05	0.001998
OPN3	765.2	-0.57808	-0.64306	1.25E-05	0.001381
INO80C	371.9	0.57505	0.70177	0.000659	0.03245
AJUBA	747	0.57157	0.65377	8.59E-05	0.006797
LRRC8C	2327.4	-0.57157	-0.70511	0.000891	0.040809
PIK3C3	6227	-0.56954	-0.63715	2.53E-05	0.002512
TSPAN7	257.4	0.56592	0.65737	0.000194	0.012467
ANXA2	1995	0.56427	0.62478	1.39E-05	0.001501
IL1RAP	795.7	-0.56395	-0.66952	0.000424	0.024203
NFKB2	609.9	0.56343	0.67862	0.000628	0.031553
BLVRB	781.5	-0.56098	-0.62694	3.12E-05	0.002991
IER2	3387.6	0.56098	0.64561	0.000153	0.010429
DENND1B	599.4	-0.55701	-0.67477	0.000829	0.038338
MAP4K5	1334.5	0.55277	0.59071	2.82E-07	5.33E-05
BCL3	644.3	0.55203	0.60895	1.56E-05	0.001661
LDB2	465.5	-0.5518	-0.6714	0.001019	0.044866
SMC6	3061.7	-0.54865	-0.62885	0.00018	0.01179
ZNF253	1646.3	-0.54837	-0.64474	0.00046	0.025497
NRN1	2783.7	-0.54527	-0.6447	0.000585	0.030165

SLC39A8	923.8	-0.54477	-0.65199	0.000815	0.037948
CIC	1809	0.54446	0.60198	2.46E-05	0.002474
SYNE3	1544.9	-0.54423	-0.60647	4.41E-05	0.004041
EVPL	980.6	-0.54063	-0.61483	0.000157	0.010539
METTL17	1465.2	-0.53989	-0.6443	0.000846	0.039027
PARVG	875.4	0.53972	0.62981	0.000445	0.025159
KLHL6	2008.1	-0.53792	-0.59875	5.01E-05	0.004447
ZNF772	554.5	0.53727	0.60117	7.17E-05	0.005934
KRT9	18.6	0.53498	6.65035	0.000955	0.043075
SETD5-AS1	404.9	0.53251	0.63055	0.000814	0.037948
IRS2	1062.6	-0.52974	-0.61918	0.000598	0.030595
TNFAIP3	10109.7	0.52792	0.56264	5.83E-07	9.41E-05
ASAP2	1227.8	-0.52222	-0.60451	0.000523	0.027621
HCP5	3037.7	0.52175	0.56108	3.25E-06	0.000412
EEF2K	859.8	0.52046	0.58695	0.000184	0.011958
PRKD2	2447.4	0.51983	0.59259	0.000309	0.018771
CTD-2368P22.1	306	0.51516	0.60814	0.001108	0.047917
ZNF70	727.1	0.50734	0.57554	0.000349	0.020819
RLTPR	4653.6	-0.5058	-0.53588	5.61E-07	9.19E-05
MYO1G	1804.3	-0.50459	-0.58325	0.000767	0.036418
TBC1D2B	1080.7	-0.50443	-0.5858	0.000894	0.040817
CORO1C	2814.4	-0.50423	-0.54246	7.24E-06	0.000851
ABHD4	962.1	0.50249	0.58571	0.001045	0.045721
TUBA1A	6080.4	-0.49898	-0.54946	8.35E-05	0.006682
XYLT1	2173.2	0.49304	0.55528	0.000372	0.021838
CAMTA2	666.3	0.488	0.54536	0.000291	0.017889
HERC3	923.4	-0.48726	-0.53755	0.000139	0.009751
PPP1R13B	1190.8	-0.48723	-0.53054	5.06E-05	0.004447
DARS	6357.7	-0.48207	-0.50954	1.17E-06	0.000172
HMGN5	399.5	0.48135	0.55117	0.000978	0.043733
RNPC3	603.8	0.47969	0.54177	0.000603	0.03067
NREP	12968.7	-0.47495	-0.53106	0.000433	0.024565
AHDC1	2906.2	0.47326	0.53736	0.000883	0.040572
STK24	4714.6	-0.47268	-0.4991	1.53E-06	0.000213
GNG2	3002.9	-0.46988	-0.5218	0.00035	0.020819
ACSS1	2289.9	-0.46887	-0.52175	0.000403	0.023211
LAT2	9833.8	0.46614	0.50333	4.94E-05	0.004418
MXRA7	1139.6	-0.45464	-0.49246	0.000101	0.007414
ADD3	2155.4	-0.45395	-0.48413	1.9E-05	0.00198
PRPSAP2	1515.8	-0.45205	-0.49128	0.000146	0.010068
KAZALD1	816.8	0.44361	0.48156	0.000177	0.011647
KIAA0930	1631	-0.442	-0.47432	6.48E-05	0.005392
CCDC117	2855	-0.44158	-0.47766	0.000141	0.009858
ZNF302	1339.8	0.43871	0.47895	0.000316	0.019048
MAPK13	1114.4	-0.43871	-0.48379	0.000588	0.030165
HLA-A	14689.3	0.42258	0.45102	7.51E-05	0.006147

ZDHHC3	1299.3	-0.41703	-0.45071	0.000304	0.018507
H2AFY	16915.2	-0.41676	-0.45876	0.000997	0.044262
PCBP1-AS1	1351.6	0.41247	0.44775	0.000489	0.02639
SSBP2	6589.7	-0.41056	-0.4359	6.44E-05	0.005392
SMARCA2	4420.1	0.40579	0.43315	0.000145	0.010068
BZRAP1	6827.9	0.38932	0.41596	0.000293	0.017946
ETS2	7236.6	0.38757	0.40978	9.69E-05	0.007272
IDH2	9359.9	-0.37641	-0.40659	0.001075	0.046676
UNG	4993.8	-0.32718	-0.3456	0.000909	0.041384
STK38	5328.8	-0.32423	-0.33965	0.000391	0.022703

Table S4. Enrichment of differentially expressed genes after *E/R* abrogation. The first column shows the altered biological processes, following by expected value, fold enrichment, raw P value and the False Discovery Rate (FDR).

GO biological process complete	Expected	Fold Enrichment	raw P value	FDR
T cell receptor V(D)J recombination	.08	39.62	1.74E-04	3.58E-02
Germinal center formation	.12	33.01	2.19E-05	1.05E-02
Negative regulation of necroptotic process	.18	22.01	7.68E-05	2.21E-02
I-kappaB kinase/NF-kappaB signaling	1.05	6.70	1.40E-04	3.20E-02
Regulation of interleukin-6 production	2.01	4.47	2.88E-04	4.75E-02
Cellular calcium ion homeostasis	6.47	3.09	1.43E-05	7.53E-03
Regulation of inflammatory response	4.98	3.01	2.23E-04	4.05E-02
Regulation of lymphocyte activation	7.72	2.72	5.35E-05	1.69E-02
Regulation of GTPase activity	7.21	2.64	1.78E-04	3.56E-02
Regulation of cell migration	12.53	2.55	2.06E-06	2.50E-03
Actin filament-based process	8.42	2.49	1.71E-04	3.60E-02
Regulation of cellular protein localization	8.04	2.49	2.52E-04	4.37E-02
Neuron projection development	9.98	2.40	1.30E-04	3.12E-02
Cell morphogenesis	10.56	2.37	1.07E-04	2.65E-02
Positive regulation of immune response	12.77	2.19	1.46E-04	3.30E-02
Negative regulation of apoptotic process	13.48	2.15	1.39E-04	3.24E-02
Positive regulation of developmental process	20.46	2.15	2.91E-06	2.87E-03
Positive regulation of multicellular organismal process	26.05	2.07	5.37E-07	1.70E-03
Cytoskeleton organization	16.12	2.05	1.54E-04	3.35E-02
Negative regulation of response to stimulus	24.14	2.03	3.45E-06	3.21E-03
Regulation of anatomical structure morphogenesis	16.05	1.99	2.70E-04	4.54E-02
Positive regulation of molecular function	26.79	1.75	2.29E-04	4.11E-02
Regulation of signal transduction	49.65	1.51	2.44E-04	4.29E-02
Positive regulation of cellular process	80.91	1.37	2.11E-04	3.88E-02
Unclassified	48.68	.49	5.25E-05	1.77E-02

Figure S1. Edited-REH sequences. Sanger sequencing of the *E/R* fusion region in REH cells. The REH cells expressing PX458 without sgRNA, used as a control, had a wild type sequence, while cells expressing G1 sgRNA, G2 sgRNA or G1 + G2 sgRNAs showed a mixture of sequences around the expected Cas9 cleavage point. sgRNA guide sequences are shown in red box.

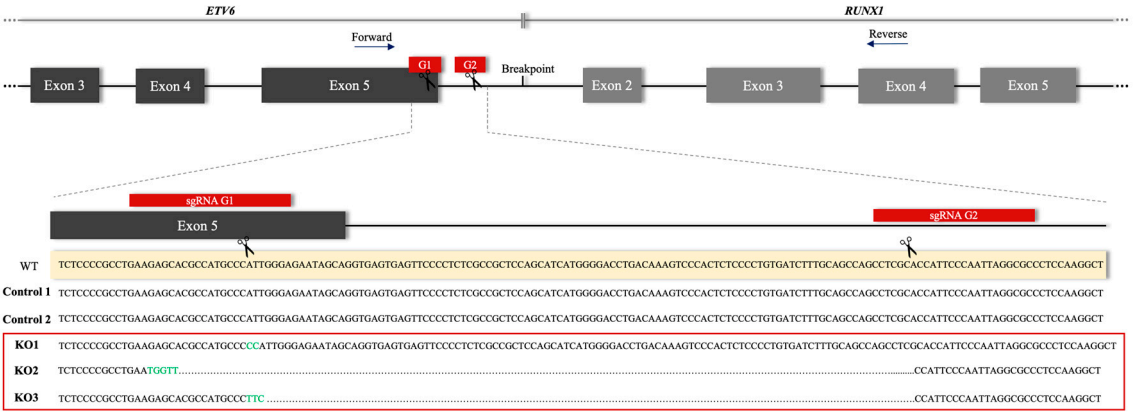

Figure S2. Edited sequences of single cell derived-cell line. The pool of REH edited-cells with both guides (G1 + G2) was separated by single cell. The sequence corresponding to the *E/R* fusion region was studied by Sanger sequencing in all clones. Two clones with single-non-edited sequence and therefore, with a wild type sequence, were selected as control clones. On the other hand, three single-edited cell clones with *E/R* KO sequence were selected as KO clones (KO1, KO2 and KO3). The pair of oligonucleotides used for ETV6/RUNX1 RT-qPCR is showed with blue arrows. These oligonucleotides were designed outside the editing region (exon 5 of *ETV6,* sense, 5 – CTCTGTCTCCCCGCCTGAA – 3 and exon 4 of

RUNX1, antisense, 5 – CGGCTCGTGCTGGCAT -3) and with a distance between them in mRNA of 143 base pairs (bps)

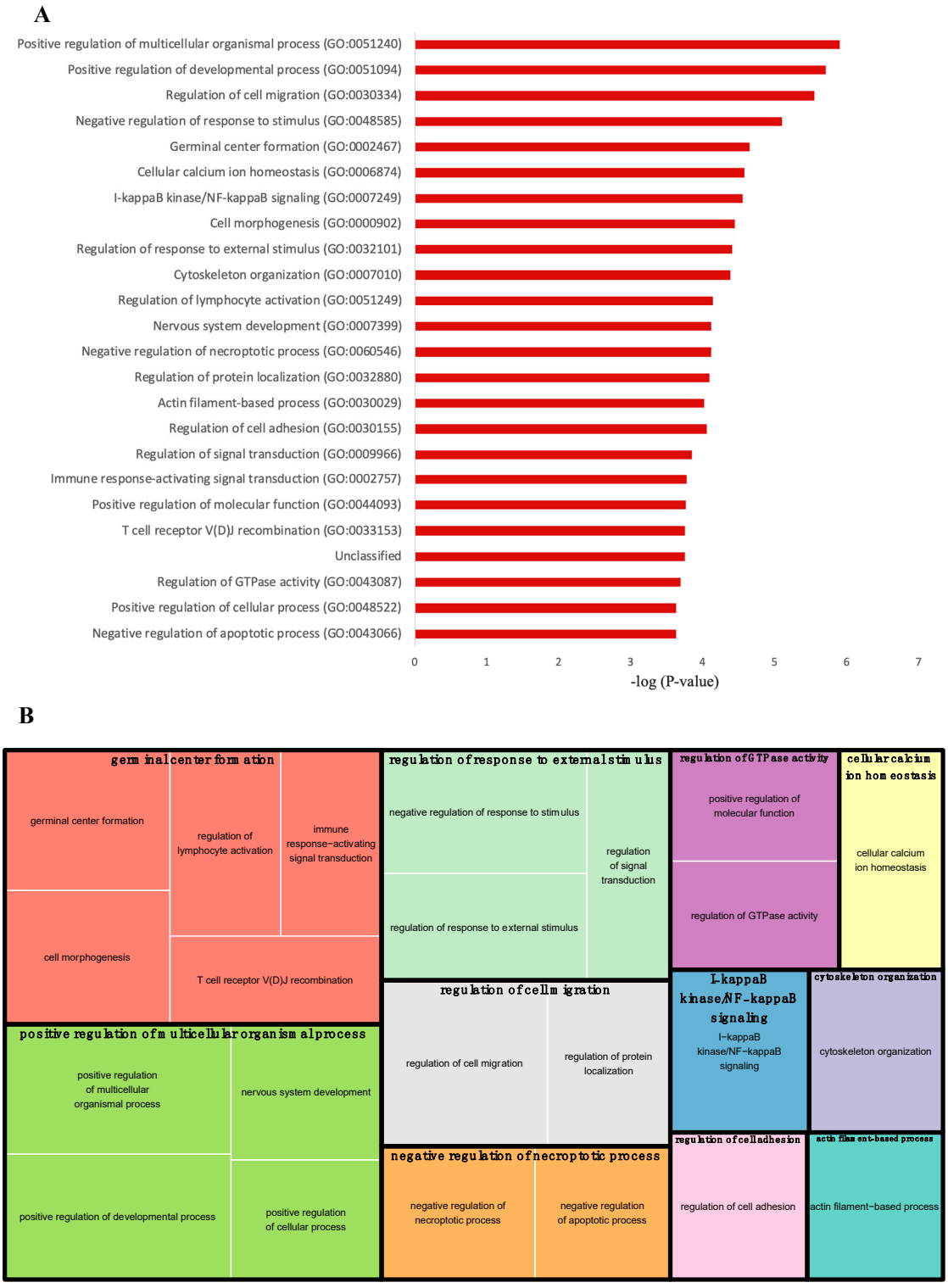

Figure S3. GO Enrichment Analysis. (A) This figure shows the biological processes obtained through enrichment analysis according to -log(P-value). (B) Each rectangle is a single cluster representative. The representatives are joined into 'superclusters' of loosely related terms, visualized with different colors. Size of the rectangles varies according to the P-value.

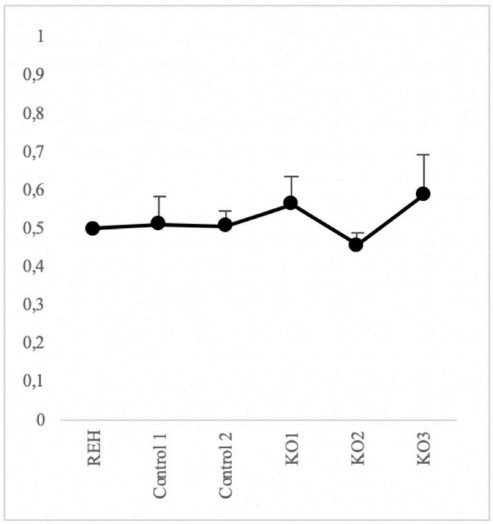

Figure S4. MTT proliferation assay. No proliferation changes were observed in E/R KO clones respected to REH cells and control clones at 72 hours by MTT assay. This experiment had 3 replicates.

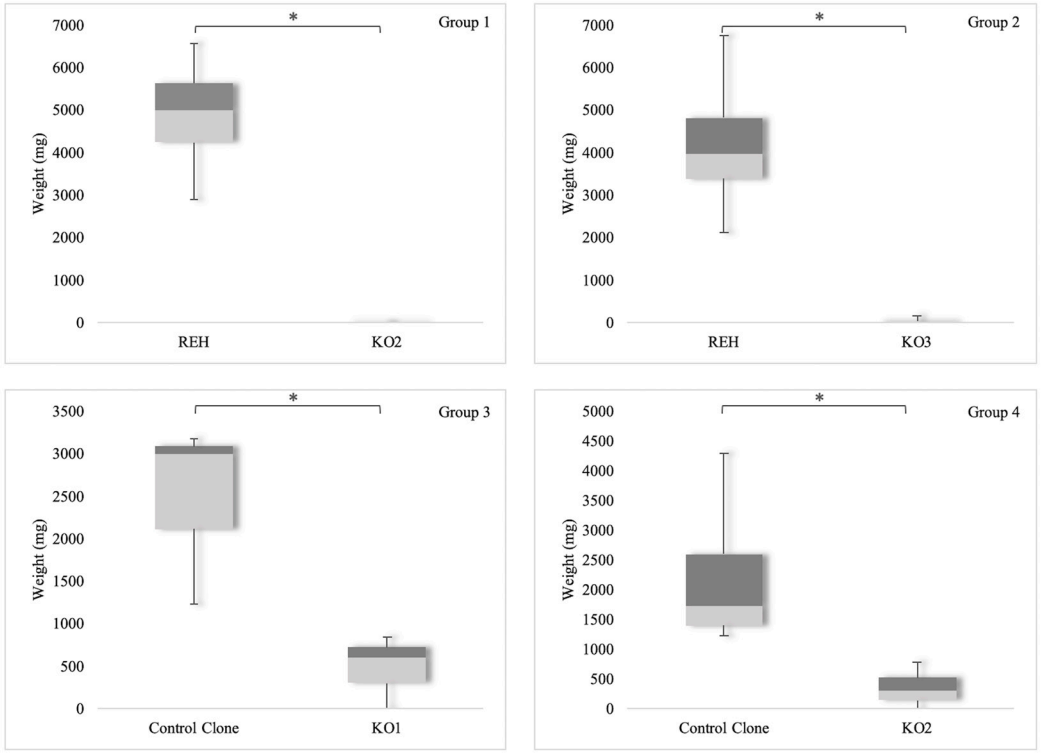

Figure S5. Measure of tumor growth. Mean of the tumor weight for each group of mice, represented by box plot, after being sacrificed at day 48 (group 1 and 2) or day 62 day (group 3 and 4). In this image, the mean of the sizes of the tumors is represented by box plot. In each group they are compared according to

the cells injected in those mice. All the mice belonging to the same group were sacrificed on the same day. Each group had 4 replicates. *P<0.05 (unpaired t-test).

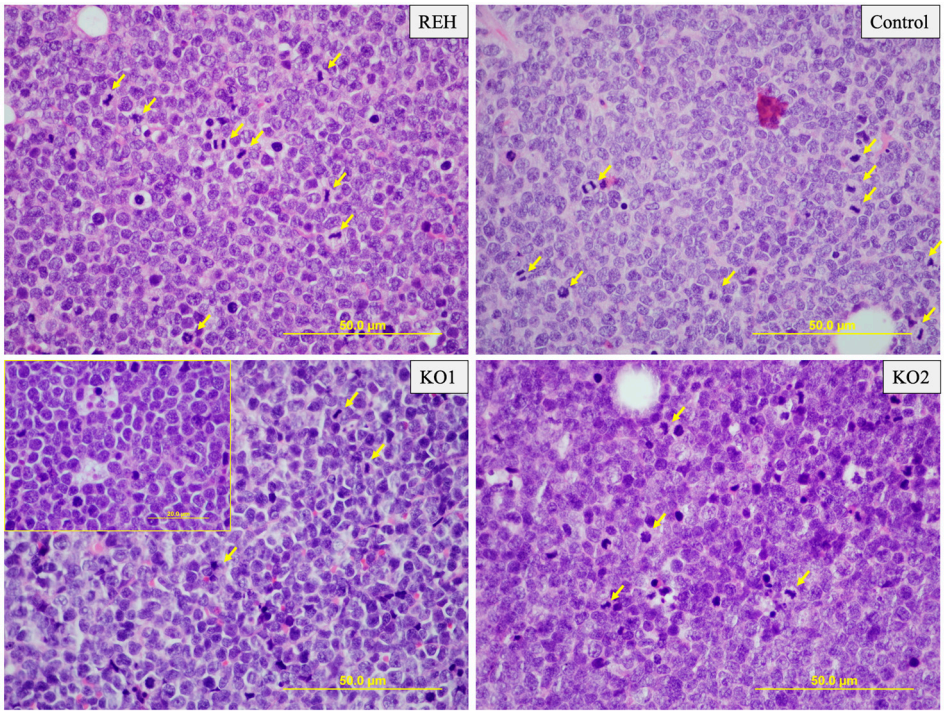

Figure S6. Tumor growth and histopathological findings. H&E representative areas of tumors from each group. Tumors were composed of monomorphic cells with round nucleus. Although mitotic figures (yellow arrows) are observed in all tumors, a higher number were observed in REH and control tumors. Macrophages are shown in KO1 clone (box in the upper left corner).

Annex IV

Paper IV. New Challenges in Targeting Signaling Pathways in Acute Lymphoblastic Leukemia by NGS Approaches. An Update

Adrián Montaño[1*], Maribel Forero-Castro[2*], Darnel Marchena-Mendoza[1,2], Rocío Benito[1&], Jesús-María Hernández-Rivas[3&**]

**AM, MFC, &RB, JMHR contributed equally to this work. **Correspondence.*

[1] IBSAL, IBMCC, Universidad de Salamanca-CSIC, Cancer Research Center; Salamanca; Spain. [2] Escuela de Ciencias Biológicas. Grupo de investigación en Ciencias Biomédicas (GICBUPTC). Universidad Pedagógica y Tecnológica de Colombia; Tunja; Colombia. [3] Universidad de Salamanca-CSIC, Hospital Universitario de Salamanca; Salamanca; Spain.

Cancers (Basel) 2018 Apr 7;10(4):110. doi: 10.3390/cancers10040110.

Supplementary material available online at:

https://www.mdpi.com/2072-6694/10/4/110#supplementary

cancers

MDPI

Review

New Challenges in Targeting Signaling Pathways in Acute Lymphoblastic Leukemia by NGS Approaches: An Update

Adrián Montaño [1,†], Maribel Forero-Castro [2,†], Darnel Marchena-Mendoza [1,2], Rocío Benito [1,†] and Jesús María Hernández-Rivas [3,*,†]

1 IBSAL, IBMCC, Universidad de Salamanca-CSIC, Cancer Research Center, 37007 Salamanca, Spain; adrianmo18@gmail.com (A.M.); darnelmarchena@hotmail.com (D.M.-M.); beniroc@usal.es (R.B.)
2 Escuela de Ciencias Biológicas, Grupo de investigación en Ciencias Biomédicas (GICBUPTC), Universidad Pedagógica y Tecnológica de Colombia, Tunja 150001, Colombia; maribel.forero@uptc.edu.co
3 Universidad de Salamanca-CSIC, Hospital Universitario de Salamanca, 37007 Salamanca, Spain
* Correspondence: jmhr@usal.es; Tel.: +34-923-291-384
† A.M., M.F.-C., R.B., J.M.H.-R. contributed equally to this work.

Received: 2 March 2018; Accepted: 5 April 2018; Published: 7 April 2018

Abstract: The identification and study of genetic alterations involved in various signaling pathways associated with the pathogenesis of acute lymphoblastic leukemia (ALL) and the application of recent next-generation sequencing (NGS) in the identification of these lesions not only broaden our understanding of the involvement of various genetic alterations in the pathogenesis of the disease but also identify new therapeutic targets for future clinical trials. The present review describes the main deletions, amplifications, sequence mutations, epigenetic lesions, and new structural DNA rearrangements detected by NGS in B-ALL and T-ALL and their clinical importance for therapeutic procedures. We reviewed the molecular basis of pathways including transcriptional regulation, lymphoid differentiation and development, TP53 and the cell cycle, RAS signaling, JAK/STAT, NOTCH, PI3K/AKT/mTOR, Wnt/β-catenin signaling, chromatin structure modifiers, and epigenetic regulators. The implementation of NGS strategies has enabled important mutated genes in each pathway, their associations with the genetic subtypes of ALL, and their outcomes, which will be described further. We also discuss classic and new cryptic DNA rearrangements in ALL identified by mRNA-seq strategies. Novel cooperative abnormalities in ALL could be key prognostic and/or predictive biomarkers for selecting the best frontline treatment and for developing therapies after the first relapse or refractory disease.

Keywords: NGS; mutations; fusion genes; pathways

1. Introduction

Acute lymphoblastic leukemia (ALL) is a malignant disorder originating from hematopoietic B- or T-cell precursors and is characterized by marked heterogeneity at the molecular and clinical levels. B-ALL and T-ALL comprise multiple subtypes defined by their primary chromosomal abnormality (mainly chromosomal translocations that give rise to chimeric fusion genes or broad aneuploidy) and defined by the cooperating secondary aberrations (deletions, amplifications, sequence mutations, and epigenetic lesions), which jointly contribute to leukemogenesis [1,2].

Although a genetic event is known to occur in the majority of cases and may be associated with outcome prediction, around 25% to 30% of pediatric and 50% of adult ALL patients have no defined genetic hallmarks of biological or clinical significance [1]. Given the increasing number of these

alterations, cytogenetics and FISH, which are methods commonly used in molecular biology, as well as small sequencing panels that focus on a limited number of genes may not be sufficient to identify new cryptic lesions especially those in lymphoid malignancies [3].

The introduction and rapid spread of DNA copy-number analysis and genome-wide DNA/RNA sequencing analysis have shown that ALL subgroups are characterized by numerous cooperating oncogenic lesions that affect genes with an established role in the proliferation and establishment of the leukemic clone. Recently, next-generation sequencing (NGS) technologies have identified many novel lesions in ALL and helped not only improve our understanding of its pathogenesis, but also helped to discover key biomarkers of diagnostic and prognostic importance [4]. The concept of NGS involves DNA, RNA, or miRNA sequencing through various approaches such as targeted sequencing, whole-exome sequencing (WES), transcriptome sequencing (messenger mRNA [mRNA-seq]), whole-genome sequencing (WGS), and epigenomics [5].

These technologies have enabled new genetic alterations to be characterized that include somatic structural DNA rearrangements, deletions of genes involved in differentiation and cell-cycle control, fusion genes that target B- or T-cell differentiation, and mutations (e.g., recurrent substitutions, indels) of genes. These mutations play crucial roles in key signaling pathways associated with the pathogenesis of ALL [1,5,6]. Similarly, many other genes become activated or inactivated due to the presence of specific somatic mutations (point or indel) or complex structural rearrangements or are affected by copy-number changes (deletions and/or amplifications) [7].

For this reason, next-generation sequencing is an important tool for detecting key genetic alterations, which directly conditions the prognosis, pathogenesis, and the evolution of patients. However, the clinical NGS applications come with great limitations. One of them is that NGS requires sophisticated bioinformatics systems, fast data processing, and large data storage capabilities, which can be costly. However, data interpretation remains a significant challenge due to the large number of variants detected by the huge molecular heterogeneity of the diseases.

In this review, we describe the alterations at the genetic level in the various signaling pathways associated with the pathogenesis of acute lymphoblastic leukemia (ALL) and the application of recent next-generation sequencing (NGS) not only for identifying and studying these lesions but also for identifying new therapeutic targets for future clinical trials.

2. Genomic Heterogeneity in Molecular Subtypes of ALL

The WHO classification divides ALL in relation to the presence of primary genetic abnormalities and it is well known that the incidence, clinical, and biological characteristics of these alterations vary with age. Additionally, many of the characteristics are strong, independent predictive factors of outcome [8,9]. As a consequence of implementation of new genomic technologies, new subtypes of ALL have been recognized in the 2016 revision of the WHO classification of myeloid neoplasms and acute leukemia [10]. This latest revision helps improve our understanding of the biology and molecular pathogenesis of ALL as well as the heterogeneity of its genetic subtypes [8,10]. Particularly, two new entities known as intrachromosomal amplification of chromosome 21 (iAMP21) and *BCR-ABL*-like B lymphoblastic leukemia/lymphoma have been recognized in the 'B lymphoblastic leukemia/lymphoma with recurrent genetic abnormalities' category [10]. A novel subgroup of T-ALL called immature early T-cell precursor leukemia (ETP-ALL) is the only subtype of T-ALL recognized as being a new entity in the 2016 WHO revision [3,10,11]. Supplemental file 1 shows the frequency and prognosis value of cytogenetic and molecular genetic abnormalities identified in ALL.

Based on the gene-expression profile analysis, in 2009 Den Boer et al. [12] and Mullighan et al. [13] independently identified a new high-risk subgroup of B-ALL called *BCR-ABL*-like or Ph-like. This group is characterized by a biological profile similar to the Philadelphia chromosome/*BCR-ABL* positive patients (Ph+) but without *BCR-ABL* fusion. It shares the same high risk of relapse and worse clinical outcome and responsiveness to tyrosine kinase inhibitors (TKIs) [8]. This subtype accounts for 15% of B-ALL, which comprises the 10% of cases of childhood B-ALL and 20% of the cases of

adult B-ALL with a peak prevalence of 28% in young adults (aged 21 to 39 years) [1,14]. Recently with NGS-based methods, a spectrum of genetic abnormalities have been detected in BCR-ABL-like ALL that extends our understanding of this leukemic subgroup, but because these are still no determinants in the diagnosis, other techniques such as FISH remain necessary. These cooperating lesions comprise the somatic mutations and gene fusions that are the most frequent lesions associated with pathogenesis of Ph-like ALL [15]. Common genomic lesions of *BCR-ABL*-like ALL include the B-lymphoid transcription factor genes (particularly *IKZF1* deletions), somatic mutations in JAK-STAT and RAS signaling (*NRAS*, *KRAS*, *PTPN11*, *NF1*), and, less commonly, kinase alterations (*FLT3*, *NTRK3*, *BLNK*, *TYK2*, *PTK2B*). Structural rearrangements have also been identified in this ALL subgroup, which affects the *CRLF2* gene, ABL-class tyrosine kinase genes, and *JAK2* and *EPOR* genes [1].

Intrachromosomal amplification of chromosome 21 (iAMP21) is a distinct subgroup of childhood ALL that is present in 2% of older children and has also been associated with a poorer outcome that improves with intensive treatment [1,10]. This abnormality has been confirmed to be a primary genetic event in B-ALL [16] and has been identified when three or more additional copies of *RUNX1* (*AML1*) are observed on a single abnormal chromosome 21 (including a total of five or more *RUNX1* copies per cell) [10,17]. iAMP is a distinct marker caused by the breakage-fusion-bridge cycle and chromothripsis, which involves tens to hundreds of genomic rearrangements with multiple regions of gain, amplification, inversion, and deletion [10,18,19].

Finally, ETP-ALL expressing ETP/stem cell genes were recently identified by whole-genome expression profiling. This new T-ALL subgroup is characterized by a high mutation load and worse survival rates than those of other T-ALL subgroups [3,10,11]. Multiple recurrent genomic lesions have recently been identified in this heterogeneous subgroup in which notable examples include the aberrant expression of the transcription factor *LYL1* and the t(2;14)(q22;q32) translocation that affects the *BCL11B* (14q32) and *ZEB2* (2q22) genes. This results in the sustained overexpression of *ZEB2*, which enhances the leukemic stem cell properties [11,20].

3. The Mutational Landscape in Signaling Pathways Involved in ALL

Somatic mutations drive oncogenic processes that promote the arrest of differentiation or can contribute to leukemogenesis by altering a wide range of cellular processes (cell cycle, epigenetic gene regulation, and apoptosis), which ultimately leads to the constitutive activation of crucial intracellular pathways associated with pathogenesis of ALL [21]. In recent years, various NGS studies of childhood and adult B-ALL and T-ALL have revealed a spectrum of somatic mutations in several genes involved in multiple canonical and non-canonical signaling pathways of ALL, such us transcriptional regulation, lymphoid differentiation and development, *TP53* and the cell cycle, *RAS* signaling, *JAK/STAT*, *NOTCH*, *PI3K/AKT/mTOR*, Wnt/β-catenin signaling, chromatin structure modifiers, and epigenetic regulators.

In particular, somatic mutations in several genes have been identified by NGS in B-ALL. These include genes associated with B-cell differentiation and development (18%; e.g., *PAX5*, *IKZF1*, *EBF1*), RAS signaling (48%; e.g., *NRAS*, *KRAS*, *PTPN11*, *FLT3*, *NF1*), JAK/STAT signaling (11%; e.g., *JAK1*, *JAK2*, *IL7R*, *CRLF2*), cell cycle regulation and tumor suppression (6%; e.g., *TP53*, *RB1*, *CDKN2A/B*), and non-canonical pathways or other/unknown genes (17%; e.g., *CREBBP*, *NT5C2*, *TBL1XR1* [22,23]. At the same time, in T-ALL, somatic mutations in the *NOTCH* signaling pathway (60%; e.g., *NOTCH1*, *NOTCH2*, *NOTCH3*, *FBXW7*, *HES1*, *JAG1*, *JAG2*), transcription factors (9–17%; e.g., *LMO2*, *TAL1(SCL)*, *TLX3*, *WT1*, *BCL11B*, *LEF1*, *ETV6*), RAS signaling (15%; e.g., *NRAS*, *KRAS*, *FLT3*, *CBL*), JAK/STAT signaling (20–30%; e.g., *JAK1*, *JAK2*, *JAK3*, *IL7R*, *STAT5B*) [24,25], PI3K/AKT/mTOR signaling (85%; e.g., *PIK3CA*, *AKT1*, *mTOR*, *PTEN*), Wnt/β-catenin signaling pathway (13%; e.g., *FAT1*, *FAT3*, *LEF1*) [24], chromatin structure modifiers and epigenetic regulators (35%; e.g., *PHF6*, *EZH2*, *DNMT3A*) [24], ribosomal processes (*RPL5*, *RPL10*, *RPL22* [25,26]), and recently discovered novel recurrent mutations in the DNA repair complex (*HER1/EGFR*), splicing factor (*ZRSR2*) [24], and various other functions (e.g., *WT1*, *CNOT3* [26], *NT5C2*, *MEF2C*) [11,24,25,27,28]. Figure 1 illustrates the pathways and significantly mutated genes in ALL and Figure 2 shows the frequency of somatic

mutations identified in ALL by using NGS methods. Supplemental file 2 details the references of Figure 2.

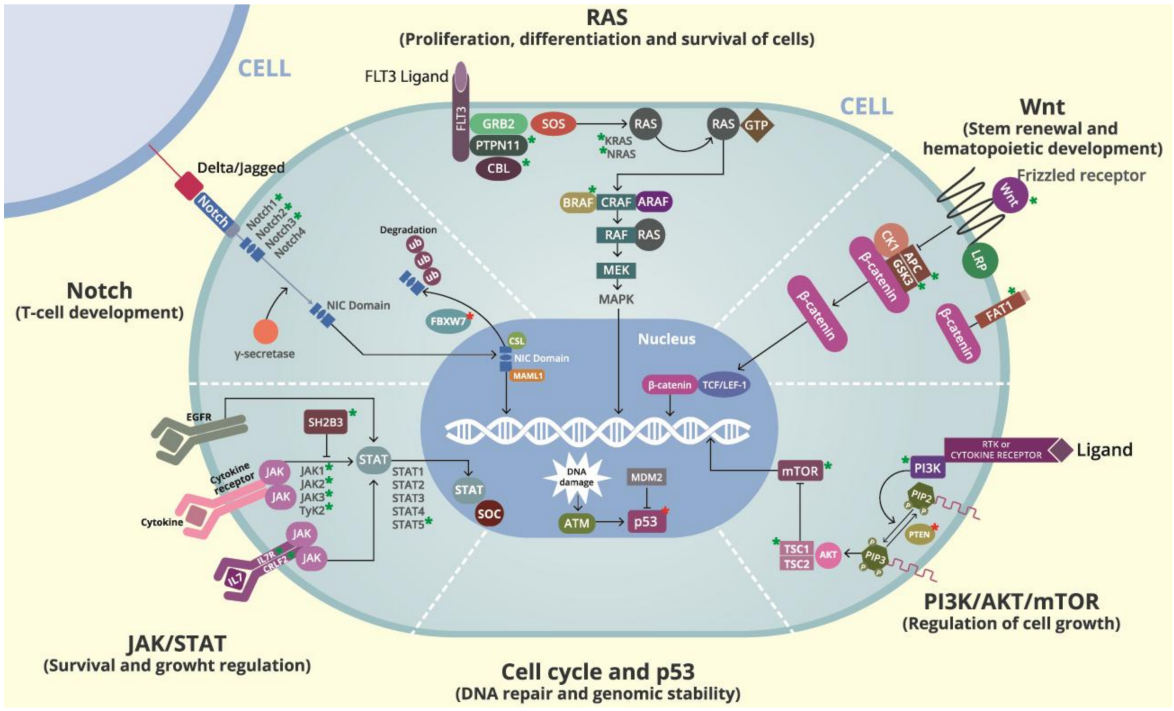

Figure 1. Cellular pathways affected by genes significantly mutated in ALL. Asterisks show the genes that are mutated in each cellular program and the biological effect of these mutations on the pathway (Green: activation mutation; Red: inactivating mutation).

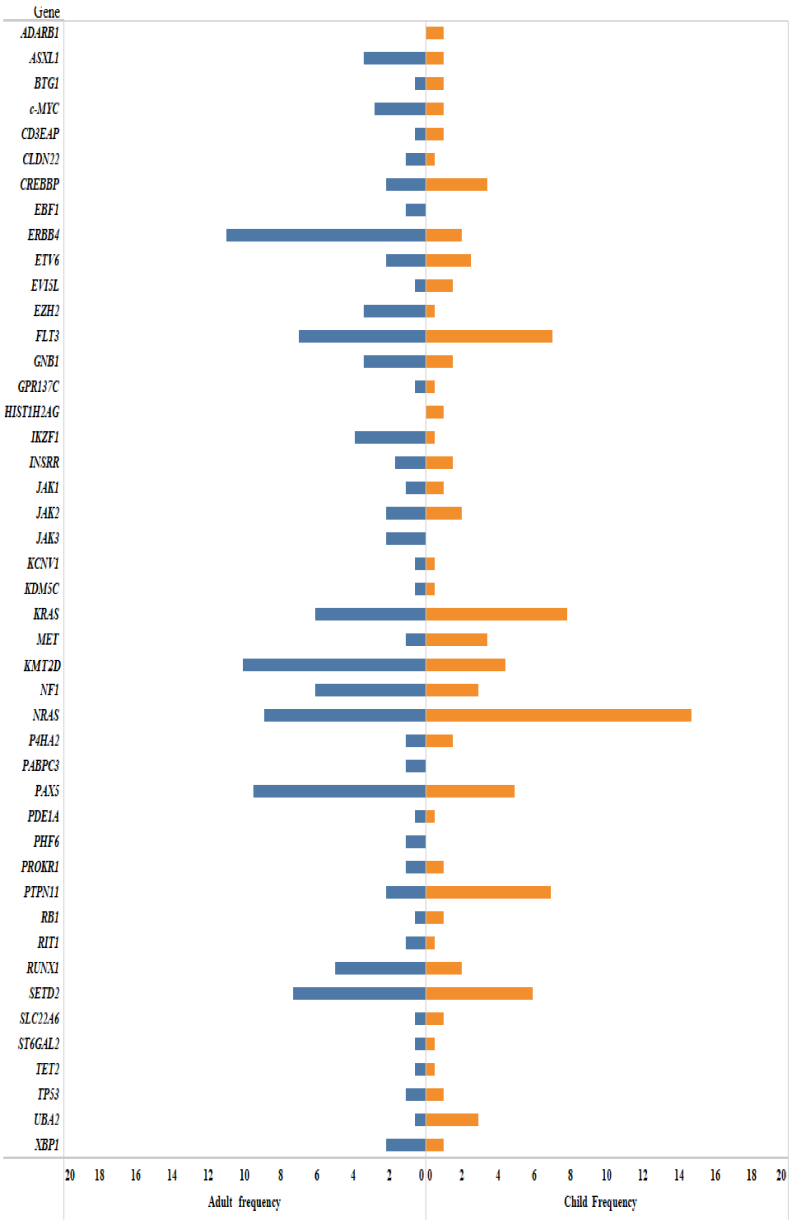

(A)

Figure 2. *Cont.*

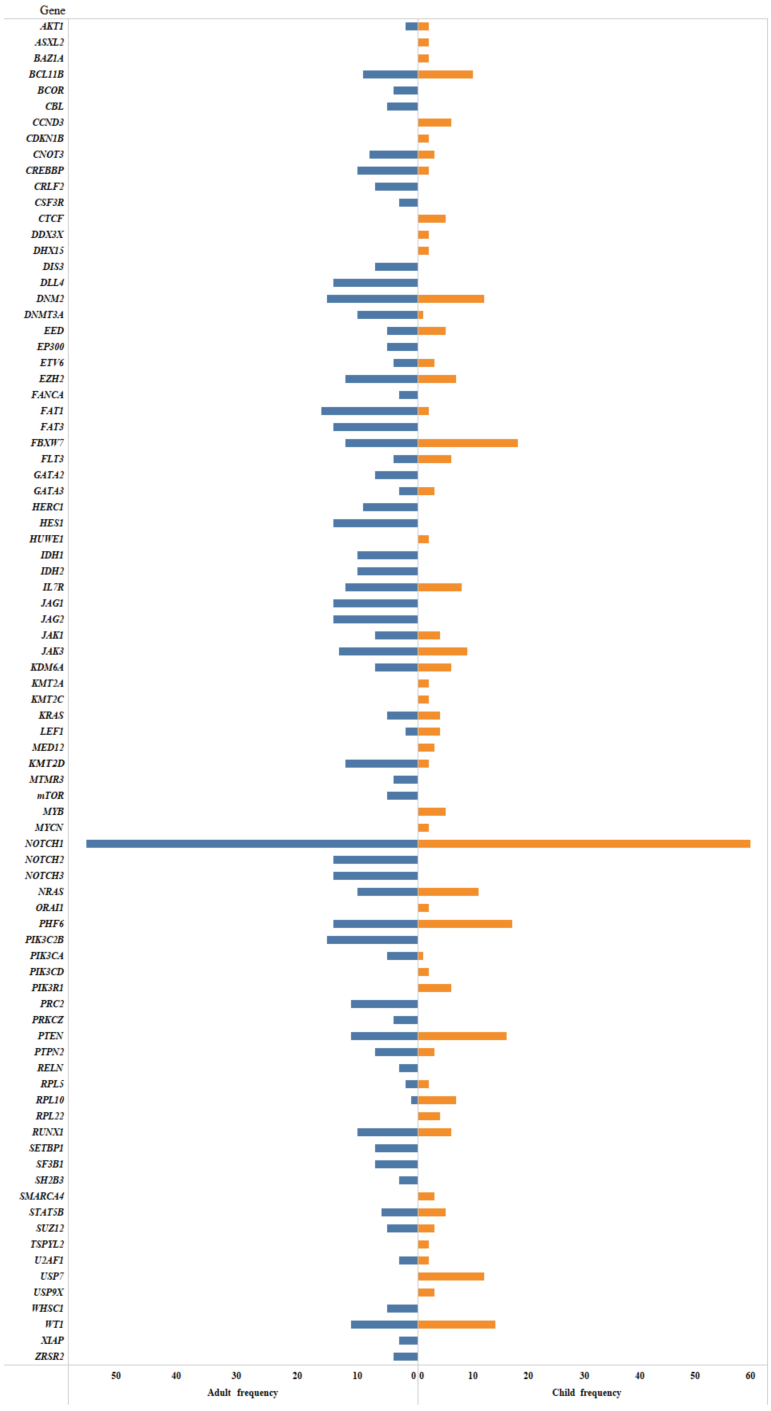

(**B**)

Figure 2. (**A**) Frequency of somatic mutations identified by NGS methods in B-ALL. The figure shows the frequency of somatic mutations in childhood and adult B-ALL. (**B**) Frequency of somatic mutations identified by NGS methods in T-ALL. The figure shows the frequency of somatic mutations in childhood and adult T-ALL.

3.1. Transcriptional Regulation and Lymphoid Differentiation and Development

Gene transcription plays a critical role in controlling normal hematopoietic differentiation. Transcription factors strongly influence cellular lineage during hematopoiesis and their genetic alterations can alter the normal mechanisms that control lymphoid differentiation and development.

Lymphoid cells are derived from pluripotent hematopoietic stem cells present in the bone marrow through stepwise maturation. This process is tightly controlled by the hierarchical activation of transcription factors and selection through functional signal transduction. The emergence of secondary genetic alterations such as deletions, amplifications, mutations, and structural rearrangements in key transcription factors disrupts lymphoid development and results in the arrest of maturation of B-lineages and T-lineages [24,29].

Important transcriptional factors involved in lymphoid development and differentiation (*EBF1*, *ETV6*, *PAX5*, *RUNX1*, and *TCF3*) participate in structural rearrangements. Many of these transcriptional factors are identified by RNA-sequencing methods, which will be described later.

NGS studies have found somatic mutations in different transcription factors involved in the pathogenesis of T-ALL such as inactivating mutations in *BCL11B*, *ETV6*, *GATA3*, *LEF1*, *RUNX1*, and *WT1* genes [11,25]. Somatic mutations in *BTG1*, *c-MYC*, *ERG*, *ETV6*, *IKZF1*, *IKZF2*, *IKZF3*, *LEF1*, *PAX5*, and *TBL1XR1* have been detected in B-ALL [29]. Sequencing the *IKZF1* gene has revealed a low frequency of somatic point mutations in B-ALL [13]. However, inherited genetic variants and rare deleterious mutations in the *IKZF1* gene play a role in the risk of developing B-ALL. *IKZF1* encodes the transcription factor IKAROS, which is indispensable for the induction of B-lineage differentiation in hematopoietic stem cells. As shown in murine models, their mutations have been recognized as being some of the most detrimental driver mutations in ALL by accelerating the onset of B-ALL in in vivo assays [1,4,29]. Deletion and mutation of other genes essential to B-cell development including *EBF1*, *RAG1*, *RAG2* and *LEF1* are also frequently detected in B-ALL [30].

Acquired somatic lesions in transcription factors correspond to non-synonymous single-nucleotide substitutions as well as frameshift and nonsense changes [11]. However, some genes such as *BCL11B*, *ETV6*, *ERG*, *GATA3*, *LEF1*, *LMO2*, *RUNX1*, *TAL1(SCL)*, *TLX1*, and *WT1* harbor some deletions in ALL cases that are difficult to detect by using NGS methods.

Focal deletions and sequence mutations in the *IKZF1* gene have been found in 15% of pediatric B-ALL and more than 80% of *BCR-ABL* cases. Recurrent mutations of *PAX5* occur in about one-third of B-ALL cases and in up to 50% of *BCR-ABL* positive cases. *EBF1* mutations occur in about 14% of *BCR-ABL* positive cases [31]. More than 80% of *BCR-ABL*-like patients have one or more alterations in genes involved in B-cell development including *IKAROS (IKZF1)*, *E2A (TCF3)*, *EBF1*, *PAX5*, and *VPREB1* [12].

IKZF2 mutations are hallmarks of low hypodiploid B-ALL. On the other hand, most cases of near-haploid ALL have a high frequency of *IKZF3* alterations [5,32]. *ETV6* mutations are found in rare B-ALL cases [30]. Deletions in *IKZF1*, *CDKN2A*, *PAX5*, *ETV6*, *RB1*, and *TCF3* genes or unbalanced translocations have been observed in high hyperdiploid B-ALL [33]. Loss-of-function mutations in transcription factors acting as hematopoietic regulators (*GATA3*, *IKZF1*, *RUNX1*, *ETV6*) have been described in ETP-ALL [5,11,27,34].

Clinical studies have demonstrated that *LEF1* mutations are associated with a favorable outcome in ALL [35]. By contrast, *IKZF1* alterations (mutation/deletion) confer resistance to therapy and promote disease relapse [4]. Similarly, *RUNX1* mutations have been associated with poor outcomes in ALL. These mutations are generally distributed across several exons but are mainly clustered in the RUNT domain (amino acids 50–177; e.g., Cys72Tyr and Arg174X) and less frequently in the TAD domain (amino acids 291–371; e.g., Pro332_Val333insTrpGly and Ile337ValfsX231) [36,37]. In particular, the high incidence of *RUNX1* mutations in early T-ALL makes the gene a novel biomarker for T-ALL because the mutations have revealed its important role in early hematopoietic development [36,37].

On the other hand, it should be noted that the B-cell receptor signaling pathway (pre-BCR signaling) is a crucial pathway early on in B-cell development. The *BTK* gene, which is essential for B-cell development, participates in this pathway. This gene is deregulated in pre-BCR ALL patients. Pre-B signaling leads to leukemic cell proliferation except in some cells that have a secondary alteration, which occurs in ALL *BCR-ABL*-positive cases. Around 15% of ALL patients are dependent on pre-BCR signaling and have been shown to be sensitive to BCR inhibitors [38–40].

3.2. RAS Signaling Pathway

The RAS signaling pathway is important for the proliferation, differentiation, and survival of the cell. Alterations in its function promote tumor transformation. Three *RAS* genes participate in this pathway including *H-RAS*, *K-RAS*, and *N-RAS*. RAS proteins are activated by guanine-nucleotide exchange factors (GEFs), inactivated by hydrolysis of GTP due to its intrinsic GTPase activity, and accelerated by the action of GTPase-activating protein (GAP). RAS activation is initiated by tyrosine kinase receptors like the epithelial growth factor receptor (EGFR), the platelet-derived growth factor receptor, and the insulin receptor. Once activated, RAS can orchestrate its effects through three major downstream pathways including the RAF family protein (C-Raf, B-Raf, A-Raf), which activates the mitogen-activated protein kinase (MAPK) to promote cell proliferation, differentiation, survival, inflammation, and the inhibition of apoptosis. Lastly, the RAS-like guanine nucleotide-dissociation stimulator (RalGDS) cascade participates in a wide variety of cellular processes [41,42] (see Figure 1).

NGS studies have identified oncogenic gain-of-function mutations in the *KRAS*, *NRAS*, *PTPN11*, *BRAF*, *FLT3*, *CBL*, and *CBLB* genes as well as loss of function mutations in the *NF1* gene, which is a negative regulator of the RAS pathway in patients with ALL [24,42,43]. The recurrent mutations in the RAS pathway involve the *KRAS* and *NRAS* genes [41]. Downstream or upstream mutations in elements of the RAS pathway constitutively activate RAS signaling by cooperating in B-lineage and T-lineage leukemogenesis [42].

Mutations in RAS genes involve mainly single nucleotide substitutions that generate missense and frameshift variations [41,43,44]. Activating mutations in *NRAS/KRAS* are recurrent in ALL. Besides the well-known hotspot mutations at codons 12, 13, and 61 (i.e., *NRAS* G13D, *KRAS*, and G12D/G13D), novel mutational sites have also been identified in ALL patients by using NGS methods (e.g., *KRAS:* V14I, V14L, K117N and A146T/P). These mutations are usually mutually exclusive, which suggests branching evolution and intra-tumoral heterogeneity [43].

NGS analysis has demonstrated that RAS pathway mutations are common in high hyperdiploid (85%), near-haploid (71%), *KMT2A(MLL1)*-rearrangements (47%), iAMP21 (60%), and ETP ALL (67%) subgroups [24,27,32,33,44,45]. In contrast, RTK- and Ras-signaling alterations are less frequent in low-near-diploid (31.8%), hypodiploid (8.8%), and non-ETP ALL (19%) cases [32].

Clinically, some sequencing studies have associated the RAS activating mutations with poor outcomes. Therefore, the presence of these mutations has been recognized as an independent predictor of poor outcome in childhood *KMT2A(MLL1)*-r ALL and the presence of *PTPN11* mutations has been associated with a good prognosis in adult B-ALL patients [46,47]. Not only do RAS mutation-positive patients have a high risk of relapse but also the prognosis for RAS mutation-negative patients remains far from favorable. Therefore, more studies are needed if we are to be able to predict the effect of RAS mutations in ALL patients [47]. The use of MAPK-ERK kinase (MEK) inhibitors and PI3K inhibitors has been proposed as a targeted therapy for the Ras/Raf/MEK/ERK signaling pathway in ALL [23,32].

3.3. JAK/STAT Signaling Pathway

Hematopoiesis is the cumulative result of intricately regulated signaling pathways that are mediated by cytokines and their receptors. Through this signaling pathway, cytokines control a variety of important biological responses related to hematopoiesis and immune function including those related to cell growth, differentiation, oncogenesis, and anti-apoptotic signals. The JAK-STAT signaling cascade consists of three main components. These are a cell surface receptor, a Janus kinase (JAK), and a two-signal transducer and activator of transcription (STAT) proteins. Mammals have four Janus kinases Jak1, Jak2, Jak3 (just another kinase) and Tyk2 (tyrosine kinase 2). The binding of various ligands, which are usually cytokines such as interferon (IFNα, IFNγ), interleukin (IL-7, IL-6), and growth factors, to cell surface receptors called GM-CSF activates associated JAKs, which increases their kinase activity. The activated STATs form heterodimers or homodimers and translocate to the cell nucleus where they induce transcription of target genes. The JAK/STAT pathway is negatively regulated at several levels (see Figure 1).

The suppressors of cytokine signaling (SOCS) are a family of STAT target genes that directly antagonize STAT activation, protein tyrosine phosphatases (PTPs) such as SRC homology2, SH2-domain-containing PTP1 (SHP1), and ubiquitin-mediated protein degradation [48].

Mutations in genes of this pathway (*JAK1*, *JAK2*, *JAK3*, *IL7R*) have been observed in B-ALL and T-ALL [24,25,49]. Mutations in *JAK* kinases and *IL7R* cause constitutive activation of the JAK-STAT pathway [27]. Activating mutations of JAKs genes (primarily *JAK2* but also *JAK1* and *JAK3*) are also associated with other genetic lesions such as *IKZF1* deletion or mutation and *CRLF2*- rearrangements (*CRFL2*-r) [49,50]. Similarly, loss-of-function mutations in the *SH2B3* gene, which is a negative regulator of *JAK2* signaling, have been identified in ALL. *SH2B3* mutations lead to the loss of regulatory functions and also lead to increased JAK2/STAT signaling [48].

JAK mutations are most commonly observed in the pseudokinase domain rather than in the kinase domain. They are usually missense mutations [51]. In particular, the missense mutations at the R683 position are common in the *JAK2* gene [49,51]. The acquired R683 *JAK2* mutations are biomarkers for B-ALL [52–54]. Recent studies have suggested that the amino acid residue p.R683 located in the linker between the N and C lobes of the JH2 domain is important for maintaining the activity, structural stability, and folding of JAK2 [55]. The mutations in p.R683 disrupt the structure of the JH2 domain, which leads to the constitutive activation of *JAK2* and the induced growth factor-independent cell proliferation of the mouse Ba/F3 hematopoietic cell line [49,53,55]. At the same time, gain-of-function mutations in the IL7R gene act as oncogenes in T-ALL and B-ALL by generally corresponding to in-frame insertions and indels in the transmembrane domain (e.g., p.L242_L243delinsLCP [49], 243InsPPCL, S185C, 246InsKCH, 241InsFSCGP, 244InsCHL, 244InsPPVCSVT [56], p.Leu242_Leu243insAsnProCys, p.Thr244_Ile245insCysProThr, p.Ile241_Thr244delinsSerAlaAsnCysGlyAla, p.Pro240_Ser246delins LeuGlnSerCys [57]).

JAK1 mutations have mainly been observed in T-ALL and high-risk B-ALL while *JAK2* mutations have been identified in Down syndrome [52] and high-risk B-ALL [34,54]. In Ph-like ALL, the patients show a high incidence of cytokine-signaling abnormalities. Mutations of *JAK* genes and *CRFL2*-r are often present in Ph-like ALL [50]. ETP ALL has also been characterized by activating mutations in *JAK1*, *JAK3*, *IL7R*, and *SH2B3* [5,34,58].

The constitutively active JAK/STAT signaling pathway results in uncontrolled proliferation of leukemia cells and has been associated with a poor outcome. JAK1/2 inhibitors (e.g., ruxolitinib) and epigenetic drugs could be useful for therapy of patients who harbor mutations in genes involved in the JAK/STAT signaling pathway [54,59]. It has recently been reported that mutations in the IL7R signaling components provide steroid resistance in T-ALL [58]. Therefore, *IL7R* signaling inhibitors could restore or enhance steroid sensitivity in patients with ALL and improve their clinical outcome [58].

3.4. TP53 and Cell Cycle Signaling Pathway

The tumor suppressor gene *TP53* is fundamental to cell cycle arrest, apoptosis, DNA repair, and genomic stability and its role in tumorigenesis is well recognized in solid and hematological malignancies. When DNA is damaged, *TP53* is activated and induces cell cycle arrest, which allows the cells to repair the damage. Alternatively, it can induce apoptosis if the DNA damage proves to be irreparable. Under normal conditions, p53 levels are low because it is associated with MDM2, which induces its ubiquitination and destruction by the proteasome [60] (see Figure 1).

CDKN2A is an important gene that codes for two proteins, which are ARF and p16. ARF regulates the *TP53* pathway by inhibiting MDM2 and the RB pathway through downregulation of tE2F-1 transcription. In addition, p16 phosphorylates RB, having been phosphorylated disassociates of the transcription factor E2F1, enters the nucleus and promotes the genes essential for transition from the G1 phase to the S phase. Inactivation of *CDKN2A* can lead to deregulation of the *TP53* and *RB* signaling pathways. In fact, both signaling pathways are altered in most human cancer cells [61].

In ALL, genomic alterations of *TP53* (mutation/deletion) are infrequent. Moreover, the *TP53* pathway is also deregulated by abnormalities other than mutations such as hypermethylation of genes

involved in the *TP53* cascade, deregulation of microRNAs (e.g., mir-126 and mir-181a), deletion of the *CDNK2A* gene, and overexpression of *MDM2* [62].

In ALL, *TP53* is usually inactivated by missense mutations that are distributed across several exons. The exons are predominantly found in evolutionarily conserved regions of this gene (e.g., L111P, T125R, R110C, H179D, C135R, Y205D, Y220C, M237I, P278S, R273P, C275F, D281N, and R282P) [49]. *TP53* mutations are uncommon in recurrent fusion genes [49,63] and are associated with patients who harbor low hypodiploidy/near triploid and *c-MYC*- rearrangements [5,32,64–66].

It should be noted that deletions of the *CDKN2A/B* and *RB1* suppressor genes are present in T-ALL (70% and 12%, respectively) and B-ALL (36% and 8%, respectively) in which they contribute to the disruption of the tumor suppressor pathways in ALL [11,67]. Deletions involving *CDKN2A/B* are also common in Ph+ ALL [31]. Genetic alterations involving the *RB1* gene are hallmarks of low-hypodiploid ALL [32].

The clinical importance of *TP53* abnormalities in ALL is tightly linked to poor prognosis and chemorefractoriness [49]. Although the *TP53* mutations are considered infrequent in ALL, these are important when it comes to relapse in childhood and adult ALL and independently predict a high-risk of treatment failure in a significant number of patients [49,68]. The presence of *TP53* mutations is associated with a reduced response rate to induction therapy [63] and with shorter survival [69]. At diagnosis, *TP53* lesions (mutation/deletion) in minor clones may confer resistance to therapy and promote disease relapse [4]. Likewise, recent studies have revealed that *TP53* mutations may also be correlated with a poor prognosis, refractoriness, and unfavorable CR rates in BLs treated with rituximab and intensive chemotherapy [70]. Currently, MDM2-targeted therapy is a promising anticancer alternative for restoring *TP53*-dependent mechanisms in ALL [62].

3.5. NOTCH Signaling Pathway

The *NOTCH* pathway is a signaling system in multicellular organisms that regulate cell proliferation, cell fate, differentiation, and apoptosis. The NOTCH receptor genes encode a family of heterodimeric transmembrane proteins (NOTCH1 to NOTCH4) that function as ligand-activated transcription factors. *NOTCH1*, *NOTCH2*, and *NOTCH3* play a pivotal role in committing cell lymphoid precursors to T-cell development. The NOTCH receptor consists of an extracellular subunit, a transmembrane subunit, and an intracellular subunit. Its activation requires cell-to-cell contact. Ligand receptor binding induces cleavage of the transmembrane subunit, which forms an intracellular cleaved form of NOTCH1 by involving the multiprotein protease complex (γ-secretase). Upon activation, the cleaved intracellular portion of the NOTCH receptors translocates into the nucleus and the NIC domain (NICD) binds the DNA-binding protein CSL as well as the SKIP protein. The trimeric complex then recruits the Mastermind-like protein (MAML), which in turn recruits additional co-activators that are required for the transcriptional regulation of the NOTCH target gene expression including the MYC and NF-kβ signaling components. Lastly, the most prominent mechanism of the NOTCH signal suppression operates through its PEST domain of the NICD, which is recognized by the FBXW7 ubiquitin protein ligase and directed towards proteasomal degradation and mediates the termination of NOTCH signaling in the nucleus [28] (see Figure 1).

In T-ALL, the constitutive activation of *NOTCH* signaling is the most prominent oncogenic pathway in T-cell transformation. The activation of this pathway occurs mainly by activating mutations of the *NOTCH1* gene and/or inactivating mutation of the *FBXW7* gene, which confers a strong growth advantage on the leukemic cell [71,72]. Activating mutations in *NOTCH1* have been identified in more than 50% of patients [24,73] and mutations in the *NOTCH2* gene have recently been found especially in adult T-ALL [24].

NOTCH1-activating mutations localized in the heterodimerization domain (HD) are mostly missense or short in-frame insertions or deletions and result in ligand-independent activation of the receptor while mutations of the negative regulatory PEST domain corresponding to indels increase NICD stability and the consequent half-life of active intracellular NOTCH1, which leads to constitutive activation of the

pathway [28,71]. At the same time, *FBXW7*-inactivating mutations are mainly of the missense type and localized at conserved amino-acid positions where they boost NOTCH1 protein stability [24,25].

Oncogenic NOTCH activation is not characteristic of B-ALL, but NOTCH1 and NOTCH2 mutations have been identified in other B-cell malignancies such as chronic lymphocytic leukemia (CLL), splenic marginal zone lymphoma (SMZL), mantle cell lymphoma (MCL), diffuse large B-cell lymphoma (DLBCL) and, rarely, follicular lymphoma (FL) [74].

Although the clinical involvement of *NOTCH1* and *FBXW7* mutations have often been associated with a favorable outcome in T-ALL, its prognostic value is controversial [28]. In T-ALL, *NOTCH1* mutations have been associated with an improved response to glucocorticoids [27]. *NOTCH* inhibitors have been used in combination with inhibitors of the *PI3K/AKT/mTOR* pathway in in vivo assays [27]. Therapeutic antibody targeting of NOTCH1 in T-ALL in combination with other drugs (e.g., glucocorticoids and dexamethasone) as a therapeutic alternative for the clinical management of T-ALL has also been tested with in vitro and in vivo assays [28,75].

3.6. PI3K/AKT/mTOR Signaling Pathway

The *PI3K/AKT/mTOR* signaling pathway is mainly involved in regulating cell growth, cell proliferation, cell motility, differentiation, inhibition of apoptosis, and modification of metabolism. In response to the exogenous growth factor or cytokine stimulation, receptor tyrosine kinases (RTKs) or G protein-coupled receptors (GPCRs) are activated and PI3Ks are recruited to the cellular membrane. PI3Ks are divided into three classes on the basis of their structures and substrate specificities [76]. Class IA PI3Ks (*PIK3CA*, *PIK3CB*, and *PIK3CD*) are the most important isoforms in cancer. They consist of a p110 catalytic domain and a non-catalytic domain, p85. PI3K phosphorylates PIP2 generate the second messenger, PIP3. This signaling cascade eventually leads to AKT activation through phosphorylation by PDK1 and the mTORC 1/2 complexes. In turn, AKT phosphorylates and several cellular proteins regulate cellular processes including cell growth. The most important negative control mechanism of this signaling pathway occurs through *PTEN* gene, which mediates the PIP3 transformation to PIP2. This inhibits the downstream cascade [77] (see Figure 1).

The PI3K/Akt/mTOR signaling pathway is often activated in leukemia and is involved in leukemogenesis [78]. Constitutive activation of this pathway results in enhanced cell metabolism, proliferation, and impaired apoptosis [11]. Its activation is a result of genetic lesions in *PI3K* genes and downstream effectors of the cascade such as *AKT* and *mTOR*. In particular, *PIK3CA* (PI3K-alpha) is a commonly mutated oncogene in T-ALL [11]. Mutational activation and overexpression of this class IA PI3K results in enhanced PI3K signaling, which is associated with oncogenic cellular transformation and cancer [79]. Inactivating mutations in the *PTEN* gene have also been observed in T-ALL patients [24,25]. *PTEN* is the main negative regulator of the PI3K-AKT pathway and its genetic lesions (mutations or deletions) trigger the hyperactivation of this oncogenic pathway in T-ALL due to the increase in AKT1 kinase activity [11].

PIK3CA mutations are mainly non-synonymous and arise from single nucleotide substitutions [79]. In addition, missense, silent, and nonsense mutations due to insertions and/or deletions have been described in *PTEN* [11].

Alterations of the *PI3K/AKT/mTOR* pathway are predominant in T-ALL (85% of cases) with respect to other leukemia types including B-ALL [80]. Moreover, *PTEN* mutations are common in T-ALL and infrequent in B-ALL [24,81]. In T-ALL patients, sequencing studies of *PTEN* have identified non-synonymous sequence mutations (nonsense or frame-shift mutations) affecting mainly exon 7. Most of these mutations correspond to small insertions or indels that truncate the protein by the premature termination of translation (e.g., Leu247fsX12, Glu242fsX15, Arg234indel, and Gly230fsX12) [82].

Within B-ALL, *PI3K/AKT/mTOR* mutations have been identified in near-haploid, low-hypodiploid, and *BCR-ABL* subgroups [83]. A marked induction of mTOR signaling occurs in *CRLF2*-rearrangements in B-ALL [81]. Moreover, although *KMT2A (MLL1)*-r has one of the lowest frequencies of somatic

mutations in childhood B-ALL, mutations in kinase-*PI3K-RAS* signaling pathway components (*FLT3*, *KRAS*, *NRAS*, *NF1*, *PTPN11*, *PIK3CA*, and *PIK3R1*) have been described in 47% of these cases [45].

From the clinical point of view, the PI3K/Akt/mTOR signaling pathway has been reported to act in T-ALL, which causes a poor prognosis and a limited response to therapy [78]. *PTEN* mutations have been associated with poor outcome in ALL. *AKT1* mutations promote glucocorticoid resistance, which is an important indicator of therapeutic failure in T-ALL [81]. PI3K inhibitors are currently being developed for clinical use in patients with mutations in genes involved in PI3K-signaling pathways [78,83]. Combined therapy to treat ALL such as *BCR-ABL* TKIs with a panel of selective PI3K/AKT/mTOR inhibitors in *NUP214(CAN)-ABL*-positive T-ALL cell lines [78] and the JAK and PI3K inhibitors ruxolitinib and rapamycin in *CRLF2*-r and JAK-mutated disease [23] are being investigated to maximize the anti-neoplastic effect of different molecular lesions in leukemic cells.

3.7. Wnt/β-Catenin Signaling Pathway

The Wnt signaling pathway is an evolutionarily conserved mechanism that is crucial for the normal development of hematopoietic stem cells (HSCs) and B-cells. Hematopoietic progenitor cells express Wnt proteins and their receptors while responding to Wnt proteins by increasing proliferation. Canonical activation usually involves Wnt protein binding to two receptor molecules, Frizzled (Fzd), which belongs to a class of seven-pass transmembrane receptors and lipoprotein receptor-related proteins 5 or 6 (LRP5/6). Wnt induces the formation of the Fzd-LRP5/6 complex to activate the Wnt signaling pathway. Without Wnt activation, β-catenin (CTNNB1) is phosphorylated by the multi-protein destruction complex and is subject to proteasomal degradation. The cellular concentration of free β-catenin is low because the APC/GSK-3/Axin complex of the adenomatous polyposis coli (APC), the glycogen synthase kinase 3β (GSK-3β), and the axin protein is responsible for regulating the level of β-catenin via GSK-3β-mediated phosphorylation of specific serin and threonine residues in β-catenin. The union of Wnt to its receptors induces the destruction of the β-catenin complex, which falls apart and leads to an excess of β-catenin accumulating in the cytoplasm. Some β-catenin is then able to enter the nucleus and cooperate with the T-cell factor (TCF) transcription factors to activate gene expression of Wnt target genes such as *LEF-1*, *c-MYC*, and cyclin D1. TCF is often in an inactive state in the nucleus. NOTCH and WNT are major players in T-cell development and self-renewal of hematopoietic stem cells pathways. In particular, they are required to turn early T-lineage into single-positive T-cells [84] (see Figure 1).

Inactivating mutations in the Fat cadherin genes *FAT1* and *FAT3* have been described in B-ALL and T-ALL [24,25,46]. These genes encode members of the FAT protocadherin family, which is a group of transmembrane proteins characterized by the presence of cadherin-type repeats. The mutational inactivation of *FAT1* has been linked to the loss of its tumor suppressor capacity and the activation of the WNT pathway [85]. Their inactivating mutations are mainly located within the cadherin domains and are predominantly missense mutations (e.g., R227C, R806C, N1594K, I1719V, and E1769G) [86].

On the other hand, mutations in the *LEF1* gene, which is of great importance in the WNT pathway, have also been described. *LEF1* also presents deletions that are difficult to detect by using NGS methods [24]. *LEF1* mutations are mainly single nucleotide substitutions that generate missense variations (e.g., H86E, K86E, and P106L) [87,88] and have been described in childhood and adult T-ALL [24].

Clinically, *LEF1*-inactivating mutations show a favorable trend towards overall survival in pediatric patients with T-ALL, which suggests that this molecular subtype of the disease may be more responsive than other subtypes to salvage therapy for relapsed T-ALL [87].

3.8. Chromatin Structure Modifiers and Epigenetic Regulators

Epigenetic mechanisms are essential factors in normal cell development and functioning. Their alteration is a central feature of cancer development. A spectrum of epigenetic regulators and chromatin structure modifiers involved in DNA methylation and histone protein modifications are part of these mechanisms. DNA hyper-methylation leads to the loss of expression of the

associated genes. Many important tumor suppressor genes are inactivated by this mechanism. On the other hand, hypo-methylation promotes cancer development through chromosomal instability (by recombination or translocation), reactivation of transposons, and loss of imprinting. Additionally, histone modifications involve acetylation and methylation processes. Acetylation results in a transcriptional activation state while de-acetylation results in a transcriptional loss of expression. The consequences of histone methylation depend on the residue and location modified [89].

ALL may feature somatic mutations in epigenetic regulators such as DNA methylation modifiers (e.g., *DNMT3A*, *TET2*, *IDH1*, and *IDH2*), histone modifiers (e.g., members of polycomb repressive complex 2 [PRC2], such as *SUZ12*, *EZH2*, *EED*, and *EP300*) and histone methyltransferases (e.g., *KMT2D(MLL2)* and *WHSC1*) [11,24]. Likewise, mutations in chromatin structure modifiers such as *PHF6* have been described in ALL [11,90,91]. It should be noted that recurrent inactivating mutations in *SETD2*, *CREBBP*, *KDM6A*, and *NR3C1* have been detected in relapsed ALL [92].

Oncogenic activating mutations in epigenetic modifiers (i.e., *IDH1/2*, *EZH2*, and *DNMT3A*) and inactivating mutations in chromatin modifiers (i.e., *KDM6A*, *CREBBP*, *EP300*, and *SMARCB1*) have been observed in ALL [24,93]. Acquired somatic lesions of chromatin structure modifiers and epigenetic regulators correspond to non-synonymous single nucleotide substitutions, frameshift, and nonsense changes [90–92,94]. Some of these genes such as *CREBBP*, *EED*, *EZH2*, *KDM6A*, *PHF6*, and *SUZ12* harbor deletions in ALL cases [11,27].

Epigenetic alterations are highly prevalent in both B-ALL and T-ALL [5,11,24,34,38,95]. Specifically, B-ALL may feature mutations in histone acetyltransferase *CREBBP* (18% in relapse ALL, rare in cases without high hyperdiploidy), methyltransferases known as *WHSC1* (14–20% in *ETV6-RUNX1* and 15% in rearranged *TCF3-PBX1*), *SETD2* (12%, *KMT2A(MLL1)*- and *ETV6-RUNX1* rearranged), *EZH2* (1.3%, hypodiploidy), phosphorylases known as *JAK2* (10% in high-risk disease, *BCR-ABL*-like, Down syndrome, high-risk disease), *KMT2A(MLL1)* (5%), and *EP300* (<1%) [33,96–98]. Somatic mutations of *CREBBP*, *WHSC1*, *KMT5B (SUV420H1)*, *SETD2*, and *EZH2* genes have been identified in high hyper-diploid childhood B-ALL [99,100].

Somatic mutations of genes involved in epigenetic functions and chromatin remodeling such as *PHF6* (11%), *KMT2D(MLL2)* (12%), *DNMT3A* (5%), *TET2* (5%), *SUZ12* (5%), and *EP300* (5%) have been identified in T-ALL [5,11,24,34]. Particularly, somatic mutations in the chromatin structure and epigenetic regulators such as *EZH2*, *SUZ12*, *EED*, *SETD2*, *DNMT3A*, and *EP300* have been found in ETP-ALL [5,24,34].

Epigenetic alterations are highly prevalent in ALL and raise the possibility that novel biomarkers could predict patient outcome [95]. *PHF6* and *DNMT3A* mutations are associated with poor outcomes in ALL [35,37]. Alterations (mutation/deletion) in the *CREBBP* gene, which is an important chromatin structure modifier, are acquired at relapse or are already present at diagnosis. They are sometimes located in subclones, which suggests their resistance to therapy (e.g., with glucocorticoids). They also promote disease relapse [4,96]. It has recently been proposed that inhibitors of the epigenetic regulator gene *EZH2* could be useful for the therapy of patients with mutations in that gene [24].

Chromatin modifiers recurrently altered in B-ALL and associated with disease outcomes include *KMT2A(MLL1)*, *CREBBP*, *WHSC1*, and *SETD2*. Clinical trials of drugs potentially targeting histone in ALL patients have been completed and others are underway. For example, in the relapsed and refractory disease, histone deacetylase inhibitors (HDACis) such as FR901228, vorinostat, panobinostat, and *JAK1/JAK2* inhibitors like ruxolitinib have been tested in phase I and II clinical trials [96].

4. Landscape of New Structural DNA Rearrangements Detected by NGS

As already indicated, B-ALL and T-ALL comprise heterogeneous subtypes defined by the presence of primary chromosomal abnormalities that are usually chromosomal translocations that help define the particular subtypes of ALL. Although new subtypes of ALL have been recognized in the 2016 revision in the WHO classification of myeloid neoplasms and acute leukemia [10], the classical structural DNA rearrangements described in this disease maintain their biological and clinical importance to their diagnosis and classification and maintain the establishment of therapeutic regimens.

ALL is the neoplasia in which the greatest number of translocations (more than one thousand) has been described of which more than 150 are recurrent and involve at least 82 fusion genes. Within B-ALL, the structural DNA rearrangements are part of the recurrent genetic abnormalities associated with this disease including hyperdiploidy, hypodiploidy, t(12;21)(p13;q22) *TEL-AML1*(*ETV6-RUNX1*), t(v;11q23) *KMT2A(MLL1)* rearranged, t(1;19)(q23;p13.3) *E2A*(*TCF3)-PBX1*, t(9;22)(q34;q11.2) *BCR-ABL(ABL1)*, t(5;14)(q31;q32) *IL3-IGH*, iAMP21, and *BCR-ABL*-like [9]. It is believed that some of the disruptions appear during fetal development especially in the case of childhood leukemia with rearrangements of the *KMT2A (MLL1)* gene and ALL with *TEL-AML1*(*ETV6-RUNX1*) translocation [4]. Important cytogenetic abnormalities in B-ALL that are associated with a poor prognosis include *KMT2A(MLL1)-AF4(AFF1)* fusion gene and hypodiploidy with fewer than 45 chromosomes. *BCR-ABL* and Philadelphia chromosome-positive (Ph+) ALL, which is commonly associated with poor outcomes, have improved their prognosis by using TKIs. In contrast, *TEL-AML1(ETV6-RUNX1)* translocation and hyperdiploidy are commonly present in childhood ALL and are subtypes associated with a favorable outcome.

In addition, in T-ALL, the T-cell receptor (TCR) and non-TCR rearrangements involve mostly chromosomal translocations as primary genetic changes in this disease. Unlike B-ALL, the clinical relevance of most subtypes of T-ALL are either unclear or controversial [3]. Gene expression profiling, cytogenetics, and immunophenotypic analyses have been used to identify nonrandom genetic lesions in T-ALL corresponding to rearrangements involving TCR genes (*TCRA/TRAC* (14q11), *TCRB/TRB* (7q34-35), *TCRG/TRG* (7p15), and *TCRD/TRD* (14q11)) and lesions with known oncogenes [101]. These lesions are usually reciprocal translocations and occur at a lower frequency than deletions, duplications, and inversions. Numerical changes are rare except for tetraploidy, which is seen in approximately 5% of cases [102].

TCR genetic lesions lead to the irregular transcription of the partner gene by juxtaposition with the regulatory region of one of the TCR loci [101]. Partner genes usually correspond to important transcription factors involved in T-cell differentiation so their deregulation disrupts normal hematopoiesis and triggers T-ALL [7]. The partner genes usually affected by these rearrangements are *TLX1/HOX11* (10q24), *TLX3/HOX11L2* (5q35), *TAL1/SCL* (1p32), *TAL2* (9q34), *LMO2/RBTN2* (11p13), *LYL1* (19p13), *BHLHB1/OLIG2* (21q22), *LMO1/RBTN1* (11p15), *LCK* (1p34), *NOTCH1/TAN1* (9q34), *c-MYC* (8q24), *TCL1*(14q32), CCND2 (12p13.32), and *MTCP1* (Xq28) [101–104].

The lesions involving known oncogenes comprise non-TCR rearrangements that result in the formation of 'fusion genes' or deletions that are associated with specific T-ALL subgroups [101]. In these translocations, parts of both genes located at the chromosomal breakpoints are fused 'in frame' and encode a new chimeric protein with oncogenic properties [104]. The 'fusion genes' that mostly define the major subtypes of T-ALL are *SIL(STIL)-TAL1(SCL)*, *PICALM(CALM)-MLLT10(AF10)*, *E2A(TCF3)/PBX1*, *NOTCH1*(*TAN1*)-fusions, *KMT2A(MLL1)*-fusions (*KMT2A(MLL1)-MLLT1(ENL)*), *NUP98*-fusions (*NUP98-SETBP1*, *NUP98-RAP1GDS1*, and *NUP98-ADD3*), *ABL1*-fusions (*EML1-ABL1*, *BCR-ABL1*), *NUP214(CAN)*-fusions (*NUP214-ABL1(ABL)*, *SET/NUP214*), and *ETV6*-fusions (*ETV6*(*TEL*)*-JAK2*, *ETV6*(*TEL*)*-ABL1*(*ABL*)) [1,101].

Recently, using a range of molecular techniques and NGS approaches such as gene expression, genome-wide sequencing, RNA Kinome Capture, and mRNA-sequencing, a large number of new cryptic DNA rearrangements have been identified in different cohorts of patients with ALL [25,105–108]. Some of these hidden lesions correspond to novel fusion patterns not identified by cytogenetics or FISH. These fusions involve mostly inter-chromosomal translocations that are caused by new genomic breakpoints and that give rise to distinct fusion transcripts [107]. However, some fusion patterns could also have originated from other types of genetic alterations such as interstitial deletions and inversions [107]. Identifying these new fusion genes provides important information for determining the most appropriate therapeutic strategy for the patient including targeted cancer therapies [107]. Figure 3 shows the fusion genes identified by NGS. The supplemental file 3 details the references of Figure 3. Besides commonly observed fusions, transcriptome sequencing studies have identified novel fusion genes in these B-ALL and T-ALL cohorts.

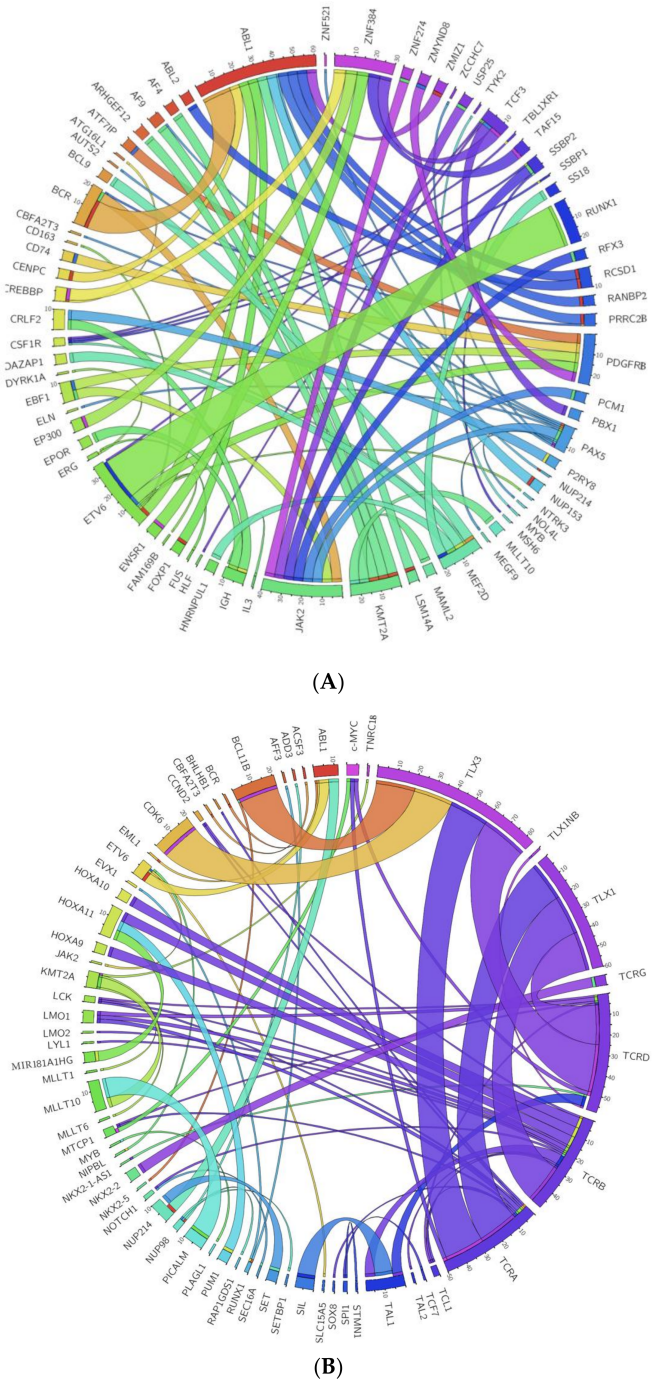

Figure 3. (**A**) New fusion genes identified by NGS approaches in B-ALL. Plot of new fusion genes identified by NGS approaches and their frequencies in B-cell acute lymphoblastic leukemia. (**B**) New fusion genes identified by NGS approaches in T-ALL. Plot of new fusion genes identified by NGS approaches and their frequencies in T-cell acute lymphoblastic leukemia.

Thus, for example, novel recurrent *MEF2D*-fusions (*BCL9*, *HNRNPUL1*, *DAZAP1*) and *ZNF384* fusions (*EP300*, *EWSR1*, *TCF3*, *TAF15*, *CREBBP*) have been described in 6.7% and 7.3% of adults, 3.4% and 3.9% of pediatric patients with B-ALL, respectively [1,105]. In particular, the *MEF2D-BCL9* fusion has recently been found to be associated with a poor prognosis. The leukemic cells with *MEF2D-BCL9* are sensitive to vorinostat and bortezomib in vitro. Therefore, these drugs could be a therapeutic option for these patients [109].

Targetable *ABL*-fusions (14.1%; *ABL1(ABL)*, *ABL2*, *CSF1R* and *PDGFRB*), and *EPOR* rearrangements or *JAK2* fusions (8.8%) have been identified in Ph-like ALL patients by RNA-sequencing [15,107]. Specifically, the novel oncogenic fusions identified in Ph-like ALL patients include *CENPC-ABL1*, *LSM14A-ABL1*, *NUP153-ABL1*, *TBL1XR1-CSF1R*, *ZMYND8-PDGFRB*, *GATAD2A-LYN*, *RFX3-JAK2*, *USP25-JAK2*, and *ZNF274-JAK2* [107]. *ABL*-fusions are sensitive to ABL1 TKIs (imatinib and dasatinib) [2] whereas *JAK2*-fusions and *EPOR*-rearrangements are sensitive to ruxolitinib in vitro [107]. It is worth mentioning that *ABL/JAK* class tyrosine kinase activating fusion genes have been found in Ph-like cases [110]. The tyrosine kinase fusions that predict activated ABL signaling include *EBF1-PDGFRB*, *SSBP1-CSF1R*, *ZMIZ1-ABL1*, *FOXP1-ABL1*, and *RCSD1-ABL2* while the tyrosine kinase fusions that predict activated JAK signaling include *PAX5-JAK2*, *BCR-JAK2*, and *TERF2-JAK2* [110].

Finally, RNA sequencing analysis has identified gene fusions associated with refractory/relapsed childhood and adult T-ALL. Besides commonly observed fusions (e.g., *TCRB/TRB-LMO2*, *STIL/TAL1(SCL)*, *TCRB/TRB-HOXA10*, *SET-NUP214(CAN)*), RNA-sequencing has revealed new non-recurrent gene fusions (e.g., *HOXA11-AS-MIR181A1HG*, *MAST3-C19orf10/MYDGF*) and rearrangements (e.g., *TCRA/TRAC-SOX8*) in T-ALL patients, which indicates that these lesions could be a hallmark of a very poor prognosis in T-ALL [106]. Figure 4 summarizes the key genes altered in the signaling pathways involved in ALL. The supplemental file 4 details the references of Figure 4.

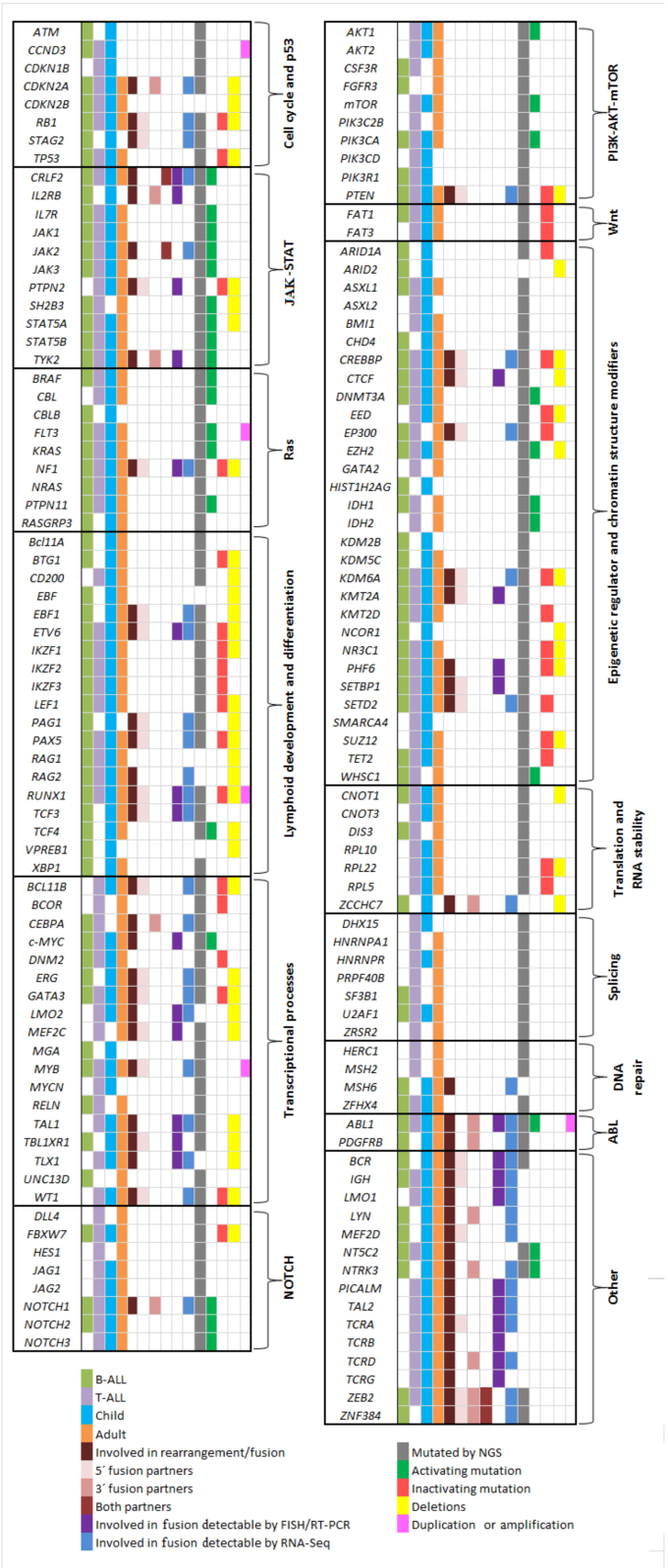

Figure 4. Summary of key genes altered in the different signaling pathways involved in ALL. The figure illustrates the genetic alterations (somatic mutations, rearrangement/fusion, deletions, and duplications) present in the main genes involved in the pathogenic pathways of ALL.

5. Conclusions

We have described the application of new NGS technologies for identifying novel cooperative abnormalities in ALL. Some of these lesions could be key prognostic and/or predictive biomarkers for selecting the best frontline treatment and for developing therapy after the first relapse or refractory disease. The identification and validation of new genetic biomarkers may add to or replace the current repertoire of biomarkers available for the clinical management of this disease.

Supplementary Materials: The following are available online at http://www.mdpi.com/2072-6694/10/4/110/s1, Supplemental File 1: Table S1. Frequency and prognosis value of cytogenetic and molecular genetic abnormalities identified in ALL; Supplemental File 2: References of Figure 2; Supplemental File 3: References of Figure 3; Supplemental File 4: References of Figure 4.

Acknowledgments: This work was supported in part by a grant from the Consejería de Educación, Junta de Castilla y León, Fondos FEDER (SA085U16), Proyectos de Investigación del SACYL, Spain (BIO/SA10/14), a grant from the Junta Provincial de Salamanca of the Asociación Española Contra el Cáncer (AECC), and a grant from the Universidad Pedagógica y Tecnológica de Colombia—Vicerrectoría de Investigación y Extensión (Grupo de Investigación en Ciencias Biomédicas UPTC—GICBUPTC, Escuela de Ciencias Biológicas).

Author Contributions: A.M., M.F.-C., D.M.-M., and R.B. wrote the paper and edited the manuscript. All authors participated in discussions and critically reviewed the manuscript. J.M.H.-R. supervised the study and corrected and approved the final version of the manuscript.

Conflicts of Interest: The authors declare no conflict of interest.

References

1. Iacobucci, I.; Mullighan, C.G. Genetic basis of acute lymphoblastic leukemia. *J. Clin. Oncol.* **2017**, *35*, 975–983. [CrossRef] [PubMed]
2. Moorman, A.V. New and emerging prognostic and predictive genetic biomarkers in B-cell precursor acute lymphoblastic leukemia. *Haematologica* **2016**, *101*, 407–416. [CrossRef] [PubMed]
3. Taylor, J.; Xiao, W.; Abdel-Wahab, O. Diagnosis and classification of hematologic malignancies on the basis of genetics. *Blood* **2017**, *130*, 410–423. [CrossRef] [PubMed]
4. Inaba, H.; Greaves, M.; Mullighan, C.G. Acute lymphoblastic leukaemia. *Lancet* **2013**, *381*, 1943–1955. [CrossRef]
5. Mullighan, C.G. Genome sequencing of lymphoid malignancies. *Blood* **2013**, *122*, 3899–3907. [CrossRef] [PubMed]
6. Bhojwani, D.; Yang, J.J.; Pui, C.H. Biology of childhood acute lymphoblastic leukemia. *Pediatr. Clin. N. Am.* **2015**, *62*, 47–60. [CrossRef] [PubMed]
7. Van Vlierberghe, P.; Pieters, R.; Beverloo, H.B.; Meijerink, J.P. Molecular-genetic insights in paediatric T-cell acute lymphoblastic leukaemia. *Br. J. Haematol.* **2008**, *143*, 153–168. [CrossRef] [PubMed]
8. Arber, D.A.; Orazi, A.; Hasserjian, R.; Thiele, J.; Borowitz, M.J.; Le Beau, M.M.; Bloomfield, C.D.; Cazzola, M.; Vardiman, J.W. The 2016 revision to the world health organization classification of myeloid neoplasms and acute leukemia. *Blood* **2016**, *127*, 2391–2405. [CrossRef] [PubMed]
9. Swerdlow, S.H.; Campo, E.; Harris, N.L.; Jaffe, E.S.; Pileri, S.A.; Stein, H.; Thiele, J.; Vardiman, J.W. *Who Classification of Tumours of Haematopoietic and Lymphoid Tissues*, 4th ed.; World Health Organization: Lyon, France, 2008.
10. Wang, S.; He, G. 2016 revision to the who classification of acute lymphoblastic leukemia. *J. Transl. Intern. Med.* **2016**, *4*, 147–149. [CrossRef] [PubMed]
11. Girardi, T.; Vicente, C.; Cools, J.; De Keersmaecker, K. The genetics and molecular biology of T-all. *Blood* **2017**, *129*, 1113–1123. [CrossRef] [PubMed]
12. Den Boer, M.L.; van Slegtenhorst, M.; De Menezes, R.X.; Cheok, M.H.; Buijs-Gladdines, J.G.; Peters, S.T.; Van Zutven, L.J.; Beverloo, H.B.; Van der Spek, P.J.; Escherich, G.; et al. A subtype of childhood acute lymphoblastic leukaemia with poor treatment outcome: A genome-wide classification study. *Lancet Oncol.* **2009**, *10*, 125–134. [CrossRef]
13. Mullighan, C.G.; Su, X.; Zhang, J.; Radtke, I.; Phillips, L.A.; Miller, C.B.; Ma, J.; Liu, W.; Cheng, C.; Schulman, B.A.; et al. Deletion of IKZF1 and prognosis in acute lymphoblastic leukemia. *N. Engl. J. Med.* **2009**, *360*, 470–480. [CrossRef] [PubMed]

14. Boer, J.M.; Koenders, J.E.; van der Holt, B.; Exalto, C.; Sanders, M.A.; Cornelissen, J.J.; Valk, P.J.; den Boer, M.L.; Rijneveld, A.W. Expression profiling of adult acute lymphoblastic leukemia identifies a BCR-ABL1-like subgroup characterized by high non-response and relapse rates. *Haematologica* **2015**, *100*, e261–e264. [CrossRef] [PubMed]
15. Yap, K.L.; Furtado, L.V.; Kiyotani, K.; Curran, E.; Stock, W.; McNeer, J.L.; Kadri, S.; Segal, J.P.; Nakamura, Y.; Le Beau, M.M.; et al. Diagnostic evaluation of RNA sequencing for the detection of genetic abnormalities associated with Ph-like acute lymphoblastic leukemia (ALL). *Leuk. Lymphoma* **2017**, *58*, 950–958. [CrossRef] [PubMed]
16. Rand, V.; Parker, H.; Russell, L.J.; Schwab, C.; Ensor, H.; Irving, J.; Jones, L.; Masic, D.; Minto, L.; Morrison, H.; et al. Genomic characterization implicates iAMP21 as a likely primary genetic event in childhood B-cell precursor acute lymphoblastic leukemia. *Blood* **2011**, *117*, 6848–6855. [CrossRef] [PubMed]
17. Kim, J.; Lyu, C.J.; Shin, S.; Lee, S.T.; Choi, J.R. Frequency and clinical characteristics of intrachromosomal amplification of chromosome 21 in korean childhood B-lineage acute lymphoblastic leukemia. *Ann. Lab. Med.* **2016**, *36*, 475–480. [CrossRef] [PubMed]
18. Rangel, N.; Forero-Castro, M.; Rondon-Lagos, M. New insights in the cytogenetic practice: Karyotypic chaos, non-clonal chromosomal alterations and chromosomal instability in human cancer and therapy response. *Genes* **2017**, *8*, 155. [CrossRef] [PubMed]
19. Gu, J.; Reynolds, A.; Fang, L.; DeGraffenreid, C.; Sterns, K.; Patel, K.P.; Medeiros, L.J.; Lin, P.; Lu, X. Coexistence of iAMP21 and *ETV6-RUNX1* fusion in an adolescent with B cell acute lymphoblastic leukemia: Literature review of six additional cases. *Mol. Cytogenet.* **2016**, *9*, 84. [CrossRef] [PubMed]
20. Goossens, S.; Radaelli, E.; Blanchet, O.; Durinck, K.; van der Meulen, J.; Peirs, S.; Taghon, T.; Tremblay, C.S.; Costa, M.; Farhang Ghahremani, M.; et al. ZEB2 drives immature T-cell lymphoblastic leukaemia development via enhanced tumour-initiating potential and IL-7 receptor signalling. *Nat. Commun.* **2015**, *6*, 5794. [CrossRef] [PubMed]
21. Cante-Barrett, K.; Spijkers-Hagelstein, J.A.; Buijs-Gladdines, J.G.; Uitdehaag, J.C.; Smits, W.K.; van der Zwet, J.; Buijsman, R.C.; Zaman, G.J.; Pieters, R.; Meijerink, J.P. MEK and PI3K-AKT inhibitors synergistically block activated IL7 receptor signaling in T-cell acute lymphoblastic leukemia. *Leukemia* **2016**, *30*, 1832–1843. [CrossRef] [PubMed]
22. Harrison, C.J. Key pathways as therapeutic targets. *Blood* **2011**, *118*, 2935–2936. [CrossRef] [PubMed]
23. Harrison, C.J. Targeting signaling pathways in acute lymphoblastic leukemia: New insights. *Am. Soc. Hematol.* **2013**, *2013*, 118–125. [CrossRef] [PubMed]
24. Neumann, M.; Vosberg, S.; Schlee, C.; Heesch, S.; Schwartz, S.; Gokbuget, N.; Hoelzer, D.; Graf, A.; Krebs, S.; Bartram, I.; et al. Mutational spectrum of adult T-all. *Oncotarget* **2015**, *6*, 2754–2766. [CrossRef] [PubMed]
25. Atak, Z.K.; Gianfelici, V.; Hulselmans, G.; De Keersmaecker, K.; Devasia, A.G.; Geerdens, E.; Mentens, N.; Chiaretti, S.; Durinck, K.; Uyttebroeck, A.; et al. Comprehensive analysis of transcriptome variation uncovers known and novel driver events in T-cell acute lymphoblastic leukemia. *PLoS Genet.* **2013**, *9*, e1003997.
26. De Keersmaecker, K.; Atak, Z.K.; Li, N.; Vicente, C.; Patchett, S.; Girardi, T.; Gianfelici, V.; Geerdens, E.; Clappier, E.; Porcu, M.; et al. Exome sequencing identifies mutation in CNOT3 and ribosomal genes RPL5 and RPL10 in T-cell acute lymphoblastic leukemia. *Nat. Genet.* **2013**, *45*, 186–190. [CrossRef] [PubMed]
27. Malinowska, I.; Glodkowska-Mrowka, E. Chapter 5—Next generation sequencing in hematological disorders. In *Clinical Applications for Next-Generation Sequencing*; Academic Press: Boston, MA, USA, 2016; pp. 75–96.
28. Tosello, V.; Ferrando, A.A. The notch signaling pathway: Role in the pathogenesis of T-cell acute lymphoblastic leukemia and implication for therapy. *Ther. Adv. Hematol.* **2013**, *4*, 199–210. [CrossRef] [PubMed]
29. Yokota, T.; Kanakura, Y. Genetic abnormalities associated with acute lymphoblastic leukemia. *Cancer Sci.* **2016**, *107*, 721–725. [CrossRef] [PubMed]
30. Zhou, Y.; You, M.J.; Young, K.H.; Lin, P.; Lu, G.; Medeiros, L.J.; Bueso-Ramos, C.E. Advances in the molecular pathobiology of B-lymphoblastic leukemia. *Hum. Pathol.* **2012**, *43*, 1347–1362. [CrossRef] [PubMed]
31. Bernt, K.M.; Hunger, S.P. Current concepts in pediatric philadelphia chromosome-positive acute lymphoblastic leukemia. *Front. Oncol.* **2014**, *4*, 54. [CrossRef] [PubMed]
32. Holmfeldt, L.; Wei, L.; Diaz-Flores, E.; Walsh, M.; Zhang, J.; Ding, L.; Payne-Turner, D.; Churchman, M.; Andersson, A.; Chen, S.C.; et al. The genomic landscape of hypodiploid acute lymphoblastic leukemia. *Nat. Genet.* **2013**, *45*, 242–252. [CrossRef] [PubMed]

33. Chen, C.; Bartenhagen, C.; Gombert, M.; Okpanyi, V.; Binder, V.; Rottgers, S.; Bradtke, J.; Teigler-Schlegel, A.; Harbott, J.; Ginzel, S.; et al. Next-generation-sequencing of recurrent childhood high hyperdiploid acute lymphoblastic leukemia reveals mutations typically associated with high risk patients. *Leuk. Res.* **2015**, *39*, 990–1001. [CrossRef] [PubMed]
34. Zhang, J.; Ding, L.; Holmfeldt, L.; Wu, G.; Heatley, S.L.; Payne-Turner, D.; Easton, J.; Chen, X.; Wang, J.; Rusch, M.; et al. The genetic basis of early T-cell precursor acute lymphoblastic leukaemia. *Nature* **2012**, *481*, 157–163. [CrossRef] [PubMed]
35. Iacobucci, I.; Papayannidis, C.; Lonetti, A.; Ferrari, A.; Baccarani, M.; Martinelli, G. Cytogenetic and molecular predictors of outcome in acute lymphocytic leukemia: Recent developments. *Curr. Hematol. Malig. Rep.* **2012**, *7*, 133–143. [CrossRef] [PubMed]
36. Grossmann, V.; Kern, W.; Harbich, S.; Alpermann, T.; Jeromin, S.; Schnittger, S.; Haferlach, C.; Haferlach, T.; Kohlmann, A. Prognostic relevance of RUNX1 mutations in T-cell acute lymphoblastic leukemia. *Haematologica* **2011**, *96*, 1874–1877. [CrossRef] [PubMed]
37. Grossmann, V.; Haferlach, C.; Weissmann, S.; Roller, A.; Schindela, S.; Poetzinger, F.; Stadler, K.; Bellos, F.; Kern, W.; Haferlach, T.; et al. The molecular profile of adult T-cell acute lymphoblastic leukemia: Mutations in RUNX1 and DNMT3A are associated with poor prognosis in T-ALL. *Genes Chromosom. Cancer* **2013**, *52*, 410–422. [CrossRef] [PubMed]
38. Geng, H.; Brennan, S.; Milne, T.A.; Chen, W.Y.; Li, Y.; Hurtz, C.; Kweon, S.M.; Zickl, L.; Shojaee, S.; Neuberg, D.; et al. Integrative epigenomic analysis identifies biomarkers and therapeutic targets in adult B-acute lymphoblastic leukemia. *Cancer Discov.* **2012**, *2*, 1004–1023. [CrossRef] [PubMed]
39. Bicocca, V.T.; Chang, B.H.; Masouleh, B.K.; Muschen, M.; Loriaux, M.M.; Druker, B.J.; Tyner, J.W. Crosstalk between ROR1 and the Pre-B cell receptor promotes survival of t(1;19) acute lymphoblastic leukemia. *Cancer Cell* **2012**, *22*, 656–667. [CrossRef] [PubMed]
40. Kohrer, S.; Havranek, O.; Seyfried, F.; Hurtz, C.; Coffey, G.P.; Kim, E.; Ten Hacken, E.; Jager, U.; Vanura, K.; O'Brien, S.; et al. Pre-BCR signaling in precursor B-cell acute lymphoblastic leukemia regulates PI3K/AKT, FOXO1 and MYC, and can be targeted by SYK inhibition. *Leukemia* **2016**, *30*, 1246–1254. [CrossRef] [PubMed]
41. Perentesis, J.P.; Bhatia, S.; Boyle, E.; Shao, Y.; Shu, X.O.; Steinbuch, M.; Sather, H.N.; Gaynon, P.; Kiffmeyer, W.; Envall-Fox, J.; et al. Ras oncogene mutations and outcome of therapy for childhood acute lymphoblastic leukemia. *Leukemia* **2004**, *18*, 685–692. [CrossRef] [PubMed]
42. Knight, T.; Irving, J.A. Ras/Raf/MEK/ERK pathway activation in childhood acute lymphoblastic leukemia and its therapeutic targeting. *Front. Oncol.* **2014**, *4*, 160. [CrossRef] [PubMed]
43. Ding, L.W.; Sun, Q.Y.; Tan, K.T.; Chien, W.; Thippeswamy, A.M.; Eng Juh Yeoh, A.; Kawamata, N.; Nagata, Y.; Xiao, J.F.; Loh, X.Y.; et al. Mutational landscape of pediatric acute lymphoblastic leukemia. *Cancer Res.* **2017**, *77*, 390–400. [CrossRef] [PubMed]
44. Ryan, S.L.; Matheson, E.; Grossmann, V.; Sinclair, P.; Bashton, M.; Schwab, C.; Towers, W.; Partington, M.; Elliott, A.; Minto, L.; et al. The role of the ras pathway in iAMP21-ALL. *Leukemia* **2016**, *30*, 1824–1831. [CrossRef] [PubMed]
45. Andersson, A.K.; Ma, J.; Wang, J.; Chen, X.; Gedman, A.L.; Dang, J.; Nakitandwe, J.; Holmfeldt, L.; Parker, M.; Easton, J.; et al. The landscape of somatic mutations in infant MLL-rearranged acute lymphoblastic leukemias. *Nat. Genet.* **2015**, *47*, 330–337. [CrossRef] [PubMed]
46. Feng, J.; Li, Y.; Jia, Y.; Fang, Q.; Gong, X.; Dong, X.; Ru, K.; Li, Q.; Zhao, X.; Liu, K.; et al. Spectrum of somatic mutations detected by targeted next-generation sequencing and their prognostic significance in adult patients with acute lymphoblastic leukemia. *J. Hematol. Oncol.* **2017**, *10*, 61. [CrossRef] [PubMed]
47. Driessen, E.M.; van Roon, E.H.; Spijkers-Hagelstein, J.A.; Schneider, P.; de Lorenzo, P.; Valsecchi, M.G.; Pieters, R.; Stam, R.W. Frequencies and prognostic impact of RAS mutations in MLL-rearranged acute lymphoblastic leukemia in infants. *Haematologica* **2013**, *98*, 937–944. [CrossRef] [PubMed]
48. Vainchenker, W.; Constantinescu, S.N. JAK/STAT signaling in hematological malignancies. *Oncogene* **2013**, *32*, 2601–2613. [CrossRef] [PubMed]
49. Forero-Castro, M.; Robledo, C.; Benito, R.; Bodega-Mayor, I.; Rapado, I.; Hernandez-Sanchez, M.; Abaigar, M.; Maria Hernandez-Sanchez, J.; Quijada-Alamo, M.; Maria Sanchez-Pina, J.; et al. Mutations in TP53 and JAK2 are independent prognostic biomarkers in B-cell precursor acute lymphoblastic leukaemia. *Br. J. Cancer* **2017**, *117*, 256–265. [CrossRef] [PubMed]

50. Gowda, C.; Dovat, S. Genetic targets in pediatric acute lymphoblastic leukemia. *Adv. Exp. Med. Biol.* **2013**, *779*, 327–340. [PubMed]
51. Mullighan, C.G. The molecular genetic makeup of acute lymphoblastic leukemia. *Am. Soc. Hematol.* **2012**, *2012*, 389–396.
52. Bercovich, D.; Ganmore, I.; Scott, L.M.; Wainreb, G.; Birger, Y.; Elimelech, A.; Shochat, C.; Cazzaniga, G.; Biondi, A.; Basso, G.; et al. Mutations of JAK2 in acute lymphoblastic leukaemias associated with down's syndrome. *Lancet* **2008**, *372*, 1484–1492. [CrossRef]
53. Mullighan, C.G. JAK2—A new player in acute lymphoblastic leukaemia. *Lancet* **2008**, *372*, 1448–1450. [CrossRef]
54. Mullighan, C.G.; Zhang, J.; Harvey, R.C.; Collins-Underwood, J.R.; Schulman, B.A.; Phillips, L.A.; Tasian, S.K.; Loh, M.L.; Su, X.; Liu, W.; et al. JAK mutations in high-risk childhood acute lymphoblastic leukemia. *Proc. Natl. Acad. Sci. USA* **2009**, *106*, 9414–9418. [CrossRef] [PubMed]
55. Li, F.; Guo, H.Y.; Wang, M.; Geng, H.L.; Bian, M.R.; Cao, J.; Chen, C.; Zeng, L.Y.; Wang, X.Y.; Wu, Q.Y. The effects of R683S (G) genetic mutations on the JAK2 activity, structure and stability. *Int. J. Biol. Macromol.* **2013**, *60*, 186–195. [CrossRef] [PubMed]
56. Shochat, C.; Tal, N.; Bandapalli, O.R.; Palmi, C.; Ganmore, I.; te Kronnie, G.; Cario, G.; Cazzaniga, G.; Kulozik, A.E.; Stanulla, M.; et al. Gain-of-function mutations in interleukin-7 receptor-α (IL7R) in childhood acute lymphoblastic leukemias. *J. Exp. Med.* **2011**, *208*, 901–908. [CrossRef] [PubMed]
57. Zenatti, P.P.; Ribeiro, D.; Li, W.; Zuurbier, L.; Silva, M.C.; Paganin, M.; Tritapoe, J.; Hixon, J.A.; Silveira, A.B.; Cardoso, B.A.; et al. Oncogenic IL7R gain-of-function mutations in childhood T-cell acute lymphoblastic leukemia. *Nat. Genet.* **2011**, *43*, 932–939. [CrossRef] [PubMed]
58. Li, Y.; Buijs-Gladdines, J.G.; Cante-Barrett, K.; Stubbs, A.P.; Vroegindeweij, E.M.; Smits, W.K.; van Marion, R.; Dinjens, W.N.; Horstmann, M.; Kuiper, R.P.; et al. IL-7 receptor mutations and steroid resistance in pediatric T cell acute lymphoblastic leukemia: A genome sequencing study. *PLoS Med.* **2016**, *13*, e1002200. [CrossRef] [PubMed]
59. Roberts, K.G.; Mullighan, C.G. How new advances in genetic analysis are influencing the understanding and treatment of childhood acute leukemia. *Curr. Opin. Pediatr.* **2011**, *23*, 34–40. [CrossRef] [PubMed]
60. Tessoulin, B.; Eveillard, M.; Lok, A.; Chiron, D.; Moreau, P.; Amiot, M.; Moreau-Aubry, A.; Le Gouill, S.; Pellat-Deceunynck, C. P53 dysregulation in B-cell malignancies: More than a single gene in the pathway to hell. *Blood Rev.* **2017**, *31*, 251–259. [CrossRef] [PubMed]
61. Leroy, B.; Anderson, M.; Soussi, T. TP53 mutations in human cancer: Database reassessment and prospects for the next decade. *Hum. Mutat.* **2014**, *35*, 672–688. [CrossRef] [PubMed]
62. Trino, S.; De Luca, L.; Laurenzana, I.; Caivano, A.; Del Vecchio, L.; Martinelli, G.; Musto, P. P53-MDM2 pathway: Evidences for a new targeted therapeutic approach in B-acute lymphoblastic leukemia. *Front. Pharmacol.* **2016**, *7*, 491. [CrossRef] [PubMed]
63. Chiaretti, S.; Brugnoletti, F.; Tavolaro, S.; Bonina, S.; Paoloni, F.; Marinelli, M.; Patten, N.; Bonifacio, M.; Kropp, M.G.; Sica, S.; et al. TP53 mutations are frequent in adult acute lymphoblastic leukemia cases negative for recurrent fusion genes and correlate with poor response to induction therapy. *Haematologica* **2013**, *98*, e59–e61. [CrossRef] [PubMed]
64. Stengel, A.; Schnittger, S.; Weissmann, S.; Kuznia, S.; Kern, W.; Kohlmann, A.; Haferlach, T.; Haferlach, C. TP53 mutations occur in 15.7% of ALL and are associated with MYC-rearrangement, low hypodiploidy, and a poor prognosis. *Blood* **2014**, *124*, 251–258. [CrossRef] [PubMed]
65. Muhlbacher, V.; Zenger, M.; Schnittger, S.; Weissmann, S.; Kunze, F.; Kohlmann, A.; Bellos, F.; Kern, W.; Haferlach, T.; Haferlach, C. Acute lymphoblastic leukemia with low hypodiploid/near triploid karyotype is a specific clinical entity and exhibits a very high TP53 mutation frequency of 93%. *Genes Chromosom. Cancer* **2014**, *53*, 524–536. [CrossRef] [PubMed]
66. Comeaux, E.Q.; Mullighan, C.G. TP53 mutations in hypodiploid acute lymphoblastic leukemia. *Cold Spring Harb. Perspect. Med.* **2017**, *7*, a026286. [CrossRef] [PubMed]
67. Carrasco Salas, P.; Fernandez, L.; Vela, M.; Bueno, D.; Gonzalez, B.; Valentin, J.; Lapunzina, P.; Perez-Martinez, A. The role of CDKN2A/B deletions in pediatric acute lymphoblastic leukemia. *Pediatr. Hematol. Oncol.* **2016**, *33*, 415–422. [CrossRef] [PubMed]

68. Hof, J.; Krentz, S.; van Schewick, C.; Korner, G.; Shalapour, S.; Rhein, P.; Karawajew, L.; Ludwig, W.D.; Seeger, K.; Henze, G.; et al. Mutations and deletions of the TP53 gene predict nonresponse to treatment and poor outcome in first relapse of childhood acute lymphoblastic leukemia. *J. Clin. Oncol.* **2011**, *29*, 3185–3193. [CrossRef] [PubMed]
69. Diccianni, M.B.; Yu, J.; Hsiao, M.; Mukherjee, S.; Shao, L.E.; Yu, A.L. Clinical significance of P53 mutations in relapsed T-cell acute lymphoblastic leukemia. *Blood* **1994**, *84*, 3105–3112. [PubMed]
70. Forero-Castro, M.; Robledo, C.; Lumbreras, E.; Benito, R.; Hernandez-Sanchez, J.M.; Hernandez-Sanchez, M.; Garcia, J.L.; Corchete-Sanchez, L.A.; Tormo, M.; Barba, P.; et al. The presence of genomic imbalances is associated with poor outcome in patients with burkitt lymphoma treated with dose-intensive chemotherapy including rituximab. *Br. J. Haematol.* **2016**, *172*, 428–438. [CrossRef] [PubMed]
71. Trinquand, A.; Tanguy-Schmidt, A.; Ben Abdelali, R.; Lambert, J.; Beldjord, K.; Lengline, E.; De Gunzburg, N.; Payet-Bornet, D.; Lhermitte, L.; Mossafa, H.; et al. Toward a NOTCH1/FBXW7/RAS/PTEN-based oncogenetic risk classification of adult T-cell acute lymphoblastic leukemia: A group for research in adult acute lymphoblastic leukemia study. *J. Clin. Oncol.* **2013**, *31*, 4333–4342. [CrossRef] [PubMed]
72. Zuurbier, L.; Homminga, I.; Calvert, V.; te Winkel, M.L.; Buijs-Gladdines, J.G.; Kooi, C.; Smits, W.K.; Sonneveld, E.; Veerman, A.J.; Kamps, W.A.; et al. NOTCH1 and/or FBXW7 mutations predict for initial good prednisone response but not for improved outcome in pediatric T-cell acute lymphoblastic leukemia patients treated on dcog or coall protocols. *Leukemia* **2010**, *24*, 2014–2022. [CrossRef] [PubMed]
73. Weng, A.P.; Ferrando, A.A.; Lee, W.; Morris, J.P.t.; Silverman, L.B.; Sanchez-Irizarry, C.; Blacklow, S.C.; Look, A.T.; Aster, J.C. Activating mutations of NOTCH1 in human T cell acute lymphoblastic leukemia. *Science* **2004**, *306*, 269–271. [CrossRef] [PubMed]
74. Chiang, M.Y.; Radojcic, V.; Maillard, I. Oncogenic notch signaling in T-cell and B-cell lymphoproliferative disorders. *Curr. Opin. Hematol.* **2016**, *23*, 362–370. [CrossRef] [PubMed]
75. Agnusdei, V.; Minuzzo, S.; Frasson, C.; Grassi, A.; Axelrod, F.; Satyal, S.; Gurney, A.; Hoey, T.; Seganfreddo, E.; Basso, G.; et al. Therapeutic antibody targeting of notch1 in t-acute lymphoblastic leukemia xenografts. *Leukemia* **2014**, *28*, 278–288. [CrossRef] [PubMed]
76. Thorpe, L.M.; Yuzugullu, H.; Zhao, J.J. PI3K in cancer: Divergent roles of isoforms, modes of activation and therapeutic targeting. *Nat. Rev. Cancer* **2015**, *15*, 7–24. [CrossRef] [PubMed]
77. Lien, E.C.; Dibble, C.C.; Toker, A. PI3K signaling in cancer: Beyond AKT. *Curr. Opin. Cell Biol.* **2017**, *45*, 62–71. [CrossRef] [PubMed]
78. Simioni, C.; Ultimo, S.; Martelli, A.M.; Zauli, G.; Milani, D.; McCubrey, J.A.; Capitani, S.; Neri, L.M. Synergistic effects of selective inhibitors targeting the PI3K/AKT/MTOR pathway or NUP214-ABL1 fusion protein in human acute lymphoblastic leukemia. *Oncotarget* **2016**, *7*, 79842–79853. [CrossRef] [PubMed]
79. Zhao, L.; Vogt, P.K. Class I PI3K in oncogenic cellular transformation. *Oncogene* **2008**, *27*, 5486–5496. [CrossRef] [PubMed]
80. Silva, A.; Yunes, J.A.; Cardoso, B.A.; Martins, L.R.; Jotta, P.Y.; Abecasis, M.; Nowill, A.E.; Leslie, N.R.; Cardoso, A.A.; Barata, J.T. Pten posttranslational inactivation and hyperactivation of the PI3K/AKT pathway sustain primary T cell leukemia viability. *J. Clin. Investig.* **2008**, *118*, 3762–3774. [CrossRef] [PubMed]
81. Fransecky, L.; Mochmann, L.H.; Baldus, C.D. Outlook on PI3K/AKT/mTOR inhibition in acute leukemia. *Mol. Cell. Ther.* **2015**, *3*, 2. [CrossRef] [PubMed]
82. Gutierrez, A.; Sanda, T.; Grebliunaite, R.; Carracedo, A.; Salmena, L.; Ahn, Y.; Dahlberg, S.; Neuberg, D.; Moreau, L.A.; Winter, S.S.; et al. High frequency of PTEN, PI3K, and AKT abnormalities in T-cell acute lymphoblastic leukemia. *Blood* **2009**, *114*, 647–650. [CrossRef] [PubMed]
83. Zuckerman, T.; Rowe, J.M. Pathogenesis and prognostication in acute lymphoblastic leukemia. *F1000Prime Rep.* **2014**, *6*, 59. [CrossRef] [PubMed]
84. Seke Etet, P.F.; Vecchio, L.; Bogne Kamga, P.; Nchiwan Nukenine, E.; Krampera, M.; Nwabo Kamdje, A.H. Normal hematopoiesis and hematologic malignancies: Role of canonical Wnt signaling pathway and stromal microenvironment. *Biochim. Biophys. Acta* **2013**, *1835*, 1–10. [CrossRef] [PubMed]
85. Morris, L.G.; Kaufman, A.M.; Gong, Y.; Ramaswami, D.; Walsh, L.A.; Turcan, S.; Eng, S.; Kannan, K.; Zou, Y.; Peng, L.; et al. Recurrent somatic mutation of FAT1 in multiple human cancers leads to aberrant Wnt activation. *Nat. Genet.* **2013**, *45*, 253–261. [CrossRef] [PubMed]

86. Neumann, M.; Seehawer, M.; Schlee, C.; Vosberg, S.; Heesch, S.; von der Heide, E.K.; Graf, A.; Krebs, S.; Blum, H.; Gokbuget, N.; et al. FAT1 expression and mutations in adult acute lymphoblastic leukemia. *Blood Cancer J.* **2014**, *4*, e224. [CrossRef] [PubMed]
87. Gutierrez, A.; Sanda, T.; Ma, W.; Zhang, J.; Grebliunaite, R.; Dahlberg, S.; Neuberg, D.; Protopopov, A.; Winter, S.S.; Larson, R.S.; et al. Inactivation of lef1 in T-cell acute lymphoblastic leukemia. *Blood* **2010**, *115*, 2845–2851. [CrossRef] [PubMed]
88. Gregoire, M.; Germain, D.; Charrin, C.; Pages, M.; Phillipe, N.; Souillet, G.; Capodano, A.; Hairion, D.; Perrimond, M.; Michel, G.; et al. Collaborative study of karyotypes in childhood acute lymphoblastic leukemias. Groupe francais de cytogenetique hematologique. *Leukemia* **1993**, *7*, 10–19.
89. San Jose-Eneriz, E.; Agirre, X.; Rodriguez-Otero, P.; Prosper, F. Epigenetic regulation of cell signaling pathways in acute lymphoblastic leukemia. *Epigenomics* **2013**, *5*, 525–538. [CrossRef] [PubMed]
90. Van Vlierberghe, P.; Palomero, T.; Khiabanian, H.; Van der Meulen, J.; Castillo, M.; Van Roy, N.; De Moerloose, B.; Philippe, J.; Gonzalez-Garcia, S.; Toribio, M.L.; et al. PHF6 mutations in T-cell acute lymphoblastic leukemia. *Nat. Genet.* **2010**, *42*, 338–342. [CrossRef] [PubMed]
91. Wang, Q.; Qiu, H.; Jiang, H.; Wu, L.; Dong, S.; Pan, J.; Wang, W.; Ping, N.; Xia, J.; Sun, A.; et al. Mutations of PHF6 are associated with mutations of NOTCH1, JAK1 and rearrangement of SET-NUP214 in T-cell acute lymphoblastic leukemia. *Haematologica* **2011**, *96*, 1808–1814. [CrossRef] [PubMed]
92. Xiao, H.; Wang, L.M.; Luo, Y.; Lai, X.; Li, C.; Shi, J.; Tan, Y.; Fu, S.; Wang, Y.; Zhu, N.; et al. Mutations in epigenetic regulators are involved in acute lymphoblastic leukemia relapse following allogeneic hematopoietic stem cell transplantation. *Oncotarget* **2016**, *7*, 2696–2708. [CrossRef] [PubMed]
93. Roy, D.M.; Walsh, L.A.; Chan, T.A. Driver mutations of cancer epigenomes. *Protein Cell* **2014**, *5*, 265–296. [CrossRef] [PubMed]
94. Li, M.; Xiao, L.; Xu, J.; Zhang, R.; Guo, J.; Olson, J.; Wu, Y.; Li, J.; Song, C.; Ge, Z. Co-existence of PHF6 and NOTCH1 mutations in adult T-cell acute lymphoblastic leukemia. *Oncol. Lett.* **2016**, *12*, 16–22. [CrossRef] [PubMed]
95. Gabriel, A.S.; Lafta, F.M.; Schwalbe, E.C.; Nakjang, S.; Cockell, S.J.; Iliasova, A.; Enshaei, A.; Schwab, C.; Rand, V.; Clifford, S.C.; et al. Epigenetic landscape correlates with genetic subtype but does not predict outcome in childhood acute lymphoblastic leukemia. *Epigenetics* **2015**, *10*, 717–726. [CrossRef] [PubMed]
96. Janczar, S.; Janczar, K.; Pastorczak, A.; Harb, H.; Paige, A.J.; Zalewska-Szewczyk, B.; Danilewicz, M.; Mlynarski, W. The role of histone protein modifications and mutations in histone modifiers in pediatric B-cell progenitor acute lymphoblastic leukemia. *Cancers* **2017**, *9*, 2. [CrossRef] [PubMed]
97. Jaffe, J.D.; Wang, Y.; Chan, H.M.; Zhang, J.; Huether, R.; Kryukov, G.V.; Bhang, H.E.; Taylor, J.E.; Hu, M.; Englund, N.P.; et al. Global chromatin profiling reveals NSD2 mutations in pediatric acute lymphoblastic leukemia. *Nat. Genet.* **2013**, *45*, 1386–1391. [CrossRef] [PubMed]
98. Sun, C.; Chang, L.; Zhu, X. Pathogenesis of ETV6/RUNX1-positive childhood acute lymphoblastic leukemia and mechanisms underlying its relapse. *Oncotarget* **2017**, *8*, 35445–35459. [CrossRef] [PubMed]
99. Paulsson, K.; Lilljebjorn, H.; Biloglav, A.; Olsson, L.; Rissler, M.; Castor, A.; Barbany, G.; Fogelstrand, L.; Nordgren, A.; Sjogren, H.; et al. The genomic landscape of high hyperdiploid childhood acute lymphoblastic leukemia. *Nat. Genet.* **2015**, *47*, 672–676. [CrossRef] [PubMed]
100. De Smith, A.J.; Ojha, J.; Francis, S.S.; Sanders, E.; Endicott, A.A.; Hansen, H.M.; Smirnov, I.; Termuhlen, A.M.; Walsh, K.M.; Metayer, C.; et al. Clonal and microclonal mutational heterogeneity in high hyperdiploid acute lymphoblastic leukemia. *Oncotarget* **2016**, *7*, 72733–72745. [CrossRef] [PubMed]
101. Chiaretti, S.; Foa, R. T-cell acute lymphoblastic leukemia. *Haematologica* **2009**, *94*, 160–162. [CrossRef] [PubMed]
102. Forero, R.M.; Hernández, M.; Rivas, J.M.H. Genetics of acute lymphoblastic leukemia. In *Leukemia*; Guenova, M., Balatzenko, G., Eds.; InTech: Rijeka, Croatia, 2013.
103. Cauwelier, B.; Dastugue, N.; Cools, J.; Poppe, B.; Herens, C.; De Paepe, A.; Hagemeijer, A.; Speleman, F. Molecular cytogenetic study of 126 unselected T-ALL cases reveals high incidence of tcrbeta locus rearrangements and putative new T-cell oncogenes. *Leukemia* **2006**, *20*, 1238–1244. [CrossRef] [PubMed]
104. Gorello, P.; La Starza, R.; Varasano, E.; Chiaretti, S.; Elia, L.; Pierini, V.; Barba, G.; Brandimarte, L.; Crescenzi, B.; Vitale, A.; et al. Combined interphase fluorescence in situ hybridization elucidates the genetic heterogeneity of T-cell acute lymphoblastic leukemia in adults. *Haematologica* **2010**, *95*, 79–86. [CrossRef] [PubMed]

105. Liu, Y.F.; Wang, B.Y.; Zhang, W.N.; Huang, J.Y.; Li, B.S.; Zhang, M.; Jiang, L.; Li, J.F.; Wang, M.J.; Dai, Y.J.; et al. Genomic profiling of adult and pediatric B-cell acute lymphoblastic leukemia. *EBioMedicine* **2016**, *8*, 173–183. [CrossRef] [PubMed]
106. Gianfelici, V.; Chiaretti, S.; Demeyer, S.; Di Giacomo, F.; Messina, M.; La Starza, R.; Peragine, N.; Paoloni, F.; Geerdens, E.; Pierini, V.; et al. RNA sequencing unravels the genetics of refractory/relapsed T-cell acute lymphoblastic leukemia. Prognostic and therapeutic implications. *Haematologica* **2016**, *101*, 941–950. [CrossRef] [PubMed]
107. Reshmi, S.C.; Harvey, R.C.; Roberts, K.G.; Stonerock, E.; Smith, A.; Jenkins, H.; Chen, I.M.; Valentine, M.; Liu, Y.; Li, Y.; et al. Targetable kinase gene fusions in high-risk B-ALL: A study from the children's oncology group. *Blood* **2017**, *129*, 3352–3361. [CrossRef] [PubMed]
108. Chen, B.; Jiang, L.; Zhong, M.L.; Li, J.F.; Li, B.S.; Peng, L.J.; Dai, Y.T.; Cui, B.W.; Yan, T.Q.; Zhang, W.N.; et al. Identification of fusion genes and characterization of transcriptome features in T-cell acute lymphoblastic leukemia. *Proc. Natl. Acad. Sci. USA* **2018**, *115*, 373–378. [CrossRef] [PubMed]
109. Suzuki, K.; Okuno, Y.; Kawashima, N.; Muramatsu, H.; Okuno, T.; Wang, X.; Kataoka, S.; Sekiya, Y.; Hamada, M.; Murakami, N.; et al. MEF2D-BCL9 fusion gene is associated with high-risk acute B-cell precursor lymphoblastic leukemia in adolescents. *J. Clin. Oncol.* **2016**, *34*, 3451–3459. [CrossRef] [PubMed]
110. Boer, J.M.; Steeghs, E.M.; Marchante, J.R.; Boeree, A.; Beaudoin, J.J.; Beverloo, H.B.; Kuiper, R.P.; Escherich, G.; van der Velden, V.H.; van der Schoot, C.E.; et al. Tyrosine kinase fusion genes in pediatric BCR-ABL1-like acute lymphoblastic leukemia. *Oncotarget* **2017**, *8*, 4618–4628. [CrossRef] [PubMed]

Annex V

Paper V. Targeted Genome Editing in Acute Lymphoblastic Leukemia. A Review

Adrián Montaño[1*], Maribel Forero-Castro[2*], Rocío Benito, Ignacio García-Tuñón, Jesús-María Hernández-Rivas[3&]

** Shared junior authorship. &Correspondence.*

[1] IBSAL, IBMCC, Universidad de Salamanca-CSIC, Cancer Research Center; Salamanca; Spain. [2] Escuela de Ciencias Biológicas. Grupo de investigación en Ciencias Biomédicas (GICBUPTC). Universidad Pedagógica y Tecnológica de Colombia; Tunja; Colombia. [3] Dept of Medicine, Universidad de Salamanca, Spain, [4] Dept of Hematology,Hospital Universitario de Salamanca; Salamanca; Spain.

BMC Biotechnol. 2018 Jul 17;18(1):45. doi: 10.1186/s12896-018-0455-9.

Montaño et al. BMC Biotechnology (2018) 18:45
https://doi.org/10.1186/s12896-018-0455-9

BMC Biotechnology

REVIEW Open Access

Targeted genome editing in acute lymphoblastic leukemia: a review

Adrián Montaño[1†], Maribel Forero-Castro[2†], Jesús-María Hernández-Rivas[1,3,4*], Ignacio García-Tuñón[1] and Rocío Benito[1]

Abstract

Background: Genome editing technologies offers new opportunities for tackling diseases such as acute lymphoblastic leukemia (ALL) that have been beyond the reach of previous therapies.

Results: We show how the recent availability of genome-editing tools such as CRISPR-Cas9 are an important means of advancing functional studies of ALL through the incorporation, elimination and modification of somatic mutations and fusion genes in cell lines and mouse models. These tools not only broaden the understanding of the involvement of various genetic alterations in the pathogenesis of the disease but also identify new therapeutic targets for future clinical trials.

Conclusions: New approaches including CRISPR-Cas9 are crucial for functional studies of genetic aberrations driving cancer progression, and that may be responsible for treatment resistance and relapses. By using this approach, diseases can be more faithfully reproduced and new therapeutic targets and approaches found.

Keywords: Acute lymphoblastic leukemia, CRISPR-Cas9, Genome editing

Background

Acute lymphoblastic leukemia (ALL) is a malignant disorder originating from hematopoietic B- or T-cell precursors, characterized by marked heterogeneity at the molecular and clinical levels. Although a genetic event is known to occur in the majority of cases, and may be associated with outcome prediction, around 25–30% of pediatric and 50% of adult ALL patients have no defined genetic hallmarks of biological or clinical significance [1].

The development of new techniques of genetic editing such as TALENs or CRISPR-Cas9 has made it possible to produce powerful animal genetic models that recapitulate the cooperating oncogenic lesions affecting genes with an established role in the proliferation and establishment of the leukemic clone [2]. In ALL, some approaches have been oriented towards analyzing the targeting of transcriptional factors such as *PAX5*, which are involved in the pathogenesis of B-ALL, and *TAL1* and *LMO2*, which are highly deregulated in T-ALL [3–5]. Targeting gene fusion expression has also been addressed through genome editing systems, as with *MLL* and *AF4*, whose fusion is associated with poor prognosis and which mainly affects B-ALL infants [6]. Other genes have been modified to gain a better understanding of the mechanism of action of several drugs, for example, *BTK*, target of ibrutinib, *XPO1*, the target of KPT-8602, and *CB1* and *CB2*, the targets of dronabinol [7, 8]. However, genome editing techniques have gone a step further and they have been used with therapeutic and clinical approaches. Their use has facilitated the design of new therapies such as chimeric antigen receptors (CARs) and have allowed the study of genes involved in the evolution of pathogenesis [9, 10].

Targeted genome editing in ALL

The development of next generation sequencing (NGS) techniques provided enormous amount of data to interpret, which generated the need to translate those data into functionally and clinically relevant knowledge that enable investigators to determinate how genotype influences phenotype. In the past decade, the integration of

* Correspondence: jmhr@usal.es
†Adrián Montaño and Maribel Forero-Castro contributed equally to this work.
[1]IBSAL, IBMCC, University of Salamanca-CSIC, Cancer Research Center, Salamanca, Spain
[3]Department of Medicine, University of Salamanca, Spain, Department of Hematology, University Hospital of Salamanca, Salamanca, Spain
Full list of author information is available at the end of the article

genome editing systems enables investigators to directly manipulate virtually any gene in a diverse range of cell types and organisms [11].

Genome editing system is based in the use of engineered nucleases composed of sequence-specific DNA-binding domains fused to a non-specific DNA cleavage module [12, 13]. These chimeric nucleases inducing DNA double-strand-breaks (DSBs) that stimulate the cellular DNA mechanisms, including error-prone non-homologous end joining (NHEJ) and homologous recombination (HR) [14]. Several approaches have been used in the last years as genome editing technologies (Fig. 1). The combination of simplicity and flexibility has hurtled zinc-finger nucleases (ZFNs), transcription activator-like effector nucleases (TALENs) and short palindromic repeats interspersed with regular intervals (CRISPR) to the forefront of genetic engineering (Fig. 2) [11].

ZFNs and TALENs were first used to generate knock-out rats in 2009 and 2011, respectively [15, 16]. TALENs system was first used in human cells in the same year [17]. CRISPR-Cas9 system, discovered as part of the prokaryotic adaptive immune system at the end of 1980s [18], was introduced some years later. This was proposed as a genetic modification system in 2005 [19] but was not tested until 2012 [20].

CRISPR-Cas9 is presented as a faster, cheaper, simpler system with the potential for multiplex genome editing [21]. The method is based on generating a directed cut in the double strand of DNA by the Cas9 nuclease. This is driven by a single 20-nucleotide RNA strand, which marks the exact breakage point. After DNA cutting, the DNA repair machinery of the host cell leads to repair errors and thereby promote a modification of the original sequence by a mutation such as an insertion, deletion or inversion, among others [22]. Based on CRISPR-Cas9 system, CRISPR interference (CRISPRi) and CRISPR activation (CRISPRa) emerged. CRISPRi uses a catalytically inactive version of Cas9 (dCas9) lacking endonucleolytic activity in combination with an sgRNA designed with a 20-bp complementary region to any gene of interest to silence a target gene [23]. While CRISPRa uses fusions of dCas9 to activator domains to activate gene expression [21].

Genome editing strategies have been used in several organisms, including *Drosophila* [24], *Caenorhabditis elegans* [25], zebrafish [26], mouse [27], rat [28], plants and humans [21] and has allowed a large number of functional studies to be carried out, based on the generation of animal and plant models. The use of genetically modified cell lines and animal models to understand the functions of genes and their pathogenesis in diseases conditioned by molecular genetics could be of help and provide insights to better understand cancer. The method used until now to generate these animal models, especially mice, is tedious and time-consuming, but CRISPR-Cas9 makes the procedure easier and more efficient [29].

Genome editing technologies, such as CRISPR-Cas9, have already been applied to the study of many diseases, including hematological diseases [30]. As exemplified by some

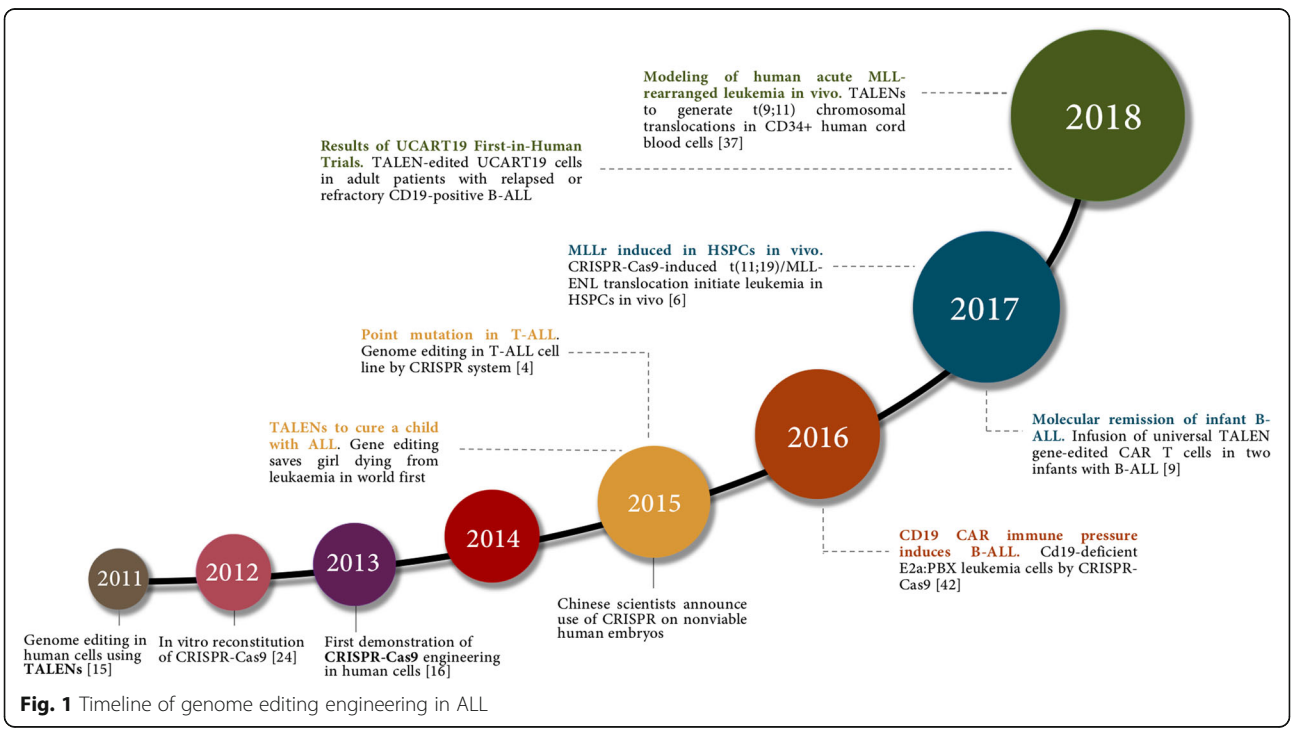

Fig. 1 Timeline of genome editing engineering in ALL

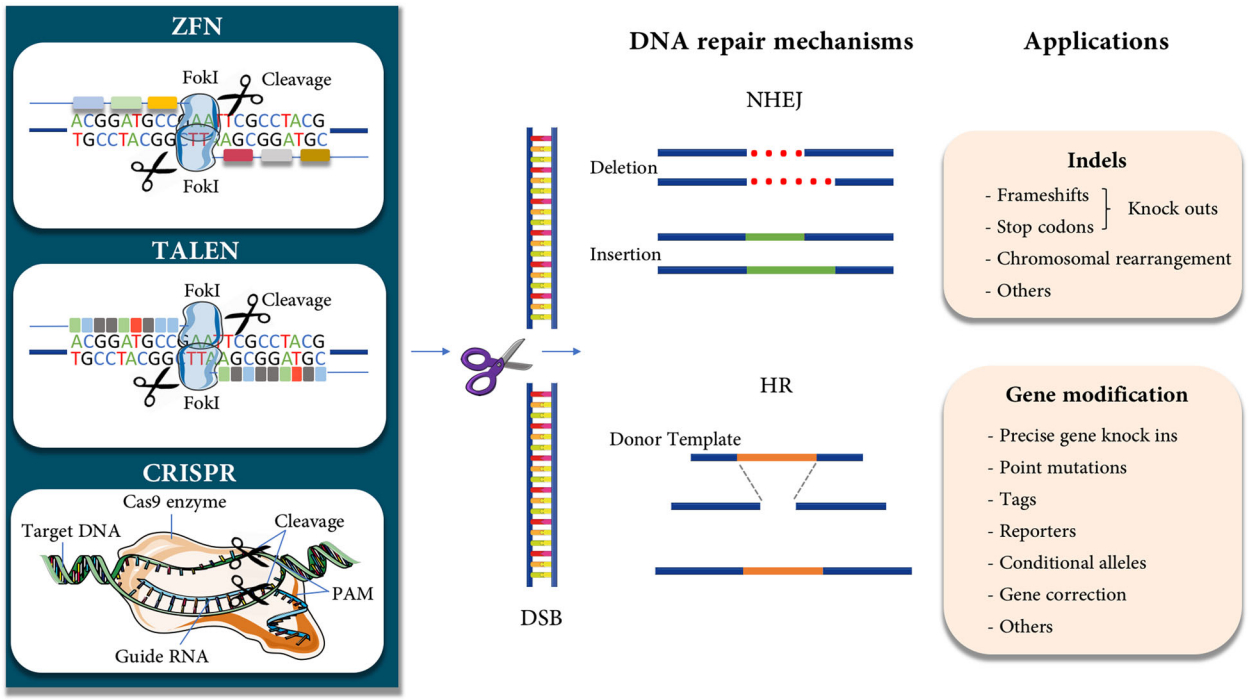

Fig. 2 The nuclease genome editing technologies in ALL. The three most commonly used types of nucleases include programmable nucleases like Zinc Finger Nucleases (ZFNs), transcription activator-like effector nucleases (TALENs) and CRISPR systems (Clustered Regularly Interspaced Short Palindromic Repeats). These nucleases were able to induce double-strand breakgs (DSBs) in the target followed by the activation of DNA repair mechanisms [30]. On induction of double-stranded breaks or nicks at targeted regions, repairing is done by either Non-homologous end joining (NHEJ) or Homologous recombination (HR) pathway. NHEJ is an error prone repair mechanism where joining of broken ends takes place, which generally results in heterogeneous indels (insertions and deletions) whereas HR is a precise repair method in which homologous donor template DNA is being used in repair DNA damage target site. HR is the ideal strategy for generating knock in models [81, 82].

very recent studies in Fanconi anemia (FA), a genetic DNA repair-deficient human disorder that results from mutations in FA genes [31] or the study of BCR-ABL oncogene in chronic myeloid leukemia [32]. Specifically, most of the genetic modification studies in ALL have been with CRISPR-Cas9, more than 20 articles since 2015. The vast majority had the purpose of knocking out genes, either by introducing mutations, insertions or deletions.

An overview of recent studies in genome editing in ALL is summarized in Table 1. Some of the most relevant studies included in the table are detailed below.

Targeting transcriptional factors

Deregulation of Transcription factors (TFs) is a common mechanism in the pathogenesis of human cancer, in particular in leukemia cells, genes encoding TFs are often amplified, deleted, rearranged via chromosomal translocation, or subjected to point mutations that result in a gain- or loss-of-function. Consequently, targeting of TFs can be highly effective in treating ALL. TFs such as *PAX5* and *IKZF1* were altered in nearly 80% of patients with B-ALL [33, 34]. These alterations affected glucose metabolism and energy supply, whereby the transcription factors act as metabolic repressors by limiting the amount of ATP available. A CRISPR-Cas9-based screen of *PAX5* and *IKZF1* transcriptional targets identified some target genes such as *NR3C1*, *TXNIP* and *CB2* as central effectors of B-lymphoid restriction of glucose and energy supply and therefore new targets for treating B-ALL [3].

In human T-cell acute lymphoblastic leukemia (T-ALL) cells, a CRISPR-Cas9 editing tool was used to disrupt *TAL1* (*SCL*) [4] or *TRIB1* (*TRB1*) [35] genes to delineate their biological functions. *TAL1* is one of the oncogenes most frequently deregulated in T-ALL [36]. This deregulation is produced by t (1;14) (p34;q11) (1–2%) or *SIL(-STIL)-TAL1* deletions (del(1)(p32)) (15–20%), although there is still a large group of patients in whom the gene is deregulated but not altered. Epigenetics must therefore play an important role in these patients [37]. CRISPR-Cas9 was used in a cell line to reproduce two known alterations in *TAL1* (insertion and deletion) and it was observed how these alterations triggered their expression. Furthermore, a change in methylation acetylation of H3K27 was observed,

Table 1 Applications of genome editing systems in ALL

	Outcome	Target Gene	SSN Technique	Modification Type	Cell type	Reference
Targeting Transcriptional factors	Point mutation (insertion/deletion)	***TAL1***	CRISPR-Cas9	HR	PEER (in vitro)	[4]
	Repress expression	***PAX5***	CRISPR-a	NA	Patient-derived pre-B ALL cells (in vitro)	[3]
	Knock out	***NR3C1***	CRISPR-Cas9	NHEJ		
		TXNIP				
		CB2				
	Knock out	***LMO2***	CRISPR-Cas9	NHEJ	PF-382 (in vitro)	[5]
Targeting gene fusion expression	Chromosomal rearrangement	**MLL/AF4**	TALEN	NHEJ	K562, HSPCS (in vitro)	[42]
		MLL/AF9				
	Knock in	**MLL/AF4 AF4/MLL**	CRISPR-Cas9	HR	HEK293 (in vitro)	[46]
	Chromosomal rearrangement	**MLL/ENL**	CRISPR-Cas9	NHEJ	HSPCS (in vitro / in vivo, xenograft)	[6]
	Chromosomal rearrangement	**MLL/AF9**	TALEN	NHEJ	CD34+ human cord blood (in vivo, xenograft)	[43]
		AF9/MLL				
	Knock in	**ETV6/RUNX1**	CRISPR-Cas9	HR	MIFF3 hIPSCs (in vitro)	[40]
Drug targts discovery and therapy	Knock out	***CB1***	CRISPR-Cas9	NHEJ	Jurkat (in vitro)	[7]
		CB2				
	Knock out	***BTK***	CRISPR-Cas9	NHEJ	RCH-ACV (in vitro / in vivo, xenograft)	[8]
		BLK				
	Knock in	***XPO1***	CRISPR-Cas9	HR	HL-60, Jurkat, K-562, and MOLT-4 (in vitro / in vivo, xenograft)	[57]
	Knock out	***ABCB1***	CRISPR-Cas9	NHEJ	HALO1 (in vitro)	[59]
Modification of CARs	Knock out	***CD19***	CRISPR-Cas9	NHEJ	NALM6, 697 (in vitro / in vivo, xenograft)	[65]
	Knock out	***CD19***	CRISPR-Cas9	NHEJ	Murine leukemia cell lines E2a:PBX (in vitro / in vivo, xenograft)	[83]
		PAX5				
		EBF1				
	Knock out	***TRAC***	CRISPR-Cas9	HR	NALM6 (in vitro / in vivo, xenograft)	[63]
	Knock in	***CD19***				
	Knock out	***CD52***	TALEN	NHEJ	Two infants (in vivo)	[9]
		TCR ab				
	Knock out	***TCR b***	CRISPR-Cas9	NHEJ	PBMC (in vitro)	[84]
	Knock out	***CD7***	CRISPR-Cas9	NHEJ	T cell lines (in vitro / in vivo, xenograft)	[85]
		TRAC				
Evolution of pathogenesis	Knock out	***CASD1***	CRISPR-Cas9	NHEJ	HAP1 (in vitro)	[70]
	Knock out	***RIP1***	CRISPR-Cas9	NHEJ	Patient-derived ALL cells (in vitro / in vivo, xenograft)	[75]
	Knock out	***CXCR4***	CRISPR-Cas9	NHEJ	NALM6 (in vitro / in vivo, xenograft)	[10]
Others	Knock out	***FLT3***	TALEN	NHEJ	K562 (in vitro)	[86]
	Knock out screen	NA	CRISPR-Cas9	NHEJ	NALM6 (in vitro)	[87]
	Knock out screen	NA	CRISPR-Cas9	NHEJ	MV4,11 (in vitro)	[88]
	Knock out	***NUDT15***	CRISPR-Cas9	NHEJ	Mouse (in vivo)	[89]
	Knock out	***DCK***	CRISPR-Cas9	NHEJ	KOPN41 (in vitro)	[90]
	Knock out	***PTCH1***	CRISPR-Cas9	NHEJ	Zebrafish embryos (in vivo, xenograft)	[91]

This table shows the main genetic editing studies carried out in ALL, classified according to the target. The different columns indicate: the outcome of edition, the target of edition (highlighted in bold), the technique used, the type of modification, the cell type and the reference

suggesting a causal relationship between mutagenesis, epigenetic modulation and expression of *TAL1* [4].

LMO2 is another gene deregulated in T-ALL. It is a potent oncogene that is essential for the formation of a large transcriptional complex in which genes such as *TAL1*, *LDB1*, *GATA1*, *GATA2*, *GATA3*, *RUNX1*, *ETS1*, and *MYB* intervene. Furthermore, its overexpression has been associated with the development of T-ALL. However, the reasons why this gene is overexpressed remain unclear, because few mutations have been described. Mutations targeted to the non-coding region of *LMO2* were introduced in a T-ALL cell line by CRISPR-Cas9 and proved to be a possible cause of the deregulation of *LMO2* expression [5].

Targeting gene fusion expression in ALL with chromosomal rearrangements

As indicated above, chromosomal translocations are very frequent in ALL and can be used to stratify the risk of ALL patients. It is well known that *MLL* rearrangements occur in a small percentage of B-ALL patients, where they are associated with very poor prognosis. Several studies have proposed that *MLL* rearrangements are an initiating event in leukemic transformation, unlike ETV6-RUNX1 and BCR-ABL translocations, in which second events are necessary to initiate leukemia [33, 38, 39]. This was demonstrated by Enver T's group, who used a homologous recombination knock-in approach by CRISPR-Cas9 to introduce the cDNA encoding of *RUNX1* exons 2–8 into the native *ETV6* locus of hIPSC. ETV6-RUNX1 expression induced a partial block of the maturation of B lymphocytes, at which time the second events required for leukemia development occurs [40].

Matthew Porteus's group wanted to test the oncogenic potential as initiator event of the *MLL* translocations, and for this purpose, they generated the MLL-AF4 and MLL-AF9 translocations by genetic modification in primary hematopoietic stem and progenitor cells (HSPCs). This strategy was based on previous studies that demonstrated that the double-stranded DNA breakage at specific positions of two chromosomes could lead to translocation [41]. They used TALENs to generate cuts directed at specific positions of MLL-AF4 and AF9, based on the breakage points described in patients. In vitro, the cells that acquired the translocation showed a proliferative advantage over the others but were not able to transform completely because they eventually disappeared from the culture [42].

Shortly after, Heckl D.'s group showed strong evidence for the formation of true t (11;19)/MLL-AF9 translocations in vitro and in vivo by CRISPR-Cas9. No full transformation was observed in liquid cultures or methylcellulose-based in vitro assays using CD34+ HSPC, while in vivo assays demonstrated that endogenous t (11;19) can initiate a monocytic leukemia-like phenotype. This study is in line with the Matthew Porteus's study, which emphasizes the importance of environmental cues for the oncogenic transformation in *MLL*r leukemias [6].

More recently, Stanford's group managed to generate t (9;11) chromosomal translocations encoding MLL-AF9 and reciprocal AF9-MLL fusion products in CD34+ human cord blood cells by TALENs. Transplantation of these cells into immune-compromised mice induced myeloid leukemias with absence of secondary lesions studied by targeted exome sequencing and RNAseq [43].

The prevailing theory is that *MLL* rearrangements occur in the uterus due to exposure to certain chemicals during pregnancy that cause errors in DNA repair, as has been demonstrated in vitro and in vivo [44, 45]. The group of Pablo Menéndez examined how it affected the expression of the fusion protein in repairing DNA damage. To this end, MLL-AF4 protein and its reciprocal, AF4-MLL were induced in the AAVS1 locus of the HEK293 cell line by CRISPR-Cas9. They subsequently induced DNA damage by exposing the cells to etoposide and ionizing radiation (IR), with no differences in repair between WT cells and those expressing proteins. Thus, they demonstrated that the expression of the fusion proteins caused by *MLL* rearrangements, did not influence susceptibility to DNA damage or repair mechanisms [46].

Drug targets discovery and therapy

The targets against which a drug acts must be identified and combined with the data provided by the NGS. This may sometimes identify patients with mutations in genes associated with some type of resistance. It can also help to generate other new drugs, when there is prior knowledge of the altered pathway we wish to attack. For example, ibrutinib has recently been proposed for the treatment of pre-BCR and *TCF3*-r-positive cases. Ibrutinib is an inhibitor kinase targeted to those ALL subtypes with affected BCR signaling. In order to understand the mechanism of action of ibrutinib in this ALL subtype, Bruton tyrosine kinase (*BTK*) KO, B lymphocyte kinase (*BLK*) KO and *BTK / BLK* KO cells have been generated by CRISPR-Cas9 [8].

The importance of *BTK* in the pathogenesis of chronic lymphocytic leukemia, diffuse large B-cell lymphoma, and other mature B-cell malignancies is well established [47–49], while there is less information about the role of *BTK* in ALL. Early studies reported unaltered levels of *BTK* in childhood ALL cells, whereas frequent *BTK* deficiency due to aberrant splicing was reported later [50, 51]. *BLK* and *BTK* were the only kinase genes overexpressed in this subtype of ALL, as revealed by arrays [52]. Only the elimination of the expression of both

kinases managed to reduce the proliferation in a similar way to ibrutinib. However, these should not be the only targets of ibrutinib since the decrease in proliferation was still greater when the drug was used. To confirm that *BTK* and *BLK* were actually drug targets, ibrutinib was tested in cell lines generated with KO genes. This indicated that ibrutinib requires the presence of both kinases for maximum effectiveness [8].

In a subsequent study, Thomas Vercruysse and coworkers focused on exportin 1 (*XPO1*). *XPO1* plays an important role in the transport through the nucleus of cycle regulatory proteins and tumor suppressor proteins, among others. The overexpression of this gene is associated with several types of cancer, and with poor patient outcome [53, 54]. *XPO1* inhibitors act by binding to the reactive cysteine residue located at position 528, preventing the export of charged proteins to the cytoplasm [55, 56]. To verify that the drug binds specifically to act against *XPO1,* a point mutation was inserted at residue 528 by CRISPR-Cas9. When this occurred, the drug was not able to act, and the cells became resistant. Therefore, this study demonstrated that the drug is highly specific to *XPO1* and is potent against ALL [57].

More recently, Dronabinol (Tetrahydrocannabinol, THC), a US Food and Drug Administration-approved cannabinoid receptor (CNB) agonist for the treatment of chemotherapy-induced nausea and vomiting, was found to induce apoptosis in acute leukaemia cells, as evidenced by the abrogation of pro-apoptotic effects of CRISPR-mediated knockout of *CB1* or *CB2* following THC treatment [7, 58].

Furthermore, new drugs are being proposed as an alternative to current therapy. An example is Carfilzomib (CFZ), as a substitute of proteasome inhibitor Bortezomib (BTZ), who demonstrated favorable clinical outcomes for refractory childhood ALL. CFZ showed significantly higher activity than BTZ in vitro, except for the P-glycoprotein-positive t (17;19) ALL cell lines. Takahashi et al. generated a knock-out of *ABCB1*, who codes for P-glycoprotein, by genome editing with a CRISPR-Cas9 system and sensitized P-glycoprotein-positive t (17;19) ALL cell line to CFZ [59].

Modification of CAR

Chemotherapy and/or radiotherapy have been standard treatments for ALL to date. However, immunological therapies have gained importance. These work by harnessing the immune system of patients to fight the disease. One example is chimeric antigen receptors (CARs), which are proteins genetically engineered to allow T cells to recognize a specific antigen in tumor cells. It had already been proposed as a standard therapy for ALL patients in 2013 by Rosenberg. In this case, the CARs were directed against CD19, an antigen of B cells [60]. Its efficacy had already been demonstrated in cases of refractory or relapsed ALL [61, 62].

CRISPR-Cas9 may be key to carry out this genetic modification. This was demonstrated by Michel Sadelain's group. The strategy followed was the combination of knock-out and knock-in. On the one hand, they interrupted the TRAC locus, and on the other, they added a CAR directed to CD19, inserting it in the AAVS1 locus. hey compared responses to CD19 antigens from these cells with those from others in which CAR had been randomly integrated. In this way, they were able to demonstrate that targeted CAR integration under the control of endogenous regulatory elements is much more effective, reduces tonic signaling, avoids the differentiation and accelerated depletion of T cells, and increases the therapeutic potential of these cells [63].

Paul Veys's group demonstrated the use of TALEN-modified T lymphocytes in two infants with refractory B-ALL. They generated universal T-cells against CD19 (CAR19), targeting the TALENs against the T-cell receptor (TCR) and simultaneously transfecting with non-human leukocyte donor cell antigens. As treated cells, they disrupted the CD52 gene, the target of the drug alemtuzumab, by TALEN, and also disrupted the expression of the αβ T cell surface receptor (TCR αβ). This minimized the risk of graft-versus-host disease (GVHD). The newborns were treated with lymphoplasty, chemotherapy and anti-CD52 serotherapy before infusion of CAR19. The results were very positive, yielding remissions within 28 days before allogeneic stem cell transplantation [9].

Despite the good results with CAR19 therapy, 10–20% of treated patients suffer relapses due to partial loss of the CD19 epitope [61, 64]. Andrei Thomas-Tikhonenko and his group have provided evidence that epitope loss is closely linked to alterations in exon 2 of CD19, detected in some samples from patients with relapses. These alterations include frameshift-type mutations and the total loss of the exon, resulting from an alternative splicing event that encodes a deficient isoform of exon 2. To assess the relevance of the detected isoforms, they eliminated CD19 expression by CRISPR-Cas9 from ALL cell lines, and then reconstituted them with different isoforms. They observed that the depleted isoform of exon 2 was located mostly in the cytosol, which could explain its mechanism of escape in front of CAR19. Thus, these deleterious mutations and the selection of isoforms resulting from alternative splicing could be the cause of this mechanism of resistance [65].

Evolution of pathogenesis

Although there have been great advances in the treatment and cure of ALL, there is still a large group of

patients who experience relapses, persistent minimal residual disease, and drug resistance, and who ultimately have a poor prognosis [66, 67]. Efforts have therefore focused on trying to understand why these resistances occur, to counteract them, and to look for new, more personalized drugs that avoid resistance.

In ALL, survival and drug resistance of lymphoblasts critically depend on 9-O-acetylation of sialic acids (Sias) [68, 69]. Baumann AM et al., generated a *CASD1* knock-out cells by CRISPR-Cas9-mediated genome editing and demonstrated that *CASD1* is essential for 9-O-acetylation [70].

Second mitochondrial-derived caspase-activators (SMACs) act by inhibiting inhibitors of apoptosis proteins (IAPs). One of the possible causes of resistance is revealed by the action of these proteins, which act to counteract the effects of drugs. These are also overexpressed in many types of cancer [71, 72]. The main mechanism of action of IAPs is the inhibition of apoptosis through proteins such as caspases [73] or receptor interaction of protein kinase 1 (*RIP1*), a potent activator of death [74]. In this study, they set out to demonstrate that SMAC acted by reactivating apoptosis of these cells, mediated by *RIP1.* They used CRISPR-Cas9 system to knock out this gene in vivo in xenograft models, and thereby eliminate its expression. The results showed that *RIP1* was necessary for the induction of cell death by SMAC [75].

CXCR4 encodes a membrane receptor whose function is to attract and confine the stromal cells of the bone marrow stromal cells (BMSCs). This interaction with BMSCs gives B cells a degree of protection, associated with increased survival, resistance to treatment, relapse and worse prognosis [76, 77]. *CXCR4* is highly expressed in B-ALL cells and has also been correlated with poor patient outcome [78]. Inhibitors of *CXCR4* have already been examined in the preclinical setting, in vitro and in vivo [79, 80] and may be *CXCR4* antagonists or agonists. To test whether the efficacy of these compounds was due to the inhibition of *CXCR4* and not to their own activity as agonists, they generated a B-ALL cell line with *CXCR4* knock-out by CRISPR-Cas9. They demonstrated that the agonistic activity of *CXCR4* antagonists did not affect antitumor activity. In addition, in vivo *CXCR4* knock-out models reduced the burden of leukemia and disease progression. In this way, the importance of *CXCR4* in the pathogenesis of B-ALL and in its use as a therapeutic target to fight drug resistance is demonstrated [10].

Conclusions, challenges and future directions

Genome editing technologies have already demonstrated its potential to study molecular biology and pathogenesis of the genetic aberrations in ALL, in vitro and in vivo.

From a future perspective, the development of the genomic editing tools could also help to the generation of murine models of leukemias that resemble the human disease. In this sense, multigenic nature of the disease entails great difficulties. In the case of ALL, murine models based on a single alteration have failed, at least in part, to fully develop the disease. Combining several of the gene alterations found in patients in a murine model, we could approach to the real pathological conditions, giving rise to a more efficient model for the investigation of this type of tumors. Until recently, to generate an animal model with several genetic alterations was a long and expensive process, however, tools such us, CRISPR-Cas9, will allow introducing multiple mutations in a single step. Thus, it will be possible to generate, in short periods of time, more complex animal models that allow us to simulate more faithfully the conditions that occur in patients, providing the appropriate platform to study and to develop new therapeutic strategies.

Furthermore, in the clinic, genome editing systems could facilitate the rapid screening of new drugs and will promote the development of personalized medicine, connecting genomics, disease phenotypes and therapeutic goals. The use of these technologies will broaden our understanding of the mechanism of action of these novel drugs and enable the identification of novel mechanisms of acquired resistance to pathway target therapeutics. However, translating genome editing technologies to the clinical setting requires two main concerns to be addressed: the safety and efficacy of treatments. The off-target effect remains one of the major obstacles of this technology. Researches will need to improve our genetic tools in order to eliminate any off-target effects and to improve the gene edition efficiency in the future. Despite this, genome editing offers new opportunities for tackling diseases such as ALL that have been beyond the reach of previous therapies.

Abbreviations

ALL: Acute lymphoblastic leukemia; AML: Acute myeloid leukemia; BCR: B-cell receptor signaling; BMSCs: Bone marrow stromal cells; CARs: Chimeric antigen receptors; CRISPR: Short palindromic repeats interspersed with regular intervals; DSBs: Double-strand breaks; HiPSC: Human induced pluripotent stem cell; HR: Homologous recombination; HSPCs: Hematopoietic stem and progenitor cells; IAPs: Inhibitors of apoptosis proteins; IR: Ionizing radiation; MMEJ: Micro-homology-mediated end-joining; NGS: Next generation sequencing; NHEJ: Non-homologous end-joining; PBMC: Peripheral blood mononuclear cell; Sias: Sialic acids; SMACs: Second mitochondrial-derived caspase-activators; TALENs: Transcription-activating type nucleases; TCR: T-cell receptor; THC: Tetrahydrocannabinol; ZFNs: Zinc finger nucleases

Acknowledgements

Part of this work was support by a grant to AM from the Junta Provincial de Salamanca of the Asociación Española Contra el Cáncer (AECC), and a grant to MFC from the Universidad Pedagógica y Tecnológica de Colombia –

Vicerrectoría de Investigación y Extensión (Grupo de Investigación en Ciencias Biomédicas UPTC – GICBUPTC, Escuela de Ciencias Biológicas).

Funding
This work was financially supported in part by a grant from the Consejería de Educación, Junta de Castilla y León, Fondos FEDER (SA085U16), Proyectos de Investigación del SACYL, Spain (BIO/SA10/14), a grant to AM from the Junta Provincial de Salamanca of the Asociación Española Contra el Cáncer (AECC), and a grant to MFC from the Universidad Pedagógica y Tecnológica de Colombia – Vicerrectoría de Investigación y Extensión (Grupo de Investigación en Ciencias Biomédicas UPTC – GICBUPTC, Escuela de Ciencias Biológicas).

Authors' contributions
AMB and MFC wrote the manuscript. All authors contributed to editing and approval of the final manuscript.

Ethics approval and consent to participate
Not applicable.

Consent for publication
Not applicable.

Competing interests
The authors declare that they have no competing interests.

Publisher's Note

Author details
[1]IBSAL, IBMCC, University of Salamanca-CSIC, Cancer Research Center, Salamanca, Spain. [2]School of Biological Sciences (GICBUPTC Research group), Universidad Pedagógica y Tecnológica de Colombia, Boyacá, Colombia. [3]Department of Medicine, University of Salamanca, Spain, Department of Hematology, University Hospital of Salamanca, Salamanca, Spain. [4]IBMCC, CIC University of Salamanca-CSIC, University Hospital of Salamanca, Salamanca, Spain.

Received: 28 February 2018 Accepted: 5 July 2018
Published online: 17 July 2018

References

1. Iacobucci I, Mullighan CG. Genetic basis of acute lymphoblastic leukemia. J Clin Oncol. 2017;35(9):975–83.
2. Nemudryi AA, Valetdinova KR, Medvedev SP, Zakian SM. TALEN and CRISPR/Cas genome editing systems: tools of discovery. Acta Nat. 2014;6(3):19–40.
3. Chan LN, Chen Z, Braas D, Lee JW, Xiao G, Geng H, Cosgun KN, Hurtz C, Shojaee S, Cazzaniga V, et al. Metabolic gatekeeper function of B-lymphoid transcription factors. Nature. 2017;542(7642):479–83.
4. Navarro JM, Touzart A, Pradel LC, Loosveld M, Koubi M, Fenouil R, Le Noir S, Maqbool MA, Morgado E, Gregoire C, et al. Site- and allele-specific polycomb dysregulation in T-cell leukaemia. Nat Commun. 2015;6:6094.
5. Rahman S, Magnussen M, Leon TE, Farah N, Li Z, Abraham BJ, Alapi KZ, Mitchell RJ, Naughton T, Fielding AK, et al. Activation of the LMO2 oncogene through a somatically acquired neomorphic promoter in T-cell acute lymphoblastic leukemia. Blood. 2017;129(24):3221–6.
6. Reimer J, Knoss S, Labuhn M, Charpentier EM, Gohring G, Schlegelberger B, Klusmann JH, Heckl D. CRISPR-Cas9-induced t(11;19)/MLL-ENL translocations initiate leukemia in human hematopoietic progenitor cells in vivo. Haematologica. 2017;102(9):1558–66.
7. Kampa-Schittenhelm KM, Salitzky O, Akmut F, Illing B, Kanz L, Salih HR, Schittenhelm MM. Dronabinol has preferential antileukemic activity in acute lymphoblastic and myeloid leukemia with lymphoid differentiation patterns. BMC Cancer. 2016;16:25.
8. Kim E, Hurtz C, Koehrer S, Wang Z, Balasubramanian S, Chang BY, Muschen M, Davis RE, Burger JA. Ibrutinib inhibits pre-BCR+ B-cell acute lymphoblastic leukemia progression by targeting BTK and BLK. Blood. 2017; 129(9):1155–65.
9. Qasim W, Zhan H, Samarasinghe S, Adams S, Amrolia P, Stafford S, Butler K, Rivat C, Wright G, Somana K, et al. Molecular remission of infant B-ALL after infusion of universal TALEN gene-edited CAR T cells. Sci Transl Med. 2017;9(374)
10. Randhawa S, Cho BS, Ghosh D, Sivina M, Koehrer S, Muschen M, Peled A, Davis RE, Konopleva M, Burger JA. Effects of pharmacological and genetic disruption of CXCR4 chemokine receptor function in B-cell acute lymphoblastic leukaemia. Br J Haematol. 2016;174(3):425–36.
11. Gaj T, Gersbach CA, Barbas CF 3rd. ZFN, TALEN, and CRISPR/Cas-based methods for genome engineering. Trends Biotechnol. 2013;31(7):397–405.
12. Urnov FD, Rebar EJ, Holmes MC, Zhang HS, Gregory PD. Genome editing with engineered zinc finger nucleases. Nat Rev Genet. 2010;11(9):636–46.
13. Carroll D. Genome engineering with zinc-finger nucleases. Genetics. 2011; 188(4):773–82.
14. Wyman C, Kanaar R. DNA double-strand break repair: all's well that ends well. Annu Rev Genet. 2006;40:363–83.
15. Geurts AM, Cost GJ, Freyvert Y, Zeitler Z, Miller JC, Choi VM, Jenkins SS, Wood A, Cui X, Meng X, et al. Knockout rats produced using designed zinc finger nucleases. Science. 2009;325(5939):433.
16. Tesson L, Usal C, Menoret S, Leung E, Niles BJ, Remy S, Santiago Y, Vincent AI, Meng X, Zhang L, et al. Knockout rats generated by embryo microinjection of TALENs. Nat Biotechnol. 2011;29(8):695–6.
17. Miller JC, Tan S, Qiao G, Barlow KA, Wang J, Xia DF, Meng X, Paschon DE, Leung E, Hinkley SJ, et al. A TALE nuclease architecture for efficient genome editing. Nat Biotechnol. 2011;29(2):143–8.
18. Ishino Y, Shinagawa H, Makino K, Amemura M, Nakata A. Nucleotide sequence of the iap gene, responsible for alkaline phosphatase isozyme conversion in Escherichia coli, and identification of the gene product. J Bacteriol. 1987;169(12):5429–33.
19. Mojica FJ, Diez-Villasenor C, Garcia-Martinez J, Soria E. Intervening sequences of regularly spaced prokaryotic repeats derive from foreign genetic elements. J Mol Evol. 2005;60(2):174–82.
20. Jinek M, Chylinski K, Fonfara I, Hauer M, Doudna JA, Charpentier E. A programmable dual-RNA-guided DNA endonuclease in adaptive bacterial immunity. Science. 2012;337(6096):816–21.
21. Mali P, Yang L, Esvelt KM, Aach J, Guell M, DiCarlo JE, Norville JE, Church GM. RNA-guided human genome engineering via Cas9. Science. 2013; 339(6121):823–6.
22. Cong L, Ran FA, Cox D, Lin S, Barretto R, Habib N, Hsu PD, Wu X, Jiang W, Marraffini LA, et al. Multiplex genome engineering using CRISPR/Cas systems. Science. 2013;339(6121):819–23.
23. Larson MH, Gilbert LA, Wang X, Lim WA, Weissman JS, Qi LS. CRISPR interference (CRISPRi) for sequence-specific control of gene expression. Nat Protoc. 2013;8(11):2180–96.
24. Yu Z, Ren M, Wang Z, Zhang B, Rong YS, Jiao R, Gao G. Highly efficient genome modifications mediated by CRISPR/Cas9 in Drosophila. Genetics. 2013;195(1):289–91.
25. Dickinson DJ, Ward JD, Reiner DJ, Goldstein B. Engineering the Caenorhabditis elegans genome using Cas9-triggered homologous recombination. Nat Methods. 2013;10(10):1028–34.
26. Chang N, Sun C, Gao L, Zhu D, Xu X, Zhu X, Xiong JW, Xi JJ. Genome editing with RNA-guided Cas9 nuclease in zebrafish embryos. Cell Res. 2013; 23(4):465–72.
27. Wang H, Yang H, Shivalila CS, Dawlaty MM, Cheng AW, Zhang F, Jaenisch R. One-step generation of mice carrying mutations in multiple genes by CRISPR/Cas-mediated genome engineering. Cell. 2013;153(4):910–8.
28. Li D, Qiu Z, Shao Y, Chen Y, Guan Y, Liu M, Li Y, Gao N, Wang L, Lu X, et al. Heritable gene targeting in the mouse and rat using a CRISPR-Cas system. Nat Biotechnol. 2013;31(8):681–3.
29. Xiong X, Chen M, Lim WA, Zhao D, Qi LS. CRISPR/Cas9 for human genome engineering and disease research. Annu Rev Genomics Hum Genet. 2016; 17:131–54.
30. Osborn MJ, Webber BR, Knipping F, Lonetree CL, Tennis N, DeFeo AP, McElroy AN, Starker CG, Lee C, Merkel S, et al. Evaluation of TCR gene editing achieved by TALENs, CRISPR/Cas9, and megaTAL nucleases. Mol Ther. 2016;24(3):570–81.
31. Osborn MJ, Gabriel R, Webber BR, DeFeo AP, McElroy AN, Jarjour J, Starker CG, Wagner JE, Joung JK, Voytas DF, et al. Fanconi anemia gene editing by the CRISPR/Cas9 system. Hum Gene Ther. 2015;26(2):114–26.
32. Garcia-Tunon I, Hernandez-Sanchez M, Ordonez JL, Alonso-Perez V, Alamo-Quijada M, Benito R, Guerrero C, Hernandez-Rivas JM, Sanchez-Martin M. The CRISPR/Cas9 system efficiently reverts the tumorigenic ability of BCR/

ABL in vitro and in a xenograft model of chronic myeloid leukemia. Oncotarget. 2017;8(16):26027–40.
33. Mullighan CG, Goorha S, Radtke I, Miller CB, Coustan-Smith E, Dalton JD, Girtman K, Mathew S, Ma J, Pounds SB, et al. Genome-wide analysis of genetic alterations in acute lymphoblastic leukaemia. Nature. 2007; 446(7137):758–64.
34. Mullighan CG, Phillips LA, Su X, Ma J, Miller CB, Shurtleff SA, Downing JR. Genomic analysis of the clonal origins of relapsed acute lymphoblastic leukemia. Science. 2008;322(5906):1377–80.
35. Miyajima C, Inoue Y, Hayashi H. Pseudokinase tribbles 1 (TRB1) negatively regulates tumor-suppressor activity of p53 through p53 deacetylation. Biol Pharm Bull. 2015;38(4):618–24.
36. Sanda T, Lawton LN, Barrasa MI, Fan ZP, Kohlhammer H, Gutierrez A, Ma W, Tatarek J, Ahn Y, Kelliher MA, et al. Core transcriptional regulatory circuit controlled by the TAL1 complex in human T cell acute lymphoblastic leukemia. Cancer Cell. 2012;22(2):209–21.
37. Ferrando AA, Herblot S, Palomero T, Hansen M, Hoang T, Fox EA, Look AT. Biallelic transcriptional activation of oncogenic transcription factors in T-cell acute lymphoblastic leukemia. Blood. 2004;103(5):1909–11.
38. Greaves MF, Wiemels J. Origins of chromosome translocations in childhood leukaemia. Nat Rev Cancer. 2003;3(9):639–49.
39. Greaves M. A causal mechanism for childhood acute lymphoblastic leukaemia. Nat Rev Cancer. 2018;
40. Boiers C, Richardson SE, Laycock E, Zriwil A, Turati VA, Brown J, Wray JP, Wang D, James C, Herrero J, et al. A human IPS model implicates embryonic B-myeloid fate restriction as developmental susceptibility to B acute lymphoblastic leukemia-associated ETV6-RUNX1. Dev Cell. 2018;44(3): 362–77. e367
41. Weinstock DM, Brunet E, Jasin M. Induction of chromosomal translocations in mouse and human cells using site-specific endonucleases. J Natl Cancer Inst Monogr. 2008;2008(39):20–4.
42. Breese EH, Buechele C, Dawson C, Cleary ML, Porteus MH. Use of genome engineering to create patient specific MLL translocations in primary human hematopoietic stem and progenitor cells. PLoS One. 2015;10(9):e0136644.
43. Schneidawind C, Jeong J, Schneidawind D, Kim IS, Duque-Afonso J, Wong SHK, Iwasaki M, Breese EH, Zehnder JL, Porteus M, et al. MLL leukemia induction by t(9;11) chromosomal translocation in human hematopoietic stem cells using genome editing. Blood Adv. 2018;2(8):832–45.
44. Bueno C, Catalina P, Melen GJ, Montes R, Sanchez L, Ligero G, Garcia-Perez JL, Menendez P. Etoposide induces MLL rearrangements and other chromosomal abnormalities in human embryonic stem cells. Carcinogenesis. 2009;30(9):1628–37.
45. Nanya M, Sato M, Tanimoto K, Tozuka M, Mizutani S, Takagi M. Dysregulation of the DNA damage response and KMT2A rearrangement in fetal liver hematopoietic cells. PLoS One. 2015;10(12):e0144540.
46. Castano J, Herrero AB, Bursen A, Gonzalez F, Marschalek R, Gutierrez NC, Menendez P. Expression of MLL-AF4 or AF4-MLL fusions does not impact the efficiency of DNA damage repair. Oncotarget. 2016;7(21):30440–52.
47. Herman SE, Gordon AL, Hertlein E, Ramanunni A, Zhang X, Jaglowski S, Flynn J, Jones J, Blum KA, Buggy JJ, et al. Bruton tyrosine kinase represents a promising therapeutic target for treatment of chronic lymphocytic leukemia and is effectively targeted by PCI-32765. Blood. 2011;117(23):6287–96.
48. Ponader S, Chen SS, Buggy JJ, Balakrishnan K, Gandhi V, Wierda WG, Keating MJ, O'Brien S, Chiorazzi N, Burger JA. The Bruton tyrosine kinase inhibitor PCI-32765 thwarts chronic lymphocytic leukemia cell survival and tissue homing in vitro and in vivo. Blood. 2012;119(5):1182–9.
49. Davis RE, Ngo VN, Lenz G, Tolar P, Young RM, Romesser PB, Kohlhammer H, Lamy L, Zhao H, Yang Y, et al. Chronic active B-cell-receptor signalling in diffuse large B-cell lymphoma. Nature. 2010;463(7277):88–92.
50. Goodman PA, Wood CM, Vassilev AO, Mao C, Uckun FM. Defective expression of Bruton's tyrosine kinase in acute lymphoblastic leukemia. Leuk Lymphoma. 2003;44(6):1011–8.
51. Feldhahn N, Klein F, Mooster JL, Hadweh P, Sprangers M, Wartenberg M, Bekhite MM, Hofmann WK, Herzog S, Jumaa H, et al. Mimicry of a constitutively active pre-B cell receptor in acute lymphoblastic leukemia cells. J Exp Med. 2005;201(11):1837–52.
52. Zhang J, Ding L, Holmfeldt L, Wu G, Heatley SL, Payne-Turner D, Easton J, Chen X, Wang J, Rusch M, et al. The genetic basis of early T-cell precursor acute lymphoblastic leukaemia. Nature. 2012;481(7380):157–63.
53. van der Watt PJ, Maske CP, Hendricks DT, Parker MI, Denny L, Govender D, Birrer MJ, Leaner VD. The Karyopherin proteins, Crm1 and Karyopherin beta1, are overexpressed in cervical cancer and are critical for cancer cell survival and proliferation. Int J Cancer. 2009;124(8):1829–40.
54. Shen A, Wang Y, Zhao Y, Zou L, Sun L, Cheng C. Expression of CRM1 in human gliomas and its significance in p27 expression and clinical prognosis. Neurosurgery. 2009;65(1):153–9. discussion 159-160
55. Lapalombella R, Sun Q, Williams K, Tangeman L, Jha S, Zhong Y, Goettl V, Mahoney E, Berglund C, Gupta S, et al. Selective inhibitors of nuclear export show that CRM1/XPO1 is a target in chronic lymphocytic leukemia. Blood. 2012;120(23):4621–34.
56. Neggers JE, Vercruysse T, Jacquemyn M, Vanstreels E, Baloglu E, Shacham S, Crochiere M, Landesman Y, Daelemans D. Identifying drug-target selectivity of small-molecule CRM1/XPO1 inhibitors by CRISPR/Cas9 genome editing. Chem Biol. 2015;22(1):107–16.
57. Vercruysse T, De Bie J, Neggers JE, Jacquemyn M, Vanstreels E, Schmid-Burgk JL, Hornung V, Baloglu E, Landesman Y, Senapedis W, et al. The second-generation Exportin-1 inhibitor KPT-8602 demonstrates potent activity against acute lymphoblastic leukemia. Clin Cancer Res. 2017;23(10):2528–41.
58. Lombard C, Nagarkatti M, Nagarkatti PS. Targeting cannabinoid receptors to treat leukemia: role of cross-talk between extrinsic and intrinsic pathways in Delta9-tetrahydrocannabinol (THC)-induced apoptosis of Jurkat cells. Leuk Res. 2005;29(8):915–22.
59. Takahashi K, Inukai T, Imamura T, Yano M, Tomoyasu C, Lucas DM, Nemoto A, Sato H, Huang M, Abe M, et al. Anti-leukemic activity of bortezomib and carfilzomib on B-cell precursor ALL cell lines. PLoS One. 2017;12(12):e0188680.
60. Kochenderfer JN, Dudley ME, Carpenter RO, Kassim SH, Rose JJ, Telford WG, Hakim FT, Halverson DC, Fowler DH, Hardy NM, et al. Donor-derived CD19-targeted T cells cause regression of malignancy persisting after allogeneic hematopoietic stem cell transplantation. Blood. 2013; 122(25):4129–39.
61. Maude SL, Frey N, Shaw PA, Aplenc R, Barrett DM, Bunin NJ, Chew A, Gonzalez VE, Zheng Z, Lacey SF, et al. Chimeric antigen receptor T cells for sustained remissions in leukemia. N Engl J Med. 2014;371(16):1507–17.
62. Lee DW, Kochenderfer JN, Stetler-Stevenson M, Cui YK, Delbrook C, Feldman SA, Fry TJ, Orentas R, Sabatino M, Shah NN, et al. T cells expressing CD19 chimeric antigen receptors for acute lymphoblastic leukaemia in children and young adults: a phase 1 dose-escalation trial. Lancet. 2015;385(9967): 517–28.
63. Eyquem J, Mansilla-Soto J, Giavridis T, van der Stegen SJ, Hamieh M, Cunanan KM, Odak A, Gonen M, Sadelain M. Targeting a CAR to the TRAC locus with CRISPR/Cas9 enhances tumour rejection. Nature. 2017;543(7643):113–7.
64. Topp MS, Gokbuget N, Zugmaier G, Klappers P, Stelljes M, Neumann S, Viardot A, Marks R, Diedrich H, Faul C, et al. Phase II trial of the anti-CD19 bispecific T cell-engager blinatumomab shows hematologic and molecular remissions in patients with relapsed or refractory B-precursor acute lymphoblastic leukemia. J Clin Oncol. 2014;32(36):4134–40.
65. Sotillo E, Barrett DM, Black KL, Bagashev A, Oldridge D, Wu G, Sussman R, Lanauze C, Ruella M, Gazzara MR, et al. Convergence of acquired mutations and alternative splicing of CD19 enables resistance to CART-19 immunotherapy. Cancer Discov. 2015;5(12):1282–95.
66. Locatelli F, Schrappe M, Bernardo ME, Rutella S. How I treat relapsed childhood acute lymphoblastic leukemia. Blood. 2012;120(14):2807–16.
67. Curran E, Stock W. How I treat acute lymphoblastic leukemia in older adolescents and young adults. Blood. 2015;125(24):3702–10.
68. Mukherjee K, Chava AK, Mandal C, Dey SN, Kniep B, Chandra S, Mandal C. O-acetylation of GD3 prevents its apoptotic effect and promotes survival of lymphoblasts in childhood acute lymphoblastic leukaemia. J Cell Biochem. 2008;105(3):724–34.
69. Parameswaran R, Lim M, Arutyunyan A, Abdel-Azim H, Hurtz C, Lau K, Muschen M, Yu RK, von Itzstein M, Heisterkamp N, et al. O-acetylated N-acetylneuraminic acid as a novel target for therapy in human pre-B acute lymphoblastic leukemia. J Exp Med. 2013;210(4):805–19.
70. Baumann AM, Bakkers MJ, Buettner FF, Hartmann M, Grove M, Langereis MA, de Groot RJ, Muhlenhoff M. 9-O-acetylation of sialic acids is catalysed by CASD1 via a covalent acetyl-enzyme intermediate. Nat Commun. 2015;6:7673.
71. LaCasse EC, Mahoney DJ, Cheung HH, Plenchette S, Baird S, Korneluk RG. IAP-targeted therapies for cancer. Oncogene. 2008;27(48):6252–75.
72. Holohan C, Van Schaeybroeck S, Longley DB, Johnston PG. Cancer drug resistance: an evolving paradigm. Nat Rev Cancer. 2013;13(10):714–26.

73. Suzuki Y, Imai Y, Nakayama H, Takahashi K, Takio K, Takahashi R. A serine protease, HtrA2, is released from the mitochondria and interacts with XIAP, inducing cell death. Mol Cell. 2001;8(3):613–21.
74. Bertrand MJ, Milutinovic S, Dickson KM, Ho WC, Boudreault A, Durkin J, Gillard JW, Jaquith JB, Morris SJ, Barker PA. cIAP1 and cIAP2 facilitate cancer cell survival by functioning as E3 ligases that promote RIP1 ubiquitination. Mol Cell. 2008;30(6):689–700.
75. McComb S, Aguade-Gorgorio J, Harder L, Marovca B, Cario G, Eckert C, Schrappe M, Stanulla M, von Stackelberg A, Bourquin JP, et al. Activation of concurrent apoptosis and necroptosis by SMAC mimetics for the treatment of refractory and relapsed ALL. Sci Transl Med. 2016;8(339):339ra370.
76. Manabe A, Coustan-Smith E, Behm FG, Raimondi SC, Campana D. Bone marrow-derived stromal cells prevent apoptotic cell death in B-lineage acute lymphoblastic leukemia. Blood. 1992;79(9):2370–7.
77. Bruggemann M, Raff T, Kneba M. Has MRD monitoring superseded other prognostic factors in adult ALL? Blood. 2012;120(23):4470–81.
78. Konoplev S, Jorgensen JL, Thomas DA, Lin E, Burger J, Kantarjian HM, Andreeff M, Medeiros LJ, Konopleva M. Phosphorylated CXCR4 is associated with poor survival in adults with B-acute lymphoblastic leukemia. Cancer. 2011;117(20):4689–95.
79. Juarez J, Bradstock KF, Gottlieb DJ, Bendall LJ. Effects of inhibitors of the chemokine receptor CXCR4 on acute lymphoblastic leukemia cells in vitro. Leukemia. 2003;17(7):1294–300.
80. Juarez J, Dela Pena A, Baraz R, Hewson J, Khoo M, Cisterne A, Fricker S, Fujii N, Bradstock KF, Bendall LJ. CXCR4 antagonists mobilize childhood acute lymphoblastic leukemia cells into the peripheral blood and inhibit engraftment. Leukemia. 2007;21(6):1249–57.
81. Jasin M, Haber JE. The democratization of gene editing: insights from site-specific cleavage and double-strand break repair. DNA repair. 2016;44:6–16.
82. Chiruvella KK, Liang Z, Wilson TE. Repair of double-strand breaks by end joining. Cold Spring Harb Perspect Biol. 2013;5(5):a012757.
83. Jacoby E, Nguyen SM, Fountaine TJ, Welp K, Gryder B, Qin H, Yang Y, Chien CD, Seif AE, Lei H, et al. CD19 CAR immune pressure induces B-precursor acute lymphoblastic leukaemia lineage switch exposing inherent leukaemic plasticity. Nat Commun. 2016;7:12320.
84. Legut M, Dolton G, Mian AA, Ottmann OG, Sewell AK. CRISPR-mediated TCR replacement generates superior anticancer transgenic T cells. Blood. 2018; 131(3):311–22.
85. Cooper ML, Choi J, Staser K, Ritchey JK, Devenport JM, Eckardt K, Rettig MP, Wang B, Eissenberg LG, Ghobadi A, et al. An "off-the-shelf" fratricide-resistant CAR-T for the treatment of T cell hematologic malignancies. Leukemia. 2018; https://doi.org/10.1038/s41375-018-0065-5.
86. Wang J, Li T, Zhou M, Hu Z, Zhou X, Zhou S, Wang N, Huang L, Zhao L, Cao Y, et al. TALENs-mediated gene disruption of FLT3 in leukemia cells: using genome-editing approach for exploring the molecular basis of gene abnormality. Sci Rep. 2015;5:18454.
87. Van Der Meer LT, Yu J, Butler M, Van der Meer JMR, Kuiper RP, van Leeuwen F. Crispr/Cas9 based Kinome screen identifies novel targets that determine sensitivity for Asparaginase therapy in acute lymphoblastic leukemia. Blood. 2015;126(23):2629.
88. Erb MA, Scott TG, Li BE, Xie H, Paulk J, Seo HS, Souza A, Roberts JM, Dastjerdi S, Buckley DL, et al. Transcription control by the ENL YEATS domain in acute leukaemia. Nature. 2017;543(7644):270–4.
89. Nishii R, Moriyama T, Janke LJ, Yang W, Suiter C, Lin TN, Li L, Kihira K, Toyoda H, Hofmann U, et al. Preclinical evaluation of NUDT15-guided thiopurine therapy and its effects on toxicity and anti-leukemic efficacy. Blood. 2018;131(22):2466–74.
90. Huang M, Inukai T, Miyake K, Tanaka Y, Kagami K, Abe M, Goto H, Minegishi M, Iwamoto S, Sugihara E, et al. Clofarabine exerts antileukemic activity against cytarabine-resistant B-cell precursor acute lymphoblastic leukemia with low deoxycytidine kinase expression. Cancer Med. 2018;7(4):1297–316.
91. Burns MA, Liao ZW, Yamagata N, Pouliot GP, Stevenson KE, Neuberg DS, Thorner AR, Ducar M, Silverman EA, Hunger SP, et al. Hedgehog pathway mutations drive oncogenic transformation in high-risk T-cell acute lymphoblastic leukemia. Leukemia. 2018; https://doi.org/10.1038/s41375-018-0097-x.